

Department of Applied Chemistry

**Size Exclusion Chromatography as a Tool for Natural
Organic Matter Characterisation in Drinking Water Treatment**

Bradley Allpike

**This thesis is presented for the Degree of
Doctor of Philosophy
of
Curtin University of Technology**

January 2008

Declaration

To the best of my knowledge and belief, this Thesis contains no material previously published by any other person except where due acknowledgement has been made.

This Thesis contains no material which has been accepted for the award of any other degree or diploma in any university.

Signature:

Date:

Acknowledgements

Firstly, I would like to thank my Principal Supervisor, A/Prof Cynthia Joll, for her advice and guidance throughout the course of my PhD program, especially during the preparation stage of this Thesis. Her capacity to always find time for discussion and the ability to make me feel like I was her most important student is greatly appreciated.

The contribution of my Co-Supervisor, A/Prof Anna Heitz, is also greatly appreciated, especially her invaluable comments regarding experimental planning and advice on technical issues. Her contribution to the preparation of this Thesis is also greatly appreciated.

I would also like to acknowledge the contribution of my Co-Supervisor, Prof Robert Kagi, in the preparation of this Thesis. As well, his advice on issues that arose during the course of this study was invaluable. Finally, I would like to thank Bob for the 'chats' in his office: there was never a dull moment.

I would also like to thank Mr Geoff Chidlow for his help, particularly with GC-MS issues, but also his contribution to the development of the organic carbon detector developed as part of this research.

The contribution of Mr Peter Chapman is also greatly appreciated, with regard to assistance with FTIR issues and also the construction to the organic carbon detector.

Also to Mr Dave Walton, whose skills in the workshop saved many hours of work, thank you.

I am also grateful for the hospitality of Prof Gary Amy and Dr Namguk Her, from the University of Colorado, and Prof Fritz Frimmel, Dr Gudrun Abbt-Braun and Dr Thomas Brinkmann, from the University of Karlsruhe. I extend my thanks to these researchers for their collaboration as described in Chapter 5 of this Thesis.

Thanks must also go to Dr Kamali Kannangara from the University of Western Sydney and A/Prof Graham Jones from Adelaide University for NMR analyses in Chapters 5 and 6 of this Thesis.

To Mr David Masters, Mr Steve O'Neill, Mr Lou Conti, Mr Paul Smith and Mr Luke Zappia of the Water Corporation, as well as the operators at the Wanneroo GWTP, I would like to extend my gratitude for their help with collection of samples and organising sampling events during the course of this study.

To the many staff and students in the Department of Applied Chemistry who assisted me, thank you. I would particularly like to thank Dr Suzy McDonald for her proof reading of this Thesis and Dr Ina Kristiana and Dr Justin Blythe for their review of Chapter 5. As well, special thanks to Justin, Daniel, Mick, Franki and Lyndon for their companionship over the years and the games of cards when times were slow.

I am grateful to the Australian Research Council (SPIRT program) and the Water Corporation for provision of an APA (I) scholarship. I would also like to acknowledge the Cooperative Research Centre for Water Quality and Treatment and the Centre for Applied Organic Geochemistry at Curtin University for financial support during this study.

Finally to my family, without their love and support, none of this would have been possible, and also to Rex, who kept me company during the long days and nights when I was preparing this Thesis. To my parents, Robyn and Peter, who have always encouraged me with everything I have done, I am eternally grateful. I would especially like to thank my Mum, who never let me forget that I eventually had to submit this Thesis for examination. Last and definitely not least, I would like to thank my wife, Jenny, who was always there for me when it really mattered.

Publications Arising from this Thesis

Refereed Journal Articles

1. **Allpike, B.P.**, Heitz, A., Joll, C.A. and Kagi, R.I. (2007) A new organic carbon detector for HPLC. *Journal of Chromatography A*, **1157**, pp 472-476
2. Warton, B., Heitz, A., Zappia, L., Masters, D., Alessandrino, M. Franzmann, P., Joll, C., **Allpike, B.P.**, O'Leary, B. and Kagi, R. (2007) Magnetic Ion Exchange (MIEX[®]) drinking water treatment in a large scale facility. *Journal of the American Water Works Association*, **99**, pp 89-101
3. **Allpike, B.P.**, Heitz, A., Joll, C.A., Kagi, R.I., Brinkman, T., Abbt-Braun, G., Frimmel, F. Her, N. and Amy, G. (2005) Size exclusion chromatography to evaluate DOC removal in drinking water treatment processes. *Environmental Science and Technology*, **37**, pp 2334-2342

Conference Presentations

1. **Allpike, B.P.**, Joll, C.J., Heitz, A., Kagi, R.I. (2007) Isolation of molecular weight fractions of natural organic matter in source waters and their behaviour in water treatment processes. *OZWATER 2007, Sydney, Australia, 4-7 March*
2. **Allpike, B.P.**, Heitz, A., Joll, C., Kagi, R. (2006) A new organic carbon detector for use with HPLC. *INTERACT – RACI, Perth, Australia, 24-28 September*
3. Joll, C., **Allpike, B.P.**, Heitz, A., Kagi, R. (2006) Isolation of molecular weight fractions of natural organic matter in source waters and their behaviour in water treatment processes. *INTERACT – RACI, Perth, Australia, 24-28 September*

4. **Allpike, B.P.**, Heitz, A., Joll, C., Kagi, R. (2006) Size exclusion chromatography with ultraviolet and organic carbon detection. *Australian Organic Geochemistry Conference, Perth, Australia, 20-23 February,*
5. **Allpike, B.P.**, Joll, C., Heitz, A., Kagi, R., Slunjski, M., Smith, P. and Tattersall, J. (2003) Size exclusion chromatography as a tool for examination of drinking water treatment processes. *OZWATER Convention and Exhibition, Perth, Australia, 6 – 10 April, CD-Rom.*
6. **Allpike, B.P.**, Heitz, A., Joll, C.A. and Kagi, R.I. (2004) HP-size exclusion chromatography to evaluate natural organic matter (NOM) removal in drinking water treatment processes. *Combined national conference of the Australian Organic Geochemists and the International Humic Substances Society, Blue Mountains, Australia, February 16-19, 2004.*
7. **Allpike, B.P.**, Joll, C.A., Heitz, A., Warton, B., Kagi, R.I., Masters, D. and O'Leary, B. (2004) Comparing natural organic matter removal by alum coagulation or MIEX[®] treatment using structural characterisation techniques, *Natural Organic Material Research: Innovations and Applications for Drinking Water, Adelaide, Australia, March 2-5, 2004.*

List of Abbreviations

alum	aluminium sulfate
AOC	assimilable organic carbon
AR	analytical reagent
AWQC	Australian Water Quality Centre
BIF	bromine incorporation factor
BOM	bioavailable organic matter
BTEX	benzene, toluene, ethylbenzenes and xylenes
CIS	critical ionic strength
CP	cross polarisation
CPMAS	cross polarisation magic angle spinning
CW	clearwater
DBP	disinfection by-product
DMTS	dimethyltrisulfide
DOC	dissolved organic carbon
EC	enhanced coagulation
FID	free induction decay
FPD	filter photometric (UV) detector
FTIR	Fourier transform infrared
GC-MS	gas chromatography-mass spectrometry
GPC	gel permeation chromatography
GWTP	groundwater treatment plant
HAA	haloacetic acid
HFM	hollow fibre membrane
HMW	high MW
HPSEC	high pressure size exclusion chromatography
IC	inorganic carbon
ICP-IDMS	inductively coupled plasma-isotope dilution mass spectrometry
ICR	inorganic carbon removal
LMW	low MW
LOD	limit of detection
LOQ	limit of quantification

MIEX [®]	magnetic ion exchange resin
MIEX [®] -C	MIEX [®] treatment followed by alum coagulation treatment
MSD	mass selective detector
MW	molecular weight
NDIR	non-dispersive infrared
NF	nanofiltration
NMR	nuclear magnetic resonance
NOM	natural organic matter
OC	organic carbon
OCD	organic carbon detector(ion)
PAH	polyaromatic hydrocarbon
PEG	polyethylene glycol
PSS	polystyrene sulfonate
py-GC-MS	pyrolysis-gas chromatography-mass spectrometry
RO	reverse osmosis
RW	aerated raw water
SEC	size exclusion chromatography
S _{Flu}	specific fluorescence
SPME	solid-phase microextraction
SRFA	Suwannee river fulvic acid
SUVA	specific UV absorbance
TDS	total dissolved solids
THM	trihalomethane
THMFP	trihalomethane formation potential
TOX	total organic halogen
TTHM	total trihalomethane
UF	ultrafiltration
USEPA	United States Environmental Protection Agency
UV	ultraviolet
WGWTP	Wanneroo groundwater treatment plant
WHO	World Health Organisation

ABSTRACT

Natural organic matter (NOM), ubiquitous in natural water sources, is generated by biogeochemical processes in both the water body and in the surrounding watershed, as well as from the contribution of organic compounds that enter the water as a result of human activity. NOM significantly affects the properties of the water source, including the ability to transport metals, influence the aggregation kinetics of colloidal particles, serve as a food source for microorganisms and act as a precursor in the formation of disinfection by-products (DBPs), as well as imparting a brown colour to the water. The reactivity of NOM is closely tied to its physicochemical properties, such as aromaticity, elemental composition, functional group content and molecular weight (MW) distribution. The MW distribution is an important consideration from a water treatment perspective for several reasons. For example, low MW NOM decreases the efficiency of treatment with activated carbon, and this fraction is thought to be the portion most difficult to remove using coagulation. The efficiency of membranes in the treatment of drinking water is also influenced by the MW distribution of NOM, while some studies have shown that the low MW fraction contributes disproportionately to the formation of bioavailable organic matter, therefore promoting the formation of biofilms in the distribution system. For these reasons, understanding the MW distribution of NOM is important for the treatment of natural waters for use as drinking waters.

Optimisation of a high pressure size exclusion chromatography (HPSEC) method for analysis of the MW distribution of NOM in natural waters is described (Chapter 2). Several parameters influencing the performance of HPSEC are tested and an optimised set of conditions illustrated. These parameters included eluent composition, ionic strength of the sample, flow rate and injection volume. Firstly, it was found that increasing the ionic strength of the HPSEC eluent resulted in less exclusion of NOM from the stationary phase. Stationary phases used in HPSEC contain a residual negative charge that can repel the negatively charged regions of NOM, effectively reducing the accessible pore volume. By increasing the ionic

strength, interactions between the stationary phase and eluent enabled a larger effective pore size for the NOM analytes. However, increasing ionic strength of the eluent also resulted in a loss of peak resolution for the NOM portion able to access the pore volume of the stationary phase. Determining the ideal eluent composition required the balancing of these two outcomes. Matching of the ionic strength of the sample with the eluent was also an important consideration. Retention times were slightly lower when the sample ionic strength was not matched with the eluent, especially for the lowest MW material, although the effect on chromatography was minimal. Flow rate had no effect on the resolution of the HPSEC chromatogram for the portion of material able to permeate the pore space of the stationary phase. Changes in the volume of sample injected had a marked effect on the elution profile of the NOM sample. Besides the obvious limitation of detection limit, only minor changes in elution profile were obtained up to an injection volume of 100 μL . Volumes above this value, however, resulted in significant peak broadening issues, as well as an undesirable effect on the low MW portion of detected DOC.

In Chapter 3, high pressure size exclusion chromatography with UV₂₅₄ and on-line detection of organic carbon (HPSEC-UV₂₅₄-OCD) was used to compare the removal of different apparent MW fractions of DOC by two process streams operating in parallel at the local Wanneroo groundwater treatment plant (GWTP). One of these two process streams included alum coagulation (operating in an enhanced coagulation mode (EC) for increased DOC removal) and the other stream included a magnetic ion exchange (MIEX[®]) process followed by alum coagulation (MIEX[®]-C). The MIEX[®] process is based on a micro-sized, macroporous, strong base anion exchange resin with magnetic properties, which has been designed to remove NOM through ion exchange of the anionic sites in NOM. Water was sampled from five key locations within these process streams, and the DOC at each location was characterised in terms of its MW distribution. HPSEC was carried out using three different on-line detector systems, namely OCD, UV absorbance detection at 254 nm, and fluorescence detection

($\lambda_{\text{ex}} = 282 \text{ nm}$; $\lambda_{\text{em}} = 353 \text{ nm}$). This approach provided significant information on the chemical nature of the DOC in the various MW fractions. The MIEX[®]-C process was found to outperform the EC process: these two processes removed similar amounts of high and low MW DOC, but the MIEX[®]-C process showed greater removal of DOC from the intermediate MW fractions. The two coagulation processes (EC and coagulation following MIEX[®]) showed good removal of the fractions of highest MW, while the MIEX[®] process alone was found to remove DOC across all MW fractions. These results seem to indicate that anionic groups, particularly susceptible to removal with MIEX[®] treatment, are well distributed across all MW fractions of NOM. In agreement with previous studies, MIEX[®]-C outperformed EC in the overall removal of DOC (MIEX[®]-C removed 25 % more DOC than EC). However, 70% of the additional DOC removed by MIEX[®]-C was comprised of a surprisingly narrow range of medium-high MW fractions.

The development of a novel online organic carbon detector (OCD) for use with HPSEC for determining the MW distribution of NOM is described in Chapter 4. With UV absorbance detection, the magnitude of the signal is based on the extinction coefficient of the chromophores in the analytes being investigated; whereas the signal from an OCD is proportional to the actual organic carbon concentrations, providing significantly more information. The development of an online OCD involved the separation of analytes using HPSEC, removal of inorganic carbon species which may interfere with organic carbon determination, oxidation of the organic carbon to carbon dioxide, separation of the produced carbon dioxide from the aqueous phase and subsequent detection of the gaseous carbon dioxide.

In the new instrument, following separation of components by HPSEC, the sample stream was acidified with orthophosphoric acid to a concentration of 20 mmol L^{-1} , resulting in a pH of ≤ 2 , in order to convert inorganic carbon to carbon dioxide. This acid dose was found to remove greater than 99 % of inorganic carbon once the acidified sample was passed through a hydrophobic polytetrafluoroethylene (PTFE) membrane allowing the passage

of dissolved gases (under negative pressure from a vacuum pump) but restricting the flow of the mobile phase. Several factors influenced the oxidation of the organic carbon in the next step, including the dose of persulfate, the type and intensity of UV radiation and the composition of the capillary through which the sample stream passes. Through optimisation of this process, it was found that a persulfate dose of 0.84 mmol L^{-1} in the sample stream was required for optimum oxidation efficiency.

A medium pressure UV lamp was compared to a vacuum UV lamp for its efficiency in oxidation of organic carbon to carbon dioxide. While the medium pressure lamp produced a far smaller percentage of its total radiation at the optimum wavelength for oxidation of organic compounds, the greater overall intensity of the medium pressure lamp was shown to be superior for this application. The composition of the capillary was shown to have a considerable effect on the oxidation efficiency. A quartz capillary, internal diameter 0.6 mm, was compared with a PTFE capillary, internal diameter 0.5 mm, for the oxidation of organic carbon by external UV treatment. While peak width, an important consideration in chromatographic resolution, was greater for the larger internal diameter quartz capillary, the lower UV transparency of PTFE combined with the shorter contact time, due to the reduced internal diameter of the capillary, resulted in a less efficient oxidation step using the PTFE capillary. The quartz capillary was therefore chosen for use in the UV/persulfate oxidation step for oxidation of organic carbon to carbon dioxide.

Separation of the produced carbon dioxide from the sample stream was achieved by sparging with nitrogen and contacting the gas/liquid mixture with a hydrophobic PTFE membrane, restricting the passage of the liquid while allowing the nitrogen and carbon dioxide gases to pass to the detection system. The only factor influencing this separation was the flow of the nitrogen sparge gas, with a flow of 2 mL min^{-1} found to be optimum. Detection of produced carbon dioxide was via a Fourier transform infrared (FTIR) spectrometer with a lightpipe accessory. The lightpipe accessory was designed for use as a detector for gas chromatography and the small size of

the detector cell was ideal for use with this application. Using the new system described, concentrations of a single peak could be determined with a detection limit of 31 ng and a determination limit of 68 ng. The development of the new OCD allowed characterisation of NOM in terms of its MW distribution and the UV and fluorescence spectral properties of each MW fraction.

Further characterisation of MW fractions of NOM from a local groundwater bore was carried out by separation of the fractions by preparative HPSEC, followed by off-line analysis. Preparative HPSEC involved the injection of a pre-concentrated groundwater sample multiple times, using a large scale HPSEC column, then collecting and combining material of identical MW. This allowed each MW fraction of the sample to be further characterised as described in Chapter 5. Preparative HPSEC has only previously been applied to a small number of samples for the concentration and fractionation of NOM, where the structural features of the various MW fractions were studied. In the current research, more extensive studies of not only the chemical characteristics, but also the disinfection behaviour, of the MW fractions were conducted.

Separation of the sample was conducted on a large diameter silica-based HPSEC column, with fraction collection based on semi-resolved peaks of the HPSEC chromatogram. Nine MW fractions were collected by this method. After concentration and dialysis to remove the buffer salts in the HPSEC mobile phase, each fraction was re-analysed by analytical HPSEC-UV₂₅₄ and showed a single Gaussian shaped peak, indicating discrete MW fractions had successfully been collected. Analysis of the collected MW fractions indicated that 57 % of the organic carbon was in Fractions 3 and 4, with 41 % in Fractions 5-9, leaving only 2 % in Fractions 1 (highest MW) and 2.

For each of the nine MW fractions, chlorine demand and 7 day trihalomethane formation potential (THMFP) were measured on dilute solutions of the same DOC concentration, and solid state ¹³C NMR spectra were recorded on some of the solid isolates obtained after lyophilisation of

the separate or combined dialysis retentates. The larger MW Fractions 3 and 4 were found to contain a greater proportion of aromatic and carbonyl carbon, and the lower MW Fractions 5 and 6 and Fractions 7-9 contained greater proportions of aliphatic and *O*-aliphatic carbon, by this technique. Chlorine demand experiments on each individual fraction with a normalised DOC concentration indicated that the largest MW fraction (Fraction 1) had the lowest chlorine demand. It was concluded that material in this fraction may be associated with inorganic colloids and unavailable for reaction with chlorine. Fraction 3 had the highest chlorine demand, just over two times more than the next highest chlorine demand (Fraction 4) and approximately three times the chlorine demand of Fraction 2. The organic material in Fraction 2 was postulated to contain a mixture of the reactive material present in Fraction 3 and the colloidal associated material present in Fraction 1. NMR analysis indicated that the difference between Fraction 3 and Fraction 4 was a reduction in reactive aromatic carbon and hence the lower chlorine demand in the latter fraction. Fractions 5-8 had similar chlorine demands, lower than Fraction 4, while Fraction 9 had a very low chlorine demand similar to that of Fraction 1. For Fractions 5-9, the lower aromatic carbon content most likely resulted in the lower chlorine demand.

The 7 day THMFP experiments showed some clear trends, with Fraction 1 and Fraction 2 producing the least amounts of THMs but having the greatest incorporation of bromine. Fractions 3 and 4 produced the greatest concentration of THMs with the lowest bromine incorporation, perhaps as they contained fast reacting THM precursors and the higher chlorine concentrations resulted in greater amounts of chlorinated THMs. Fraction 5 and Fraction 6 produced similar levels of THMs over 7 days to Fractions 7-9 (approximately 75% of the amount formed by Fractions 3 and 4), however, Fractions 7-9 formed these THMs more quickly than Fractions 5 and 6, with slightly greater amounts of bromine incorporation. It was thought that the increased speed of formation was due to the smaller MW of these fractions and a simpler reaction pathway from starting material to formation of THMs, as well as some structural differences. This research marks the first report of significantly resolved MW fractions being isolated and their behaviour in the

presence of a disinfectant being determined. While the high MW fractions had the greatest chlorine demands and THMFPs, these fractions are also the easiest to remove during coagulation water treatment processes, as shown in Chapter 3. The lowest MW material formed significant amounts of THMs, and also formed THMs more quickly than other MW fractions. This has important implications from a water treatment perspective, as the lowest MW material is also the most difficult to remove during conventional treatment processes.

Solid samples of NOM were isolated from water samples taken from four points at the Wanneroo GWTP using ultrafiltration and subsequent lyophilisation of the retained fractions, as described in Chapter 6. The sampling points were following aeration (Raw), following treatment by MIEX[®], following treatment by MIEX[®]-C and following treatment by EC. Elemental analysis, FTIR spectroscopy, solid state ¹³C NMR spectroscopy and HPSEC-UV₂₅₄-OCD analysis were used to compare the four isolates. Treatment with MIEX[®]-C was found to remove the greatest amount of NOM. Additionally, treatment with MIEX[®]-C was able to remove the largest MW range of NOM, with the remaining material being depleted in aromatic species and having a greater proportion of aliphatic and O-aliphatic carbon. EC treatment completely removed the NOM components above 5000 Da, but NOM below this was not well removed. NOM remaining after the EC train had a lower aromatic content and more aliphatic oxygenated organic matter than the RW. The remaining organic matter after MIEX[®] treatment contained less aromatic material compared to the RW, but had a greater aromatic content than either of the EC or MIEX[®]-C samples.

HPSEC was a significant analytical technique used throughout this research. Initial optimisation of an HPSEC method was an important development which allowed improved resolution of various MW fractions. The application of this technique and comparison of three detection systems for the study of DOC removal showed, for the first time, the performance of MIEX[®] treatment at a full scale groundwater treatment facility. The use of various HPSEC detection systems allowed significant characterisation of the MW fractions,

more information than had previously been gathered from such a sample set. This work demonstrated the need for OCD when applying HPSEC to the study of NOM. As such, a system was constructed that built on previously developed systems, with the use of a small detector cell enabling detection limits capable of measuring even the most dilute natural and treated water samples. To study the individual MW fractions in detail, preparative HPSEC was applied and, for the first time, the disinfection behaviour of various MW fractions was examined. Interestingly, the lowest MW fractions, acknowledged to be the most recalcitrant to conventional water treatment processes, produced significant quantities of THMs. Also the formation kinetics of THMs from the low MW fractions indicated that THMs were formed as quickly as, or perhaps even at faster rates than from the larger MW fractions. Finally, structural characterisation of NOM at four stages of the Wanneroo GWTP indicated MIEX[®]-C treatment was superior to EC, of significant interest for the water industry.

TABLE OF CONTENTS

Declaration	I
Acknowledgments	II
Publications	IV
List of Abbreviations	VI
Abstract	VIII
1. INTRODUCTION	1
1.1. Drinking Water Sources Supplying the Perth Metropolitan Region	1
1.2. Hydrogeology of Perth's Groundwater Sources	3
1.3. Natural Organic Matter	6
1.4. Treatment of Groundwater in Perth	8
1.4.1. Treatment of Groundwater at the Wanneroo Groundwater Treatment Plant	9
1.4.2. Magnetic Ion Exchange (MIEX [®]) Resin	13
1.5. Isolation and Characterisation of Natural Organic Matter	19
1.5.1. NOM Isolation Techniques	20
1.5.2. NOM Characterisation Techniques	23
1.5.2.1. Tier 1 NOM Characterisation Techniques	24
1.5.2.2. Tier 2 NOM Characterisation Techniques	25
1.5.2.2.1. Elemental Composition	25
1.5.2.2.2. Nuclear Magnetic Resonance Spectroscopy	25
1.5.2.2.3. Fourier Transform Infrared Spectroscopy	28
1.5.2.2.4. Pyrolysis-Gas Chromatography-Mass Spectrometry	29
1.5.2.3. Tier 3 NOM Characterisation Techniques	30
1.5.2.4. Tier 4 NOM Characterisation Techniques	31
1.5.3. Size Exclusion Chromatography	32
1.5.3.1. Mechanisms of Size Exclusion Chromatography Separation	34
1.5.3.1.1. Geometric Models for Size Exclusion Chromatography Separation	37
1.5.3.1.2. Thermodynamic Model for Size Exclusion Chromatography Separation	39
1.5.3.2. The Application of Size Exclusion Chromatography to NOM	40
1.5.3.3. Organic Carbon Detection for High Pressure Size Exclusion Chromatography	44
1.6. Scope of Study	49
	XVI

2. HIGH PRESSURE SIZE EXCLUSION CHROMATOGRAPHY METHOD DEVELOPMENT 52

2.1.	Introduction	52
2.1.1.	Scope of Study	56
2.2.	Experimental	56
2.2.1.	Samples	56
2.2.2.	Materials and Methods	57
2.2.2.1.	Purified Laboratory Water	57
2.2.2.2.	High Pressure Size Exclusion Chromatography	57
2.3.	Results and Discussion	59
2.3.1.	Effect of the Mobile Phase Composition on HPSEC Performance	59
2.3.2.	Effect of the Ionic Strength of the Sample on HPSEC Performance	68
2.3.3.	Effect of the Flow Rate on HPSEC Performance	71
2.3.4.	Effect of the Injection Volume on HPSEC Performance	76
2.3.5.	Analysis of Aquatic NOM Sample Using Optimised HPSEC Conditions	81
2.4.	Conclusions	84

3. THE USE OF HIGH PRESSURE SIZE EXCLUSION CHROMATOGRAPHY TECHNIQUES TO STUDY THE EFFECTIVENESS OF A RANGE OF DRINKING WATER TREATMENT PROCESSES 86

3.1.	Introduction	86
3.1.1.	Scope of Study	87
3.2.	Experimental	88
3.2.1.	Samples	88
3.2.2.	Materials and Methods	89
3.2.2.1.	Purified Laboratory Water	89
3.2.2.2.	Measurement of Constituents and Water Quality Parameters in Water Samples	89
3.2.2.3.	Measurement of Dissolved Organic Carbon Concentration	89
3.2.2.3.1.	Materials	89
3.2.2.3.1.1.	Phosphoric Acid Solution	89
3.2.2.3.1.2.	Persulfate Oxidiser Solution	90
3.2.2.3.2.	Preparation of Standard Solutions	90
3.2.2.3.3.	Measurement of Dissolved Organic Carbon Concentration	90
3.2.2.4.	High Pressure Size Exclusion Chromatography	91

3.2.2.5.	Method A	91
3.2.2.6.	Method B	92
3.2.2.7.	Method C	93
3.2.2.8.	High Pressure Size Exclusion Chromatography Data Treatment	93
3.3.	Results and Discussion	94
3.3.1.	Comparison of HPSEC Methods	94
3.3.2.	Raw Water Characteristics	102
3.3.3.	Evaluation of Water Treatment Processes	105
3.3.4.	High Pressure Size Exclusion Chromatography-Fluorescence Spectroscopy	111
3.4.	Conclusions	115
 4. DEVELOPMENT OF A DISSOLVED ORGANIC CARBON DETECTOR FOR USE WITH HPSEC		 117
4.1.	Introduction	117
4.1.1.	Oxidation of Dissolved Organic Carbon Using UV/Persulfate	118
4.1.2.	Methods for Removal of Inorganic Carbon in HPSEC with Organic Carbon Detection	121
4.1.3.	Scope of Study	122
4.2.	Experimental	122
4.2.1.	Samples	122
4.2.2.	Materials and Methods	123
4.2.2.1.	Ultra-pure Laboratory Water	123
4.2.2.2.	Reagents	123
4.2.2.3.	HPSEC Column Systems	123
4.2.3.	Organic Carbon Detector Development: Wet Chemistry System for Oxidation of Dissolved Organic Carbon and Carbon Dioxide Removal	124
4.2.4.	Standard HPSEC Operating Conditions	125
4.3.	Results and Discussion	126
4.3.1.	HPSEC-OCD System	126
4.3.2.	Removal of Inorganic Carbon	126
4.3.3.	Oxidation of Organic Matter Using Persulfate and UV Treatment	132
4.3.3.1.	UV Radiation	133
4.3.3.2.	Effect of Persulfate on the Oxidation of Organic Compounds	135
4.3.3.3.	Influence of UV radiation Exposure Time on the Oxidation of Organic Compounds	137

4.3.3.4.	Effect of pH on the Oxidation of Organic Carbon	143
4.3.4.	Dose Rate of Orthophosphoric Acid and Sodium Persulfate	144
4.3.5.	Detection of Carbon Dioxide Produced from Organic Carbon Species	146
4.3.6.	Column Selection in HPSEC-DOC Analysis	148
4.3.7.	Calibration of OCD and Statistical Parameters for Quantitative Analysis	153
4.3.8.	Application of HPSEC-UV ₂₅₄ -OCD to Study the Molecular Weight Distribution of NOM	159
4.4.	Conclusion	161

5. DISINFECTION BEHAVIOUR OF MOLECULAR WEIGHT FRACTIONS ISOLATED BY PREPARATIVE HIGH PRESSURE SIZE EXCLUSION CHROMATOGRAPHY

162

5.1.	Introduction	162
5.1.1.	Scope of Study	168
5.2.	Experimental	168
5.2.1.	Samples	168
5.2.2.	Materials and Methods	170
5.2.2.1.	Purified Laboratory Water	170
5.2.2.2.	Reagents	170
5.2.2.3.	Preparative HPSEC Separation	170
5.2.2.4.	Analytical HPSEC	171
5.2.2.5.	Chlorine Demand and Trihalomethane Formation Potential Measurements	172
5.2.2.6.	Solid State ¹³ C Nuclear Magnetic Resonance Spectroscopy of Individual MW Fractions	174
5.2.2.7.	Analysis of Bromide	174
5.2.2.8.	Measurement of Constituents and Water Quality Parameters in Water Samples	175
5.2.2.9.	Measurement of Dissolved Organic Carbon Concentration	175
5.3.	Results and Discussion	175
5.3.1.	Isolation and Fractionation of Aquatic NOM by Preparative HPSEC	175
5.3.2.	Recovery of Dissolved Organic Carbon from Preparative HPSEC Separation	181
5.3.3.	Solid State ¹³ C NMR Spectroscopy of Individual MW Fractions	183
5.3.4.	Effects of Chlorine on Individual MW Fractions	188
5.3.4.1.	Chlorine Demand of Individual MW Fractions	188
5.3.4.2.	Trihalomethane Formation Potential of Individual MW Fractions	192

5.3.4.2.1.	7 Day Total Trihalomethane Formation	192
5.3.4.2.2.	Trihalomethane Speciation	196
5.4.	Conclusions	205

6. ISOLATION AND CHARACTERISATION OF NOM FROM VARIOUS STAGES AT THE WANNEROO GWTP FOR EVALUATION OF THE PERFORMANCE OF TREATMENT PROCESSES FOR NOM REMOVAL

208

6.1.	Introduction	208
6.1.1.	Scope of Study	210
6.2.	Experimental	210
6.2.1.	Samples	210
6.2.1.1.	Ultrafiltration Treatment for Sample Isolation	211
6.2.2.	Materials and Methods	213
6.2.2.1.	Purified Laboratory Water	213
6.2.2.2.	Measurement of Constituents and Water Quality Parameters in Water Samples	213
6.2.2.3.	Measurement of Dissolved Organic Carbon Concentration	214
6.2.2.4.	Biodegradable Organic Carbon Concentration	214
6.2.2.5.	Assimilable Organic Carbon Concentration	214
6.2.2.6.	HPSEC Analysis	215
6.2.2.7.	Elemental Analysis	215
6.2.2.8.	Fourier Transform Infrared Spectroscopy of Solid NOM Isolates	215
6.2.2.9.	Pyrolysis-Gas Chromatography-Mass Spectrometry of Solid NOM Isolates	216
6.2.2.10.	Solid State ¹³ C Nuclear Magnetic Resonance Spectroscopy of Solid NOM Isolates	216
6.3.	Results and Discussion	217
6.3.1.	Analysis of Water Samples Prior To Ultrafiltration	217
6.3.1.1.	Water Quality Parameters of Water Samples	217
6.3.1.2.	HPSEC-UV ₂₅₄ -OCD Analysis of Water Samples	222
6.3.2.	Analysis of Ultrafiltration Isolated NOM Samples	226
6.3.2.1.	Elemental Analysis of NOM Isolates	226
6.3.3.	Pyrolysis-GC-MS Analysis of NOM Isolates	229
6.3.4.	Infrared Spectroscopy of NOM Isolates	237
6.3.5.	Solid State ¹³ C Nuclear Magnetic Resonance Spectroscopy of Solid NOM Isolates	241

XX

6.4.	Conclusions	245
7.	THESIS CONCLUSIONS	249
	APPENDICES	253
	REFERENCE LIST	263

LIST OF FIGURES

Chapter One

Figure 1.1 Location map showing the Perth metropolitan region and six groundwater schemes. Surface water reservoirs are located to the east of the Darling Scarp (modified from Hirschberg, 1989).	2
Figure 1.2 Flow chart of the Wanneroo GWTP treatment scheme.	11
Figure 1.3 Geometric models: a) conical-pore opening, b) cylindrical pore opening (taken from Mori and Barth, 1999).	37
Figure 1.4 Schematic of the thin film OCD system (taken from Huber and Frimmel, 1991).	46

Chapter Two

Figure 2.1 Influence of mobile phase on the HPSEC of aquatic NOM a) purified laboratory water (mobile phase A), b) 10 mmol L ⁻¹ sodium acetate (B), c) 10 mmol L ⁻¹ phosphate buffer (C), d) 10 mmol L ⁻¹ phosphate buffer + 26 mmol L ⁻¹ sodium sulfate ($\mu = 100$ mmol L ⁻¹ (D)), e) 20 mmol L ⁻¹ phosphate buffer (E), f) 20 mmol L ⁻¹ phosphate buffer + 20 mmol L ⁻¹ sodium sulfate ($\mu = 100$ mmol L ⁻¹ (F)). Injection volume was 100 μ L, flow rate 1 mL min ⁻¹ and sample ionic strength adjusted to match that of the mobile phase.	64
Figure 2.2 Comparison of total peak area, area of peak eluting at V_0 (1 st peak) and sum of the area of peaks eluting after V_0 (2 nd peak group) for six mobile phases tested; purified laboratory water (mobile phase A), 10 mmol L ⁻¹ sodium acetate (B), 10 mmol L ⁻¹ phosphate buffer (C), 10 mmol L ⁻¹ + 26 mmol L ⁻¹ sodium sulfate ($\mu = 100$ mmol L ⁻¹) (D), 20 mmol L ⁻¹ phosphate buffer (E), 20 mmol L ⁻¹ + 20 mmol L ⁻¹ sodium sulfate ($\mu = 100$ mmol L ⁻¹) (F). Areas taken from chromatograms in Figure 2.1.	65
Figure 2.3 Influence of sample ionic strength on the HPSEC of aquatic NOM. Mobile phase tested was 20 mmol L ⁻¹ phosphate buffer, $\mu = 40$ mmol L ⁻¹ (mobile phase C), injection volume = 100 μ L and flow rate 1 mL min ⁻¹ ; a) Sample ionic strength lower than mobile phase, b) sample ionic strength same as mobile phase ($\mu = 40$ mmol L ⁻¹).	69
Figure 2.4 Influence of mobile phase flow rate on the HPSEC of aquatic NOM. Flow rates: a) 0.5 mL min ⁻¹ , b) 0.8 mL min ⁻¹ , c) 1 mL min ⁻¹ , d) 1.2 mL min ⁻¹ are compared. x axis expressed as elution time. Mobile phase was 20 mmol L ⁻¹ phosphate buffer (mobile phase D), injection volume was 100 μ L and sample ionic strength was unaltered.	73
Figure 2.5 Influence of mobile phase flow rate on the HPSEC of aquatic NOM. Flow rates: a) 0.5 mL min ⁻¹ , b) 0.8 mL min ⁻¹ , c) 1 mL min ⁻¹ , d) 1.2 mL min ⁻¹ are compared. x axis expressed as elution volume (V_e). Mobile phase was 20 mmol L ⁻¹ phosphate buffer (mobile phase D), injection volume was 100 μ L and sample ionic strength was unaltered.	74

Figure 2.6 Influence of injection volume on the HPSEC of aquatic NOM. Chromatograms from injection volumes of 500, 50, 20 and 10 μL are compared to the chromatogram from injection of a volume of 100 μL . Mobile phase was 20 mmol L^{-1} phosphate buffer (mobile phase D), flow rate was 1 mL min^{-1} and sample ionic strength was unaltered..... 77

Figure 2.7 Influence of injection volume on the HPSEC of aquatic NOM. The aerated raw water sample was diluted with purified laboratory water for injection volumes 20 μL , 50 μL , 100 μL and 500 μL so DOC concentrations equalled the sample injected with a 10 μL injection volume. a) 500 μL injection, sample diluted 50:1, b) 100 μL injection, sample diluted 10:1, c) 50 μL injection, sample diluted 5:1, d) 20 μL injection, sample diluted 10:1, e) 100 μL injection, sample not diluted. Mobile phase was 20 mmol L^{-1} phosphate buffer (mobile phase D), flow rate was 1 mL min^{-1} and sample ionic strength was unaltered..... 79

Figure 2.8 Typical chromatogram using the optimised HPSEC conditions. Mobile phase composition: 10 mmol L^{-1} KH_2PO_4 + 10 mmol L^{-1} Na_2HPO_4 ; sample buffered so ionic strength of sample equalled that of mobile phase ($\mu = 40 \text{ mmol L}^{-1}$), injection volume = 100 μL , flow rate 1 mL min^{-1} . The sample was aerated raw water from the Wanneroo GWTP..... 82

Chapter Three

Figure 3.1 Schematic of Wanneroo GWTP, showing sampling locations (*) and sample names. 88

Figure 3.2 HPSEC-UV₂₅₄ chromatograms (Method B, 300 mm x 7.8 mm column) of water samples from the Wanneroo GWTP: a) RW, b) MIEX[®], c) MIEX[®]-C, d) EC, e) clear water. Peaks in each chromatogram are numbered as referred to in the text. 97

Figure 3.3 HPSEC-UV₂₅₄-OCD chromatograms (Method A, 250 mm x 20 mm column) of water samples from the Wanneroo GWTP: a) RW, b) MIEX[®], c) MIEX[®]-C, d) EC, e) clear water. Peaks in each chromatogram are numbered as referred to in the text. Black line = DOC response; dashed line = UV₂₅₄ response. 98

Figure 3.4 HPSEC-UV₂₅₄-OCD chromatograms (Method C, 250 mm x 20 mm column) of water samples from the Wanneroo GWTP: a) RW, b) MIEX[®], c) MIEX[®]-C, d) EC, e) clear water. Peaks in each chromatogram are numbered as referred to in the text. Black line = DOC response; dashed line = UV₂₅₄ response. 101

Figure 3.5 DOC concentrations (mg L^{-1}) in MW fractions from samples from the Wanneroo GWTP. Values above bars represent DOC concentrations in each fraction (mg L^{-1}) 106

Figure 3.6 MW specific-SUVA chromatograms (Method C, 250 mm x 20 mm column) of water samples from the Wanneroo GWTP: a) RW, b) MIEX[®], c) MIEX[®]-C, d) EC, e) clear water..... 109

Figure 3.7 Chromatograms from HPSEC-Flu (Method C, 250 mm x 20 mm column, excitation wavelength of 282 nm and emission wavelength of 353 nm) of water samples from the Wanneroo GWTP: a) RW, b) MIEX[®], c) MIEX[®]-C, d) EC, e) clear water..... 112

Figure 3.8 MW S_{Flu} chromatograms (Method C, 250 mm x 20 mm column) of water samples from the Wanneroo GWTP: a) RW, b) MIEX[®], c) MIEX[®]-C, d) EC, e) clear water.

..... 114

Chapter Four

Figure 4.1 Relative Spectral emittance from low pressure and medium pressure lamps. (Taken from Bolton, 2001). 119

Figure 4.2 Pathway of photoreactions of NOM (NOM* = NOM at an excited state; $h\nu$ = UV irradiation; NOM' and NOM'' are NOM with slightly different structures) (Taken from Frimmel, 1994) 120

Figure 4.3 Layout of HPSEC-OCD system. 126

Figure 4.4 Interference in HPSEC-OCD caused by inorganic carbon species, a) inorganic carbon not removed, b) inorganic carbon removed. Chromatograms were obtained using a semi-preparative column and conditions as described in Section 4.2.4. 127

Figure 4.5 Scheme of HFM bundle used for removal of inorganic carbon. 128

Figure 4.6 Influence of orthophosphoric acid concentration on removal of inorganic carbon species. Shaded area represents portion of chromatogram where IC eluted. Acid concentrations in solution: a) 0 mmol L⁻¹, b) 3.7 mmol L⁻¹, c) 8.7 mmol L⁻¹, d) 13.1 mmol L⁻¹, e) 17.4 mmol L⁻¹, f) 20.0 mmol L⁻¹, g) 26.0 mmol L⁻¹, h) 30.4 mmol L⁻¹. Chromatograms were obtained using a semi-preparative column and conditions as described in Section 4.2.4. . 129

Figure 4.7 Removal of inorganic carbon using a orthophosphoric acid concentration of 20.0 mmol L⁻¹ and a HFM bundle a) 100 mg L⁻¹ inorganic carbon, b) 5mg L⁻¹ inorganic carbon, c) 100 mg L⁻¹ inorganic carbon dosed with 20.0 mmol L⁻¹ orthophosphoric acid and passed through HFM bundle, d) 5 mg L⁻¹ inorganic carbon dosed with 20.0 mmol L⁻¹ orthophosphoric acid and passed through HFM bundle. The signal was collected using conditions as described in Section 4.2.4..... 132

Figure 4.8 Influence of persulfate concentration on oxidation of organic carbon in a sample of RW. Persulfate concentrations, from 0 to 2.52 mmol L⁻¹ in solution, dosed at 10 μ L min⁻¹, the signal was collected without using a chromatographic column, using conditions described in Section 4.2.4..... 136

Figure 4.9 Oxidation efficiency of organic carbon subjected to a medium pressure UV lamp with quartz capillary of varying length. a) 300 mm, b) 600 mm, c) 900 mm, d) 1200 mm. The signal was collected without a chromatographic column, using conditions described in Section 4.2.4. 138

Figure 4.10 Conversion of the DOC component of post-aeration WGWTP water to CO₂ versus quartz capillary length..... 139

Figure 4.11 Schematic of HPSEC-UV₂₅₄-OCD system used to test effect of residence time (system volume) on peak resolution. 140

Figure 4.12 Influence of quartz capillary on peak width and residence time. a) black line = without quartz capillary present, b) red line = with quartz capillary present. Chromatograms

were obtained without a chromatographic column using conditions described in Section 4.2.4.	141
Figure 4.13 Comparison of a) black line = quartz capillary and b) red line = PTFE capillary on peak width. Signals were obtained without a chromatographic column using conditions described in Section 4.2.4.	142
Figure 4.14 Influence of hydrogen ions on the oxidation of organic carbon by UV/persulfate. Black line a) 0 mmol L ⁻¹ orthophosphoric acid, red line b) 3.7 mmol L ⁻¹ orthophosphoric acid. Chromatograms were obtained with a semi-preparative chromatographic column using conditions described in Section 4.2.4.	143
Figure 4.15 Influence of the concentration of persulfate and orthophosphoric acid dose on removal of inorganic carbon and oxidation of organic carbon. a) 0 μL min ⁻¹ , b) 5 μL min ⁻¹ , c) 10 μL min ⁻¹ , d) 20 μL min ⁻¹ , e) 30 μL min ⁻¹ , f) 50 μL min ⁻¹ , g) 100 μL min ⁻¹ . Chromatograms were obtained with a semi-preparative chromatographic column using conditions described in Section 4.2.4.	145
Figure 4.16 Recovery of CO ₂ through the hydrophobic PTFE membrane with varying nitrogen flows, a) 2 mL min ⁻¹ , b) 3 mL min ⁻¹ , c) 5 mL min ⁻¹ , d) 7.5 mL min ⁻¹ , e) 10 mL min ⁻¹ and f) 20 mL min ⁻¹ . Signals were obtained without a chromatographic column using conditions described in Section 4.2.4.	147
Figure 4.17 FTIR background signal of blank injection showing CO ₂ contribution in HPSEC-OCD using a) HW-50s column (250 mm x 22 mm i.d.) and b) TSK G3000SW _{xl} (300 mm x 7.8 mm i.d.) column contribution. Chromatograms were obtained using conditions described in Section 4.2.4.	149
Figure 4.18 HPSEC UV ₂₅₄ and OCD chromatograms of raw water on a) analytical column (300 mm x 7.8 mm i.d.), b) semi-preparative column (250 mm x 10 mm i.d.) and c) preparative column (250 mm x 22 mm i.d.). Chromatograms were obtained using column system as mentioned above using conditions described in Section 4.2.4.	151
Figure 4.19 Calibration graph for organic carbon concentrations taken from Table 4.3.	155
Figure 4.20 Repeatability investigation: different coloured curves represent the five different injections; HPSEC-OCD chromatogram of raw aerated water from GWTP, a) is the OCD signal and b) is the UV ₂₅₄ signal. Chromatograms were obtained with a semi-preparative chromatographic column conditions described in Section 4.2.4.	158
Figure 4.21 HPSEC-UV ₂₅₄ -OCD chromatogram of raw aerated water from GWTP, a) is the OCD signal and b) is the UV ₂₅₄ signal. Chromatograms were obtained with a preparative chromatographic column conditions described in Section 4.2.4.	159

Chapter Five

Figure 5.1 Location of production Bore W300.	169
--	-----

Figure 5.2 Preparative HPSEC-UV ₂₅₄ chromatogram of UF treated W300 bore water, indicating positions of nine collected fractions. Numbers in red are the number attributed in the text to each fraction. The column was a BioSep SEC-S 3000 (300 mm x 21.2 mm i.d.) silica base HPSEC column and the mobile phase was a 20 mmol L ⁻¹ phosphate buffer. The flow rate was 2 mL min ⁻¹ and the injection volume was 2 mL.....	177
Figure 5.3 a) Analytical HPSEC-UV ₂₅₄ chromatogram (TSK G3000SW _{xl} 300 mm x 7.8 mm column) of UF treated W300 water. Numbers above chromatogram represent the elution volume at which fractions were collected. Numbers in red are the number attributed to each fraction in the text. Red lines mark intervals where fractions were collected; b) HPSEC-UV ₂₅₄ chromatograms of individual fractions after analysis on the analytical column. Volume above represents elution volume of individual fractions. Numbers in red are numbers attributed to fractions in text.....	178
Figure 5.4 Solid state ¹³ C NMR spectra of isolated samples. a) Fractions 7-9, b) Fractions 5 & 6, c) Fraction 4, d) Fraction 3.	184
Figure 5.5 Relative proportions of carbon types in the solid state ¹³ C NMR spectra of the isolated NOM samples: Fraction 3 only, Fraction 4 only, Fractions 5 and 6 combined and Fractions 7-9 combined. The relative percentage of the four different carbon types in each sample is listed above the corresponding bar.....	185
Figure 5.6 Total THM concentration plotted against time for each of the nine individual MW fractions. Colours refer to individual fractions as stated in the legend.	193
Figure 5.7 Relative molar concentrations of individual THMs found after exposure to chlorine and bromine for 168 hours for the nine MW fractions collected from preparative HPSEC. CHCl ₃ = chloroform, CHCl ₂ Br = bromodichloromethane, CHClBr ₂ = dibromochloromethane, CHBr ₃ = bromoform.....	197

Chapter Six

Figure 6.1 Schematic of the WGWTP showing sampling locations and sample names. ...	211
Figure 6.2 Schematic of ultrafiltration system	212
Figure 6.3 HPSEC-OCD chromatograms of water samples: a) RW, b) MIEX [®] , c) MIEX [®] -C and d) EC	222
Figure 6.4 HPSEC-UV ₂₅₄ -OCD chromatograms of water samples: a) RW, b) MIEX [®] , c) MIEX [®] -C and d) EC. The black line represents the OCD signal and the red line represents the UV ₂₅₄ signal.....	224
Figure 6.5 Pyrograms obtained by Py-GC-MS of NOM isolates from a) RW and b) MIEX [®] . Numbers above chromatograms refer to identification key in Table 6.4.	230
Figure 6.6 Pyrograms obtained by Py-GC-MS of NOM isolates from a) MIEX [®] -C and b) EC. Numbers above chromatograms refer to identification key in Table 6.4.	231
Figure 6.7 Relative yield of pyrolysis products of various biopolymer origin from NOM isolated from a) RW, b) MIEX [®] , c) MIEX [®] -C and d) EC.....	234

Figure 6.8 FTIR spectra of four solid NOM isolates: a) RW, b) MIEX[®], c) MIEX[®]-C, d) EC.
.....238

Figure 6.9 Solid state ¹³C CPMAS NMR spectra of NOM isolates: a) RW, b) MIEX[®], c)
MIEX[®]-C, d) EC.....241

LIST OF TABLES

Chapter Two

Table 2.1 Tested mobile phase composition, ionic strength and pH.....	58
Table 2.2 Distance of peak maximum from point of injection (t_R), peak width at half height ($w_{1/2}$) and calculated number of theoretical plates (N) for the six mobile phases tested using a Tosoh TSK G3000SW _{xl} column. Injection volume was 100 μ L and mobile phase flow was 1 mL min ⁻¹ . Sample ionic strength was adjusted to equal the mobile phase by adding a concentrated solution of the mobile phase to the sample prior to analysis.	60

Chapter Three

Table 3.1 Water quality and chemical dose parameters at sample locations at the Wanneroo GWTP.....	89
Table 3.2. Molecular weight parameters (Mn, Mw and ρ) for Wanneroo raw water (excluding Fraction 1) determined using two different HPSEC methods with two different detection methods.....	103

Chapter Four

Table 4.1 Influence of orthophosphoric acid concentration on integrated area of each chromatogram obtained in Figure 4.6.	130
Table 4.2 Oxidation efficiency of the medium pressure UV lamp and the vacuum UV lamp measured on seven organic compounds (DOC = 10 mg L ⁻¹ . The signal was collected using conditions described in Section 4.2.4. Peak areas were calibrated against potassium hydrogen phthalate (Section 4.3.7).....	134
Table 4.3 Peak areas and RSD (n=5) of standards used to calibrate organic carbon concentrations.....	154
Table 4.4 Limits of detection and determination for organic carbon detection.....	156
Table 4.5 Comparison of DOC concentration from Shimadzu TOC analyser and HPSEC-UV ₂₅₄ -OCD system, showing hydrophobic organic carbon content in raw water sample from WGWTP.	157
Table 4.6 Repeatability data of chromatograms plotted in Figure 4.20.....	158

Chapter Five

Table 5.1 Characteristics of Bore water W300.....	176
Table 5.2 Distribution of DOC by Preparative HPSEC-UV ₂₅₄ and Nominal MWs of the Separated Size Fractions. ^a calculated from measured DOC concentration of solution. ...	182

Table 5.3 Chlorine demands of the nine fractions obtained by preparative HPSEC. All fractions had a DOC concentration of 2 mg L ⁻¹ . Chlorine demand values are chlorine concentrations required to obtain a chlorine residual of 0 mg L ⁻¹ after 168 hours of contact.	189
Table 5.4 Bromine incorporation factors for THMs (BIF (THMs)) for each of the nine fractions collected by preparative HPSEC. BIF (THMs) calculated using Equation 5.1.....	199
Table 5.5 Chlorine and bromine incorporation into THMs as a percentage of the total chlorine and bromine dosed to fractions.....	201

Chapter Six

Table 6.1 Water quality parameters of samples from the WGWTP: raw water following aeration (RW), following MIEX [®] treatment (MIEX [®]), following MIEX [®] and coagulation treatment (MIEX [®] -C), and following enhanced coagulation treatment only (EC). n.d. = not determined	218
Table 6.2 Elemental composition of the four NOM isolates. (n.d. = not detected).....	228
Table 6.3 Most abundant compounds identified in pyrograms of four NOM isolates. Category of compound type relates to Figure 6.5 and 6.6.....	232
Table 6.4 Relative proportions of carbon types in the solid state ¹³ C NMR spectra of the NOM isolates: Integration results from solid state ¹³ C NMR analysis of RW, MIEX [®] , MIEX [®] -C and EC (Figure 6.9). % = percentage of peak area of total spectrum, ppm is chemical shift of peak in parts per million.	242

1. INTRODUCTION

1.1. Drinking Water Sources Supplying the Perth Metropolitan Region

Perth, the capital city of the State of Western Australia, has a population of approximately 1.5 million, 75 % of the State's population (Australian Bureau of Statistics, 2007). The Perth region is bounded by the Gingin Brook to the north, the South Dandalup River to the south, the Darling Scarp to the east and the Indian Ocean to the west (Figure 1.1). This area is almost entirely on the Swan Coastal Plain, except for a small portion in the north east which is situated on the Dandaragan Plateau. The region covers an area of approximately 4000 km², and extends from the Perth central business district to Guilderton, 80 km to the north, and to Mandurah, 70 km to the south (Davidson, 1995). Perth experiences a Mediterranean type climate with hot, dry summers and mild, wet winters. Average yearly rainfall ranges from approximately 860 mm in the northern coastal area to about 1200 mm on the Darling Plateau southeast of Perth (Australian Bureau of Statistics, 2007). Almost 90 % of rainfall occurs between April and October, with the remaining months, especially December to February, being hot and dry, resulting in large evaporation losses from wetlands. Also, with changing world and local climates, average rainfall in the south west of Western Australia, including the Perth region, has been gradually decreasing over recent decades, with local surface reservoirs now mostly less than 50 % of capacity (Water Corporation, 2007). This has presented new challenges for the Water Corporation of WA, the State's major water utility, responsible for the supply of potable water to the majority of Western Australia. As a result of the reduced annual rainfall, approximately 55 % of Perth's water is extracted from groundwater sources, 15 % produced from seawater desalination and the remaining 30 % of supply extracted from eleven storage reservoirs in the Darling Range (Water Corporation, 2007). These reservoirs are located in largely pristine, uninhabited Jarrah forest, on predominantly nutrient-poor

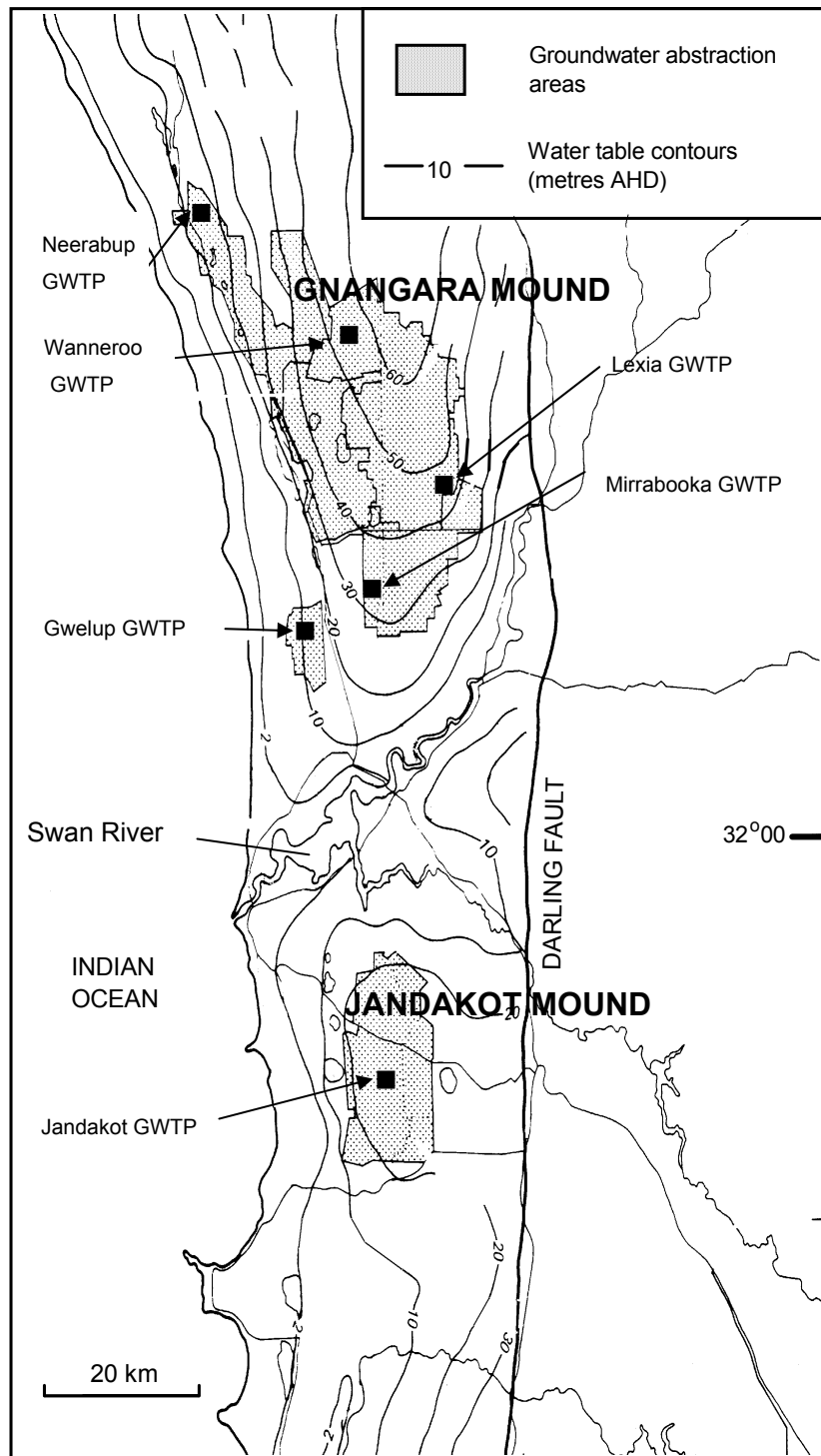


Figure 1.1 Location map showing the Perth metropolitan region and six groundwater schemes. Surface water reservoirs are located to the east of the Darling Scarp (modified from Hirschberg, 1989).

lateritic sediment, and water quality is usually good, requiring no treatment other than disinfection (Water Corporation, 2007). Recharge of these storage reservoirs is almost exclusively by winter rainfall and local runoff. Conversely, the groundwater is extracted from over 180 bores from various

confined and unconfined aquifers and is often of poorer quality and requires substantial treatment in order to meet current Australian drinking water guidelines.

1.2. Hydrogeology of Perth's Groundwater Sources

Water permeates the superficial formations beneath the Swan Coastal Plain and the underlying geological formations of the Perth Basin to create underground storage aquifers. This groundwater occupies the pores and regions between particles of the underlying geological formations. According to Davidson (1995), fresh water has been found at depths of at least 1000 m due mainly to direct rainfall recharge on the coastal plain with a small component derived from runoff from the Darling Scarp and Dandaragan Plateau. Perth's underground water stores have been divided into six different aquifers. These aquifers are the unconfined superficial aquifer containing the Gnangara and Jandakot mounds and the semi-confined and confined Rockingham, Kings Park, Mirrabooka, Leederville and Yarragadee aquifers. The work in this Thesis has almost exclusively been conducted with water drawn from the unconfined superficial aquifer. Accordingly, a detailed description of this aquifer is given below.

The superficial aquifer, or as it is referred to locally the 'unconfined' or 'shallow' aquifer, is a complex, unconfined multilayered formation lying within the quaternary sediments of the Swan Coastal Plain (Davidson, 1995). This aquifer extends west from the Darling Scarp and covers most of the Swan Coastal Plain. The sediments that comprise the aquifer range from clay in the east alongside the Darling Scarp, through a sandy succession in the central coastal plain to predominantly limestone in the far west on the coastal extreme. The superficial aquifer varies in thickness from 45 m in the northern Perth region to 20 m in the south, with a maximum thickness of approximately 70 m. It has been calculated that the capacity of the superficial aquifer, represented by the amount of water in pore spaces available to bores if the sediments were de-watered, is approximately 25 000 GL and varies in age from the present at the watertable to

approximately 2000 years at the aquifer base. The upper limit of the superficial aquifer is the watertable. The watertable varies significantly in depth throughout the Swan Coastal Plain, mainly dependent on topography, with lesser influences being the permeability of sediments and location within the groundwater flow system. The watertable is at its highest during September-October, and at its lowest during April and May immediately before the winter rainfall period. The level of the watertable fluctuates significantly outside these periods as recharge is almost exclusively through rainfall infiltration (Davidson, 1995).

Two groundwater mounds within the superficial aquifer contain approximately 85 % of the groundwater within the aquifer (Department of Water, 2007). These are the Gnangara and Jandakot mounds (Figure 1.1). These mounds are critically important to the groundwater supply, with approximately 40 % of production bores drawing water from these mounds (Department of Water, 2007). The mounds are refreshed directly by rainfall infiltration, and develop due to a superior rate of vertical rainfall infiltration when compared to the rate of horizontal groundwater flow through the aquifer (Davidson, 1995). These mounds also significantly influence the groundwater flow within the superficial aquifer. Groundwater flows through the aquifer under the influence of gravity away from the crests of the mounds and foothills of the Darling and Dandaragan Plateaus towards the discharge boundaries of the Swan Coastal Plain, namely the Indian Ocean, Gingin Brook, Swan River, Canning River, Serpentine River and the North and South Dandalup Rivers. Also, some lakes act as boundaries for groundwater flow (Davidson, 1995).

There are many permanent and transient lakes and swamps within the Swan Coastal Plain forming the upper limit of the watertable. These lakes and swamps exist in shallow interdunal and interbarrier depressions of the land surface. Some of the lakes and most of the swamps exist in swales in otherwise flat terrain. The majority of lakes in the Swan Coastal Plain are shallow, ranging in depth from approximately 0.5 to 3 m (Department of Water, 2007). They are often surrounded by vegetation and contain

sediments of biogenic origin consisting of peat and peaty sands, together with diatomite, calcareous clay and fresh water marly limestone (Davidson, 1995). Following periods of rainfall, hydraulic connection is developed between the lake water and groundwater of the superficial aquifer. Thus, it is apparent that these lake systems are intricately linked with water quality in the superficial aquifer. Some of the swamps of the coastal plain are perched above the watertable, with seepage into the superficial aquifer inhibited by a ferruginous hardpan sediment ('coffee rock'). Typically, these swamps are seasonally waterlogged, containing water following heavy rainfall. There are swamps which are in direct contact with the watertable, but as they are extremely shallow, they only contain water during the winter rainfall period. Most of these shallow wetlands are evaporative basins with highly variable salinity. At the end of winter, the water in these basins is at its freshest; however, during periods of hot dry weather, evaporation results in increasingly saline water. After heavy rainfall, this water, with increased salinity, is flushed into the groundwater forming a brackish plume from these wetlands, which is capable of altering the groundwater salinity in the region surrounding the wetlands. Due to the direct contact between lakes and swamps and the groundwater of the superficial aquifer, it is clear that they can impart some influence on the water quality and are thus of critical importance (Davidson, 1995).

Geological location and position within the groundwater flow system exert the most influence on the chemical and physical properties of the groundwater in the superficial aquifer (Davidson, 1995). Thus, there is temporal variation in the quality of groundwater in this aquifer. Salinity within the superficial aquifer ranges from approximately 130 to 12 000 mg L⁻¹ total dissolved solids (TDS), but rarely exceeds 1000 mg L⁻¹ TDS. Salinity is generally lowest at points of aquifer recharge and increases in the direction of the groundwater flow and is at its highest at rivers and the ocean which are the points of discharge. The lowest salinity in the superficial aquifer is at the crest of the Gnangara and Jandakot mounds. The pH of groundwater in the superficial aquifer ranges from 4 at the watertable in the east and central coastal plain and increases to between 6.5 and 7.5 at the base. The limestone sediment

on the coastal fringe has a pH between 7 and 8. Colour can be used as an indicator of the content of organic matter in natural waters (Clesceri *et al.*, 1998). For the superficial aquifer, the colour varies significantly, with the highest values in the upper section of the aquifer, where leaching from vegetation and peat deposits on the surface is passed to the watertable as a result of infiltration (Davidson, 1995). Groundwater in the superficial aquifer contains dissolved iron at concentrations of less than 1 mg L⁻¹ to more than 50 mg L⁻¹, with concentrations generally increasing towards the base of the aquifer. Dissolved iron is present as ferrous ion, which is readily oxidised to ferric ion on contact with air. Sulfate is present in concentrations generally below 100 mg L⁻¹, although increased concentrations can be found in areas surrounding peaty wetlands due to the oxidation of sulfides. Hardness, which is measured as an equivalent quantity of calcium carbonate, also increases in the direction of groundwater flow. Concentrations of less than 50 mg L⁻¹ are found in the sandy soils of the central coastal plain, with concentrations up to 500 mg L⁻¹ in the limestone sediment in the coastal area. The confined aquifer system extends from the Darling Scarp in the east to several kilometres offshore in the west and has been investigated to a depth of more than 1100 m (Davidson, 1995). Five confined or semi-confined aquifers have been identified. Water in these aquifers is considerably different in quality to the superficial aquifer; generally it is lower in colour, as well as containing much lower sulphide concentrations (Davidson, 1995).

1.3. Natural Organic Matter

Natural organic matter (NOM) in source waters originates from the degradation and leaching of organic detritus within the watershed and the introduction of organic compounds from human activity, and is transported by streams and groundwater flow (Croué, 2004). The chemical characteristics of aquatic NOM are not only influenced by the source materials, but also by the biogeochemical processes involved in carbon cycling within the terrestrial and aquatic systems (Croué *et al.*, 1999). NOM may control the mobilities of trace metals (Cabaniss and Shuman, 1988) and hydrophobic organic

compounds (Murphy *et al.*, 1990), as well as the aggregation kinetics of colloidal particles (Liang and Morgan, 1990). Moreover, NOM plays an important role in a wide range of photochemical reactions (Gao and Zepp, 1998), and serves as a source of organic carbon for microorganisms (Hunt *et al.*, 2000). The reactivity of NOM is closely tied to its physicochemical properties such as molecular weight (MW), aromaticity, elemental composition, and functional group content (Cabaniss *et al.*, 2000). NOM in source waters also significantly affects many aspects of water treatment processes, including the performance of unit processes (*i.e.* oxidation, coagulation and adsorption), application of disinfectants and biological stability (Matilainen *et al.*, 2002). As a result, NOM acts upon potable water quality by contributing to disinfection by-products, biological regrowth in the distribution system, colour, taste and odour (Owen *et al.*, 1995). Various water treatment processes can either directly or indirectly, and to varying degrees, remove aquatic organic matter from raw water, depending on their operational conditions and the specific characteristics of the NOM, such as MW distribution, carboxylic acidity and humic substance content (Collins *et al.*, 1985). High MW NOM is more amenable to removal than low MW NOM while NOM with the highest carboxylic acidity, and hence charge density, is generally more difficult to remove by conventional treatment (Collins *et al.*, 1986) but should be removed by ion exchange processes such as the magnetic ion exchange (MIEX[®]) resin process (Singer and Bilyk, 2002, Warton *et al.*, 2007). Water with high MW humic material (5 000-10 000 Da) is a good candidate for chemical coagulation (Amy *et al.*, 1992), while low MW species are reportedly more amenable to adsorption processes (McCreary and Snoeyink, 1980).

The term NOM encompasses all organic matter in the watershed, that is, insoluble particulate matter such as microorganisms, bacteria and colloidal material, as well as dissolved organic carbon (DOC) (Thurman, 1985). DOC is an operationally defined term and includes all organic material able to pass through a 0.45 µm membrane (Clesceri *et al.*, 1998), while Amy (1993) has stated that approximately 90 % of NOM is present as DOC. The DOC

fraction of NOM can be further divided into humic and non-humic substances (Thurman, 1985), with the humic fraction typically accounting for approximately 50 % of the DOC in water but can contribute as much as 90 % in highly coloured sources (Croué *et al.*, 1999). For most natural waters, the remaining 50% of DOC is divided between hydrophilic acids, contributing approximately 30 % of the DOC, with the remaining 20 % present as identifiable compounds (Thurman, 1985).

The humic fraction of DOC is further divided into humic and fulvic acids classified depending on their solubility in acid. Fulvic acids are soluble at any pH while humic acids are insoluble below a pH of 1 (Thurman and Malcolm, 1981, Thurman, 1985, Malcolm, 1990). The humic acid fraction contributes only 10-20 % of the total DOC (Thurman, 1985). Generally, humic acids are less soluble due partly to the higher average MW, ranging from 1 000-10 000 Da (Malcolm, 1990), and low carboxylic acid content, from 3.5-4.5 mM g⁻¹ (Thurman, 1985). Fulvic acids reportedly comprise 80-90 % of the humic fraction and are more soluble, due partly to the lower average MW of 600-1 000 Da (Malcolm, 1990) and greater carboxylic acid content, 5-6 mM g⁻¹ (Thurman, 1985). It has been proposed by Leenheer (1981) that the hydrophilic acids are a mixture of organic compounds that are both simple organic acids, as well as complex polyelectrolytic acids containing many hydroxyl and carboxylic acid functional groups. The remaining 20 % of organic matter consists of compounds of much simpler structures including proteins, peptides, lipids, carbohydrates, carboxylic acids, amino acids, hydrocarbons, fats and other low molecular weight organic molecules (Thurman, 1985).

1.4. Treatment of Groundwater in Perth

Scheme water supplying the Perth metropolitan area is derived from six groundwater treatment plants (GWTPs), located at Wanneroo, Mirrabooka, Neerabup, Gwelup and Lexia, north of Perth, and Jandakot in the south (Figure 1.1), as well as surface water sources and seawater desalination. The variety of sources and the mixing of groundwater from such a large

number of bores at the treatment plants results in a complex system to supply the population of Perth with potable water. Water at the GWTPs is usually a blend of different quality sources (both confined and unconfined groundwater) mixed to obtain a relatively stable composition product, which, upon treatment, will produce water meeting current drinking water guidelines (NH&MRC, 1996). By constantly changing the bores used to produce this water blend, the water resources of the region are managed so as not to exhaust supplies, while still supplying high quality treated water. While the major water quality parameters remain relatively constant, the specific nature of these components, especially the NOM present, will be constantly changing and this can have downstream implications.

1.4.1. Treatment of Groundwater at the Wanneroo Groundwater Treatment Plant

The Wanneroo GWTP is the largest plant supplying the city of Perth, capable of producing 225 ML of water per day (ML d^{-1}). Water from up to 50 unconfined and confined bores is used in the raw water blend. Water entering the Wanneroo GWTP is usually high in iron and DOC, with the plant optimised to remove iron, turbidity and DOC. During the summer months, raw water is often of a lower quality as water from an increased number of bores must be used in order to meet seasonal demand. Until June 2001, treatment at the Wanneroo GWTP involved spray aeration to oxidise iron, sulphide and DOC, and to remove volatile components, coagulation with aluminium sulfate (alum) and a high MW anionic polyacrylamide polyelectrolyte to aid in flocculation, with sedimentation to remove NOM and turbidity, rapid sand filtration for removal of particulates and final disinfection.

Water distributed from the Wanneroo GWTP was hampered for many years by the production of an intermittent 'swampy' odour, identified by researchers at Curtin University of Technology as being caused by the presence of dimethyltrisulfide (DMTS) (Wajon *et al.*, 1986, Heitz *et al.*, 2000, Heitz, 2002). The researchers found that the problem was most pronounced at the extremities of the distribution system where free chlorine concentrations

were at their lowest. Early in the investigation, the mechanism of DMTS formation was unclear, but the problem was found to be controlled by maintaining adequate chlorine residuals in the distribution system. Wajon *et al.* (1986) demonstrated that free chlorine residuals of greater than 0.35 mg L^{-1} at the outlet of the Wanneroo GWTP decreased numbers of complaints by up to 90 %. It was later discovered by Heitz and co-workers (2000) that reactions occurring in pipewall biofilms in the distribution system played an important role in the formation of DMTS. A pool of reduced sulfur, potentially important in swampy odour formation, was found to be provided by microbial sulfate-reducing and sulfur-reducing mechanisms occurring in pipewall biofilms. The pipewall biofilm was also found to absorb organic and inorganic polysulfides and acted as a protective barrier against oxidative attack by chlorine and dissolved oxygen in the bulk water, aiding in the formation of DMTS. While the actual mechanism of DMTS formation is still not yet known, it is clear that reactions in the biofilm and chlorine residuals play an important role (Heitz *et al.*, 2000). As well as controlling chlorine residuals, it was thought that reducing the DOC content of water emanating from the Wanneroo GWTP may reduce biofilm formation in the distribution system and eliminate or reduce the occurrence of DMTS outbreaks (Franzmann *et al.*, 2001, Heitz *et al.*, 2002).

In order to achieve this reduction in DOC concentration, in June 2001, the world's first full scale magnetic ion exchange (MIEX[®]) treatment facility was integrated into the existing process at the Wanneroo GWTP. The MIEX[®] plant has a maximum capacity of 112 ML d^{-1} , half of the capacity of the overall plant. The current treatment scheme at the Wanneroo GWTP is shown in Figure 1.2. The current treatment scheme has two process trains, capable of running simultaneously if demand is sufficiently high, with water exiting the aeration pits either fed to the MIEX[®]-coagulation treatment stream or the enhanced coagulation stream or both. After treatment, these two streams are combined and fed to the 'clearwater' tank for final disinfection and distribution.

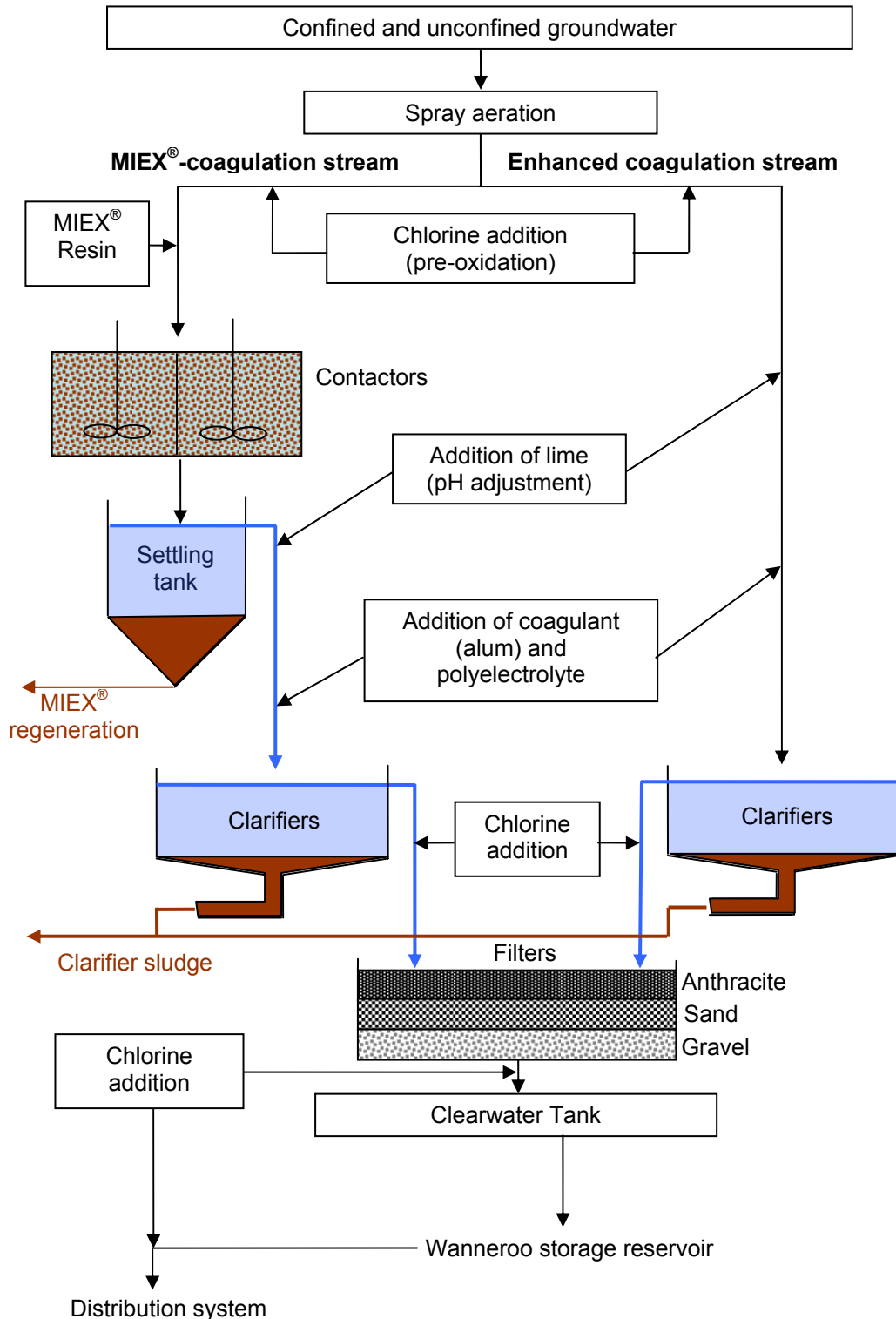


Figure 1.2 Flow chart of the Wanneroo GWTP treatment scheme.

In the MIEX[®]-coagulation stream (Figure 1.2), following aeration, chlorine (3-5 mg L⁻¹) is added for the oxidation of iron (II) to iron (III). Upon entering the contactors, water and the MIEX[®] resin (30 mL L⁻¹) are mixed for 10

minutes, and the slurry transferred to the settling tanks. The magnetic properties of the resin cause high settling rates, and resin recoveries of greater than 99.9 % are reported to be achieved in MIEX[®] processes (Morran *et al.*, 1996). Following separation of the resin and water, 90 % of the used resin is returned to the contactors for continued treatment, with the remaining 10 % sent to a regeneration process. The continuous treatment capability of the process makes the MIEX[®] resin an attractive treatment option. In the regeneration tank, a concentrated brine solution is used to displace DOC on the resin with chloride ions. The regenerated resin slurry is then pumped back to the contactor. Fresh virgin resin is added to make up for the resin lost or degraded during the process. Water leaving the MIEX[®] treatment process then passes to clarifiers where alum is dosed at between 40 and 50 mg L⁻¹. A high MW anionic polyacrylamide polyelectrolyte is also added at approximately 0.6 mg L⁻¹ to aid in the flocculation process. The clarifiers typically operate at an upflow velocity of 3.5 m h⁻¹. Water exiting from the clarifiers is combined with water that has been treated in the enhanced coagulation-only treatment train.

Enhanced coagulation is generally used to describe a coagulation treatment where an increased coagulant dose is employed and the pH has been optimised for maximum DOC removal (Edzwald and Tobiason, 1999). At the Wanneroo GWTP, on the enhanced coagulation side of the plant, the alum dose from the original coagulation process was increased, without pH optimisation, to increase the removal of DOC, and the process was locally termed 'enhanced' coagulation. This term will also be used in this Thesis to refer to this treatment stream at the Wanneroo GWTP. In this stream, water leaving the aeration pits is chlorinated (3-5 mg L⁻¹), with alum (90-100 mg L⁻¹) and anionic polyacrylamide polyelectrolyte (0.8 mg L⁻¹) added for clarification of the water. Supernatant water from the clarifiers is then chlorinated and combined with water from the MIEX[®] / coagulation train and the combined water flows through one of twelve concrete filters packed with sand (0.3 m depth, particle size 0.6 mm) and anthracite coal (0.6 m depth, particle size 1.2 mm) at a linear velocity of 15 m h⁻¹. These filters are periodically backwashed with chlorinated water. Water emanating from the filters then

flows to the 'clearwater' tank where it is chlorinated for disinfection (dose: 4-5 mg L⁻¹). From the clearwater tank, water is then pumped to the Wanneroo storage reservoir. During the course of the current study, before reaching the storage reservoir, water extracted from the confined Yarragadee aquifer was introduced at flows of up to 20 ML d⁻¹ to the product water of the Wanneroo GWTP. Since the conclusion of this study, this water from the Yarragadee aquifer is now added to the raw water entering the GWTP and subjected to full treatment. At the reservoir, water is again chlorinated, with the aim to achieve a chlorine residual of approximately 1 mg L⁻¹ at the reservoir outlet, prior to distribution to consumers.

1.4.2. Magnetic Ion Exchange (MIEX[®]) Resin

MIEX[®], an acronym for **M**agnetic **I**on **E**xchange, is an ion exchange resin developed jointly by the Australian Water Quality Centre (AWQC), the CSIRO and Orica Watercare (formally ICI Watercare) more than 15 years ago (Morran *et al.*, 1996). Early work into ion exchange resins for DOC removal was carried out by Bursill and co-workers (1985) and Hine and Bursill (1987). They discovered that certain anion exchange resins, when used in a simple stirred system, were highly effective for the removal of DOC which had previously been found to cause fouling problems when the resin was used in a column setup. Following extensive work over a number of years by the three organisations, a new magnetic anion exchange resin was developed which exhibited excellent properties (Morran *et al.*, 1996). The MIEX[®] resin is a conventional strong base anion exchange resin including quaternary ammonium functional groups, with a polyacrylic macroporous structure, and several unconventional qualities, such as a particle size 2-5 times smaller than conventional resins (180 µm approximate resin diameter) (Slunjski *et al.*, 1999, Slunjski *et al.*, 2000a). This smaller particle size reduces the reliance on slow, intraparticle diffusion that is associated with active sites inside the resin beads and results in increased exchange rates of DOC and the exchangeable ion, chloride, due to an increase in available external area of exchange (Singer and Bilyk, 2002). The major innovation of

the MIEX[®] resin, however, is the incorporation of a magnetic iron oxide into the resin structure (Bourke *et al.*, 1999, Slunjski *et al.*, 1999, Cadee *et al.*, 2000, Singer and Bilyk, 2000). After stirring of the MIEX[®] resin-water mixture is stopped, the fine resin beads rapidly agglomerate into larger, faster settling particles. Cadee *et al.* (2000) reported that the settling rate of these magnetically agglomerated beads was two orders of magnitude higher than that predicted by the Stokes free settling rates of individual resin beads. The result is that conventional upflow settlers can be used for the resin-water separation, with treated water collected as overflow from the settling tanks and the resin collected as a concentrated underflow stream. Greater than 99.9 % of the resin was found to be recovered at extremely high settler rise rates of 10 m h⁻¹ (Cadee *et al.*, 2000).

There has been extensive research into the performance of the MIEX[®] resin for removal of DOC in drinking water. Much of this work dates back to the late 1980s and early 1990s during the process development phase; however, a large percentage of this work remained confidential for extended periods of time due to pending patents that have since been taken out on this product. It was not until midway through the 1990s that research became available detailing the MIEX[®] resin performance characteristics. One of the first reports of the on the MIEX[®] process was by Morran *et al.* (1996) who reported the use of MIEX[®] for the removal of NOM in a pilot plant. These researchers illustrated that the resin had several desirable features, both from an operational and treatment perspective. Firstly, they demonstrated that the 'open packed' resin structure and high void volume allowed the resin to be pumped in slurry form throughout the plant, for convenient addition to untreated water. By adding the resin as a suspension, the dose of MIEX[®] resin could be adjusted to achieve target DOC removal. This was demonstrated by constantly changing the inlet water DOC levels to simulate changes in raw water quality normally experienced in a GWTP. The researchers found that, by simply increasing or decreasing the amount of resin in the system, target DOC levels could be obtained within one hour from the time of change. This rapid change in removal was attributed to the small particle size of the resin allowing for rapid sorption rates. It was

concluded that this could result in smaller plant sizes and/or reduced contact times (Morran *et al.*, 1996). The magnetic component of the resin was also found to facilitate particle agglomeration and rapid settling, assisting recovery of the resin. This property of the resin was reported to allow it to be used in a continuous, rather than batch or column, process. Another feature allowing it to be used in a continuous process was its high capacity for sorption of organic compounds. This resulted in more than 90 % of the resin being able to be returned directly to the contactor, representing an average of ten cycles for the resin before the need for regeneration. The speed of the regeneration process was also found to be a desirable feature, with only a small volume of sodium chloride required for fast exchange of anions, which reportedly allowed a decreased total resin inventory for the process (Morran *et al.*, 1996).

Morran *et al.* (1997) also noted the capability of the MIEX[®] resin to reduce the trihalomethane formation potential (THMFP) over a 7 day period of treated waters. Four waters from different Australian sources were compared, and total THMs after 7 days were found to be reduced to levels below the World Health Organisation (WHO) limit of 250 $\mu\text{g L}^{-1}$ (World Health Organisation, 2004) by employing regenerated MIEX[®] resin treatment. There have been a number of published reports (Singer and Bilyk, 2002, Drikas *et al.*, 2003, Fearing *et al.*, 2004, Boyer and Singer, 2005) that have found similar benefits through the use of MIEX[®] resin for treatment of raw waters with various initial DOC concentrations. Drikas and co-workers (2003) demonstrated that regenerated MIEX[®] treatment of waters with moderate (5.8 mg L^{-1}) and high (10 mg L^{-1}) DOC concentrations reduced total THM concentrations, measured over 7 days, by greater than 75 % for the moderate DOC water and almost 80 % for the high DOC water. Combining MIEX[®] and conventional coagulation with alum further reduced THM levels, as well as resulting in improvements to the overall water quality. Parameters used to gauge water quality were DOC concentration, UV absorbance at 254 nm, specific UV absorbance (SUVA, defined as the UV absorption in m^{-1} divided by the DOC concentration in mg L^{-1}) and colour.

All of these measured parameters were lower after combined treatment with MIEX[®] and alum than after only alum coagulation (Drikas *et al.*, 2003). Singer and Bilyk (2002) reported similar results to those of Drikas *et al.* (2003) in an examination of, the removal of DOC and UV absorbing species, as well as bromide, by both MIEX[®] treatment and MIEX[®] in series with alum coagulation treatment using virgin MIEX[®] resin. In their study, nine water samples were chosen with varying levels of DOC and alkalinity, measured as equivalent mg L⁻¹ concentrations of calcium carbonate. These samples were chosen to fit the United States Environmental Protection Agency (USEPA) enhanced coagulation matrix which sets minimum removal percentages of DOC for waters fitting a certain cell on the matrix. MIEX[®] resin as a pre-treatment for alum coagulation was found to significantly increase removal of DOC when compared to only alum coagulation. It was also found that, with MIEX[®] pre-treatment, the doses of alum could be significantly reduced to obtain similar turbidity levels to those obtained without a MIEX[®] pre-treatment. A greater than 50 % reduction in bromide concentrations of waters following contact with virgin MIEX[®] resin was also found. For raw water with low initial alkalinity ($\leq 20 \text{ mg L}^{-1}$ as CaCO₃), bromide levels were reduced to less than 10 $\mu\text{g L}^{-1}$ after treatment with virgin MIEX[®] resin from initial levels in the raw water of 160 $\mu\text{g L}^{-1}$. It was thought that as the alkalinity increased, carbonate and bicarbonate ions competed for the charged sites on the MIEX[®] resin, and were preferentially removed compared to bromide (Singer and Bilyk, 2002). Fearing and co-workers (2004) investigated the effect of MIEX[®] pre-treatment, in conjunction with the use of ferric chloride as a coagulant, on DOC removal and DBP formation, specifically THMs. In their work, they also assessed the impact on of MIEX[®] treatment on particular fractions of NOM. They used XAD-7 and XAD-4 resins to separate NOM in raw and treated waters into fractions identified as a non-acid hydrophilic fraction, a hydrophilic acid fraction, a fulvic acid fraction and a humic acid fraction. The combination of regenerated MIEX[®] resin pre-treatment, followed by coagulation with ferric chloride, was shown to be extremely effective for overall DOC removal from a surface water. A removal of greater than 85 % of the DOC was achieved by MIEX[®] followed

by ferric chloride treatment. The non-acid hydrophilic fraction was the fraction found to be most recalcitrant when conventional coagulation was employed; but, by using MIEX[®] resin as a pre-treatment step, increased removal of this fraction was obtained. MIEX[®] pre-treatment was also shown to increase the removal of the fulvic acid fraction, but was ineffective in increasing the removal of the humic acid and hydrophilic acid fractions. In regard to total THMFP, MIEX[®] plus ferric chloride treatment was able to reduce by 50 % the concentrations observed when compared to a single ferric chloride coagulation treatment (Fearing *et al.*, 2004). Boyer and Singer (2005) expanded on this approach by investigating the effect on haloacetic acid (HAA) formation in potable water of a virgin MIEX[®] resin/alum sequence, compared to virgin MIEX[®] resin treatment only, and alum treatment only. Here, it was shown that treating the water with only MIEX[®] resin decreased the formation of total HAAs by up to 70 % when compared to alum coagulation only. Surprisingly, combining MIEX[®] and alum treatment did not further reduce the total HAA formation potential achieved by only MIEX[®] resin treatment (Boyer and Singer, 2005).

Combining MIEX[®] treatment with a turbidity removal step, such as coagulation with ferric or aluminium salts is necessary, as MIEX[®] will only remove the dissolved component of raw waters (Singer and Bilyk, 2000, Bourke *et al.*, 2001, Pelekani *et al.*, 2001). Bourke *et al.* (2001) investigated using regenerated MIEX[®] resin as a pre-treatment prior to ultrafiltration or microfiltration. It was noted that neither ultrafiltration nor microfiltration removed significant quantities of DOC but were able to adequately control the turbidity. Thus, a combined regenerated MIEX[®] resin/microfiltration process was trialled to see if both DOC and turbidity could be controlled. Combining MIEX[®] pre-treatment with microfiltration was found to control turbidity to desired levels while not damaging the membrane. Membrane fouling was not a problem as, following backwashing, initial flux rates across the membranes could be re-established, and DOC levels were reduced by over 50 % compared to the raw water throughout the period of the trial (Bourke *et al.*, 2001).

The research into MIEX[®] resin performance described above was carried out on relatively small volumes of water on a laboratory scale, pilot scale or small operating scale (2 ML d⁻¹). There have been a number of studies of water quality from pilot scale studies of MIEX[®] treatment of Wanneroo GWTP water and MIEX[®] plus alum coagulation treatment on a pilot scale (Bourke *et al.*, 1999, Cadee *et al.*, 2000, Slunjski *et al.*, 2000b) as well as studies of the world's first full-scale MIEX[®] treatment plant and combined MIEX[®] and alum coagulation stream at the Wanneroo GWTP (Smith *et al.*, 2001, Smith *et al.*, 2003). The most extensive study on the performance of the combined processes, however, was carried out by Warton and co-workers (2005, 2007), who examined the water quality at various stages within the Wanneroo GWTP in typical summer and winter periods. This research was the first of its kind, and studied the performance of MIEX[®] treatment, both as a single treatment step and in combination with alum coagulation, as well as the enhanced coagulation stream at the Wanneroo GWTP. Further, the combined MIEX[®]/alum coagulation treatment stream was compared with the enhanced coagulation treatment stream in terms of a number of water quality parameters, including THMFP over 7 days, DOC, assimilable organic carbon (AOC) and biodegradable organic carbon (BDOC) concentrations, and specific NOM characteristics, such as MW distribution, assessed by high pressure size exclusion chromatography (HPSEC). Warton *et al.* (2005, 2007) found that, regardless of the characteristics of inlet water in summer and winter periods, DOC concentrations after treatment with MIEX[®]/alum coagulation were almost identical. Similarly, for enhanced coagulation treatment, DOC concentrations after treatment of seasonal raw water blends were virtually the same. During the summer period, the period of highest demand, an inlet DOC concentration of 6.85 mg L⁻¹ was measured. After treatment with the combined MIEX[®]/alum process, 1.65 mg L⁻¹ of DOC remained, compared with 2.25 mg L⁻¹ DOC after the enhanced coagulation treatment. During the winter sampling, an inlet DOC concentration of 4.15 mg L⁻¹ was measured, with treatment using the combined MIEX[®]/alum method resulting in 1.60 mg L⁻¹ DOC remaining, and with enhanced coagulation, 2.15 mg L⁻¹ DOC remained. This indicates that, while the combined treatment was more effective at removing DOC when compared to

enhanced coagulation, there remained a recalcitrant DOC fraction that was not removed by either process. HPSEC analysis with UV₂₅₄ detection was consistent with this idea, with waters from both treatment processes during the summer and winter periods having identical MW characteristics in the UV₂₅₄-active material. Pre-treatment with MIEX[®] was found to increase the efficiency of the coagulation process and enabled the use of lower doses of the coagulant chemicals. Combining MIEX[®] treatment and coagulation also significantly reduced the THMFP and chlorine demand of the product water compared to enhanced coagulation treatment. The only exception to the advantages of combining MIEX[®] treatment and coagulation was an increased AOC concentration, a measure of the bioavailability of the DOC in the water. This parameter increased after the combined treatment compared to enhanced coagulation, however, this was attributed to carryover of excessively high concentrations of the commercial polyelectrolyte used in the coagulation process. Overall, Warton *et al.* (2005, 2007) concluded that the combination of MIEX[®] resin treatment with a coagulation step was an effective treatment option for removal of DOC and for improvement in overall water quality.

1.5. Isolation and Characterisation of Natural Organic Matter

Although some characterisation methods for dissolved aquatic NOM can be applied directly to raw filtered samples, isolation and concentration of NOM are required for many analytical procedures (Croué *et al.*, 1999). Ultraviolet and visible absorbance spectroscopy and fluorescence spectroscopy, liquid chromatography, and organic acidity can be studied in dilute solutions ($\sim 10 \text{ mg C L}^{-1}$), but typically 10-100 mg of solid NOM sample is required for elemental analysis. Solid state ¹³C nuclear magnetic resonance (NMR) spectroscopy, a fundamental technique for characterising NOM, requires amounts in the order of 50 mg or greater of solid NOM sample, while Fourier transform infrared (FTIR) spectroscopy and pyrolysis-gas chromatography-mass spectrometry (Py-GC-MS) require solid isolates of at least 1 mg (Croué *et al.*, 1999).

1.5.1. NOM Isolation Techniques

The method of isolation of a NOM sample plays a major role in determining the properties of the sample. Croué *et al.* (2000) have published a detailed review of currently used methods for the concentration, isolation and fractionation of aquatic NOM. Evaporation of the water at reduced pressure, freeze drying (lyophilisation), membrane partitioning and sorption techniques are used extensively. The practice of direct reduced pressure evaporation and lyophilisation was dismissed as an impractical option by Croué and co-workers (2000), since it is inherently slow at removing large volumes of water, and does not discriminate between NOM and inorganic salt, leaving sample residues with an undesirably high inorganic content. However, if the inorganic salts are removed by other techniques, lyophilisation is perhaps the best method for obtaining solid NOM isolates that have been minimally altered from their dissolved composition (Croué *et al.*, 2000).

The use of membrane techniques such as nanofiltration (NF) and reverse osmosis (RO) are attractive NOM isolation alternatives. Croué *et al.* (2000) noted that several factors were important for the successful application of these techniques, namely, the membrane composition and pore size, the volume concentration factor, and the ionic strength of the sample being treated. According to Croué *et al.* (2000), the advantages of membrane techniques over sorption based techniques are: firstly, that a comparatively large volume of water can be processed in a short period of time; secondly, that the NOM is never subjected to extreme pH values which have the potential to alter its structural properties; and thirdly, that, according to at least one report, membranes seem to be more effective than resin techniques at collecting polysaccharides and polypeptides (Serkiz and Perdue, 1990). The major drawback of membrane concentration is that, similar to evaporation and lyophilisation, the membrane concentration techniques do not remove inorganic salts from the NOM, and, in the case of RO, actually concentrate the inorganic salt component (Serkiz and Perdue, 1990, Sun *et al.*, 1995). Another prospective problem with the use of membranes for NOM concentration is the possibility of membrane fouling by

the NOM. There have been a number of researchers (e.g., Wiesner and Chellam, 1992, DiGiano *et al.*, 1993, Amy and Cho, 1999, Cho *et al.*, 1999, Aoustin *et al.*, 2001) that have reported the sorption of NOM onto membranes, particularly higher MW substances (such as humic materials). If the NOM concentration near the membrane reaches some critical value, a gel-like layer can form, increasing water flux (Chang and Benjamin, 1996, Chang *et al.*, 1998)

An attraction of sorption-based isolation techniques is their ability to simultaneously concentrate, isolate and fractionate NOM (Thurman and Malcolm, 1981). Several sorbents have previously been used for the isolation of NOM. Materials such as iron and aluminium oxides (Levashkevich, 1966, Parfitt *et al.*, 1977, Parfitt and Russell, 1977, Tipping and Cooke, 1982, Dzombak and Morel, 1990) have been used for decades, however, low MW NOM, low polarity NOM and NOM with a small residual negative charge will not be adsorbed by iron or aluminium sorbents (Semmens and Staples, 1986, Sinsabaugh *et al.*, 1986, Korshin *et al.*, 1997a). Also, co-elution of inorganic anions has been problematic with these sorbents (Croué *et al.*, 2000). Activated carbon has also been used for the concentration and isolation of NOM, but only half to two-thirds of the adsorbed NOM could be eluted, and there was some evidence that eluted NOM had been chemically altered (Leenheer, 1984). Presently, the most extensively used sorption-based procedure for isolating NOM is sorption onto non-ionic, macroporous resins, such as the XAD-type resins. Three decades ago, Leenheer and Huffman (1976) proposed using the acrylic ester XAD-8 resin, the crosslinked aromatic polymer XAD-4 resin and anion exchange resins, in a hierarchical fractionation procedure, characterising aquatic NOM components based on their hydrophobic-hydrophilic and acid-base properties. This procedure has been refined several times (Leenheer, 1981, Leenheer and Noyes, 1984, Leenheer, 1997), but still provides the framework for most sorption fractionation procedures.

In any version of this sorption fractionation procedure, the aquatic NOM is separated into two fractions referred to as either humic and non-humic or

hydrophobic and hydrophilic (Leenheer, 1981). The hydrophobic fraction contains material that is sorbed at acidic pH on the XAD-8 resin and desorbed with base, while the hydrophilic fraction is the material that is not sorbed by the XAD-8 resin (Leenheer, 1981). Recovery of material sorbed on the XAD-8 resin is typically greater than 90 % (Croué *et al.*, 2000). The fractionation procedure has been used to obtain another fraction termed the transphilic fraction (Malcolm and MacCarthy, 1992, Croué *et al.*, 1993), where material that is not sorbed on the XAD-8 resin is passed at acidic pH through an XAD-4 resin. Approximately 80 % of material adsorbed on this resin can be desorbed with base and is termed the transphilic fraction (Malcolm and MacCarthy, 1992, Croué *et al.*, 1993). The fractions can be further fractionated with alternative resins to obtain acidic, basic and neutral fractions, but these steps offer diminishing returns with more effort required to collect progressively smaller incremental amounts of NOM (Croué *et al.*, 2000). The obvious advantage of this sorption technique is that the hydrophobic and transphilic fractions collected are free from salts and have been significantly concentrated; however, only about 75 % of the total NOM can be collected and this procedure is very time consuming when compared to membrane techniques (Leenheer, 1981, Croué *et al.*, 2000). The NOM remaining in the water is termed the hydrophilic fraction, and is, as a result of the fractionation procedure, enriched in salts. If this fraction is to be isolated for characterisation, complicated and time consuming procedures such as ion-exchange and precipitation or co-precipitation need to be employed (Croué *et al.*, 2000).

Piccolo *et al.* (2002) and Peuravuori and Pihlaja (2004) proposed an alternative means of isolation of NOM, involving fractionation HPSEC in a preparative mode. The mechanisms of HPSEC separation and operation will be discussed in Section 1.5.3; however, unlike analytical HPSEC, where resolution of chromatograms to obtain accurate and reproducible results is the critical factor, in a preparative mode, recovery of sample mass in a specified time is the most important consideration. SEC, or gel permeation chromatography (GPC) as it is also known, has been used extensively and for a number of decades for the isolation of natural organic components

including biopolymers and proteins (Law, 1969, Barlow *et al.*, 1971, Unger, 1983), however, it was not until Piccolo *et al.* (2002) applied this technique to aquatic humic matter that it was considered as a technique for the isolation of NOM. Unlike analytical HPSEC, where sample volume or mass is minimised, in preparative HPSEC, it is important and often advantageous to apply a much larger sample amount to the column. Although it has been shown that with increasing sample size (volume or mass), the retention volumes of all components and their peak widths increase and resolution will decrease (Mori and Barth, 1999), by increasing the mass of sample introduced onto the column and using higher eluent flow rates, larger amounts of fractionated NOM can be collected. Repeating this procedure several times allows for the collection of NOM separated on the basis of MW. Both Piccolo *et al.* (2002) and Peuravuori and Pihlaja (2004) collected up to 8 fractions for future study. Enough material in each fraction was obtained by repeating the analysis several times and combining corresponding MW fractions for further study. This technique allowed recoveries of greater than 90 % of the NOM (Piccolo *et al.*, 2002, Peuravuori and Pihlaja, 2004). Some of the advantages of using preparative HPSEC to isolate and fractionate aquatic NOM are that extreme pH conditions are not required and labour intensity is low, as automated HPSEC fractionation systems can be used (Peuravuori and Pihlaja, 2004). However, due to the buffers used in HPSEC separation, NOM fractions contain high concentrations of salts. To overcome this issue, dialysis using a MW cut-off of 1000 Da was successfully applied to remove the buffer salts and fractions could be concentrated easily by lyophilisation (Piccolo *et al.*, 2002, Peuravuori and Pihlaja, 2004).

1.5.2. NOM Characterisation Techniques

The size, chemical composition, structure, functional group content and polyelectrolytic characteristics of NOM may vary greatly depending on the origin and age of material (Aiken *et al.*, 1985, Chin *et al.*, 1994). However, because of the complexity of NOM, no single analytical tool can provide definitive structural or functional information about NOM. Rather, as

Schnitzer and Khan (1972) suggested: “significant progress in our knowledge of the chemistry and reactions of humic substances may be possible only by the combined application of a variety of spectroscopic and wet-chemical techniques.” Croué *et al.* (2000) separated NOM characterisation techniques into four tiers depending on the information gained. The first tier techniques address the chemical identities of individual species included in the NOM macromolecules, such as amino acids and carbohydrates. The second tier techniques investigate the nature and abundance of structural units in the NOM molecules, and include techniques such as elemental composition, ^{13}C and ^1H nuclear magnetic resonance (NMR) spectroscopy, Fourier transform infrared (FTIR) spectroscopy, and gas chromatography-mass spectrometry (GC-MS) utilising various forms of sample introduction including thermal degradation (e.g. pyrolysis). Analysis with both Tier 1 and 2 techniques provides chemically specific information; however, these techniques require substantial sample preparation. The third tier of techniques addresses issues related to chemical behaviour of NOM, focussing on its polymeric nature. Techniques to investigate MW, or more correctly molecular size, distribution, acid-base and hydrophobic-hydrophilic properties, and NOM reactivity are included in this group. These types of analyses usually require less sample preparation than either Tier 1 or Tier 2 analyses. Tier 4 analyses comprise techniques not explicitly exploring chemical identities of functional groups or molecules, but measure a spectral signature of NOM *in situ*, such as ultraviolet/visible (UV/vis) absorbance spectroscopy and fluorescence spectroscopy. Due to the simplicity and sensitivity of these latter techniques, sample analysis can be performed without sample concentration or isolation (Croué *et al.*, 2000). In the following sections, techniques from each Tier used in the current study will be described.

1.5.2.1. Tier 1 NOM Characterisation Techniques

No Tier 1 techniques were applied for characterisation of NOM in the current study.

1.5.2.2. Tier 2 NOM Characterisation Techniques

1.5.2.2.1. Elemental Composition

Elemental analysis is generally the first technique applied to the study of NOM (Croué *et al.*, 2000). The elements analysed include carbon, hydrogen, oxygen, nitrogen and sulfur and the fraction of NOM which is not oxidised is referred to as 'ash' and indicates the amount of inorganic species present (Croué *et al.*, 2000). The results of these analyses are usually given in percent by weight and also specific ratios of elements present.

Abbt-Braun and Frimmel (1999) have stated that the higher the carbon to hydrogen ratio, the greater the aromatic content, while a reduction of this ratio indicates a higher degree of aliphatic carbon. The carbon to oxygen ratio indicates the proportion of oxygenated functional groups and, similarly, the nitrogen to carbon ratio indicates the proportion of nitrogenous functional groups, such as proteins.

1.5.2.2.2. Nuclear Magnetic Resonance Spectroscopy

NMR spectroscopy is a powerful technique allowing molecular level structural elucidation (Knicker and Nanny, 1997). The advantages of NMR spectroscopy over many other structural characterisation techniques are that it is non-destructive, can be used to identify individual functional groups and can aid in determining structures of large macromolecules. Humic substances have been studied by NMR since Schnitzer and Barton (1963) applied solution state ^1H NMR spectroscopy to investigate the structural features of humic acids. The development of the Fourier transform NMR spectroscopic technique allowed low concentrations of organic matter to be studied, hence, natural abundance ^{13}C NMR spectra in the liquid state could be investigated (Ernst and Anderson, 1966). Gonzalez-Vila *et al.* (1976) first applied ^{13}C solution state NMR to the study of humic materials. The development of high resolution ^{13}C solid state cross-polarisation magic angle spinning (CPMAS) allowed solid state analysis of complex macromolecules such as NOM. Schafer and Stejskal (1976), Newman *et al.* (1980) and

Hatcher *et al.* (1980) were the first researchers to apply this solid state technique to the study of NOM.

The determination of chemical shifts is the principal application of NMR spectroscopy by which structural information can be obtained (Nanny *et al.*, 1997). For the study of NOM, determination of these chemical shifts allows semi-quantitative and qualitative assignment of carbon and hydrogen (from the study of ^{13}C and ^1H NMR spectroscopy, respectively) bonded to different chemical structures (Nanny *et al.*, 1997). For ^1H solution NMR spectroscopy, chemical shifts of between 1 and 10 ppm are typically obtained. Croué *et al.* (2000) provide chemical shifts from ^1H solution NMR spectroscopy for various chemical linkages in NOM. ^1H Solution NMR spectroscopy was not used in the current study. For ^{13}C NMR spectroscopy, Keeler *et al.* (2006) studied the chemical shifts of various structural features from a humic acid sample. Both solution and solid state ^{13}C NMR spectroscopy produce chemical shifts in the same region of the spectrum, and the differences between solid and liquid state NMR techniques will be discussed below. Typically, five broad regions are investigated in ^{13}C NMR spectroscopy: these are 0-60 ppm (assigned as aliphatic carbon), 60-100 ppm (assigned to carbohydrates or O-aliphatic carbons), 100-165 ppm (assigned to aromatic carbon), 165-190 ppm (assigned to carboxyl carbon), and 190-230 ppm (ketones and aldehydes) (Malcolm, 1990). However, far more information can be obtained from good quality spectra. For example, Croué *et al.* (2000) and Keeler *et al.* (2006) identified far more peaks corresponding to different types of carbons. A broad peak at 20 ppm was due to terminal methyl groups of alkyl chains, while methylene carbons in alkyl chains and polypeptides and methyl groups of acetyl groups attached to aliphatic structures produced a peak at 30 ppm. A peak at ~60 ppm was due to carbon attached to aliphatic alcohols, esters and ethers, while a peak at ~70 ppm was associated with carbonyl carbons of cellulose and hemicellulose. Glucose fragments from carbohydrates produced a peak at ~100 ppm, while a broad signal at 130 ppm was due to aromatic carbon, and a peak at 150 ppm was associated with substituted aromatic carbon, as well as a contribution from O-substituted carbon in aromatic structures. Peaks

centered at ~170 ppm were typically due to carbonyl/carboxyl carbons from structures such as hemicellulose, amides and polypeptides. Peaks at 190 ppm and above were generally due to the presence of ketone functionalities (Croué *et al.*, 2000, Keeler *et al.*, 2006).

For the study of NOM, solid and liquid ^{13}C NMR and solution ^1H NMR spectroscopy can be applied and all three techniques have associated advantages and disadvantages. The use of solution NMR spectroscopy is not as favoured as solid state NMR spectroscopy for several reasons. The first reason is the low solubility of aquatic NOM in NMR solvents and the differential solubility of various components of NOM, resulting in sample fractionation (Malcolm, 1989, Wilson, 1989). In addition, certain chemical shifts of the sample can be obscured by solvent peaks and the solvent can affect the chemical shifts of the sample. More technical problems through the use of solution NMR spectroscopy are the long relaxation times and nuclear Overhauser effect, which relates to variations in the relaxation of different chemical linkages, affecting quantification of peaks. The advantage of solution NMR spectroscopy is a reduction in peak broadening, and hence an increase in peak resolution, due to the natural rotation or 'tumbling' of molecules in solution (Malcolm, 1989). Solid state NMR spectroscopy is limited to the study of the ^{13}C nucleus. The major reason for the limitation on solid state proton NMR spectroscopy is due to problems with line broadening experienced by solid state experiments. For proton NMR spectroscopy, techniques such as CPMAS are not sufficient to reduce line broadening to enable sufficient resolution (Wilson, 1987, 1989). The advantages of ^{13}C solid state NMR spectroscopy for the study of NOM are elimination of the nuclear Overhauser effect, rapid relaxation rates, solubility of samples is not an issue and also samples, which often require extensive separation and isolation procedures, can be recovered in an uncontaminated state (Wilson, 1989). However, there are some important considerations in the use of solid state ^{13}C NMR spectroscopy, including the incomplete cross polarisation of certain carbon atoms in a NOM molecule. This results in some carbon types being underestimated in solid state spectra, typically aromatic carbons,

which results in issues with quantification of the spectra (Alamany *et al.*, 1983, Wilson, 1987, 1989, Knicker and Nanny, 1997).

1.5.2.2.3. Fourier Transform Infrared Spectroscopy

Analysis of pure compounds with FTIR spectroscopy results in complex spectra due to the many absorption bands generated. The analysis of NOM by FTIR spectroscopy, however, produces much simpler spectra as only the strongest absorption bands can be identified, due to the heterogeneous nature of the sample (Croué *et al.*, 2000). FTIR spectroscopy is a technique used to study the molecular structure of a molecule and is based on the absorption of infrared radiation by the vibrational modes of bonded atoms (Bloom and Leenheer, 1989). FTIR spectroscopy is particularly useful for examining the nature of oxygen in organic molecules, as the intensity of absorption is to a great extent a function of the change in dipole moment involved in the vibration. In this regard, FTIR spectroscopy is, in fact, superior to NMR spectroscopy for the analysis of oxygen in NOM as NMR provides only indirect spectral information through the effects of oxygen on ^1H or ^{13}C nuclei (Bloom and Leenheer, 1989).

For FTIR analysis of NOM, several main absorption bands are found. These include a broad band from $3\,600\text{--}2\,400\text{ cm}^{-1}$, characteristic of hydrogen bonded hydroxyl groups or water. Aliphatic C-H stretching typically produces a band at $\sim 2\,900\text{ cm}^{-1}$ and carbonyl stretching of carboxylic acids and ketones produces a strong band at $1\,720\text{ cm}^{-1}$. Aromatic carbon stretching and hydrogen bonded carbonyl groups have a band at $1\,610\text{ cm}^{-1}$, while C-O stretching of carboxylic acids, ethers and esters displays a characteristic peak at $1\,250\text{ cm}^{-1}$ (Stevenson, 1982).

One significant disadvantage of FTIR spectroscopy is that only qualitative information on the structure of NOM can be derived (Bloom and Leenheer, 1989). This is because the various stretching, vibrational and rotational motions which absorb infrared radiation have a wide range of molar absorptivities and the absorptivity of each group in the molecule must be

known for quantitative determination. Another difficulty in quantitative and, in fact, qualitative determinations of functional group type is the overlap of bands from the multiple infrared active groups in NOM. Another issue with FTIR spectroscopy is that samples are typically prepared as KBr discs, and this method may introduce a broad band at $3\ 500\text{-}3\ 300\ \text{cm}^{-1}$ due to the presence of water adsorbed onto the sample from the atmosphere (Bloom and Leenheer, 1989).

1.5.2.2.4. Pyrolysis-Gas Chromatography-Mass Spectrometry

Thermal degradation of NOM, termed pyrolysis, gives specific by-products that can be linked to macromolecules synthesised from natural biopolymers (Croué *et al.*, 2000). Analytical pyrolysis involves rapid heating of a sample at temperatures usually ranging from $300\ ^\circ\text{C}$ to $800\ ^\circ\text{C}$ (Hatcher and Clifford, 1994). Typically, the sample is heated to the target temperature within milliseconds to seconds and this temperature is maintained for up to 20 seconds. Products from the on-line thermal degradation of the NOM sample are trapped on the front of a gas chromatography (GC) column, then separated by GC and identified by mass spectrometry (MS); this technique is termed pyrolysis-GC-MS (Py-GC-MS). While Py-GC-MS cannot be used as a strictly quantitative analytical technique, it can provide a specific fingerprint of a NOM sample (Bracewell *et al.*, 1989).

Pyrolysis followed by GC-MS has been used to differentiate between different humic fractions and to identify some precursors of NOM. For example, Peschel and Wildt (1988) investigated the pyrolysis products of several carbohydrates and proteins and identified a number of characteristic products. They showed that methylfurans, furfural and methyl furfural were always produced from thermal degradation of the selected carbohydrates, while acetonitrile, pyrrole and acetamide were always produced after the proteins were thermally degraded (Peschel and Wildt, 1988). Similarly, Saiz-Jimenez and de Leeuw (1986) identified a range of pyrolysis products from natural products, including lignins, polysaccharides and proteins. Analysis of

the pyrolysis products from several whole soil samples allowed them to identify the portion of each of the described macromolecular groups in their soil samples (Saiz-Jimenez and De Leeuw, 1986). Page *et al.* (2002) used Py-GC-MS to identify organic compounds which may act as markers of terrestrially derived bio-macromolecules in pyrograms. Lignin, chitosan, bovine serum albumin, tannic acid and cellulose were used as models for macromolecular precursors and products from the degradation techniques in turn were linked to each reference macromolecule (Page *et al.*, 2002).

The low yield of compounds analysed upon thermal degradation of NOM is one of the major disadvantages of Py-GC-MS. Often less than 25 % of the NOM is detected as individual compounds (Gaffney *et al.*, 1996). Also, Py-GC-MS suffers from several serious limitations that need to be considered when interpreting results. Secondary reactions can occur between pyrolysis products and reactive intermediates, and the resultant compounds identified may not always directly represent moieties in the original macromolecule (Saiz-Jimenez, 1994). According to Saiz-Jimenez (1994), one of the most intriguing facts in NOM structural characterisation is the presence of aromatic structures containing carboxylic acids often found by other methods, such as chemical oxidation and NMR spectroscopic studies, but which are not observed in thermal degradation analysis. In Py-GC-MS, carboxylic acid moieties were found to be converted to carbon dioxide, which is often also present as a contaminant due to gas leaks in the GC-MS system, making estimations of carboxylic acid content difficult (Saiz-Jimenez, 1994).

1.5.2.3. Tier 3 NOM Characterisation Techniques

A detailed discussion of HPSEC is presented in Section 1.5.3.

1.5.2.4. Tier 4 NOM Characterisation Techniques

The absorption of both ultraviolet (UV) and visible (vis) light at $\lambda > \sim 230$ nm by surface waters and groundwaters is widely attributed to the aromatic chromophores present in aquatic NOM (Christman *et al.*, 1989, Chin *et al.*, 1994). One of the disadvantages of using UV/vis spectroscopy for studying NOM is that the spectra are typically broad and nearly featureless (Wang *et al.*, 1990). As a result, information gained from UV/vis spectroscopy for the study of NOM has often been limited to monitoring the absorbance at 253.7 nm (usually quoted as 254 nm) or higher wavelengths, such as 400 nm (Clesceri *et al.*, 1998). The absorbance at 254 nm has been attributed to aromatic moieties, while the absorbance at 400 nm measures the 'colour' of the sample, possibly due to quinone like structures and conjugated ketonic C=O structures (Stevenson, 1982). A parameter, termed the E_4/E_6 ratio, is also used: it is defined as the ratio of the absorbance at 465 nm to the absorbance at 665 nm (Stevenson, 1982). Chen *et al.* (1977) showed that the E_4/E_6 ratio decreased with increasing MW and condensation and proposed that it may serve as an index of humification. A low E_4/E_6 ratio may be indicative of a relatively high degree of condensation of aromatic constituents, and a high ratio may reflect a low degree of aromatic condensation and imply the presence of relatively more aliphatic structures (Chen *et al.*, 1977). Similarly, the specific UV absorbance (SUVA) at 254 nm, a measure of the UV absorbance at 254 nm per mg of DOC in 1 L of sample, is an indication of the aromatic, hydrophobic character of NOM (Traina *et al.*, 1990, Novak *et al.*, 1992).

While the UV/vis spectra are typically broad and nearly featureless, in theory, the spectrum could be deconvoluted into separated spectra which are the result of distinct chromophores. However, this is effectively impossible as the number of individual chromophores is high, their concentrations are unknown and none of the chromophores possess a unique and easily distinguishable absorption spectrum (Korshin *et al.*, 1997b). This has meant the potential of UV spectroscopy has largely not been investigated. Korshin

et al. (1996, 1997b), as an alternative to simply measuring individual wavelengths, has proposed modelling the UV absorbance spectrum of NOM as a composite of three absorption bands, representing certain electronic transitions in aromatic chromophores in NOM molecules. These transitions were based on known electronic transitions of benzene and termed the local excitation, benzoid and electron transfer transitions which have peaks at 180, 203 and 253 nm respectively. The three model spectra can be superimposed on the UV spectra of NOM and when summed, closely resemble the experimental spectra. Modelling these transition has shown that their relative intensities provide useful information about the structural features of NOM as well as providing information on NOM reactions (Korshin *et al.*, 1996, Korshin *et al.*, 1997b).

1.5.3. Size Exclusion Chromatography

The MW or molecular size plays a critical role in determining the mechanical, bulk and solution properties of polymeric material (Mori and Barth, 1999). Compared to small organic molecules, which have discrete, well-defined MWs, organic macromolecules can be comprised of hundreds or thousands of chains of varying MWs, so the MW distribution is also an important factor controlling the properties of polymers (Mori and Barth, 1999). Synthetic polymers do have a distinctive MW distribution depending on the polymerisation mechanism, kinetics and conditions applied during their formation (Yau *et al.*, 1979). Conversely, natural polymers and macromolecules, such as lignins, polysaccharides and humic substances, can have characteristic MWs, depending on their source, histories and method of isolation (Yau *et al.*, 1979).

The MW distribution of aquatic NOM is an important consideration in drinking water treatment process operations for several reasons. For example, previous research has demonstrated that low MW NOM components decrease the efficiency of treatment with activated carbon because they compete for adsorption sites with target compounds (Newcombe *et al.*, 1997). The low MW components are also thought to comprise the fraction

that is the most difficult to remove using conventional coagulation treatment (Chow *et al.*, 1999, Drikas *et al.*, 2003). Certain fractions of NOM have also been shown to be significant factors in the fouling of membranes used in drinking water treatment (Aoustin *et al.*, 2001). Some studies have shown that the low MW fractions contribute disproportionately to bioavailable organic matter (BOM), and therefore promote biofilm formation in drinking water distribution systems (Volk *et al.*, 2000, Hem and Efraimsen, 2001). Knowledge of changes in the MW distribution of NOM during water treatment is therefore of considerable interest to the water industry, and substantial efforts have been made to develop techniques to identify the MW distribution of organic matter present in a water sample.

A variety of techniques have been used to characterise MW distribution, including analytical ultrafiltration (Buffle *et al.*, 1978), field flow fractionation (Giddings *et al.*, 1987) and vapour pressure osmometry (Figini and Marx-Figini, 1981). Disadvantages of these techniques are that, while the MW can be determined, statistical averages cannot be calculated. In the case of field flow fractionation, instrumentation is often complex, analysis time long and sample preparation extensive. MW averages can also be measured independently by physical methods, such as boiling point elevation, freezing point depression, membrane osmometry, vapour pressure osmometry and light scattering. A major limitation of these techniques is that the overall shape of the MW distribution remains unknown (Mori and Barth, 1999). Hence, two macromolecular samples may have the same average MWs but completely different MW distributions. The most popular, and by far the most convenient, method of determining average MWs and MW distributions is HPSEC. This technique allows the determination of MW distributions and all the statistical averages in a relatively short time period with little sample volume or sample preparation.

For soluble macromolecular material, the MW distribution can be determined using chromatography on a porous gel or resin using a suitable detection system. In HPSEC, the high MW compounds are excluded from the resin and elute first, while smaller species are able to permeate the pore space of

the resin and thereby progress through the column more slowly and elute later. To define the MW distribution of a polymer or macromolecular material, statistical averages of the distribution are calculated. These parameters include the number averaged MW (M_n ; the weight of 'average' molecules in the mixture), weight averaged MW (M_w ; weight of the molecule to which the 'average' atom belongs) and polydispersity (ρ), calculated as shown below:

$$M_n = \frac{\sum_{i=1}^N h_i}{\sum_{i=1}^N \frac{h_i}{M_i}} \quad 1.1$$

$$M_w = \frac{\sum_{i=1}^N h_i (M_i)}{\sum_{i=1}^N h_i} \quad 1.2$$

$$\rho = \frac{M_w}{M_n} \quad 1.3$$

where h_i is the height of the sample HPSEC curve eluted at volume i and M_i is the molecular weight of the i th volume (Chin *et al.*, 1994). For a pure substance having a single MW, M_n will be equal to M_w and $\rho = 1$; whereas for a mixture of molecules, $M_n < M_w$ and $\rho > 1$ (Zhou *et al.*, 2000).

1.5.3.1. Mechanisms of Size Exclusion Chromatography Separation

SEC is an attractive option for determining the MW distribution of organic polymers and macromolecular samples due to the ease of operation, simplicity of sample preparation and requirement of minimal sample volumes. SEC separates predominantly on the basis of molecular hydrodynamic volume or size, rather than by enthalpic interactions with the stationary phase, as is the case with other modes of liquid chromatography, such as adsorption, partition, or ion-exchange (Mori and Barth, 1999). In SEC, as a mixture of solutes of different size pass through a column packed with porous particles, the molecules that are too large to penetrate the pores

of the packing material elute first, passing straight through the column. Smaller molecules that can penetrate or diffuse into the pores, elute at a later time or elution volume, depending on the degree of permeation into the pore space of the resin phase. Thus, a sample is separated or fractionated by molecular size, the profile of which describes the MW distribution or size distribution of the sample (Mori and Barth, 1999). If the SEC system is calibrated with a series of compounds with known MW, a relationship between MW and elution volume can be obtained. This relationship can then be used as a calibration curve to determine the MW distribution of a sample.

Following injection of a sample containing a mixture of different sized molecules, those which are too large to penetrate the pores of the stationary phase elute first within the interstitial or void volume (V_0) of the column, i.e., the volume of the mobile phase that is located between the particles of the stationary phase (Mori and Barth, 1999). Smaller solutes approaching the average pore size of the stationary phase penetrate or partition into the pores of the stationary phase and elute at a longer elution time. Solute with a molecular size which is relatively small with respect to the pore size will freely diffuse into the pores, sampling the total pore volume of the stationary phase (V_i). The elution volume of small solutes will be equal to the total mobile phase volume or permeation volume (V_p) of the packed SEC column:

$$V_p = V_0 + V_i \quad 1.4$$

The chromatographic behaviour of the solutes separated by HPSEC can be described by the general chromatographic equation:

$$V_e = V_0 + K_{SEC} V_i \quad 1.5$$

where V_e is the elution volume of a solute and K_{SEC} is the SEC distribution coefficient. K_{SEC} is a thermodynamic parameter defined as the ratio of the average concentration of the solute in the pore volume $[c]_i$ to that in the void volume $[c]_0$:

$$K_{SEC} = \frac{[c]_i}{[c]_0} \quad 1.6$$

From equation 1.4 and equation 1.5, it is clear that K_{SEC} has defined limits of $0 \leq K_{SEC} \leq 1$. As a result, the product of the void volume and the accessible

pore volume, $K_{SEC}V_i$, governs the retention volume of a sample. If $K_{SEC} > 1$, the separation is controlled by enthalpic interactions which depend on the chemical composition of the solute and not necessarily on its MW. This is a major problem in using SEC to separate aquatic NOM, and it is necessary to reduce the enthalpic interactions as much as possible. Where these effects can not be eliminated, equation 1.5 becomes:

$$V_e = V_0 + K_{SEC} V_i + K_{part} V_s + K_{ads} S \quad 1.7$$

where K_{part} is the partition coefficient, V_s is the volume of the stationary phase, K_{ads} is the adsorption coefficient, and S is the surface area of the packing. If the last two terms of equation 1.7 are zero, then only size exclusion effects are responsible for separation, however, in practice, this is virtually impossible to achieve due to the complex nature of aquatic NOM and the presence of charged regions in the stationary phase. Therefore, K_{SEC} can be defined by:

$$K_{SEC} = K_D K_p \quad 1.8$$

where K_D is the distribution coefficient for pure size exclusion and K_p is the distribution coefficient for solute-stationary phase interaction effects (Mori and Barth, 1999).

There have been a number of mechanisms used to describe SEC including geometric considerations (Ogston, 1958, Laurent and Killander, 1964, Squire, 1964, Casassa, 1967, Giddings *et al.*, 1968, Casassa, 1971, van Kreveld and van Den Hoed, 1973, Hager, 1980, Kubin and Vozka, 1980), restricted diffusion (Smith and Kollmansberger, 1965, Yau and Malone, 1967, DiMarzio and Guttman, 1969), separation by flow (Cheng, 1986), and thermodynamic models (Chang, 1968, Yau *et al.*, 1968a, Yau *et al.*, 1968b, Dawkins, 1976, Kopaciewicz and Regnier, 1982). The geometric approach and thermodynamic model appear to be the most useful to users as they offer the clearest and most practical explanation (Mori and Barth, 1999).

1.5.3.1.1. Geometric Models for Size Exclusion Chromatography Separation

The simplest method to describe the mechanism by which SEC separates molecules of various sizes is by using geometric considerations. These approaches assume either conical (Figure 1.3a) or cylindrical (Figure 1.3b) pore openings (Mori and Barth, 1999). Although pore structures of SEC stationary phases are more complex than these models and enthalpic interactions between stationary phase and solutes are impossible to eliminate, the two models offer useful insights into the separation process. In exploring these models, one has to bear in mind that they only take into account spherically shaped molecules (Yau *et al.*, 1979).

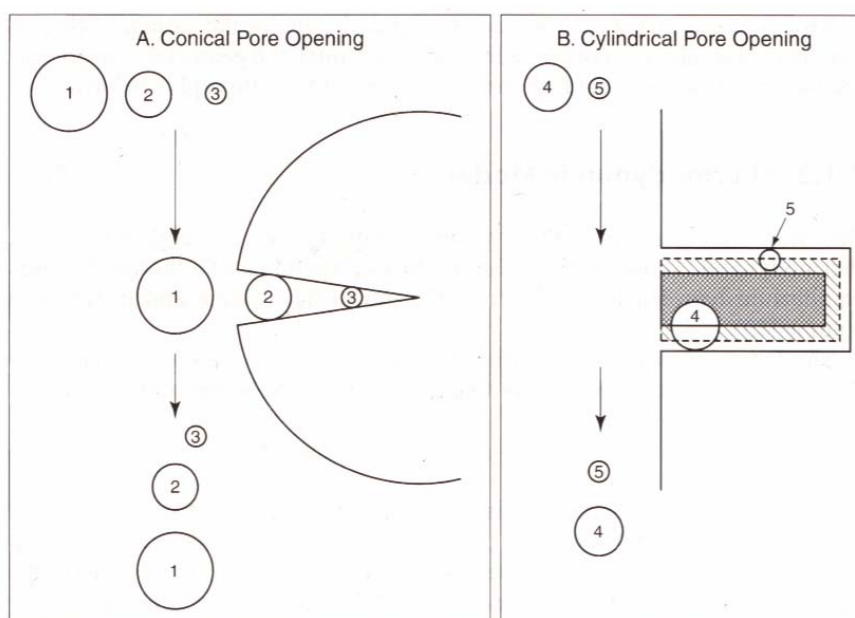


Figure 1.3 Geometric models: a) conical-pore opening, b) cylindrical pore opening (taken from Mori and Barth, 1999).

The conical model, first proposed by Porath (1963) assumes the pores of the stationary phase narrow with increasing depth. Spherical molecules penetrate the pores to certain depths depending on the ratio of the molecule diameter to pore diameter (Mori and Barth, 1999). In Figure 1.3a, molecules (1) with diameters larger than that of the pore cannot penetrate the pore and are totally excluded from the pore structure. These large molecules pass through the column without being impeded, and elute at V_0 . An intermediate molecule (2) can penetrate into the pore structure until it reaches a diameter

comparable to its own. Such molecules are slightly impeded and elute at various points between V_o and V_p , depending on their molecular diameters. The smallest molecules can reach deep into the pore structure and penetrate almost the entire pore volume. Such molecules are retained to the greatest extent and elute latest, at or close to V_p , again depending on their molecular diameter. Thus, for this simplified example, the molecules elute in order of decreasing molecular diameter, i.e. 1, 2 then 3 (Mori and Barth, 1999). This model is obviously a simplified version of what actually takes place inside the stationary phase of a SEC column. Interactions between the stationary phase and solutes are not taken into account and, the model assumes that at any point in time only one molecule can be positioned inside a single pore of the stationary phase.

The cylindrical pore model is an improvement on the conical pore model (Mori and Barth, 1999). However, this model still assumes that there is no interaction between the stationary phase and the solute affecting V_e . The cylindrical pore model assumes a constant diameter throughout the inside of the pore (Mori and Barth, 1999). The accessible pore volume is limited to the radius of the molecule from the pore wall: Giddings *et al.* (1968) and Kubin and Vozka (1980) described this phenomenon as the wall or excluded volume effect. This is shown in Figure 1.3b, where the larger molecule (4) is able to access a smaller amount (the cross shaded area surrounded by a solid line) of the pore volume when compared to the smaller molecule (5) (diagonally shaded area surrounded by a dotted line), and so elutes earlier from the column (Mori and Barth, 1999). The cylindrical model, while still not able to fully define the separation process, provides a better method of describing the separation mechanism of SEC. Here, a number of molecules are able to both enter and exit the pore volume at any point in time. However, because the pore structures of the stationary phases and the molecular conformation of polymer molecules cannot be defined with certainty, both the conical and cylindrical pore models are useful, but only provide a simplified picture of SEC behaviour (Mori and Barth, 1999).

1.5.3.1.2. Thermodynamic Model for Size Exclusion Chromatography Separation

The more widely accepted, and more realistic, approach to conceptualising SEC is based on thermodynamic considerations. It invokes the establishment of a thermodynamic equilibrium between the solute in the void volume and the solute in the pore volume, as described by Dawkins (1976), Yau *et al.* (1979) and Mori and Barth (1999). In Section 1.5.3.1 the general chromatographic equation for the separation of solutes by SEC was shown to be:

$$V_e = V_0 + K_{SEC} V_i \quad 1.5$$

The standard free energy change, ΔG° , for the transfer of solute molecules from the mobile phase to the stationary phase is related to K_{SEC} by (Dawkins, 1976):

$$\Delta G^\circ = kT \ln K_{SEC} \quad 1.9$$

where k is the Boltzmann's constant and T is temperature. Also, the standard free energy change depends on the standard enthalpy change, ΔH° , and the standard entropy change, ΔS° , as follows:

$$\Delta G^\circ = \Delta H^\circ - T\Delta S^\circ \quad 1.10$$

Thus, combining equations 1.9 and equation 1.10 gives:

$$K_{SEC} = \exp\left(\frac{-\Delta H^\circ}{kT}\right) \times \exp\left(\frac{\Delta S^\circ}{k}\right) \quad 1.11$$

At ideal SEC conditions, ΔH° is equal to zero and there are no enthalpic interactions between the stationary phase and the solute. Thus, equation 1.11 becomes (Dawkins, 1976, Mori and Barth, 1999):

$$K_{SEC} = \exp\frac{\Delta S^\circ}{k} \quad 1.12$$

In reality, this is not the case and ΔH° is usually slightly positive or slightly negative, depending on the overall charge of the stationary phase and the solute molecule (Dawkins, 1976). This results in either adsorption of the solute to the stationary phase surface, when ΔH° is negative, and hence V_e slightly higher than would be expected, or repulsion interactions, when ΔH° is positive, and hence V_e slightly lower than would otherwise be expected.

Since the conformational degrees of freedom of the solute are more restricted inside the pores of the stationary phase, as compared to being in the void volume, the conformational entropy of the solute chain decreases during permeation into the pores. The driving force behind ΔS° arises from the concentration gradient of the solute developed between the void and pore volumes. The loss in conformational entropy when the solute transfers from the mobile phase to within a pore governs SEC separation (Dawkins, 1976).

1.5.3.2. The Application of Size Exclusion Chromatography to NOM

Since Porath and Flodin (1959) first reported the use of Sephadex[®] gels for the separation of glucose from dextrans of various MWs, there have been thousands of published reports on the use of SEC for MW based separations. The large majority of these publications describe the separation of synthetic polymers, desalting of organic samples and isolation of proteins and other natural macromolecules for further study. Application of this technique for determining the MW distribution of naturally occurring organic material began shortly after the Porath and Flodin (1959) report, with Posner (1963) and then Gjessing (1965) reporting the estimation of MWs of humic substances in natural waters.

The first MW determinations of humic material by low pressure SEC were conducted using Sephadex[®] gels (Posner, 1963, Gjessing, 1965). Porath and Flodin (1959) described these gels as 'prepared by cross-linking dextran in such a way that the polysaccharide chains form a macromolecular network of great stability'. The gels had several advantages over previous substrates, such as starch and agar, which had been used for size-based separations but had proved to be of little practical value (Porath and Flodin, 1959). It was found that aqueous solutions filtered rapidly through Sephadex[®] gels at atmospheric pressure, and the gel was not appreciably dissolved in neutral, acidic or basic solutions (Porath and Flodin, 1959). Several different Sephadex[®] gels are available, covering a range of MW

exclusion limits. These exclusion limits, along with calibration with a number of macromolecules of established MW, were used to determine the MW distribution of aquatic NOM. Several researchers (Gjessing, 1965, Gjessing and Lee, 1967, Ghassemi and Christman, 1968, Kemp and Wong, 1974, Ishiwatari *et al.*, 1980, Tuschall and Brezonik, 1980, Davis and Gloor, 1981) used Sephadex[®] gels in low pressure SEC to determine the MW of aquatic NOM, with reported values of between 500 and 2 000 000 Da. It has been shown, however, that the MW distributions of humic substances determined by SEC can be higher than those determined by other methods, due to calibration with standards that are likely to have different molecular dimensions (conformations) than the components of the aquatic NOM being analysed (Schnitzer and Skinner, 1968). In addition, elution volumes of NOM can be both increased and decreased, depending upon interactions between the solute organic material and the stationary phase. Sephadex[®] gels, as well as other stationary phases used for SEC, are known to have a negative charge on the gel surface, which results in an ion exclusion effect on the negatively charged regions known to occur in the structure of aquatic NOM components (Marinsky, 1986). The aromatic character of aquatic NOM can also lead to sorption on the stationary phase (Hatcher *et al.*, 1981). To overcome these phenomena, Gelotte (1960) and Posner (1963) advocated the use of electrolytes in the mobile phase to increase its ionic strength. They found, however, that increasing the ionic strength led to adsorption of certain functionalities within the aquatic NOM to the stationary phase. It was concluded that a fine balance between adsorption and exclusion effects needed to be found. The major disadvantage of using Sephadex[®] in SEC, however, is the weak matrix of the gel, with associated softness, which means it is not able to withstand the higher pressures required for increasing the speed of analysis (Mori and Barth, 1999). This results in the need to use low flow rates and, hence, analysis times of greater than 24 hours. In order to increase the speed of analysis, several new packing materials were developed, including porous glasses or silicates, and soft and rigid organic gels. The advantage of these new packings was their ability to be used under higher pressure, resulting in significantly higher flow rates and, hence, shorter analysis times (Mori and Barth, 1999).

The effect of adsorption and exclusion on the MW distribution of aquatic NOM continues to be a problem, even with the development of superior phases able to be used at high pressure (HPSEC). HPSEC was used exclusively in this thesis and all SEC will be referred to as HPSEC from this point forward. According to Peuravuori and Pihlaja (1997), the choice of eluent, rather than the stationary phase, is the most critical factor in achieving suitable separation of aquatic NOM. Berdén and Berggren (1990) investigated the effect of ionic strength (μ) and eluent pH of the mobile phase on the elution behaviour of a humic substance using a Toyo Soda (now Toyopearl) TSK G2000 SW_{xL} silica-based HPSEC column and the use of polystyrene sulfonates (PSSs) for MW calibration of the column. These researchers found that both parameters strongly affected the retention behaviour of humic substances, and that a high ionic strength and low pH resulted in an increased elution volume. Berdén and Berggren (1990) explained this in terms of exclusion effects from interactions between the sample and stationary phase and also intramolecular interactions of the humic substance. Stevenson (1982) described humic substances as coiled relatively unbranched chains of 2- to 3-dimensionally crosslinked molecules, having ionised carboxylate groups distributed throughout the molecule. Thus, an increase in the ionic strength of the mobile phase would result in a decrease in ion exclusion effects between the sample and stationary phase, due to cationic competition for anionic sites, and a decreased repulsion between different ionic parts of the humic macromolecule. The latter would decrease the hydrodynamic volume of the macromolecule. Both the decreased ion exclusion effects and the decreased hydrodynamic volume of the macromolecule would lead to an increased elution volume. Barth (1980) however, reported that adsorption of the sample to the stationary phase increased with increasing ionic strength and recommended an ionic strength of 0.1 mol L⁻¹ to minimise both exclusion and adsorption effects. Berdén and Berggren (1990) also found that a mobile phase pH of 7 minimised both adsorption and exclusion effects and advocated the use of a mobile phase ionic strength of 0.1 mol L⁻¹. Peuravuori and Pihlaja (1997) further

investigated the effect of mobile phase composition and standards for MW calibration. Here, they argued that a mobile phase consisting of 10 mmol L⁻¹ sodium acetate was superior for the MW separation of aquatic NOM. The researchers compared a number of eluents and demonstrated that a 10 mmol L⁻¹ sodium acetate buffer achieved superior resolution of MW fractions when compared to a number of different concentration phosphate buffers and sodium azide. With regard to MW standards, the researchers employed a slightly different approach to that taken in previous work (Barth, 1980, Beckett *et al.*, 1987, Berdén and Berggren, 1990, Chin and Gschwend, 1991, Chin *et al.*, 1994), using a number of different types of compounds as MW standards. They argued that, while PSSs were relatively similar to humic substances when compared to other available macromolecules, aquatic NOM was more branched and cross-linked, and, thus, they utilised polyethylene glycols (PEGs), as well as a number of proteins and simple organic molecules, for MW calibration (Peuravuori and Pihlaja, 1997).

The choice of standards for MW calibration, as well as statistical methods for calculating MW averages, has been a contentious issue since SEC was first used to study aquatic NOM. Different types of compounds used for calibrating SEC columns include dextrans (Ghassemi and Christman, 1968, Engelhardt and Mathes, 1977), various proteins (Engelhardt and Mathes, 1977, Hashimoto *et al.*, 1978), PEGs (Engelhardt and Mathes, 1977, Plechanov, 1983), polyacrylic acids (Thurman *et al.*, 1982), PSSs (Barth, 1980, Beckett *et al.*, 1987, Berdén and Berggren, 1990, Chin and Gschwend, 1991, Chin *et al.*, 1994), and a combination of the above (Peuravuori and Pihlaja, 1997). There has been no general consensus on the best approach for MW calibration, but perhaps Zhou and co-workers (2000) have provided the most conclusive analysis. Here, they demonstrated the variability that can be obtained in determination of MWs and MW averages (M_n and M_w) when analysing samples on the same instrument with different columns or standards and when analysing samples in different laboratories. They reported that variability of between 10-20 percent could be expected for MW averages. This becomes critical when analysing samples of similar origins when variations in MW averages of less than 10 percent could be expected.

Zhou *et al.* (2000) identified two critical conditions that need to be met for accurate MW determinations. First, a need for standards of the same molecular type as the analytes, *i.e.*, similar MWs and charge distribution, and second, efficient data processing of HPSEC chromatograms, including baseline corrections and selection of appropriate MW cut-offs for average calculations. Zhou and co-workers (2000) used PSSs for calibration, due to the similarities with aquatic NOM when compared to other available macromolecules, however, they also suggested the use of salicylic acid and acetone as low MW standards. The processing of data is an area that has not been extensively covered, however, it was shown to be crucial in accurate calculation of MW averages (Zhou *et al.*, 2000). The MW cutoff was also shown to be a critical factor in determining MW averages for NOM. Zhou and co-workers (2000) suggested that a high MW cutoff at the point where the chromatogram returns to <2 % of the maximum chromatogram height and a low MW cutoff of <1 % of the maximum chromatogram height but not less than 50 Da.

1.5.3.3. Organic Carbon Detection for High Pressure Size Exclusion Chromatography

A major limitation of many current HPSEC methods for determination of the MW distribution of aquatic NOM is that UV absorbance is used to determine the concentration of DOC in the eluent, while UV detectors are sensitive only to UV-absorbing species. This detection method is also not quantitative for organic carbon because the magnitude of the absorbance is very susceptible to structural features, rather than to the mass of organic carbon. Zhou and co-workers (2000) investigated the effect of increasing UV detector wavelength on the detection response of humic substances. They found that the M_n and M_w values increased with increasing wavelength, making MW determinations by this method unreliable.

For these reasons, organic carbon detectors (OCDs) have been developed for use with HPSEC systems (Huber and Frimmel, 1991, Vogl and Heumann, 1998, Specht and Frimmel, 2000, Her *et al.*, 2002). The major advantage of

these methods is that the detector signal is directly proportional to the concentration of organic carbon in the eluent and, irrespective of functionality; any type of organic species can be detected. Three of the four techniques are based on the UV/wet chemical oxidation method (Huber and Frimmel, 1991, Huber and Frimmel, 1994, Specht and Frimmel, 2000, Her *et al.*, 2002) for quantitative determination of organic carbon. The principle of these methods is the oxidation of NOM to carbon dioxide and subsequent quantitative detection of the carbon dioxide, enabling determination of the organic carbon concentration. Currently, this technology is limited to only a few research groups throughout the world. An alternative method for detecting organic carbon following HPSEC was developed by Vogl and Heumann (1998). This technique employed inductively coupled plasma-isotope dilution mass spectrometry (ICP-IDMS) for the quantitative determination of organic carbon. The method of Vogl and Heumann is unique and extremely difficult to replicate and is no longer in operation (Heumann, 2003).

Huber and Frimmel (1991) were the first to develop the HPSEC-OCD technique. Their detector is a complicated system based on production of an extremely thin film of sample that is first separated by HPSEC and then falls under gravity once introduced at the top of the system. A schematic of the system is shown in Figure 1.4.

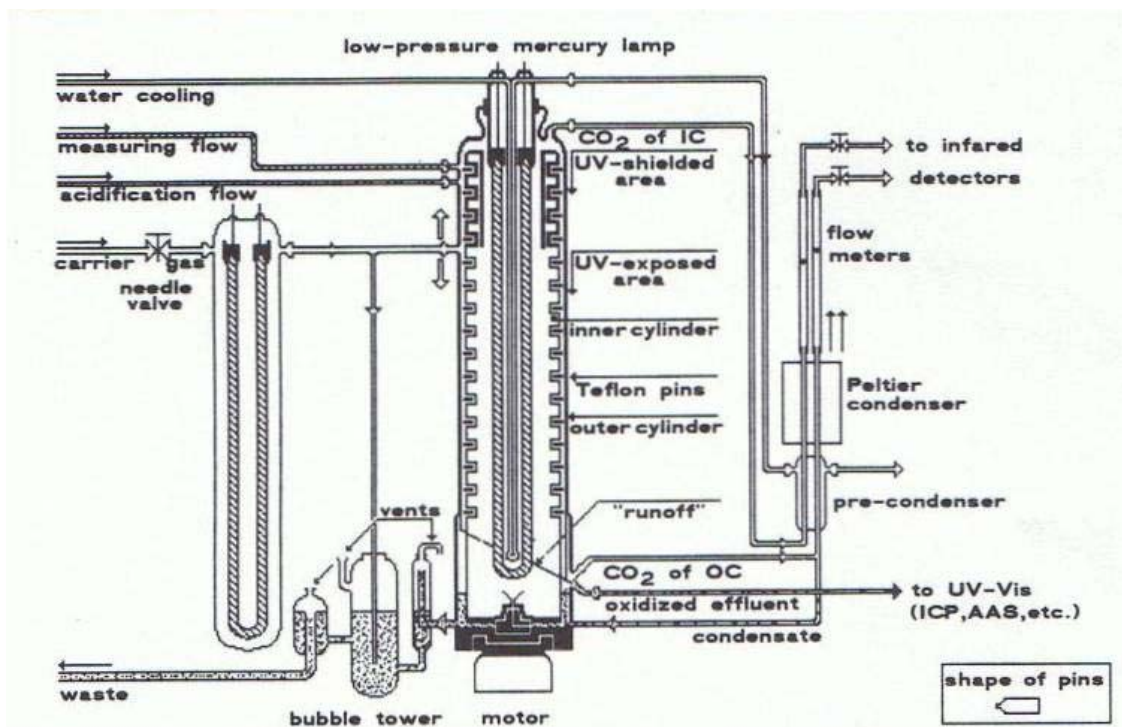


Figure 1.4 Schematic of the thin film OCD system (taken from Huber and Frimmel, 1991).

The sample to be measured is fed into a continuous flow of very pure water buffered with phosphate salts. This flow enters the upright reactor at its upper end and flows downward under gravity. At the lower end, the flow leaves the reactor either by reason of hydrostatic pressure differences inside and outside the reactor, and/or by means of pumping through a separate outlet. The reactor has two distinct features: the online removal of carbon dioxide produced from inorganic carbon (IC), and the mechanism by which the flow is spread out as a thin film to improve the oxidation of organic carbon to carbon dioxide and removal of carbon dioxide produced from solution. For the removal of IC, nitrogen gas enters the reactor and is forced, after splitting, to flow in opposite directions. In the upstream direction, the nitrogen passes a part of the reactor shielded from the UV lamp and purges carbon dioxide from the acidified measuring flow. The nitrogen/carbon dioxide gas mixture leaves the reactor *via* a small opening at the top carrying carbon dioxide derived from IC. In the downstream direction, nitrogen gas passes the UV-irradiated part of the reactor and purges carbon dioxide produced from UV oxidation of non-volatile organic carbon (OC). The

mechanism of oxidation in this downstream section is the unique part of this system. Due to the low penetration depth of UV light in water, the sample is spread out as a thin film by action of a spinning cylinder, with Teflon pins added to help spread the sample. This thin film allows the penetration of UV light and also improves the removal of carbon dioxide produced from OC in the sample stream. The flow of nitrogen and carbon dioxide in this downstream section is then dried and fed to a non-dispersive infrared detector (NDIR) to measure produced carbon dioxide (Huber and Frimmel, 1991). While this reactor is extremely efficient for online measurement of OC, there are two issues which arise during its use. The first arises from the use of buffer systems containing high concentrations of salts (Specht and Frimmel, 2000). The design of the system means that a build up of salts will occur in the thin film reactor, leading to its destruction. The other issue with the thin film reactor is the amount of sample required for analysis. The infrared detector used for this analysis has a sample cell with a volume of approximately 20 mL. As a result of such a large cell, it is necessary to make use of a high flow of gas to ensure the sample cell is continually being flushed. This high nitrogen flow rate and large sample cell result in larger aquatic NOM sample sizes being required. The method thus has a high detection limit and low sensitivity (Specht and Frimmel, 2000).

Since the development of this first organic carbon detection system some 15 years ago, there have been two other systems built for detection of OC, after separation by HPSEC, using UV oxidation. Her and co-workers (2002) and Specht and Frimmel (2000) developed similar systems using slightly different technology to that of Huber and Frimmel (1991). These two systems, while different from the thin film instrument of Huber and Frimmel (1991), employ the same basic principles for separation of inorganic carbon and organic carbon, and oxidation of organic carbon to carbon dioxide. Her and co-workers (2002) separate the inorganic carbon after the chromatography step using a hydrophobic membrane bundle, which allows gas to permeate under vacuum, but the aqueous sample is retained for further treatment. The sample is first acidified with orthophosphoric acid to convert IC to carbon dioxide gas and then passed through the bundle of hollow fibre membranes

(HFM). These membranes are hydrophobic and thus, retain any water while allowing gas to pass through. The carbon dioxide gas is forced through the membrane, due to a negative pressure being applied on the outside of the HFM bundle. After the inorganic carbon removal step, a persulfate solution is introduced to aid in the oxidation of OC prior to UV treatment (Her and co-workers, (2002). The application of UV light to the sample in the method of Her and co-workers (2002b) is slightly different to the thin film method employed by Huber and Frimmel (1991), with the sample being passed through a quartz capillary situated directly alongside a low pressure mercury discharge lamp. This method proved to be equally effective as the thin film reactor for oxidation of OC to carbon dioxide (Her *et al.*, 2002).

The mode of detection of the produced carbon dioxide in the method of Her and co-workers (2002) is also different to the technique used by Huber and Frimmel (1991). Her and co-workers (2002) utilise a commercial conductivity detector to measure the carbon dioxide produced, thus avoiding the need to remove the carbon dioxide from solution. The drawback however, is that not all the carbon dioxide is measured, and therefore sensitivity is lowered. In fact, the commercial conductivity instrument uses a hydrophobic Gortex[®] membrane to partition the carbon dioxide between the sample stream and an ultra pure water stream. The carbon dioxide diffuses through the membrane into the ultra pure water stream, and the conductivity is measured up to several times per second. As not all of the carbon dioxide permeates across the membrane, detection limits may be higher than with a NDIR detector.

The system developed by Specht *et al.* (2000) is basically a combination of the designs of Her and co-workers (2002) and Huber and Frimmel (1991). Following the chromatographic separation, inorganic carbon in the eluent is converted into carbon dioxide by the addition of orthophosphoric acid, and the acidified mixture purged with nitrogen gas. This gas/liquid mixture is fed to an open chamber where the carbon dioxide derived from IC is allowed to escape and the eluent, containing OC, pumped by action of a peristaltic pump through the remainder of the system (Specht *et al.*, 2000). The oxidation of organic carbon is performed in the same manner as used by Her

and co-workers (Her *et al.*, 2002), where sample is passed through a quartz capillary running parallel to a low pressure mercury discharge UV lamp and nitrogen added to again purged the OC derived carbon dioxide from solution. The carbon dioxide/nitrogen mixture separated by using a cooling module to “freeze out” the water, and the gas mixture dried before being analysed in an NDIR detector similar to that used by Huber and Frimmel (1991). While this system overcomes the problem of the high salt concentrations that may affect the thin film reactor, the issue of requirement of large sample sizes was not overcome. The large sample cell in the NDIR detector requires large volumes of both nitrogen gas and also OC.

1.6. Scope of Study

The characteristics of NOM are an important consideration in the treatment of natural waters. The presence of NOM in groundwater and surface water sources used for drinking water leads to a number of problems necessitating treatment of these sources prior to distribution. As well, disinfection required to achieve microbiologically safe water results in the formation of a number of disinfection by-products, due to reactions between NOM and the disinfectant. For these reasons, it is important to investigate the structure of NOM and to develop new methods for NOM structural characterisation.

The MW distribution is an important characteristic of NOM, as it has been shown that different treatment methods preferentially remove different size fractions of NOM. Thus, methods of determining the MW distribution of NOM are important from a treatment perspective. Chapter 2 of this thesis focuses on the development of an HPSEC analytical method for accurately determining the MW distribution of NOM. Several parameters were investigated for optimisation of separation of NOM components in HPSEC. These parameters were eluent composition, injection volume, flow rate and sample ionic strength.

An investigation of the two different treatment streams at the Wanneroo GWTP in terms of their MW characteristics was conducted and is reported in

Chapter 3. The Wanneroo GWTP is of particular interest as it includes the world's first large scale MIEX[®] treatment process, and the configuration of the plant allows comparison of MIEX[®] treatment followed by coagulation with enhanced coagulation on identical inlet water. The MW distribution of NOM at various points in these two treatment streams was investigated with three HPSEC techniques. These techniques included HPSEC with UV₂₅₄ detection, using an analytical scale column for maximum resolution of MW peaks, and HPSEC with OCD and UV₂₅₄ detection, utilising a larger scale column achieving slightly lower peak resolution, but having the advantage of detecting all NOM present with the OCD system. These two methods used virtually identical mobile phases. The third HPSEC method involved OCD, UV₂₅₄ and fluorescence detection, with a column of similar dimensions to the second method, but with a different mobile phase to the first two methods. Significant information on NOM removal during different stages of the treatment process was obtained, as well as the superior overall MW information obtained with an on-line OCD system.

The attractiveness of OCD in HPSEC analysis, as a system which can detect all NOM in a sample, as well as provide concentrations of organic carbon in each MW fraction, prompted the development of an OCD system. In Chapter 4, the construction of an OCD is described and each section of the detector outlined. These sections include inorganic carbon removal and dosing of reagents; the oxidation of organic carbon and subsequent removal of produced carbon dioxide from solution; the detection of the carbon dioxide for concentration determination; and the calibration of the system to achieve accurate DOC concentrations for an entire sample, as well as individual peaks.

While the analytical determination of the MW distribution of aquatic NOM is valuable in terms of its likely behaviour in water treatment, this technique does not give any information about the NOM structure. In Chapter 5, HPSEC is used in a preparative mode to collect discrete MW fractions of a sample of groundwater from the Gngangara mound. The method for collecting nine MW fractions is described, as well as information on the

character of the organic matter isolated in each fraction. The isolated MW fractions were then treated with chlorine and the formation of disinfection by-products measured. This body of information allowed structural features of organic matter in each fraction to be identified and correlated with disinfection behaviour.

Chapter 6 of this Thesis describes the isolation and characterisation of NOM from four stages of the Wanneroo GWTP. Water samples after aeration, following MIEX[®] treatment, after MIEX[®] and coagulation treatment, and following enhanced coagulation were collected. The samples were concentrated, inorganic material was removed and the samples lyophilised to obtain solid isolates. Solid isolates were analysed using solid state ¹³C NMR spectroscopy, Py-GC-MS, and FTIR spectroscopy as well as investigating the MW distribution, DOC content other water quality parameters of the dilute solutions prior to isolation. It was found that treatment removed aromatic material leaving a greater proportion of hydrophilic oxygenated carbon.

2. HIGH PRESSURE SIZE EXCLUSION CHROMATOGRAPHY METHOD DEVELOPMENT

2.1. Introduction

In high pressure size exclusion chromatography (HPSEC), the quality of the chromatography may be influenced by mobile phase composition and pH, flow rate, injection volume and sample pre-treatment. It is important, therefore, to optimise these parameters. In certain cases, non-ideal filtration mechanisms can have a substantial influence on HPSEC chromatographic performance. The most important of these interactions are hydrophobic interactions, ion exchange, ion exclusion and intramolecular electrostatic repulsive interactions (Berdén and Berggren, 1990, Chin and Gschwend, 1991, Specht and Frimmel, 2000). At high ionic strengths, hydrophobic interactions will prevail, and at low ionic strengths, electrostatic interactions dominate (Mori and Barth, 1999). Opinion on the ideal mobile phase composition seems mixed, with some researchers proposing a mobile phase ionic strength of between 0 and 0.04 mol L⁻¹ (Huber and Frimmel, 1991, Hongve *et al.*, 1996, Peuravuori and Pihlaja, 1997), whilst others favour an ionic strength of 0.1 mol L⁻¹ or above (Mori *et al.*, 1987, Chin *et al.*, 1994). Berdén and Berggren (1990) investigated the effect of increasing mobile phase concentration and ionic strength, as well as different mobile phase pH, on HPSEC chromatographic performance. Using a TSK G2000 SW_{XL} silica based column, the mobile phase pH was altered by using either sodium nitrate (pH 6.0) or ammonium acetate/sodium nitrate (1:3, pH 7.0) and ionic strengths adjusted to 0.05, 0.10, 0.15 and 0.2 mol L⁻¹. Resolution of the humic acid solution investigated was poor for all conditions tested. However, at high ionic strength, retention volumes increased markedly and irreversible adsorption on the surface of the stationary phase also increased, and this phenomenon was more pronounced at a lower pH. The authors stated that the ionised acid groups (COO⁻) of humic molecules and the residual negative charge of the silica based stationary phase may result in exclusion effects, increasing the retention volume. They also suggested that, with increasing

ionic strength, sample adsorption on the stationary phase may become problematic (Berdén and Berggren, 1990).

Chin and Gschwend (1991) also investigated the effect of ionic strength on HPSEC chromatographic performance using a Waters 300SW silica based HPSEC column. They found that the ionic strength of the mobile phase needed to be above a pre-determined critical value, which they termed the critical ionic strength (CIS). Values below this CIS resulted in ion exclusion, caused by the residual negative charge of the silica stationary phase and negative regions of humic materials which resulted in exclusion from the pores of the stationary phase. The result was retention volumes greater than what would be expected by the molecular weight (MW) of the sample. The effect of adsorption of the analyte on the stationary phase due to high ionic strengths was not addressed (Chin and Gschwend, 1991). Peuravuori and Pihlaja (1997) investigated several mobile phase compositions with varying ionic strengths using a TSK G3000SW silica based column. Their study showed poor chromatographic resolution of a humic acid solution using a 1 mmol L⁻¹ phosphate buffer and a 1 mmol L⁻¹ phosphate buffer with 100 mmol L⁻¹ sodium chloride added to adjust the ionic strength to approximately 0.1 mol L⁻¹. At the lowest ionic strength (1 mmol L⁻¹), ion exclusion effects were apparently too great to allow the humic material to permeate the pores of the stationary phase, resulting in poor resolution of peaks and low retention volumes. Increasing the ionic strength with the addition of sodium chloride increased the elution volume due to the reduction of ion exclusion but resulted in little if any improvement in the chromatographic resolution. A 20 mmol L⁻¹ phosphate buffer was also tested and resolution was slightly improved, but not to the same extent as when a 10 mmol L⁻¹ sodium acetate solution was utilised. According to Peuravuori and Pihlaja (1997), the ion exclusion effect was sufficiently minimised with a 10 mmol L⁻¹ sodium acetate mobile phase to allow the sample to permeate the pores of the stationary phase. The authors acknowledged, however, the work of Becher *et al.* (1985), who used a 20 mmol L⁻¹ phosphate buffer as the mobile phase on a different isolated humic acid sample to achieve similar separation to that of Peuravuori and Pihlaja (1997) using a 10 mmol L⁻¹ sodium acetate solution

for the separation their isolated humic acid sample. Similarly, Huber and Frimmel (1994, 1996) obtained well resolved chromatograms using a 28 mmol L⁻¹ phosphate buffer as the mobile phase when studying a surface water derived humic acid.

The effect of flow rate on HPSEC chromatographic performance was studied by Cooper *et al.* (1973), who investigated polystyrene elution parameters at flow rates between 0.21 and 1.05 mL min⁻¹ using tetrahydrofuran as the mobile phase. The authors found that that elution volumes and number of theoretical plates remained constant over a range of polystyrene MWs at the flow rates tested (Cooper *et al.*, 1973). However, Mori (1977) demonstrated an increase in the number of theoretical plates of a high MW polystyrene standard (MW 200 000 Da) with decreasing flow rate when using toluene as the mobile phase. Mori and Barth (1999) also reported an increase in retention volumes with increasing flow rate, and an improvement in resolution with lower flow rates, due possibly to the increased time the sample was in contact with the stationary phase. Similarly, Cheng and Hollis (1987), using dichloromethane as the mobile phase in a study of polystyrene, noted that an increase in flow rate resulted in a reduction in the number of theoretical plates and an increase in retention volumes, but stated that in practice the effects were insignificant. The effect of flow rate in aqueous HPSEC was investigated by Ricker and Sandoval (1996) using phosphate salts as the mobile phase when studying water soluble proteins. Here, increasing flow rate was shown to reduce peak resolution, due apparently to the slow diffusion rates of polymers into the stationary phase and hence a reduced time for interaction between the sample and particles of the stationary phase (Ricker and Sandoval, 1996). Also, a study by Saito and Hayano (1979) showed that flow rate actually had no effect on the resolution of humic or fulvic acids extracted from marine sediments. However, unlike the size exclusion separation of polymers of known MW, humic material is macromolecular and thus small increases in resolution or changes in retention volume may not be noticeable when considering the separation of such materials.

The retention volume of a sample studied in HPSEC will increase as the injection volume increases (Mori, 1977). At the same time, the number of theoretical plates decreases as the injection volume increases as a result of band broadening (Mori, 1977). Ricker and Sandoval (1996) also investigated injection volume effects on the resolution of water soluble proteins using phosphate salts as the mobile phase. They observed a loss of resolution as injection volume was increased, due to band broadening, however, the effect was minimal from injection volumes of 2 μL to 200 μL . The authors also noted that it was in fact the volume of sample injected and not the concentration of sample which was responsible for the loss of resolution, and an increase in sample concentration, while maintaining a constant injection volume, should maintain resolution until the viscosity of the sample increased significantly (Ricker and Sandoval, 1996).

The importance of matching the ionic strength of the sample and mobile phase in HPSEC was first reported by Chin and Gschwend (1991). In their study of humic acids, they demonstrated that a lower sample ionic strength compared to the mobile phase ionic strength allowed the humic material to 'uncoil' and increase its hydrodynamic volume and, as a result, appear to have a larger MW than in fact was the case. This phenomenon prevented the humic material permeating into the pores of the stationary phase to the degree predicted by its MW and hence the humic material eluted at an earlier retention volume (Chin and Gschwend, 1991). A similar study by Specht and Frimmel (2000) investigated the chromatographic behaviour of a highly coloured surface water sample without the matching of sample and mobile phase ionic strength. In their study, a sharp peak at what the authors referred to as the 'salt boundary' was shown. The salt boundary was at the point of the chromatogram where the lower ionic strength sample solvent had moved through the stationary phase, eluting at the permeation volume of the column. At this point, the lower ionic strength of the sample solvent, water in the case of this study, was not able to counter the residual negative charge of the stationary phase, and hence electrostatic ion exclusion would occur at this point of the chromatogram. This process would prevent molecules from diffusing into the pores of the stationary phase and thus they would elute at a

point earlier than would be expected by their MW. In fact, all low MW charged components should elute at the salt boundary. The matching of the mobile phase and sample ionic strength was advocated, therefore, to achieve accurate MW determinations of the low MW portion of humic material (Specht and Frimmel, 2000).

2.1.1. Scope of Study

The objective of the work in this Chapter was the optimisation of an HPSEC method for the MW characterisation of NOM. The chromatographic effect of mobile phase composition, sample ionic strength, flow rate and injection volume were tested and optimised for a groundwater sample taken following aeration at the Wanneroo GWTP. These conditions were then used in the studies reported in the remainder of this Thesis.

2.2. Experimental

2.2.1. Samples

Four litre glass Winchesters for sampling were cleaned by soaking in Pyroneg[®] detergent for 24 hours, rinsing with deionised water and then heating at 550 °C for 12 hours. A water sample (8 L) was collected in two 4 L glass Winchesters from a sampling point after the aeration stage at the Wanneroo GWTP. Samples were stored in the dark at 4 °C prior to analysis. Sub-samples of this sample were used throughout the HPSEC method development phase of the study. Each sub-sample was filtered through a 0.45 µm nylon membrane (Pall Acrodisc), which had previously been rinsed with purified laboratory water (500 mL, this volume has previously been found sufficient to remove residual DOC from this type of membrane (Alessandrino *et al.*, 2006)) and sample water (40 mL). For work investigating the sample ionic strength, just prior to analysis, the ionic strength of each sub-sample was adjusted to equal the ionic strength of the mobile phase by diluting the sample with an aliquot of concentrated mobile phase. In each case, a stock solution of mobile phase was prepared at 10

times its usual concentration, and 1 mL of this was added to 9 mL of sample so that the ionic strength of the injected sub-sample equalled that of the mobile phase.

2.2.2. Materials and Methods

2.2.2.1. Purified Laboratory Water

Purified laboratory water was obtained by passing tap water first through an Ibis[®] reverse osmosis system. The system comprised a 5 μm pre-filter, followed by an activated charcoal filter, and two mixed-bed ion exchange purification packs in series. Product water was then passed through a reverse osmosis membrane and the permeate water stored in a 60 L polypropylene tank. Water from the storage tank was then fed to a Purelab Ultra Analytic purification system (Elga, UK), comprising microfiltration, mixed bed ion-exchange and final UV disinfection, as required, producing water with a conductivity of $18.2 \text{ M}\Omega \text{ cm}^{-1}$ and a dissolved organic carbon concentration of $1 \mu\text{g L}^{-1}$. This high purity water is referred to as “purified laboratory water” in this Thesis.

2.2.2.2. High Pressure Size Exclusion Chromatography

HPSEC was performed using a macroporous silica based TSK G3000SW_{xl} (7.8 x 300 mm, particle size 5 μm , pore size 250 Å ; Tosoh BioSep, Japan). The HPLC instrumentation used was a Hewlett Packard Model 1090 Series II equipped with a filter photometric UV detector (FPD) allowing only a wavelength of 254 nm to pass. The mobile phases tested, their ionic strength (μ) and pH are listed in Table 2.1; all chemicals were AR grade (Sigma-Aldrich). Samples were injected manually using a Rheodyne 7125 6-port injection valve. Typically, a 100 μL sample loop was utilised. For experiments where the effects of injection volume were tested, the sample loop was exchanged as required. The mobile phase flow rate was 1 mL min^{-1} for most experiments, except for those evaluating the effect of

flow rate, where flow rate was altered as needed. HP Chemstation software was used for data analysis of the FPD signal.

Table 2.1 Tested mobile phase composition, ionic strength and pH.

Mobile phase	Mobile phase Composition	Ionic Strength (μ)	pH
A	Purified laboratory water	0 mmol L ⁻¹	7.2
B	10 mmol L ⁻¹ CH ₃ COONa	10 mmol L ⁻¹	8.0
C	5 mmol L ⁻¹ Na ₂ HPO ₄ + 5 mmol L ⁻¹ KH ₂ PO ₄	20 mmol L ⁻¹	6.9
D	5 mmol L ⁻¹ Na ₂ HPO ₄ + 5 mmol L ⁻¹ KH ₂ PO ₄ + 26 mmol L ⁻¹ Na ₂ SO ₄	100 mmol L ⁻¹	6.8
E	10 mmol L ⁻¹ Na ₂ HPO ₄ + 10 mmol L ⁻¹ KH ₂ PO ₄	40 mmol L ⁻¹	6.8
F	10 mmol L ⁻¹ Na ₂ HPO ₄ + 10 mmol L ⁻¹ KH ₂ PO ₄ + 20 mmol L ⁻¹ Na ₂ SO ₄	100 mmol L ⁻¹	6.9

The void volume (V_0) (5.5 mL) and total permeation volume (V_p) (13.3 mL) of the column were determined using Dextran blue (MW 200 kDa) and acetone (MW 58.1 Da), respectively. Elution parameters were calculated as a distribution coefficient (K_d') (Peuravuori and Pihlaja, 1997)

$$K_d' = \frac{(V_e - V_0)}{(V_p - V_0)} \quad 2.1$$

where V_e is the elution volume of the solute.

The column system was calibrated with polystyrene sulphonate (PSS) standards (840, 4 400, 6 530, 15 200, 35 300 and 81 800 Da; Polymer Scientific Services, USA) in order to estimate the molecular weight averages (Appendix 1). A series of other compounds with a range of different functional groups were used to confirm the PSS based calibration (trypan blue 960 Da, cyanocobalamin (vitamin B12) 1355 Da, tannic acid 1 701 Da, ribonuclease A 13 700 Da and albumin 66 000 Da; Sigma-Aldrich). The calibration standards and other compounds used for testing were dissolved in the mobile phase (10 mg L⁻¹). The calibration curve was linear ($R^2=0.977$) over the MW range tested (Appendix 1).

2.3. Results and Discussion

2.3.1. Effect of the Mobile Phase Composition on HPSEC Performance

The chromatographic performance in HPSEC is highly dependent on the properties of both the mobile phase and the stationary phase (Peuravuori and Pihlaja, 1997). This is primarily due to interactions other than size exclusion, such as adsorption, hydrophobic interactions, ion exclusion, ion exchange and intermolecular electrostatic repulsion interactions (Robards *et al.*, 1994, Peuravuori and Pihlaja, 1997, Zhou *et al.*, 2000). Clearly, a complex variety of interactions can occur between solute and mobile phase, solute and stationary phase or between mobile phase and stationary phase, and, therefore, the retention time of a given analyte is highly dependent on the type of stationary phase, the type, concentration and ionic strength of the mobile phase and the difference in ionic strength between the sample and the mobile phase (Mori *et al.*, 1987, Robards *et al.*, 1994, Specht and Frimmel, 2000, Her *et al.*, 2002b). Choice of a mobile phase with an appropriate ionic strength is particularly important for minimising non-size exclusion interactions between analyte and stationary phase (Peuravuori and Pihlaja, 1997). For the analysis of aquatic NOM, aqueous mobile phases containing sodium azide, acetate or phosphate, amongst others, have been used as the mobile phase (Huber and Frimmel, 1991, Chin *et al.*, 1994, Peuravuori and Pihlaja, 1997); however, there does not seem to be a general consensus on the ideal mobile phase for this application.

Six different mobile phases (purified laboratory water: mobile phase A; 10 mmol L⁻¹ sodium acetate: mobile phase B; 10 mmol L⁻¹ phosphate buffer: mobile phase C; 10 mmol L⁻¹ phosphate buffer with 26 mmol L⁻¹ sodium sulfate added: mobile phase D; 20 mmol L⁻¹ phosphate buffer: mobile phase E; and 20 mmol L⁻¹ phosphate buffer with 20 mmol L⁻¹ sodium sulfate added: mobile phase F) were selected to study the chromatographic performance of HPSEC using a TSK G3000 SW_{XL} HPSEC column applied to NOM (Table 2.2). This column is reported to have relatively low adsorption characteristics and a well-defined pore-size distribution, which should enhance separation efficiency (Peuravuori and Pihlaja, 1997, Conte and Piccolo, 1999), and its

performance in the separation of humic substances has been reported to be superior to that of comparable columns (Myllykangas *et al.*, 2002). The mobile phases listed were chosen to compare both high and low ionic strength systems, as well as the difference between sodium acetate, which according to at least one report (Peuravuori and Pihlaja, 1997) is superior in the separation of NOM, and phosphate buffers.

To measure the column efficiency or resolving power for the six mobile phases investigated in this work, the number of theoretical plates, N , was calculated using equation 2.2 and tested on a PSS standard (MW 6530 Da). PSS was chosen due to its narrow MW distribution and hence likely separation of a single peak using the HPSEC conditions chosen, simplifying theoretical plates calculations.

$$N = 5.545 \left(\frac{t_R}{w_{1/2}} \right)^2 \quad 2.2$$

where t_R is the distance of the peak maximum from the point of injection in minutes, and $w_{1/2}$ is the width of the peak at half height in minutes (Scott, 1976). Table 2.2 lists the values required to calculate the number of theoretical plates, as well as the number itself. Chromatograms for the polystyrene sulphonate standard using each of the six mobile phases are shown in Appendix 2.

Table 2.2 Distance of peak maximum from point of injection (t_R), peak width at half height ($w_{1/2}$) and calculated number of theoretical plates (N) for the six mobile phases tested using a Tosoh TSK G3000SW_{xl} column. Injection volume was 100 μ L and mobile phase flow was 1 mL min^{-1} . Sample ionic strength was adjusted to equal the mobile phase by adding a concentrated solution of the mobile phase to the sample prior to analysis.

Mobile phase	t_R (min)	$w_{1/2}$ (min)	N
Purified laboratory water (A)	5.84	1.05	172
10 mmol L^{-1} sodium acetate (B)	6.43	0.52	847
5 mmol L^{-1} KH_2PO_4 + 5 mmol L^{-1} Na_2HPO_4 (C)	7.18	0.68	618
5 mmol L^{-1} $\text{M KH}_2\text{PO}_4$ + 5 mmol L^{-1} Na_2HPO_4 + 26 mmol L^{-1} Na_2SO_4 (D)	9.51	1.04	463
10 mmol L^{-1} KH_2PO_4 + 10 mmol L^{-1} Na_2HPO_4 (E)	8.32	0.79	615
10 mmol L^{-1} KH_2PO_4 + 10 mmol L^{-1} Na_2HPO_4 + 20 mmol L^{-1} Na_2SO_4 (F)	9.55	1.05	459

Purified laboratory water (mobile phase A), with the lowest ionic strength produced the lowest theoretical plate value (Table 2.2). The distance of the peak maximum from the point of injection was the shortest of all the mobile phases. This is most likely a result of residual negative charge on the stationary phase surface. In solution, the PSS standard will have an overall negative charge and, if there is a residual negative charge on the stationary phase, the charge exclusion will result in an earlier retention time and, hence, a lower number of theoretical plates. In purified laboratory water, the residual negative charge on the stationary phase can not be offset, however, a buffered mobile phase can offset this charge. Sodium acetate (10 mmol L⁻¹; mobile phase B) was found to have the highest number of theoretical plates, even though this mobile phase had an ionic strength lower than the four phosphate buffers under investigation. The value of t_R for sodium acetate was slightly higher than purified laboratory water, but shorter than the phosphate buffers tested. The peak width at half height for sodium acetate, however, was narrower than for all the other mobile phases tested, resulting in the highest number of theoretical plates. The comparison of these eluents with regard to the calculation of theoretical plates does not appear to be addressed in the literature when studying polystyrene sulphonates. However, Peuravuori and Pihlaja (1997) stated that when using sodium acetate as a mobile phase, charged humic materials were able to permeate the pores of the stationary phase being unhindered by charge exclusion effects, and that sample resolution was superior to other mobile phases tested, including phosphate buffers of 1 mmol L⁻¹, 20 mmol L⁻¹ and 100 mmol L⁻¹. Since humic substances have been found to behave similarly to polystyrene sulphonates and have similar hydrodynamic properties (Beckett *et al.*, 1987, Berdén and Berggren, 1990), the results of Peuravuori and Pihlaja (1997) can be applied to explain the observations of the current study. Thus, for sodium acetate, the reduction of charge exclusion, enabling increased sampling of the total pore volume, may be the reason for the greater number of theoretical plates observed.

Surprisingly, the 10 mmol L⁻¹ and 20 mmol L⁻¹ phosphate buffers (mobile phases C and E, respectively) had almost identical numbers of theoretical

plates. The elution parameters for the two mobile phases were slightly different, with the 10 mmol L⁻¹ phosphate buffer resulting in a t_R of 7.18 min compared to the 20 mmol L⁻¹ phosphate buffer with a t_R of 8.32 min. These results are consistent with literature reports that reducing mobile phase ionic strength reduces the elution volume of a given substance (Berdén and Berggren, 1990, Chin and Gschwend, 1991, Peuravuori and Pihlaja, 1997), since the 20 mmol L⁻¹ phosphate buffer had an ionic strength of 40 mmol L⁻¹, while the 10 mmol L⁻¹ phosphate buffer had an ionic strength of 20 mmol L⁻¹. While a reduction by half of the ionic strength resulted in a reduction in elution time of 1.14 min, it also resulted in an increase in $w_{1/2}$ of 0.11 min, with the overall effect that the number of theoretical plates was practically identical for the two mobile phases (618 for the 10 mmol L⁻¹ phosphate buffer and 615 for the 20 mmol L⁻¹ phosphate buffer).

Increasing the ionic strength of each of the 10 mmol L⁻¹ and 20 mmol L⁻¹ phosphate buffers to 100 mmol L⁻¹ with the addition of sodium sulfate (mobile phases D and F, respectively) reduced the number of theoretical plates of the original buffers, again to very similar values (463 and 459). Peak broadening upon addition of the sodium sulfate was significant for these two mobile phases, with $w_{1/2}$ values of 1.04 and 1.05 minutes for the mobile phases D and F, respectively, compared to 0.68 and 0.79 for the mobile phases C and E, respectively. While increasing the ionic strength of the original phosphate mobile phases did result in increased elution volumes (t_R), the concurrent peak widening was so significant that the theoretical plate values of the higher ionic strength mobile phases D and F decreased, compared to C and E, respectively.

From the calculation of theoretical plates for these six mobile phases, purified water (mobile phase A) was shown to be unsuitable for MW determinations in HPSEC. The charge exclusion experienced without added charge imparted by ions in the mobile phase resulted in the negatively charged PSS likely being excluded from the pore space of the stationary phase and hence insufficient separation was achieved. Sodium acetate (10 mmol L⁻¹; mobile phase B) performed best as a mobile phase for the study of PSS. The ionic

strength of sodium acetate was sufficient to allow the PSS to permeate into the pore space of the stationary phase and be separated as a narrow peak in the chromatogram. However, for reasons that will be discussed below, sodium acetate was not used in the remainder of this Thesis. Briefly, organic carbon detection is not possible with the use of this organic salt as mobile phase and issues arise with loss of sample on to the stationary phase with its use in the study of NOM. The use of either a 10 mmol L⁻¹ phosphate buffer or 20 mmol L⁻¹ phosphate buffer (mobile phases C and E, respectively) as the mobile phase also performed well and resulted in a high number of theoretical plates, again likely as a result of sufficient charge in the mobile phase to negate the residual negative charge of the stationary phase. Increasing the ionic strength to 100 mmol L⁻¹ through the addition of sodium sulphate (mobile phases D and F, respectively), as suggested (Chin and Gschwend, 1991), resulted in significant peak broadening and hence increased numbers of theoretical plates. This is possibly a result of adsorption onto the stationary phase, but, in any case, it would appear that, at this ionic strength, resolution would be lost in the study of a complex mixture such as NOM.

The effect of the six different mobile phases on the size exclusion chromatography of a solution of natural organic matter in water was then investigated. A sample of raw water following aeration at the Wanneroo GWTP was subjected to HPSEC-UV₂₅₄ using the six different mobile phases (A-F, Table 2.1) and the resulting chromatograms are presented in Figure 2.1. Identical conditions to those used in the determination of theoretical plates with a PSS standard were employed in this study with sample ionic strength being matched to that of the mobile phase by addition of a concentrated solution of the particular mobile phase to the sample just prior to analysis.

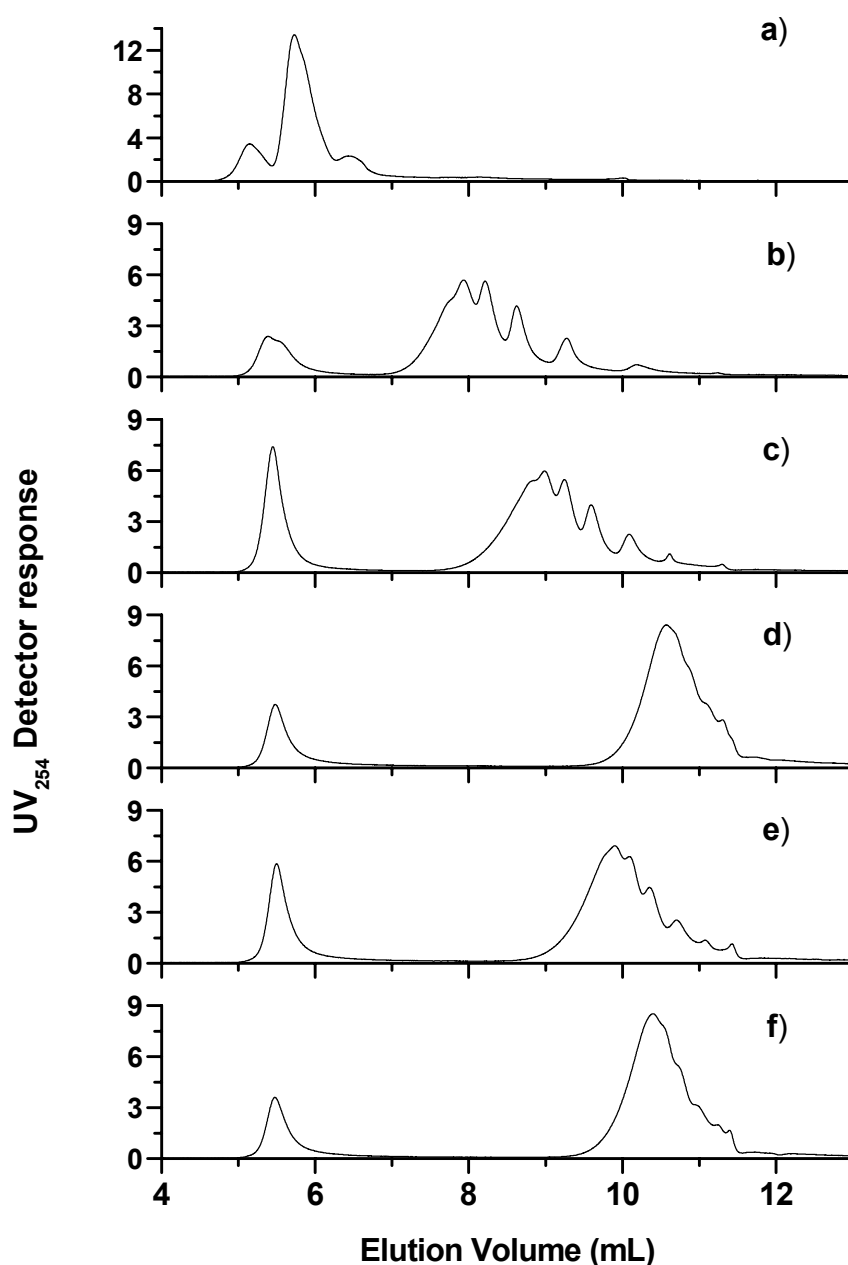


Figure 2.1 Influence of mobile phase on the HPSEC of aquatic NOM a) purified laboratory water (mobile phase A), b) 10 mmol L⁻¹ sodium acetate (B), c) 10 mmol L⁻¹ phosphate buffer (C), d) 10 mmol L⁻¹ phosphate buffer + 26 mmol L⁻¹ sodium sulfate ($\mu = 100$ mmol L⁻¹ (D)), e) 20 mmol L⁻¹ phosphate buffer (E), f) 20 mmol L⁻¹ phosphate buffer + 20 mmol L⁻¹ sodium sulfate ($\mu = 100$ mmol L⁻¹ (F)). Injection volume was 100 μ L, flow rate 1 mL min⁻¹ and sample ionic strength adjusted to match that of the mobile phase.

Changes in the concentration and ionic strength of the mobile phases markedly affected the elution behaviour of the UV₂₅₄-active substances in the sample, as predicted by the calculation of theoretical plates for each mobile phase. A noticeable feature of the chromatograms in Figure 2.1a-f is that the

area of the first peak, having an elution volume of approximately 5 - 6 mL, changed considerably with changes in mobile phase ionic strength and concentration. This peak eluted at the void volume, V_0 (Section 2.2.2.2), of the column, indicating that the material represented by this peak had not been subjected to any size exclusion effects (i.e. it was excluded from the pores of the stationary phase). The area of the first peak (elution volume 5-6 mL), the area of the remaining group of peaks (termed 2nd peak group) and the total peak area of the whole chromatogram for the six different mobile phases are presented in Figure 2.2.

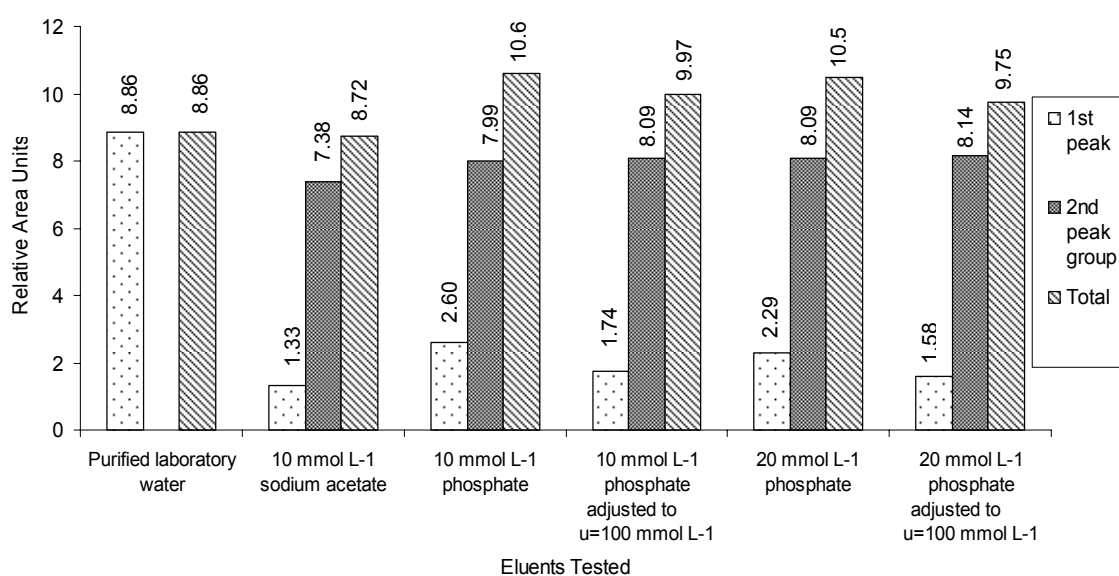


Figure 2.2 Comparison of total peak area, area of peak eluting at V_0 (1st peak) and sum of the area of peaks eluting after V_0 (2nd peak group) for six mobile phases tested; purified laboratory water (mobile phase A), 10 mmol L⁻¹ sodium acetate (B), 10 mmol L⁻¹ phosphate buffer (C), 10 mmol L⁻¹ + 26 mmol L⁻¹ sodium sulfate ($\mu = 100$ mmol L⁻¹) (D), 20 mmol L⁻¹ phosphate buffer (E), 20 mmol L⁻¹ + 20 mmol L⁻¹ sodium sulfate ($\mu = 100$ mmol L⁻¹) (F). Areas taken from chromatograms in Figure 2.1.

The area of the first peak gives an indication of the relative proportion of UV₂₅₄-active substances that were excluded from the stationary phase and, hence, indicates the effect of ionic strength on the size exclusion process. The chromatograms in Figure 2.1 and peak areas in Figure 2.2 show that altering the ionic strength of the mobile phase changed not only the elution volume of aquatic NOM components, but also changed the effective pore size of the stationary phase. In the case where purified laboratory water was

used as the mobile phase (Figure 2.1a, mobile phase A), i.e. at the lowest ionic strength, the peak at V_0 (the group of peaks here are considered one peak for the purpose of this experiment since they all elute at or close to V_0) was considerably larger than when phosphate and acetate buffers were used. This indicates that, when purified laboratory water was used as the mobile phase (mobile phase A), more of the sample was excluded from the pores of the stationary phase than when the mobile phase had a higher ionic strength. These observations compliment the chromatogram for aquatic NOM in Figure 2.1a where all UV₂₅₄-active material eluted at or close to V_0 . This is likely to be due to the charge exclusion effect, where the effective pore size was reduced, due to negative charges in the aquatic NOM repelling the residual negative charge on the surface of the stationary phase. Increasing the ionic strength to 20 mmol L⁻¹ or 40 mmol L⁻¹ using phosphate buffers (mobile phases C and E, respectively) reduced the area of the peak at V_0 and hence increased the size of the 2nd group of peaks, indicating a greater proportion of sample had permeated the pores of the stationary phase. Increasing the ionic strength to 100 mmol L⁻¹ for the two different phosphate buffer concentrations (mobile phases D and F) actually decreased the amount of material eluting at V_0 , indicating less charge exclusion occurring, however, the total amount of UV₂₅₄-active DOC detected was also slightly reduced. This may possibly be due to increasing sorption of UV₂₅₄-active DOC onto the stationary phase with the overall increase in charge in these two buffer systems as observed in the work of (Berdén and Berggren, 1990).

The effect of mobile phase on the separation of UV₂₅₄-active DOC is also apparent from the chromatograms in Figure 2.1. Purified laboratory water as the mobile phase (mobile phase A) resulted in virtually the entire sample being excluded from the column (Figure 2.1a). Using a 10 mmol L⁻¹ phosphate buffer as the mobile phase (mobile phase C, Figure 2.1c) produced excellent separation of UV₂₅₄-active DOC. The 2nd group of peaks in this case was spread over an elution volume of approximately 5 mL, and the peaks were more clearly resolved than with the other mobile phases. At a higher phosphate buffer concentration of 20 mmol L⁻¹ (mobile phase E,

Figure 2.1e), the elution volume of the 2nd group of peaks was reduced to approximately 4 mL, with decreased resolution of peaks. The advantage of the 20 mmol L⁻¹ phosphate buffer (mobile phase E) over the 10 mmol L⁻¹ phosphate buffer (mobile phase C), however, was in relation to the amount of excluded material. The total amount of measured UV₂₅₄-active material was virtually equal for the 10 mmol L⁻¹ and 20 mmol L⁻¹ phosphate buffer mobile phases (10.6 units and 10.5 units, respectively), however, the excluded fraction decreased from 2.60 units to 2.29 units, respectively. The addition of sodium sulfate to the two phosphate buffered mobile phases (mobile phases D and F, Figure 2.1d and Figure 2.1f) reduced the amount of excluded UV₂₅₄ - active DOC, but the resolution of the 2nd group of peaks was severely affected and the elution volume of this fraction was unfavourably reduced to approximately 2 mL in each case.

Previous research (Peuravuori and Pihlaja, 1997, Myllykangas *et al.*, 2002) has shown that the use of a 10 mmol L⁻¹ acetate buffer (mobile phase B, Figure 2.1b) can reduce intermolecular electrostatic repulsion and also minimise adsorption effects, and that excellent resolution is obtained for humic and fulvic acids. Comparison of the similar chromatograms from use of mobile phase B (Figure 2.1b; 10 mmol L⁻¹ sodium acetate) and mobile phase C (Figure 2.1c; 10 mmol L⁻¹ phosphate buffer) shows only a minor improvement in the resolution of the 2nd group of peaks. Also, while the amount of excluded material is less for mobile phase B, the total amount of material detected is also less. This observation is counter to what has been found in the literature (Peuravuori and Pihlaja, 1997), as lower ionic strengths should result in more ion exclusion. However, as this mobile phase was not to be used in further studies due to its incompatibility with organic carbon specific detectors this phenomenon was not further investigated. Possibly, this loss of material could be sample specific but further experiments were not conducted.

Results of theoretical plate experiments, as well as testing of a natural water sample, indicated that use of a 10 mmol L⁻¹ phosphate buffer (mobile phase C) resulted in resolution of NOM to a similar extent as the previously

favoured 10 mmol L⁻¹ sodium acetate mobile phase (mobile phase B), but due to ion exclusion effects, a significant portion of material was excluded from the pore space of the stationary phase. As a result, a 20 mmol L⁻¹ phosphate buffer (mobile phase E) was chosen as the mobile phase for future study, since the resolution achieved with this mobile phase was only marginally less than that achieved with the 10 mmol L⁻¹ phosphate buffer and the 20 mmol L⁻¹ phosphate buffer resulted in inclusion of a larger portion of the sample into the pore space of the stationary phase. Increasing the ionic strength of the mobile phase to 100 mmol L⁻¹ (mobile phases D and F) resulted in less charge exclusion, but at the cost of sample resolution, and so was discounted as a practical option for the chromatographic system being used.

2.3.2. Effect of the Ionic Strength of the Sample on HPSEC Performance

The interactions of the chosen mobile phase with the analytes and with the stationary phase are very important with regard to HPSEC performance. However, there are several other factors which contribute to resolution. One of these factors is the difference between the ionic strength of the mobile phase and that of the sample being introduced to the HPSEC system. For example, Specht and Frimmel (2000) found, for a natural coloured surface water, that when the ionic strength of the mobile phase was greater than that of the sample ionic strength, a sharp peak at the end of the chromatogram (the permeation volume) was present and in general, peaks eluted earlier than when the mobile phase ionic strength and sample ionic strength were equal. In addition, under these conditions of equal mobile phase and sample ionic strength, the sharp peak at the end of the chromatogram, which they identified as the salt boundary, was eliminated (Specht and Frimmel, 2000).

In the current experiment, a NOM sample was subjected to HPSEC using a 20 mmol L⁻¹ phosphate buffer as the mobile phase, a flow rate of 1 mL min⁻¹ and injection volume of 100 µL. The sample was tested with the ionic strength unchanged, and then the chromatographic performance of the same

sample was compared to when the ionic strength was adjusted to equal that of the mobile phase. The chromatograms obtained for a sample with the same ionic strength as the mobile phase, and one with a lower ionic strength, are shown in Figure 2.3. Note that the lower overall peak intensity of the sample with the ionic strength increased to be the same as the mobile phase is due to dilution effects through the addition of buffer (diluted 10 % by an aliquot of buffer of 10 times the concentration of the mobile phase). After integration of the total peak area of the two chromatograms, values of 10.18 area units and 9.24 area units were obtained for the samples with an unaltered ionic strength and with increased ionic strength, respectively. This represented an area of 90 % of the altered sample compared to the unaltered one, confirming that the difference in peak area was entirely due to dilution.

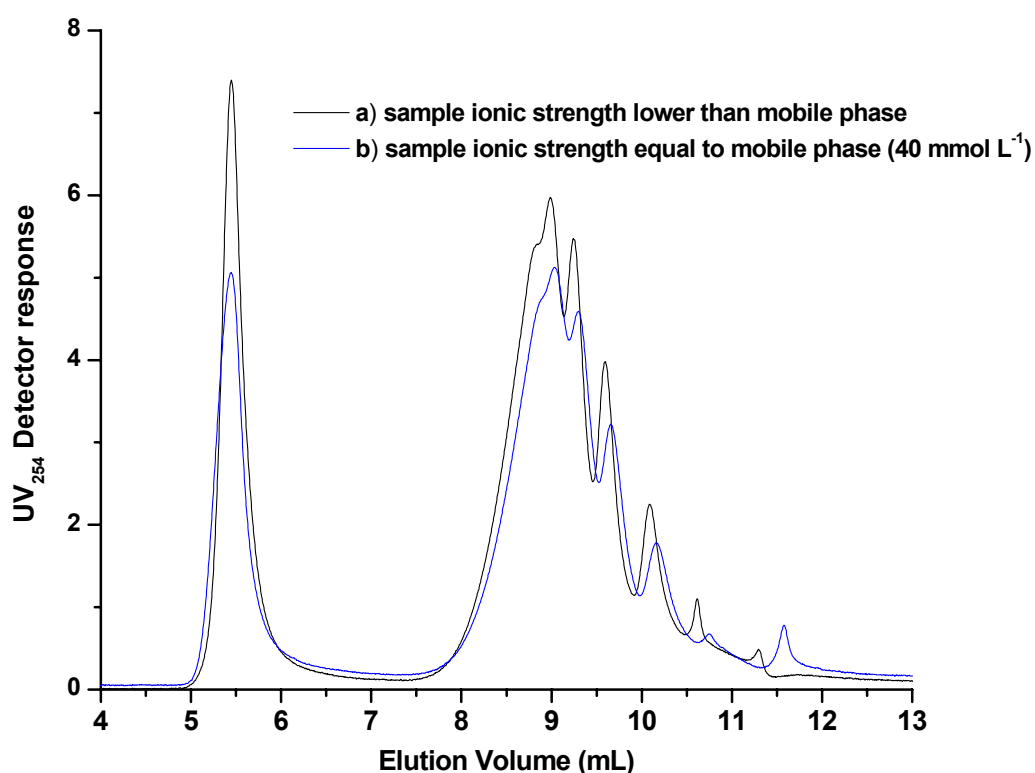


Figure 2.3 Influence of sample ionic strength on the HPSEC of aquatic NOM. Mobile phase tested was 20 mmol L⁻¹ phosphate buffer, $\mu = 40$ mmol L⁻¹ (mobile phase C), injection volume = 100 μ L and flow rate 1 mL min⁻¹, a) Sample ionic strength lower than mobile phase, b) sample ionic strength same as mobile phase ($\mu = 40$ mmol L⁻¹).

The chromatograms presented in Figure 2.3 are consistent with the findings of Specht and Frimmel (2000) in terms of the elution volume being slightly

lower after the ionic strength was increased to equal to that of the mobile phase. For example, the largest peak of the 2nd group of peaks, eluted at an elution volume of 9.00 mL when the sample ionic strength was less than that of the mobile phase, while adjusting the sample ionic strength to equal that of the mobile phase resulted in an elution volume for the corresponding peak of 9.05 mL. Several authors (DeHaan *et al.*, 1987, Ceccanti *et al.*, 1989, Chin and Gschwend, 1991) noted a similar effect in their studies of NOM by HPSEC, with elution volumes greater when sample ionic strength was lower than that of the mobile phase compared to when the ionic strengths were matched. This was attributed to a change in the molecular configuration of NOM under different ionic strengths. The work of Gosh and Schnitzer (1980) and Cornel *et al.* (1986) showed changes in the ionic strength of the sample could significantly influence the hydrodynamic volume of humic material. For the study of NOM using HPSEC, lower ionic strength of the sample means a more loosely coiled humic molecule, resulting in what appears to be higher MW peaks. Increasing the ionic strength of the sample to equal that of the mobile phase means a tighter coiled structure and causes a shift towards slightly lower MWs (DeHaan *et al.*, 1987, Ceccanti *et al.*, 1989, Chin and Gschwend, 1991).

Specht and Frimmel (2000) also noted in their experiment that the sharp peak at the end of the chromatogram ($V_e \cong 11.3$ mL in Figure 2.3) was replaced with a long tailing flank when the sample ionic strength was adjusted to equal the mobile phase ionic strength. However, in the current study, the sharp peak at ~11.3 mL is small, although still noticeable, in the chromatogram where sample and mobile phase ionic strengths were not matched (Figure 2.3a), and so the effect on this peak was less pronounced. By matching the sample and mobile phase ionic strength, the sharp peak has been removed and the long tail is apparent, but a further small peak at ~11.6 mL has appeared. This is possibly sample specific and may simply be a result of low MW components present in the sample. There is also a reduction of the peak at ~10.6 mL after the matching of sample and mobile phase ionic strengths; this material is possibly being included in the lower MW peak at ~11.6 mL. Specht and Frimmel (2000) explained that at this

point in the chromatogram, the salt boundary, the low MW components elute at the same point as the sample solvent and, due to the lower ionic strength at this point in the chromatogram, charged low MW material may elute at a point greater than would be expected by its MW due to an increase in charge exclusion.

By increasing the ionic strength of the sample to equal that of the mobile phase, there has been a slight reduction in elution volume due to the coiling of NOM at higher ionic strengths. NOM molecular configuration has been shown to change according to pH, concentration and, more importantly for this application, ionic strength (Gosh and Schnitzer, 1980, Cornel *et al.*, 1986). As a result, increasing sample ionic strength will slightly alter MW determinations, however, the effect is minimal. More important for the study of NOM by HPSEC is the greater accuracy of MW determinations for the low MW component. For the NOM sample studied in this research, the salt boundary effect was minimal and an anomaly of the appearance of a further peak at lower retention times has reduced the effect. However, the benefits of matching the ionic strength of the sample and mobile phase can still be seen and this process is an important consideration for the study of NOM by HPSEC.

2.3.3. Effect of the Flow Rate on HPSEC Performance

The mobile phase flow rate is another parameter which can potentially influence resolution of MW fractions in HPSEC. While there have been hundreds of reports on the use of HPSEC to characterise aquatic NOM, there seems to be no consensus on the ideal flow rate. Conte and Piccolo (1999) chose a flow rate of 0.6 mL min^{-1} , Nissinen and co-workers (2001) decided on a rate of 0.7 mL min^{-1} , Peuravuori and Pihlaja (1997) operated at an mobile phase flow rate of 0.8 mL min^{-1} , while Zhou *et al.* (2000) and Huber and Frimmel (1991) used an mobile phase flow rate of 1 mL min^{-1} . No explanation of flow rates chosen were given in these studies.

In the current study, four flow rates (0.5, 0.8, 1 and 1.2 mL min⁻¹) were chosen to evaluate the effect of mobile phase flow rate on HPSEC separation using the Tosoh TSK G3000SW_{XL} column, a 20 mmol L⁻¹ phosphate buffer mobile phase (mobile phase E), an injection volume of 100 μL, while leaving the ionic strength of the sample unadjusted to evaluate the effect on the salt boundary at different flow rates. The chromatograms, as a function of elution time, achieved with the four different flow rates are presented in Figure 2.4. Elution time rather than volume was used to represent this data to show the increase in time taken for analysis with lower flow rates.

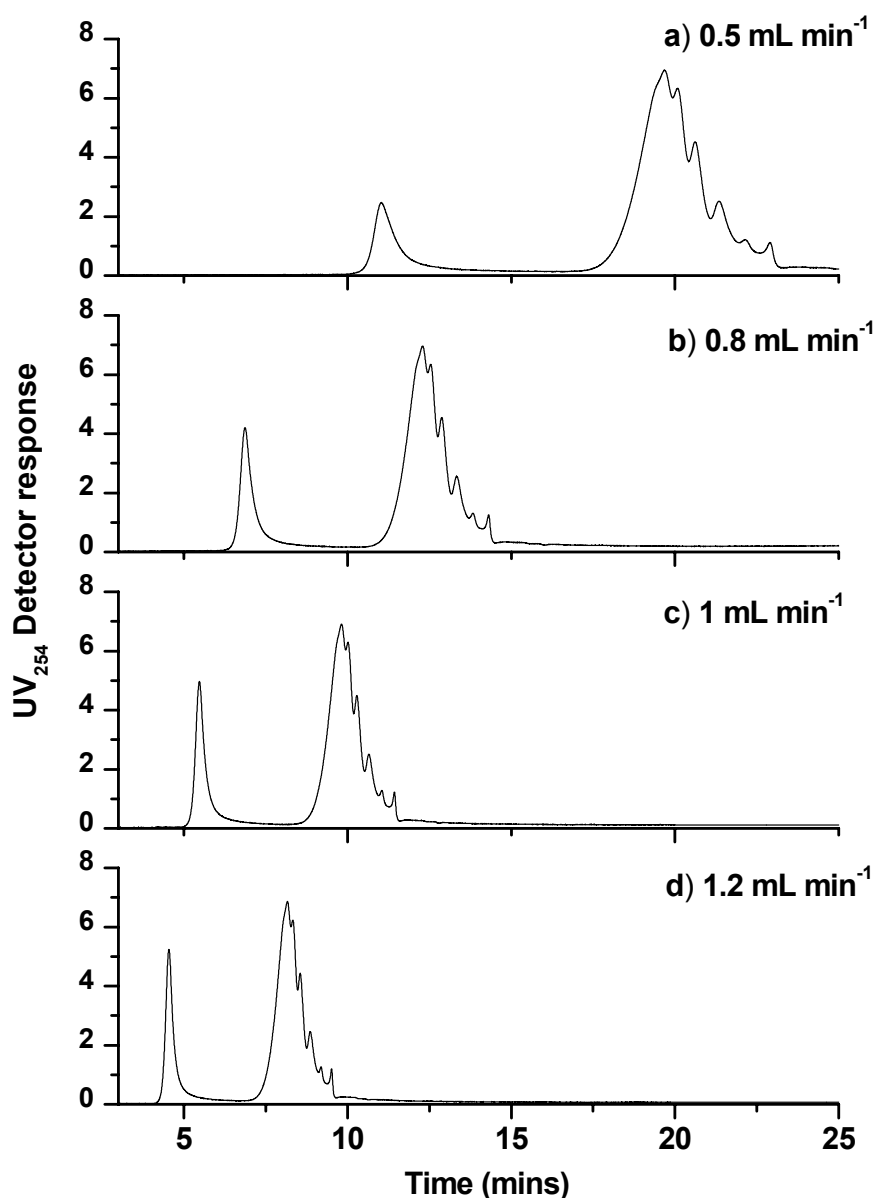


Figure 2.4 Influence of mobile phase flow rate on the HP size exclusion chromatography of aquatic NOM. Flow rates: a) 0.5 mL min^{-1} , b) 0.8 mL min^{-1} , c) 1 mL min^{-1} , d) 1.2 mL min^{-1} are compared. x axis expressed as elution time. Mobile phase was 20 mmol L^{-1} phosphate buffer (mobile phase D), injection volume was $100 \mu\text{L}$ and sample ionic strength was unaltered.

Reduction of the flow rate agreed with the findings of Saito & Hayano (1979) with no noticeable change in sample resolution observed (Figure 2.5).

Changing the flow rate did, however, appear to influence the amount of material that was excluded from the column (material eluting at V_0). To more clearly observe this effect, the four chromatograms in Figure 2.5 are

presented as a function of elution volume, rather than elution time, in Figure 2.5.

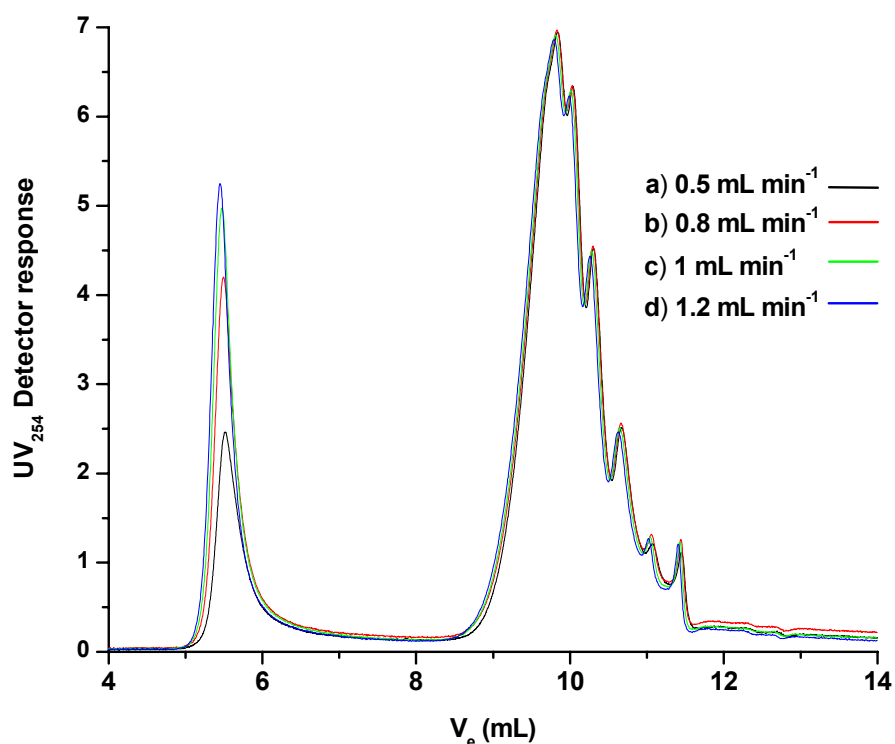


Figure 2.5 Influence of mobile phase flow rate on the HPSEC of aquatic NOM. Flow rates: a) 0.5 mL min^{-1} , b) 0.8 mL min^{-1} , c) 1 mL min^{-1} , d) 1.2 mL min^{-1} are compared. x axis expressed as elution volume (V_e). Mobile phase was 20 mmol L^{-1} phosphate buffer (mobile phase D), injection volume was $100 \mu\text{L}$ and sample ionic strength was unaltered.

From Figure 2.5, it is apparent that the shapes of the peaks representing the included fraction of NOM are unaffected by the changes in flow rate. In fact, the four chromatograms from elution volume 8.5 to 11.5 mL are virtually identical. However, increasing the flow rate clearly resulted in increasing amounts of material excluded from the column (material eluting at V_0). Integration of the areas of the peak at approx 5.5 mL showed that the amount of NOM excluded increased from 9.6 area units for a flow rate of 0.5 mL min^{-1} , to 10 area units at 0.8 mL min^{-1} , to 10.5 area units at 1 mL min^{-1} , and finally to 10.6 area units at 1.2 mL min^{-1} . The reasons for this increase in the excluded fraction with an increase in flow rate are unclear, and this phenomenon does not appear to be addressed in the literature. It is possible that the reason for an increase in the proportion of

the NOM which was excluded was simply due to a reduction in time the material had to undergo adsorption on the stationary phase. By increasing the flow rate, the material being analysed was forced through the column faster and hence had less time to interact with the stationary phase, resulting in a larger peak at V_0 . However, at lower flow rates, the included fraction would be expected to correspondingly increase, since there is more time for the NOM to permeate into the pores of the stationary phase, but this was not observed. At higher flow rates, more UV₂₅₄-active material was recovered than at lower flow rates. One possibility for the fate of the unrecovered material at the lower flow rates is that it was adsorbed by the stationary phase as a result of the longer contact time; another possibility is that the difference in recoveries may simply be an artefact of the detection system for this large material. Future work could include a more thorough investigation of this peak, possibly including a study using different UV detector wavelengths (other than 254 nm), or the use of different detection systems, e.g. organic carbon, fluorescence or refractive index detection. Alternatively, the material comprising the excluded fraction peak could be collected using preparative HPSEC at the various flow rates and changes in characteristics of the material could then be studied.

For the current study, a flow rate of 1 mL min^{-1} was selected as the flow rate of choice. Resolution of peaks was found to be virtually identical for all four flow rates tested. Low flow rates have previously been reported to have the potential to provide greater resolution due to greater interaction time between sample and stationary phase (Ricker and Sandoval, 1996, Popovici and Schoenmakers, 2005), but this was not observed in the current research. Practically, high flow rates are preferable since they decrease analysis time and thus enable greater sample throughput. The flow rate of 1 mL min^{-1} was selected over 1.2 mL min^{-1} , because of concerns of the possible loss of resolution that the higher flow rate may produce.

2.3.4. Effect of the Injection Volume on HPSEC Performance

The volume of sample injected onto the stationary phase is another important parameter that can influence the chromatographic performance of HPSEC separation. According to Mori and Barth (1999), the retention volume of a solute increases with an increase in injection volume. At the same time, the number of theoretical plates decreases as the injection volume increases, due to band broadening resulting in a loss of resolution. Again, there seems to be no general consensus in the literature on the ideal injection volume for HPSEC of aquatic NOM, with volumes ranging from 25 μL (Saito and Hayano, 1979) to 2 mL (Huber and Frimmel, 1991, Specht and Frimmel, 2000, Her *et al.*, 2002b)

The effect of varying the injection volume was examined in this study using a mobile phase comprising a 20 mmol L^{-1} phosphate buffer solution (mobile phase E), flow rate of 1 mL min^{-1} while leaving sample ionic strength unaltered to observe the salt boundary effect while changing injection volume. A sample of aerated raw water from Wanneroo GWTP was analysed after injection of five different volumes of the same sample (10 μL , 20 μL , 50 μL , 100 μL and 500 μL). Initially sample concentration was not changed to account for the variation in injection volume and results are shown in Figure 2.6. From review of the literature (e.g. Berdén and Berggren, 1990, Chin and Gschwend, 1991, Peuravuori and Pihlaja, 1997), it appears that 100 μL is the most common injection volume used with 7.8 mm internal diameter HPSEC columns and, hence, the chromatograms from the other injection volumes are compared directly to the chromatogram from injection of the 100 μL volume.

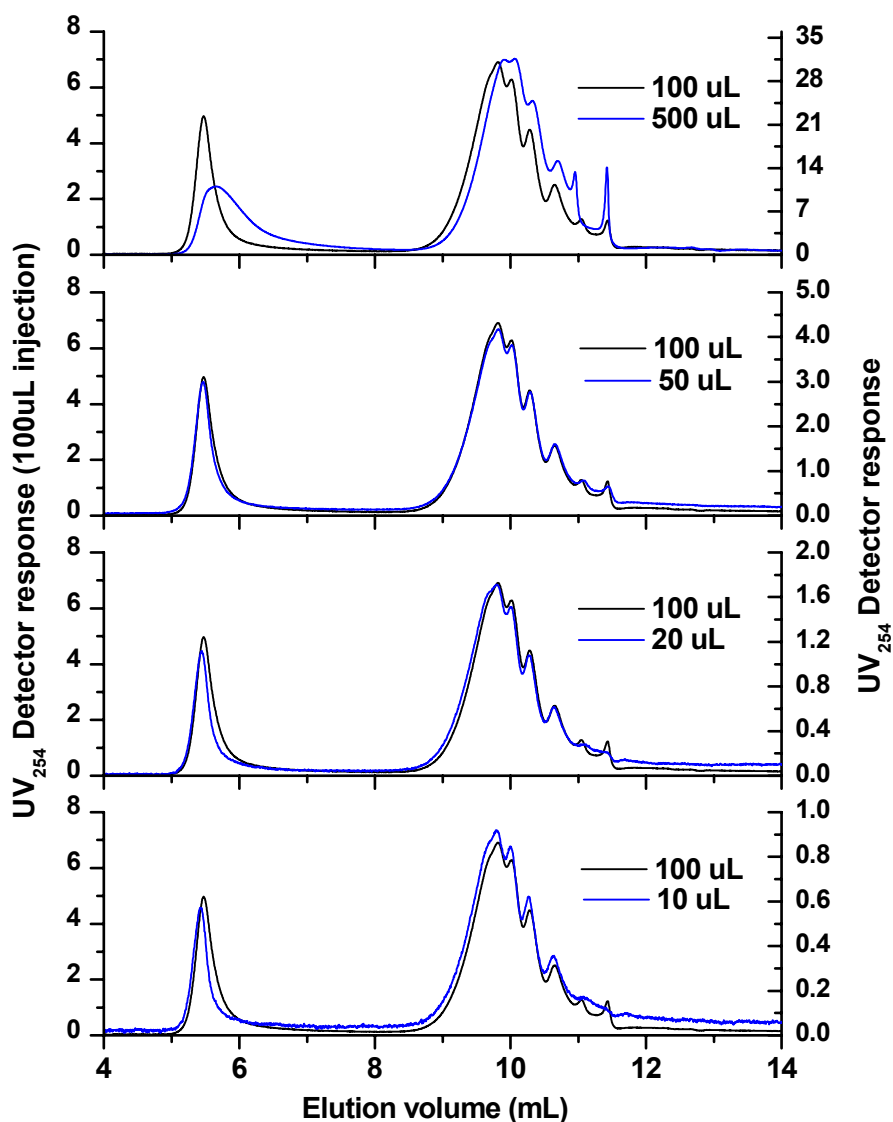


Figure 2.6 Influence of injection volume on the HPSEC of aquatic NOM. Chromatograms from injection volumes of 500, 50, 20 and 10 μL are compared to the chromatogram from injection of a volume of 100 μL . Mobile phase was 20 mmol L^{-1} phosphate buffer (mobile phase D), flow rate was 1 mL min^{-1} and sample ionic strength was unaltered.

The difference between an injection volume of 100 μL and 50 μL was minimal (Figure 2.6). Further reductions in injection volume to 20 μL and 10 μL (Figure 2.6) resulted in a slight improvement in peak resolution, likely due to reductions in band broadening, as outlined by Mori (1977) and Mori and Barth (1999). Also noticeable from Figure 2.6 is the reduction in the sharp peak present at the salt boundary in the 10 μL and 20 μL chromatograms. This observation will be discussed later in this Section.

Injection of 500 μL of sample onto the column resulted in significant peak broadening and a loss in resolution of peaks Figure 2.6. This was especially pronounced for the peak eluting at the void volume, i.e. the excluded fraction, of the sample. To test that this effect was not simply a result of the increased amount of material being injected onto the column, the aerated raw water sample was systematically diluted with purified laboratory water, apart from the 10 μL sample, and re-injected using the same injection volumes (500, 100, 50, 20 and 10 μL) so that identical amounts of DOC were injected onto the column. The resulting chromatograms are presented in Figure 2.7.

As observed by Mori and Bath (1999), the increased injection volume in fact resulted in a loss of resolution. The peak at V_o was the most affected, but there was also a noticeable deterioration in resolution of the peaks between 9 and 12 min for all injection volumes compared to the 10 μL injection volume. The 10 μL and 20 μL injection volumes (Figure 2.7a and Figure 2.7b) produced virtually identically shaped chromatograms while a loss of resolution was observed increasing injection volume to 50 μL (Figure 2.7c) and a further loss of resolution found when 100 μL (Figure 2.7d) of sample was injected. This is likely due to a gradual increase in band broadening as the injection volume is increased. Also an increase of the peak at the salt boundary ($V_e \cong 11.5 \text{ mL}$) becomes evident when injecting 50 μL of sample and even more evident when injecting 100 μL of sample. Injecting 500 μL of sample resulted in the poorest resolution and also the largest peak at the salt boundary. While the loss of resolution observed here is consistent with the findings of Mori and Barth (1999), that is a result of band broadening, a shift to greater retention times with an increase in injection volume was not observed in this case.

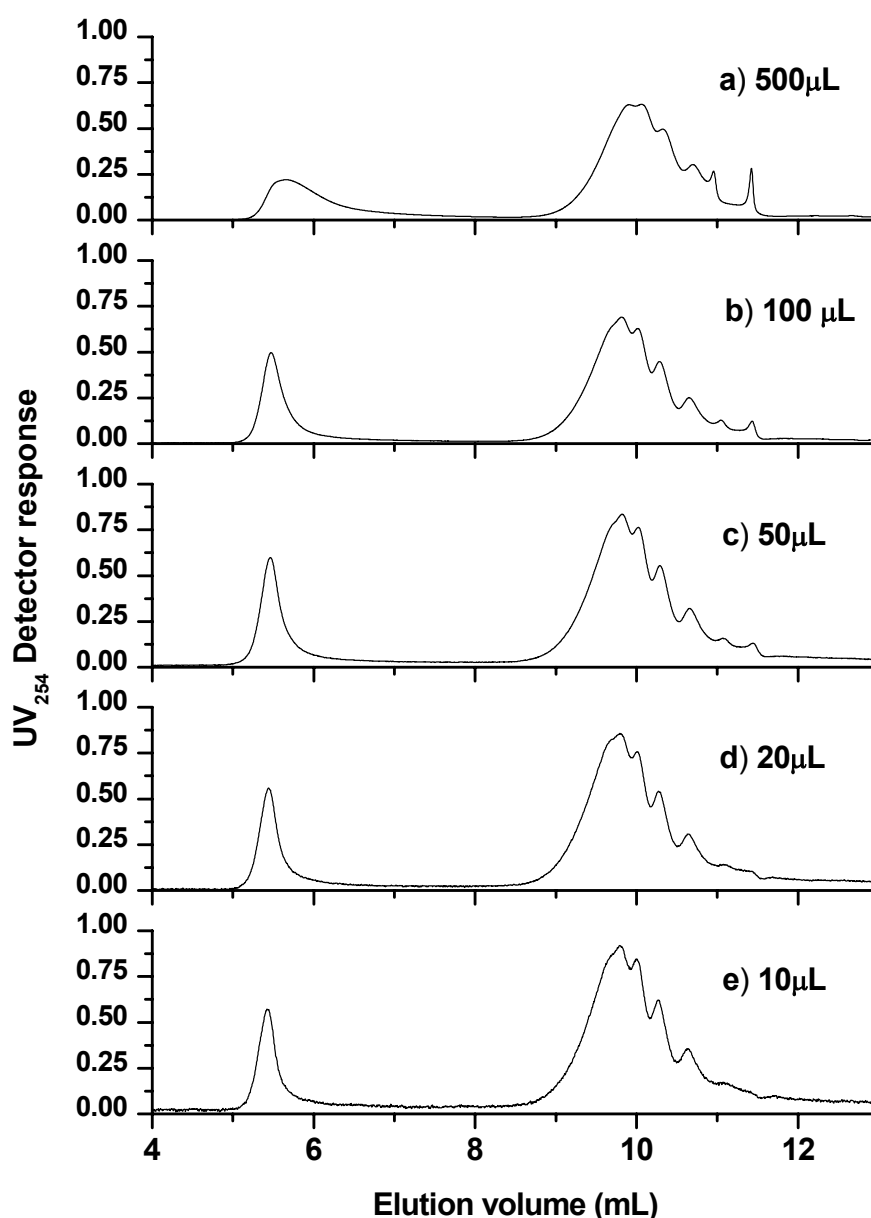


Figure 2.7 Influence of injection volume on the HPSEC of aquatic NOM. The aerated raw water sample was diluted with purified laboratory water for injection volumes 20 μL , 50 μL , 100 μL and 500 μL so DOC concentrations equalled the sample injected with a 10 μL injection volume. a) 500 μL injection, sample diluted 50:1, b) 100 μL injection, sample diluted 10:1, c) 50 μL injection, sample diluted 5:1, d) 20 μL injection, sample diluted 10:1, e) 100 μL injection, sample not diluted. Mobile phase was 20 mmol L^{-1} phosphate buffer (mobile phase D), flow rate was 1 mL min^{-1} and sample ionic strength was unaltered.

The above experiments, testing the effects of altering injection volumes, also provide a very good illustration of salt boundary effects (Figure 2.6). The ionic strength of the samples tested in these experiments was not adjusted to match that of the buffer. Hence, increasing the sample injection volume also

increased the volume of water (at much lower ionic strength than the mobile phase) that was injected onto the column during introduction of the sample. As discussed previously (Section 2.3.2), the salt boundary is the point where the water from the sample elutes from the column. At this point, the ionic strength of the system is lowered due to dilution of the mobile phase. This results in increased charge exclusion between the negative charges of solute molecules and the negatively charged regions of the stationary phase. In Figure 2.6 and Figure 2.7, the larger the injection volumes, the more pronounced the effect on DOC eluting at the salt boundary ($V_e \cong 11.5$ mL) and the greater the amount of DOC eluting at the salt boundary. Specht and Frimmel (2000) have stated that the material that elutes at the salt boundary is likely to have an overall negative charge. With increasing injection volume, the difference between mobile phase ionic strength at the salt boundary and the mobile phase ionic strength during the rest of the analysis increases. Hence, with increasing injection volume, more of the sample components would elute at the salt boundary, explaining the differences in the relative areas of the salt boundary peaks observed at different injection volumes in Figure 2.6 and Figure 2.7. At an injection volume of 50 μ L, the salt boundary effect was still noticeable, but when the amount of sample injected was decreased to very low volumes (10 and 20 μ L; Figure 2.7a and b), the effect was minimal, with only a very small peak apparent at the salt boundary. This demonstrates that when utilising injection volumes lower than about 20 μ L in this system, it may not be necessary to match the ionic strength of the sample to that of the mobile phase.

For the study of NOM by HPSEC, utilising as small an injection volume as possible is desirable. The reduction in band broadening and hence increase in peak resolution and minimisation of the salt boundary effect is greatest at lower injection volumes. However, for samples with low concentrations of detectable DOC, the sample may not be detected if insufficient material reaches the detector. As a result, an injection volume of 100 μ L was chosen for the remainder of this research.

2.3.5. Analysis of Aquatic NOM Sample Using Optimised HPSEC Conditions

In the current study, the optimised conditions for analysis of the MW distribution of aquatic NOM from natural waters using HPSEC have been determined to be as follows: 1. mobile phase E, i.e. 20 mmol L⁻¹ phosphate buffer, comprised of 10 mmol L⁻¹ Na₂HPO₄ + 10 mmol L⁻¹ KH₂PO₄, pH of 6.8 and ionic strength = 40 mmol L⁻¹; 2. injection volume 100µL; 3. flow rate 1 mL min⁻¹; 4. ionic strength of the sample adjusted to equal that of the mobile phase by adding 1 mL of a 10 times concentrated solution of the mobile phase to 9 mL of the sample. Conversion of the x-axis from elution volume to MW was achieved using the calibration curve developed in Section 2.2.2.2 and illustrated in Appendix 1. These optimised conditions were then applied to analyse the sample of aerated raw water from the Wanneroo GWTP and the resulting chromatogram is presented in Figure 2.8.

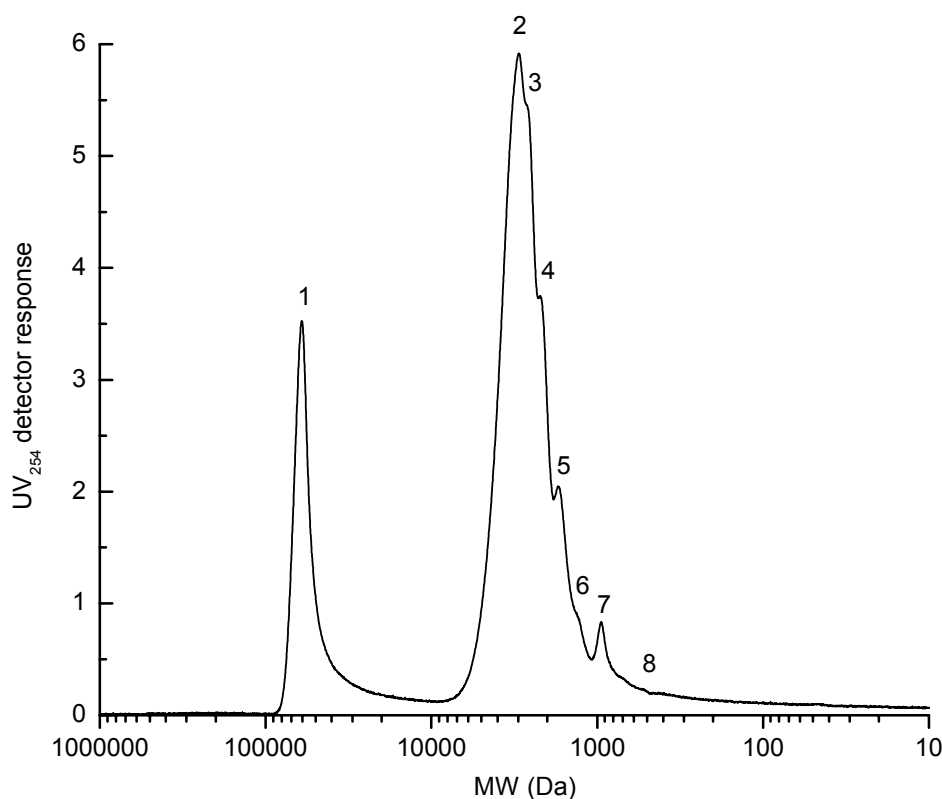


Figure 2.8 Typical chromatogram using the optimised HPSEC conditions. Mobile phase composition: $10 \text{ mmol L}^{-1} \text{ KH}_2\text{PO}_4 + 10 \text{ mmol L}^{-1} \text{ Na}_2\text{HPO}_4$, sample buffered so ionic strength of sample equalled that of mobile phase ($\mu = 40 \text{ mmol L}^{-1}$), injection volume = $100 \mu\text{L}$; flow rate 1 mL min^{-1} . The sample was aerated raw water from the Wanneroo GWTP.

The HPSEC chromatogram in Figure 2.8, analysing NOM taken after aeration from the Wanneroo GWTP, shows the sample was resolved into 8 peaks. This compares favourably to the work of Peuravuori and Pihlaja (1997) who stated that a 10 mmol L^{-1} sodium acetate mobile phase was superior than a 20 mmol L^{-1} for the resolution of NOM in HPSEC. In their study, NOM of various origins was separated into either 7 or 8 peaks (Peuravuori and Pihlaja, 1997) and resolution was similar to that achieved in the current study. From this comparison, the current optimised HPSEC method performed well for the study of NOM.

As shown in Figure 2.8, approximately 20 % (determined by integration) of the UV_{254} detectable NOM was not subjected to any size exclusion and eluted at V_0 (Peak 1). Huber and Frimmel (1996) reported that this material

is likely to comprise inorganic colloids, while Allpike *et al.* (2005) suggested that the material could also contain organic colloidal substances perhaps bound to iron and/or sulfur. Both of these hypotheses could explain why this material is not able to enter the pore space of the stationary phase, as colloids would likely be larger than the pore volume of the stationary phase utilised. Also the significant signal in the UV₂₅₄ spectrum would result due to light scattering of the particulate matter. The remaining 80 % of UV₂₅₄-active material eluted within a relatively small MW range, between about 7 000 Da and 300 Da. From this included portion, six peaks (Peaks 2-7) were resolved, with a further small portion (Peak 8) unresolved between a MW of 600 - 300 Da. Most of the UV₂₅₄ active NOM was present at a MW between 7 000 and 2 000 Da (Peaks 2-4).

Water from this sampling point, after aeration at the Wanneroo GWTP, has been well studied due to the implementation of the world's first large scale MIEX[®] resin treatment plant at the Wanneroo GWTP. As a result, a number of HPSEC studies have been reported in the literature on samples taken from this point in the process at the Wanneroo GWTP (Cadee *et al.*, 2000, Slunjski *et al.*, 2000a, Slunjski *et al.*, 2000b, Bourke *et al.*, 2001). HPSEC conditions in these studies included a Shodex KW-802.5 column (Shoko, Japan), a 1 mmol L⁻¹ phosphate buffer with ionic strength adjusted to 100 mmol L⁻¹ with sodium chloride as the mobile phase, a flow rate of 1 mL min⁻¹, an injection volume of 100 µL, with samples adjusted so their ionic strength was equal to that of the mobile phase, according to the method of (Chin *et al.*, 1994). Utilising these conditions, the aerated raw NOM sample has previously only been separated into 3 peaks, with a large portion eluting at V₀ of the system and only two resolved peaks eluting in the included fraction. While the bore waters contributing to the samples taken after aeration at the Wanneroo GWTP would have been different at each sampling event, the overall water quality of the blended water is kept reasonably constant. It is therefore clear that the method described in this Chapter is far superior than the previous methods for the separation of Wanneroo-type NOM.

2.4. Conclusions

On a Tosoh TSK G3000SW_{xl} column, using UV₂₅₄ detection, a mobile phase consisting of a buffer of 10mmol L⁻¹ Na₂HPO₄+10 mmol L⁻¹ KH₂PO₄, a flow rate of 1 mL min⁻¹, with 100 μL of sample injected, achieved the greatest resolution of MW fractions during HPSEC of NOM from a sample of raw aerated water from the Wanneroo GWTP. It was also shown that adjusting the ionic strength of the sample to match that of the mobile phase had a small but noticeable effect on elution volume, as has been described by Chin & Gschwend (1991). This was attributed to an increase in the coiled nature of NOM at higher ionic strengths resulting in apparent lower MW material and hence higher elution volumes. The impact on retention volume was minimal but matching the ionic strength of sample and mobile phase had a greater effect on small MW material eluting at the salt boundary. When using small injection volumes (10-20 μL), the salt boundary effect was minimal, but for samples with low concentrations of DOC requiring larger injection volumes, the effect was significant and resulted in incorrect MW determinations.

From the experiments conducted, the composition of the mobile phase had the greatest effect on peak resolution of all the method parameters tested. This is consistent with observations by Peuravuori and Pihlaja (1997), who also showed that the most critical factor in peak resolution was the composition of the mobile phase. Chin *et al.* (1994) and Zhou and co-workers (2000) showed that the ionic strength of the buffer needed to be maintained at 0.1 mol L⁻¹ to reduce unwanted interactions between the stationary phase and solutes. However, in the present study, it was demonstrated that increasing the ionic strength of the buffer to 0.1 mol L⁻¹ actually increased adsorption of the solute onto the stationary phase and less resolution of the included fraction was achieved. Also, when the ionic strength of the buffer was too low, the exclusion effect described by Chin *et al.* (1994) indeed had an effect: a significant portion of the sample was excluded from the pores of the stationary phase and not separated to any degree. The best mobile phase for the chosen system was therefore the

20 mmol L⁻¹ phosphate buffer, of intermediate ionic strength (mobile phase E).

The flow rate and injection volume were shown to have minimal effect on peak resolution, although at very high injection volumes (500 µL on a 7.8 mm ID column) significant band broadening occurred, resulting in a loss of resolution. In cases where the ionic strength of the sample had not been matched to that of the buffer, it was found that the salt boundary effect contributed substantially to the overall shape of the chromatogram with high injection volumes. Injection of sample volumes of 100 µL or greater resulted in a decrease in ionic strength at the salt boundary and, hence, intermolecular exclusion of solute molecules. The larger the sample volume, the greater was the salt boundary effect, and the more material which eluted at the salt boundary. While the resolution was not substantially improved by decreasing the injection volume below values of 100 µL, less dilution resulted in higher ionic strengths of the samples and the salt boundary effect was reduced. While this is advantageous for HPSEC studies of NOM, lowering the injection volume will increase detection limits and for samples with low DOC concentrations may result in UV₂₅₄-active DOC being undetected. For this reason, a 100 µL injection volume was chosen for use. The only influence of flow rate was an increase in retention time with decreasing flow rate. By optimising the above parameters, it was possible to identify 8 fractions from the aerated raw water sample taken from the Wanneroo GWTP.

3. THE USE OF HIGH PRESSURE SIZE EXCLUSION CHROMATOGRAPHY TECHNIQUES TO STUDY THE EFFECTIVENESS OF A RANGE OF DRINKING WATER TREATMENT PROCESSES

The research in this Chapter has been published in:

Allpike, B.P., Heitz, A., Joll, C.A., Kagi, R.I., Abbt-Braun, G., Frimmel, F.H., Brinkmann, T., Her, N. and Amy, G. (2005) Size Exclusion Chromatography to Characterise DOC Removal in Drinking Water Treatment. Environmental Science and Technology, 39, pp 2334-2342.

3.1. Introduction

The MIEX[®] process is an innovative, new water treatment process jointly developed by SA Water, Orica Australia Pty Ltd and CSIRO Australia (Slunjski *et al.*, 2000b, Pelekani *et al.*, 2001, Slunjski *et al.*, 2002). The process is based on a micro-sized, macroporous, strong base anion exchange resin with magnetic properties, which is used in a continuous process that incorporates a resin regeneration side-process. The world's first full-scale MIEX[®] water treatment plant was commissioned at the Wanneroo GWTP, in December 2001 (Smith *et al.*, 2003). At the Wanneroo GWTP the MIEX[®] process is operated in combination with a conventional alum clarifier for maximum removal of DOC. The plant was configured such that the combined MIEX[®] coagulation process can be operated in parallel with the pre-existing coagulation process. In this way, the raw water supplying the two process streams is identical, and water can be sampled from comparable locations in the parallel streams, facilitating accurate comparison of the two processes. The MIEX[®] resin treatment was developed with the aim of reducing the overall DOC content of treated water, especially those fractions that are resistant to removal by coagulation processes (Slunjski *et al.*, 2000b). DOC reduction was a major objective for the introduction of the MIEX[®] process at the Wanneroo GWTP, specifically to

(a) decrease DBP formation; (b) decrease biofilm regrowth in the distribution system; and (c) to improve the stability of chlorine (disinfectant) residuals in finished water. However, characterisation of the product water had previously been limited to measurements of bulk water quality parameters such as DOC concentrations, UV_{254} , colour and specific UV absorbance (SUVA) for example as well as HPSEC- UV_{254} measurements. Previous studies had shown that the combined MIEX[®] and coagulation process appeared to preferentially remove the lower MW DOC components, while enhanced coagulation treatment appeared to preferentially remove those of higher MW (Slunjski *et al.*, 2000b and references therein, Drikas *et al.*, 2003). However, these previous investigations had been conducted using HPSEC with UV_{254} detection only, and were hampered by the lack of availability of an OCD system. Furthermore, they had been conducted on either pilot scale or laboratory simulation experiments, which cannot fully represent on-plant conditions. In the present research, these previous investigations were extended, firstly by studying real-world samples from a full-scale MIEX[®] treatment plant, and secondly, by conducting the analyses using HPSEC coupled with UV_{254} , OCD and fluorescence detectors. These additional methods of characterisation provided information on the effects of the treatment processes on the MW and molecular (spectroscopic) characteristics of the DOC that was not previously available.

3.1.1. Scope of Study

The objective of the work in this Chapter was to evaluate the drinking water treatment processes used at the Wanneroo GWTP with regard to their MW distribution. The performance of analytical and preparative scale HPSEC as well as UV_{254} , fluorescence and OC detection was compared for samples from the Wanneroo GWTP after various stages of treatment.

3.2. Experimental

3.2.1. Samples

Glassware for sampling was cleaned according to the procedure outlined in Chapter 2.2.1. Samples (4 L) were collected from five points at the Wanneroo GWTP on the 14th May 2002 (Figure 3.1) in four litre glass Winchesters prepared as in Section 2.2.1. Samples analysed were stored at 4 °C until required. Sub-samples used for HPSEC analysis were prepared by filtration as described in Chapter 2.2.1. The ionic strength of the samples was adjusted to equal that of the mobile phase by addition of a ten times concentrated solution of the mobile phase as described in Chapter 2.2.1.

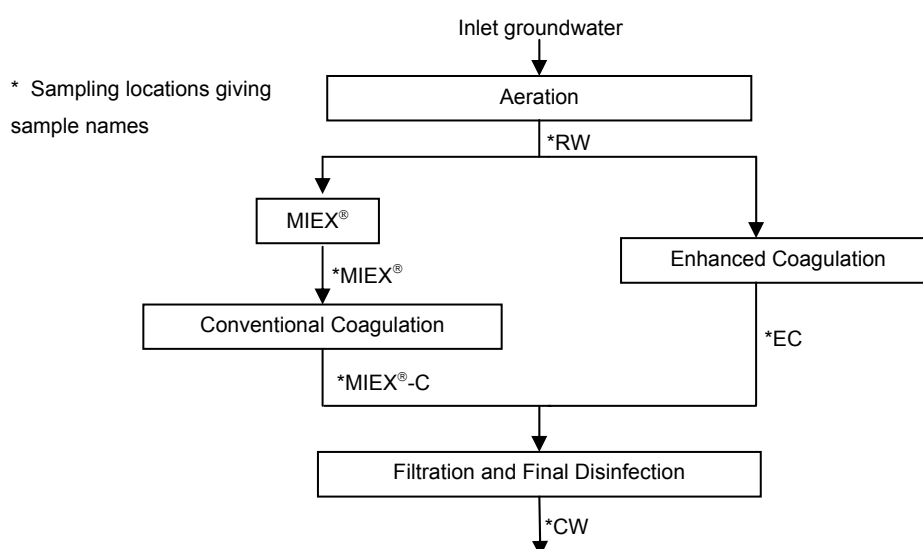


Figure 3.1 Schematic of Wanneroo GWTP, showing sampling locations (*) and sample names.

The samples collected were (a) the aerated raw water (RW); (b) water after treatment with MIEX[®] only (MIEX[®]); (c) water after treatment with MIEX[®] followed by conventional coagulation (MIEX[®]-C); (d) water after treatment with enhanced coagulation only (EC; that is coagulation geared for maximum NOM removal by optimising alum dose) and; and (e) “clear water”, after filtration, pH adjustment and chlorination for disinfection (CW). Data on chemical doses, plant operating parameters and raw water chemistry are provided in Table 3.1. A thorough description of the treatment processes at the WGTP is provided in Section 1.4.1.

Table 3.1 Water quality and chemical dose parameters at sample locations at the Wanneroo GWTP.

Water quality parameter/ chemical dose	Raw water (RW)	MIEX [®] treated (MIEX [®])	MIEX [®] -coagulation (MIEX [®] -C)	Enhanced coagulation (EC)	Clear water (CW)
Alum dose (mg L ⁻¹)	-	-	55	70	-
Polyelectrolyte dose (mg L ⁻¹)	-	-	0.75	0.62	-
DOC concentration (mg L ⁻¹)	5.7	2.46	1.59	2.14	1.74
Colour (@ 400 nm)	45	29	2	3	2
UV ₂₅₄ (cm ⁻¹)	0.326	0.175	0.025	0.047	0.035
SUVA (L mg ⁻¹ m ⁻¹)	5.7	7.1	1.6	2.2	2.0
pH	7.2	7.4	6.6	6.4	6.7

3.2.2. Materials and Methods

3.2.2.1. Purified Laboratory Water

Purified water was obtained as outlined in Chapter 2.2.2.1

3.2.2.2. Measurement of Constituents and Water Quality Parameters in Water Samples

Water quality parameters, including colour, UV₂₅₄ and pH were determined by SGS Australia Pty Ltd.

3.2.2.3. Measurement of Dissolved Organic Carbon Concentration

3.2.2.3.1. Materials

3.2.2.3.1.1. Phosphoric Acid Solution

Phosphoric acid (BDH, 100 mL, 85 % w/v) was added to purified laboratory water and the volume made up to 500 mL.

3.2.2.3.1.2. Persulfate Oxidiser Solution

Sodium persulfate (60 g, Sigma-Aldrich 98 %) and phosphoric acid (15 mL, 85 %) were added to purified laboratory water and the volume made up to 500 mL.

3.2.2.3.2. Preparation of Standard Solutions

Organic carbon solutions (100 mg C L⁻¹): a stock solution of potassium hydrogen phthalate (Aldrich, 2.125 g), previously dried at 100 °C for 2 hours and cooled in a desiccator, was prepared in purified laboratory water (1 L). The stock solution of potassium hydrogen phthalate was serially diluted to produce solutions of 0.10, 0.20, 0.50, 1.00, 1.50, 2.00, 2.50, 3.00, 4.00, 5.00, 6.00, 8.00 and 10.00 mg organic carbon L⁻¹ for construction of calibration curves.

3.2.2.3.3. Measurement of Dissolved Organic Carbon Concentration

Nylon membranes (Pall Acrodisc, 0.45µm) were pre-washed with purified laboratory water (500 mL) and sample water (40 mL). Water samples were filtered using a pre-washed nylon membrane. The filtered water was collected in an annealed glass vial (40 mL) and analysed using a Shimadzu Total Organic Carbon Analyser (TOC-Vws) using a Non-purgable Organic Carbon (NPOC) method. The NPOC parameters included 3 to 5 injections of 2.5 mL of sample per injection (with a maximum standard deviation of 0.05 mg L⁻¹), with 2 washes. An aliquot of the phosphoric acid solution (75 µL) was added and the sample sparged with nitrogen gas for 3 minutes. An aliquot of the persulfate oxidiser solution (1.5 mL) was added and the sample irradiated by UV light to oxidise organic carbon. The resulting carbon dioxide was detected using an infrared detector.

3.2.2.4. High Pressure Size Exclusion Chromatography

The HPSEC systems that were used in this study included (a) a system utilising a preparative scale column (250 mm x 22 mm, particle size 30 μm) coupled with a UV₂₅₄ detector in series with an organic carbon detector (OCD) (Huber and Frimmel, 1991) (Method A); (b) a system utilizing an analytical column, to provide optimum separation, coupled with a UV₂₅₄ detector (Method B); and (c) a system using a preparative scale column interfaced with UV₂₅₄, fluorescence and OCD-specific detectors in series (Her *et al.*, 2002a, Her *et al.*, 2002b) (Method C).

3.2.2.5. Method A

In this method, HPSEC of filtered samples was performed according to a previously described method using a 'preparative' polymer based stationary phase, TSK HW-50S column (length 250 mm, inner diameter 20 mm, particle size 30 μm , pore size 125 Å, Toyopearl, Japan), a 26.8 mmol L⁻¹ phosphate mobile phase (Na₂HPO₄·2H₂O = 1.5 g L⁻¹, KH₂PO₄ = 2.5 g L⁻¹, pH 6.6, ionic strength 39.0 mmol L⁻¹), and on-line UV₂₅₄ and OCD systems (Huber and Frimmel, 1994, 1996) at Karlsruhe University, Karlsruhe Germany. The flow rate was 1 mL min⁻¹ and the injection volume was 2 mL. In the OCD system, a cylindrical thin film reactor with a rotating inner cylinder and a low-pressure mercury lamp in the middle served to oxidise DOC to carbon dioxide, which in turn was quantified by a non-dispersive infrared (NDIR) detector (Huber and Frimmel, 1991). The void volume of the column (V_0 = 21 mL) was determined using dextran blue and the permeation volume of the column (V_p = 47 mL) was determined by injecting deionised water and using an electrical conductivity detector. Standards for MW calibration were polystyrene sulfonates (PSS): (35 700, 15 800 and 4 480 Da, Polymer Scientific Services).

The irreversible adsorption of some sample components onto the stationary phase of the column meant that not all of the sample eluted from the column.

The recovery of DOC through the column from each sample was determined by measuring DOC concentrations after the sample had passed through the HPSEC column and for a sample in which the column was bypassed. The concentration of the 'lost' fractions of DOC was determined by comparing the peak area of a sample that eluted from the column with the peak area of the same sample that had bypassed the column. Potassium hydrogen phthalate standards served to calibrate the OCD. Recoveries of DOC through the column ranged from 78-91%, which is consistent with previous observations of HPSEC analysis of NOM, and model compounds used to represent NOM (Specht and Frimmel, 2000).

3.2.2.6. Method B

In this method, HPSEC was performed using an 'analytical' silica based stationary phase, TSK G3000SW_{xl} column (length 300 mm, inner diameter 7.8 mm, particle size 5 μm , pore size 250 \AA , Tosoh BioSep, Japan) and a Hewlett Packard 1090 Series II HPLC instrument with filter photometric detection (FPD) at $\lambda = 254 \text{ nm}$ at Curtin University of Technology. The column had a $V_0 = 5.5 \text{ mL}$, as determined with dextran blue, and a $V_p = 13.3 \text{ mL}$, as determined with acetone. The mobile phase was a 20 mmol L^{-1} phosphate buffer (1.36 g L^{-1} KH_2PO_4 and 3.58 g L^{-1} Na_2HPO_4 , pH 6.8 and ionic strength = 40 mmol L^{-1}). Samples were injected manually using a Rheodyne 7125 6-port injection valve equipped with a 100 μL sample loop. The flow rate was 1 mL min^{-1} . Data analysis was performed using HP Chemstation software. The void volume of the column ($V_0 = 5.5 \text{ mL}$) was determined using dextran blue and the permeation volume of the column ($V_p = 13.3 \text{ mL}$) was determined using acetone. The system was calibrated using PSS standards (840, 4 400, 6530, 15 200, 35 300 and 81 800 Da, Polymer Scientific Services). The calibration curve was linear ($R^2 = 0.98$) over the MW range tested.

3.2.2.7. Method C

In this method, HPSEC was performed using a polymer based stationary phase, TSK-50S column (length 250 mm, inner diameter 20 mm, particle size 30 μm , pore size 125 \AA , Toyopearl, Japan) coupled with a UV₂₅₄ detector (SPD-6A Shimadzu), a fluorescence detector (Waters 470 Scanning Fluorescence Detector) scanning at an excitation wavelength of 282 nm and an emission wavelength of 353 nm, and a OCD system (Modified Sievers TOC 800 Turbo) (Her *et al.*, 2002a, Her *et al.*, 2002b) at the University of Colorado, Boulder, Colorado. The mobile phase system consisted of a phosphate buffer (2.4 mmol L⁻¹ NaH₂PO₄ + 1.6 mmol L⁻¹ Na₂HPO₄, pH 6.8), containing sodium sulfate (25 mmol L⁻¹), to achieve an ionic strength of 100 mmol L⁻¹. The mobile phase flow rate was 1 mL min⁻¹ and the sample volume was 2 mL. The void volume of the column ($V_0 = 28.17$ mL) was determined using dextran blue and the permeation volume of the column ($V_p = 61.3$ mL) was determined using acetone. Polyethylene glycol (PEG) MW standards (200 – 10 000 Da, Phenomenex) were used for determination of MW. This method is described in detail elsewhere (Her *et al.*, 2002a, Her *et al.*, 2002b).

3.2.2.8. HPSEC Data Treatment

Calculation of number average molecular weight (M_n) and weight average molecular weight (M_w) was based on the method of (Zhou *et al.*, 2000), who recommended a value of 1 % of the maximum chromatogram height as the high molecular weight (HMW) cut-off, and 2 % of the maximum chromatogram height as the low molecular weight (LMW) cut-off. Careful selection of the LMW cut-off is especially important because this has a marked effect on the calculation of MW. For Wanneroo raw water, Peak 1 eluted outside the calibration range in all of the methods that were used (i.e. has a very high MW), so this fraction was not included in the calculation of MW parameters, and the values listed in Table 3.2 relate to Peaks 2-8 only. However, omission of Peak 1 led to complications in selection of the HMW

cut-off for chromatograms obtained using Method A. Incomplete resolution of Peaks 1 and 2 meant that the detector response did not decrease to 1 % of the maximum response prior to the commencement of elution of Peak 2, and the HMW cut-off could not be determined using the specified method. In the case of Method A, the HMW cut-off was therefore taken as the minimum detector response between Fractions 1 and 2.

3.3. Results and Discussion

In order to study the MW characteristics of treated ground water and to evaluate two different treatment processes, water from five points of the Wanneroo GWTP were collected during autumn in May of 2002. The five sampling points were following aeration of the raw water (RW), following MIEX[®] resin treatment of the raw water (MIEX[®]), following MIEX[®] and alum coagulation of the raw water (MIEX[®]-C), following enhanced coagulation of the raw water (EC) and after filtration and final disinfection of the two treated water types (MIEX[®]-C and EC) had been combined (Figure 3.1).

3.3.1. Comparison of HPSEC Methods

To gauge the validity of using HPSEC for MW determinations and to gain spectroscopic as well as DOC-specific information, the samples (raw, MIEX[®], MIEX[®]-C, EC and clear water) were analysed using three different HPSEC methods in operation at three different laboratories around the world.

Method A involved the use of a preparative scale TSK-50s HPSEC column (length 250 mm, inner diameter 20 mm, particle size 30 μm , pore size 125 \AA) and OCD and UV₂₅₄ detection using a phosphate buffer, 8.4 mmol L⁻¹ Na₂HPO₄·2H₂O + 18.4 mmol L⁻¹ KH₂PO₄, as the mobile phase. Analysis with this method was performed by the author in the research group led by Professor Frimmel and with assistance from Dr Thomas Brinkman, at Karlsruhe University, Germany. Analysis with Method B utilized an analytical scale TSK G3000 SW_{XL} HPSEC column (length 300 mm, inner diameter 7.8 mm, particle size 5 μm , pore size 250 \AA) with UV₂₅₄ detection using a

phosphate buffer, $10 \text{ mmol L}^{-1} \text{ Na}_2\text{HPO}_4 + 10 \text{ mmol L}^{-1} \text{ KH}_2\text{PO}_4$, as the mobile phase, performed by the author at Curtin University. Method C involved the use of a preparative scale TSK-50s HPSEC column (length 250 mm, inner diameter 20 mm, particle size $30 \mu\text{m}$, pore size 125 \AA) and OCD and UV_{254} detection. The mobile phase system consisted of a phosphate buffer ($2.4 \text{ mmol L}^{-1} \text{ NaH}_2\text{PO}_4 + 1.6 \text{ mmol L}^{-1} \text{ Na}_2\text{HPO}_4$, pH 6.8), containing sodium sulfate (25 mmol L^{-1}), to achieve an ionic strength of 100 mmol L^{-1} . Detection was *via* OCD and UV_{254} methods. Analyses using this method were performed by the author in the laboratories at the University of Colorado, USA, with the kind invitation of Professor Gary Amy and the assistance of Dr Namguk Her.

Chromatograms utilizing Method A are shown in Figure 3.3, Method B in Figure 3.2 and Method C in Figure 3.4. Chromatograms obtained with Method C are not included in the initial comparisons of chromatographic separation due to the different nature of the mobile phase. The higher ionic strength mobile phase used for this method resulted in a different elution profile compared to Methods A and B and as such, results for method C are not introduced until after the separation of NOM has been discussed. In the two methods using OCD (Methods A and C), large diameter (20 mm) columns were used, since these detectors were not sufficiently sensitive to be compatible with the smaller injection volumes, and hence smaller amounts of analytes, which can be used with smaller diameter columns. The chromatographic results from these methods were compared with those from Method B, in which a smaller diameter column (7.8 mm) was interfaced with a UV_{254} detector. Comparison of chromatograms obtained using Methods A and B showed that the chromatographic separation obtained using the smaller diameter column (Method B; Figure 3.2) was superior to that which could be obtained with the large diameter columns (Method A; Figure 3.3). Further, the analysis time required was more than four-fold greater than that required for the method utilising the small diameter column (67 min and 15 min, respectively). However, the chromatograms produced by the two methods showed a similar elution pattern in all samples, and these

similarities suggest that direct comparison of results obtained using these two methods will be valid.

Similarities in the elution pattern of the two methods support the findings of Peuravuori and Pihlaja (1997) who stated that 'the most critical step in studying aquatic humic solutes in HPSEC is the choice of the eluent'. In the current study, two vastly different types of HPSEC stationary phases, silica based compared to polymer based phases, but using very similar mobile phases, were compared. Method A used an HW-50s material made from copolymerisation of ethylene glycol and methacrylate type polymers. This material has a particle size of 20 - 40 μm (mean particle size 30 μm) and a pore size of 125 \AA . Method B employed a TSK G3000SW_{xl} media with an organic phase bonded to a silica based resin, a particle size of 5 μm and a pore size of 250 \AA . Method A used a 26.8 mmol L^{-1} phosphate buffer at pH 6.6 with an ionic strength of 39.0 mmol L^{-1} , while Method B utilised a 20.0 mmol L^{-1} phosphate buffer at pH 6.8 with an ionic strength of 40 mmol L^{-1} . While the actual compositions of the two eluents were different, it was the ionic strength of the mobile phase which had the greatest influence on the separation. In solution, neutral, acidic and basic salts are dissociated into their respective ions according to their dissociation constant. Therefore, the measure of the electrolyte concentration is not the molar concentration of the salts themselves, but the ionic strength (Mori and Barth, 1999). The two eluents with very similar ionic strengths resulted in similar separation performance on these two completely different types of HPSEC media. Thus, it can be seen that it is the composition of the mobile phase, and, more specifically, the ionic strength of the mobile phase, that exerts the most influence on separation, rather than the composition of the stationary phase.

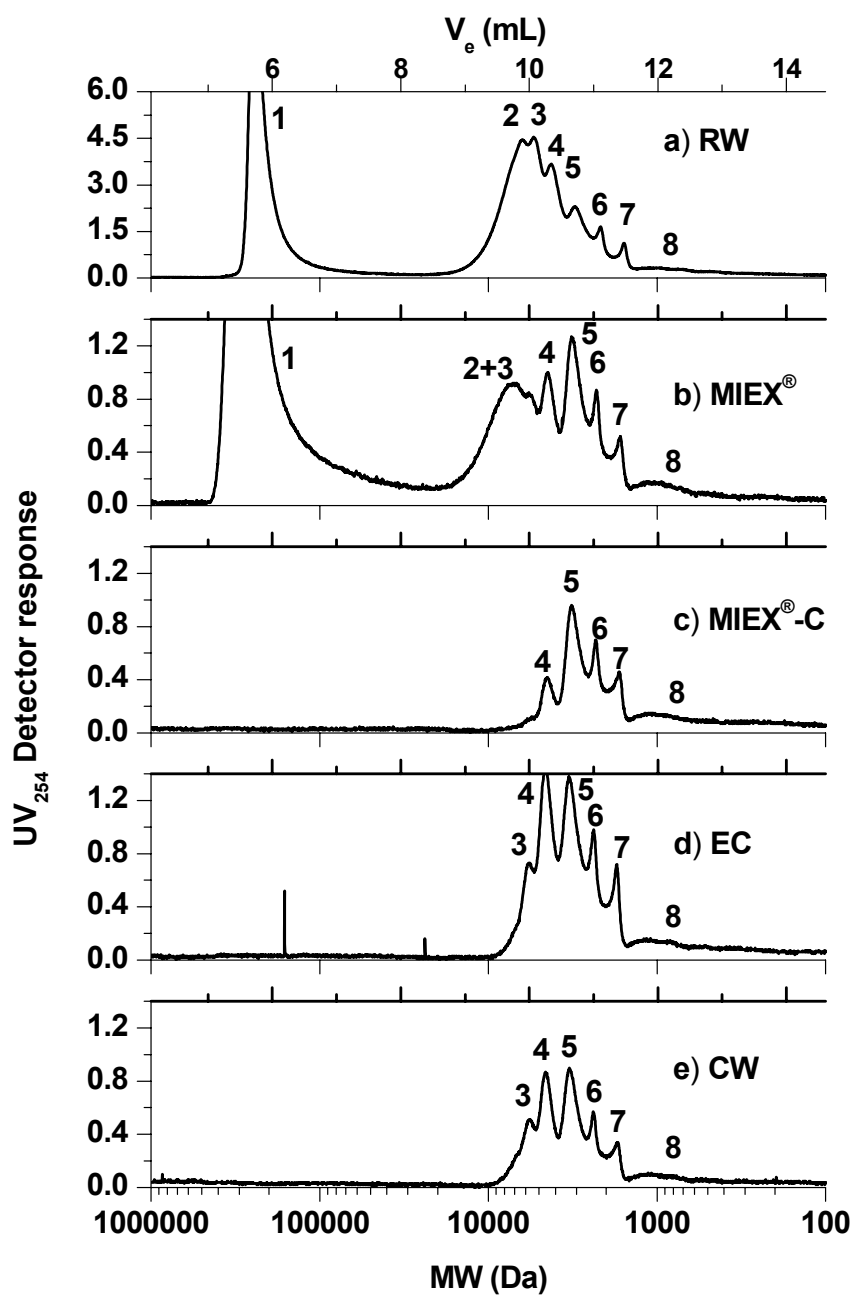


Figure 3.2 HPSEC-UV₂₅₄ chromatograms (Method B, 300 mm x 7.8 mm column) of water samples from the Wanneroo GWTP: a) RW, b) MIEX[®], c) MIEX[®]-C, d) EC, e) clear water. Peaks in each chromatogram are numbered as referred to in the text.

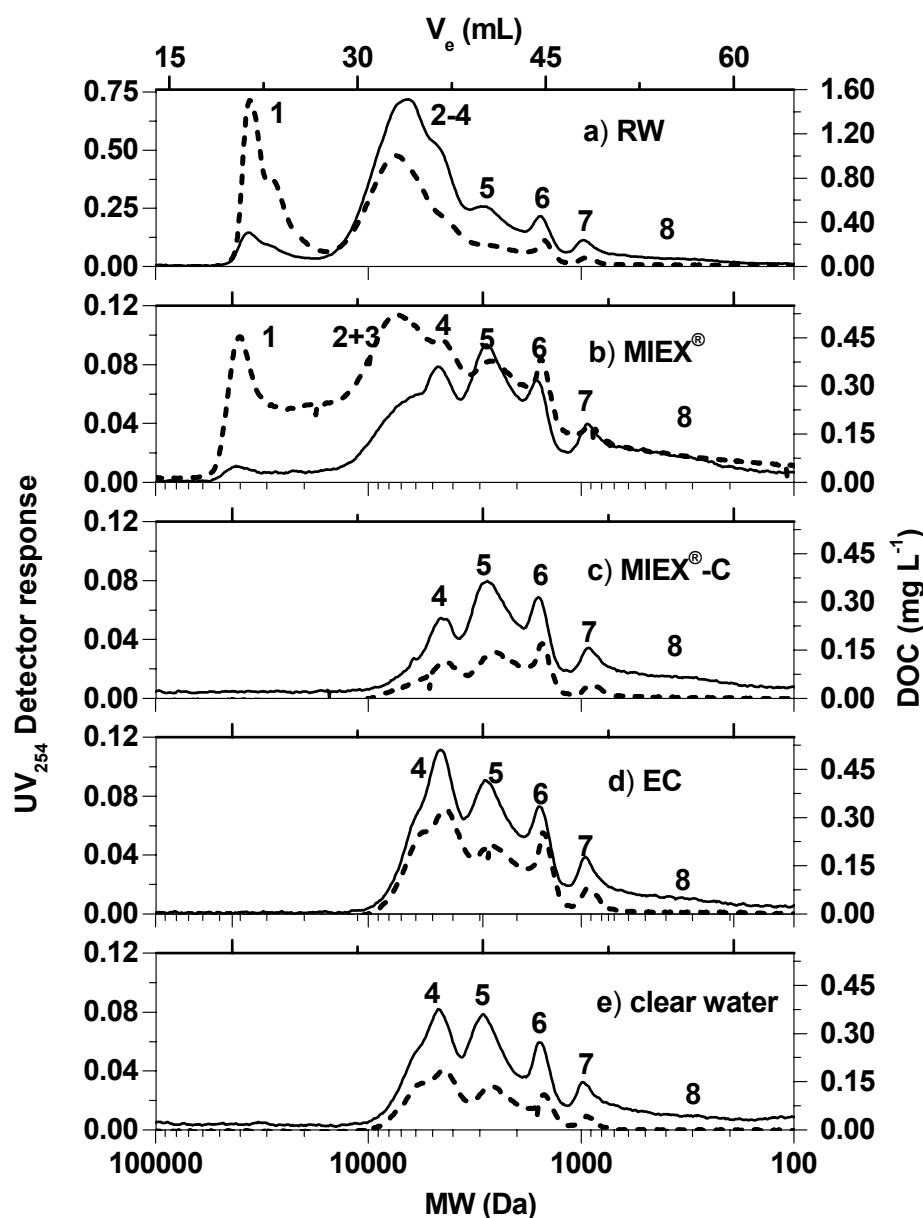


Figure 3.3 HPSEC-UV₂₅₄-OCD chromatograms (Method A, 250 mm x 20 mm column) of water samples from the Wanneroo GWTP: a) RW, b) MIEX[®], c) MIEX[®]-C, d) EC, e) clear water. Peaks in each chromatogram are numbered as referred to in the text. Black line = DOC response; dashed line = UV₂₅₄ response.

The profiles of DOC and UV₂₅₄-active DOC from the use of Methods A and B consisted of a peak at V_0 , which was present in both the raw water (Figure 3.2a and Figure 3.3a) and in the MIEX[®]-treated samples (Figure 3.2b and Figure 3.3b), and a smaller, later-eluting group of peaks, which was present in all of the samples. The material represented by the peak at V_0 (Peak 1) was completely excluded from the stationary phases of both columns (as

shown by Dextran blue, MW 200 KDa), and was therefore not subjected to the size exclusion separation process. While this peak represents only a small fraction of the total DOC, the same material represents a major proportion of the total UV₂₅₄-active substances in the sample, illustrating the significant discrepancies that occur between UV₂₅₄ detection and OC detection. The material represented by the later-eluting group of peaks (Peaks 2-8) did permeate the pores of the stationary phases, and provides a valid comparison of the separation efficiency of each column. For example, in the case of the RW sample (Figure 3.2a and Figure 3.3a) this material was separated into six semi-resolved peaks when using the 300 mm x 7.8 mm column, but into only three semi-resolved peaks with some shoulders when using the 250 mm x 20 mm column. In the experiment using the larger diameter column, even the material eluting at V_0 was not completely resolved from the later-eluting material, but these areas of material were clearly well separated, to the baseline, by the smaller diameter column.

In the case of two of the treated water samples, EC-treated (Figure 4.2d and Figure 4.3d) and CW (Figure 3.2e and Figure 3.3e), Peaks 3 and 4 could not be resolved using the larger diameter column, while these were well separated using the smaller diameter column. With its improved resolution, the smaller diameter column clearly has the potential to provide more information on the character of DOC, and on the fractions of DOC that were removed by the water treatment processes, than is available when using the larger diameter column. These observations illustrate the need for OC detectors that have signal-to-noise characteristics that are compatible with these smaller diameter columns.

Method C used the same column as in Method A, i.e. a HW-50s polymer based resin with a mean particle size of 30 μm and a pore size of 125 \AA . The mobile phase was different, however, to that utilised in Methods A and B. In Method C, the mobile phase consisted of a 4 mmol L^{-1} phosphate buffer at pH 6.8 with sodium sulphate (25 mmol L^{-1}) added to bring the ionic strength of the buffer system to 100 mmol L^{-1} . It has been established (Chin

and Gschwend, 1991, Chin *et al.*, 1994, Peuravuori and Pihlaja, 1997, Mori and Barth, 1999) that higher ionic strength buffers, particularly above 100 mmol L^{-1} , may reduce the effect of ion exclusion and increase the elution volume of molecules. The effect on ion exclusion with the use of the high ionic strength mobile phase in Method C is difficult to determine but there is no doubt that elution time increased with the increased ionic strength of this buffer system (Figure 4.4). It is also evident from comparison of Figure 3.4 with Figure 3.2 and Figure 3.3 that there was a considerable loss in resolution with the increase in ionic strength of the mobile phase. When compared to the chromatograms from analysis of raw water by Method B (Figure 3.3 a), where six semi-resolved peaks could be identified for the included fraction, and Method A (Figure 3.2 a), where 3 semi-resolved peaks and some shoulders could be identified, the chromatogram from use of Method C (Figure 3.4 a) showed only one broad peak with a long tail that never fully returns to the baseline. Comparison of the treated water chromatograms showed a similar trend. Analysis of EC and CW samples showed four semi-resolvable peaks for Method A (Figure 3.3 d and Figure 3.3 e) and five semi-resolvable peaks for Method B (Figure 3.2 d and Figure 3.2 e). In comparison, analysis of these two samples by Method C showed two broad peaks at increased elution volume.

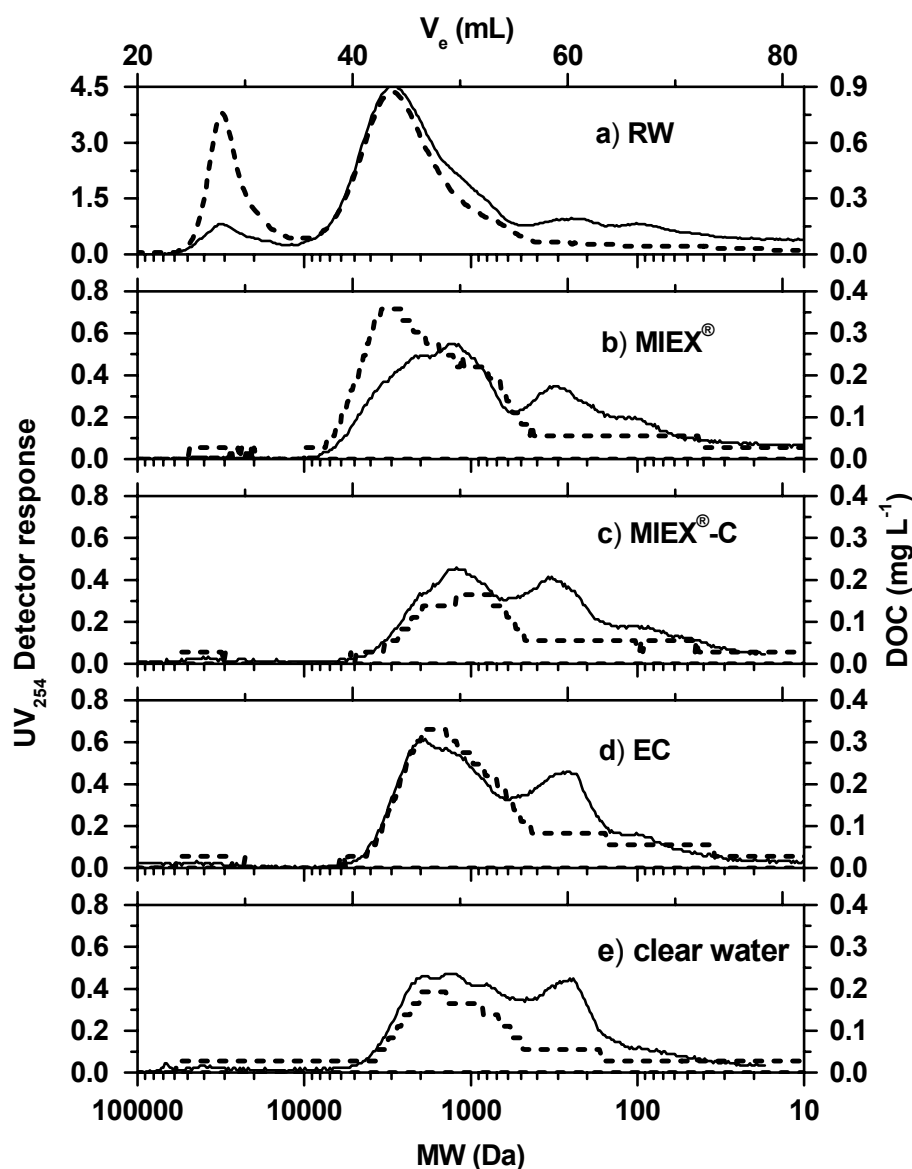


Figure 3.4 HPSEC-UV₂₅₄-OCD chromatograms (Method C, 250 mm x 20 mm column) of water samples from the Wanneroo GWTP: a) RW, b) MIEX[®], c) MIEX[®]-C, d) EC, e) clear water. Peaks in each chromatogram are numbered as referred to in the text. Black line = DOC response; dashed line = UV₂₅₄ response.

As previously mentioned, it is difficult to determine the effect of the mobile phase on ion exclusion processes, however, the increase in elution volume is indicative that the sample molecules were able to penetrate further into the pores of the stationary phase and were therefore more retained. It is also evident, especially for the RW sample (Figure 3.4 a), that the tailing peak at higher elution volume never fully returned to the baseline well past the

permeation volume of this system, representing molecules continuing to be slowly eluted from the column.

Thus, increasing the mobile phase ionic strength increased the elution volume of sample components by allowing greater permeation into the pores of the stationary phase or by promoting adsorption of sample components onto the stationary phase. Use of a lower ionic strength buffer appeared to resolve the DOC into a greater number of peaks, as observed in results from Methods A and B. The improved resolution of these fractions with the lower ionic strength buffers allowed more precise comparison of the different water treatment processes in this study.

3.3.2. Raw Water Characteristics

In order to compare the MW characteristics of DOC in the Wanneroo raw water with those of DOC from other sources, number average molecular weight (M_n) and weight average molecular weight (M_w) were calculated for two of the three methods. Values of M_n and M_w obtained for Wanneroo raw water (Table 3.2) agreed reasonably well, even though different methods of detection and calibration were used. Values of M_w were remarkably consistent for Method A (with OCD) and Method B, but M_w was high for Method A when using UV₂₅₄ detection. This high value was probably caused by the incomplete resolution of peaks 1 and 2 in this chromatogram, and was exacerbated by the high UV₂₅₄ response of peak 1. Zhou *et al.* (2000) suggested a HMW cutoff of 1 % of the maximum chromatographic height when calculating MW parameters. However, due to incomplete resolution of peaks 1 and 2 using Method A with UV₂₅₄ detection the chromatogram never reaches a value of 1 % of the maximum chromatographic height, as a result the M_w is higher than would be expected. Values of M_n were highly dependent on the LMW cut-off chosen, especially in the case of Method A (OCD), where significant peak tailing occurred. Peak tailing was much less evident in the case of both of the chromatograms obtained using UV₂₅₄ detection, and this may explain the relatively high values of M_n obtained by these methods.

Molecular weight parameters determined using both Method A and Method B showed that M_n and M_w for DOC in Wanneroo raw water were relatively high when compared to published values for NOM from other sources. For example, previously established values of M_n for the IHSS reference material Suwannee River Fulvic Acid (SRFA) range from 1 160 – 1 385 Da, while those for M_w range from 2 114 – 3 120 Da (Perminova *et al.*, 2003). Although comparison with published values is complicated by differences in methodologies (e.g. use of different calibration standards, mobile phase systems and HPSEC columns), even when these differences are taken into consideration, values for Wanneroo raw water appear to be more similar to those of northern European swamp water fulvic acids (Perminova *et al.*, 2003) and lake waters (Peuravuori and Pihlaja, 1997). For example, the values for M_n and M_w for Nordic Reference Fulvic Acid were reported as being 3 870 Da and 6 100 Da, respectively, and these appeared to be typical of waters from some Finnish lakes (Peuravuori and Pihlaja, 1997).

Table 3.2. Molecular weight parameters (M_n , M_w and ρ) for Wanneroo raw water (excluding Fraction 1) determined using two different HPSEC methods with two different detection methods.

Detection method	M_n	M_w	ρ
Method A (OCD)	2 405	5 319	2.21
Method A (UV ₂₅₄)	4 273	6 371	1.49
Method B (UV ₂₅₄)	3 407	5 294	1.55

The MW distribution of both UV₂₅₄-active DOC and total DOC in Wanneroo raw water is broadly bimodal in nature, as shown in chromatograms using both UV₂₅₄ detection and OCD (Figure 3.2a and Figure 3.3a). The peak denoted as Peak 1 in these chromatograms represents material eluting at V_0 , and this material is the principal cause of the high SUVA in this sample. Although the high MW and very high SUVA values of this peak are suggestive of humic substances that are highly aromatic, it is more likely that this material is colloidal in nature, and may also comprise some inorganic substances. Although samples were filtered (0.45 μ m Nylon membrane) prior to injection onto the HPSEC column, colloidal material is well known to permeate membranes of much smaller pore size (Buessler *et al.*, 1996).

Previous workers (Huber and Frimmel, 1996, Schmitt *et al.*, 2003) observed similar characteristics in a German lake water sample, and attributed a similar early eluting fraction with high SUVA to inorganic colloidal material (which would produce a UV_{254} signal due to light-scattering effects), speculating that it may contain silicates, iron oxyhydroxides and aluminium. The presence of colloidal material in this aerated raw water sample is entirely consistent with the composition of the source water and the sample history: prior to aeration, the raw groundwater from this aquifer contains appreciable levels of sulfide, iron (II) and DOC and it is depleted in oxygen ($<1 \text{ mg L}^{-1}$). Thus, one potential source of colloidal material is from the formation of iron oxyhydroxides from oxidation of ferrous iron in the aeration step. Iron from this water source is strongly complexed with organic matter (Heitz, 2002), and precipitated iron would be associated with organic matter, which could explain why some DOC was observed in this peak (Figure 3.3a). Alternatively, the material in Peak 1 may consist of sulfur species associated with organic matter, either in colloidal form as elemental sulfur or in solution (partially oxidised sulfur compounds such as polythionates and polysulfides absorb at $\lambda = 254 \text{ nm}$). Elemental sulfur is a product of the oxidation of sulfide, but in the presence of organic matter, as occurs in the groundwaters in this study, the formation of crystalline sulfur is inhibited, and “dirty” sulfur is formed instead (Heitz, 2002). Dirty sulfur consists of liquid-like clusters of cyclic sulfur (S_6 - S_8), incorporating hydrophobic organic molecules. This does not crystallize and separate from solutions in the same way that pure elemental sulfur does (Steudel, 1996). Either colloidal sulfur in solution or dirty sulfur, both associated with organic matter, or colloidal iron associated with organic matter could therefore produce the DOC and UV_{254} responses observed for Fraction 1.

The later-eluting UV_{254} -active and OCD peaks (Peaks 2-8 in Figure 3.2 and Figure 3.3) are more alike than the earlier-eluting fraction discussed above, but there are nevertheless some notable differences. Peaks 2, 3 and 4, which elute as one unresolved peak in Figure 3.3a and three partly resolved peaks in Figure 3.2a, are likely to be enriched in humic substances of relatively high MWs (up to around 10 000 Da). Humic substances are rich in

aromatic functional groups (Thurman, 1985), and these are easily detected by both OCD and UV₂₅₄ detectors. In our sample, the signals for Peaks 5-7 are moderate using UV₂₅₄ compared to OCD, and may thus comprise fulvic acids, conjugated unsaturated acids or keto-acids, as have been observed in previous studies (Huber and Frimmel, 1996, Specht and Frimmel, 2000). Peak 8 is comprised of DOC of the lowest MW, which eluted as a broad band of poorly resolved material that eluted with a long tailing peak. This lowest MW DOC material is thought to be important in drinking water treatment as this material is reported to be poorly removed by conventional processes and considered to be bioavailable (Volk *et al.*, 2000). Significantly, in this study, the UV₂₅₄ detection method underestimated the relative proportion of this important fraction.

3.3.3. Evaluation of Water Treatment Processes

Analysis using both the HPSEC-UV₂₅₄ (Figure 3.2a-e) and the HPSEC-UV₂₅₄-OCD (Figure 3.3a-e) methods showed that significant proportions of the DOC in the aerated raw water were removed by the combined MIEX[®]-C process and by the EC process. In order to quantitatively demonstrate the effects of these treatment processes on each of the DOC MW peaks shown in Figure 3.3, the concentration of DOC represented by each peak or group of peaks (Fractions 2-4) was also calculated, and the results are presented in Figure 3.5. In general, the results in Figure 3.3 and Figure 3.5 show that the coagulation processes preferentially removed the higher MW material, while MIEX[®] appeared to remove organic matter over a wide MW distribution, favouring the medium MW range.

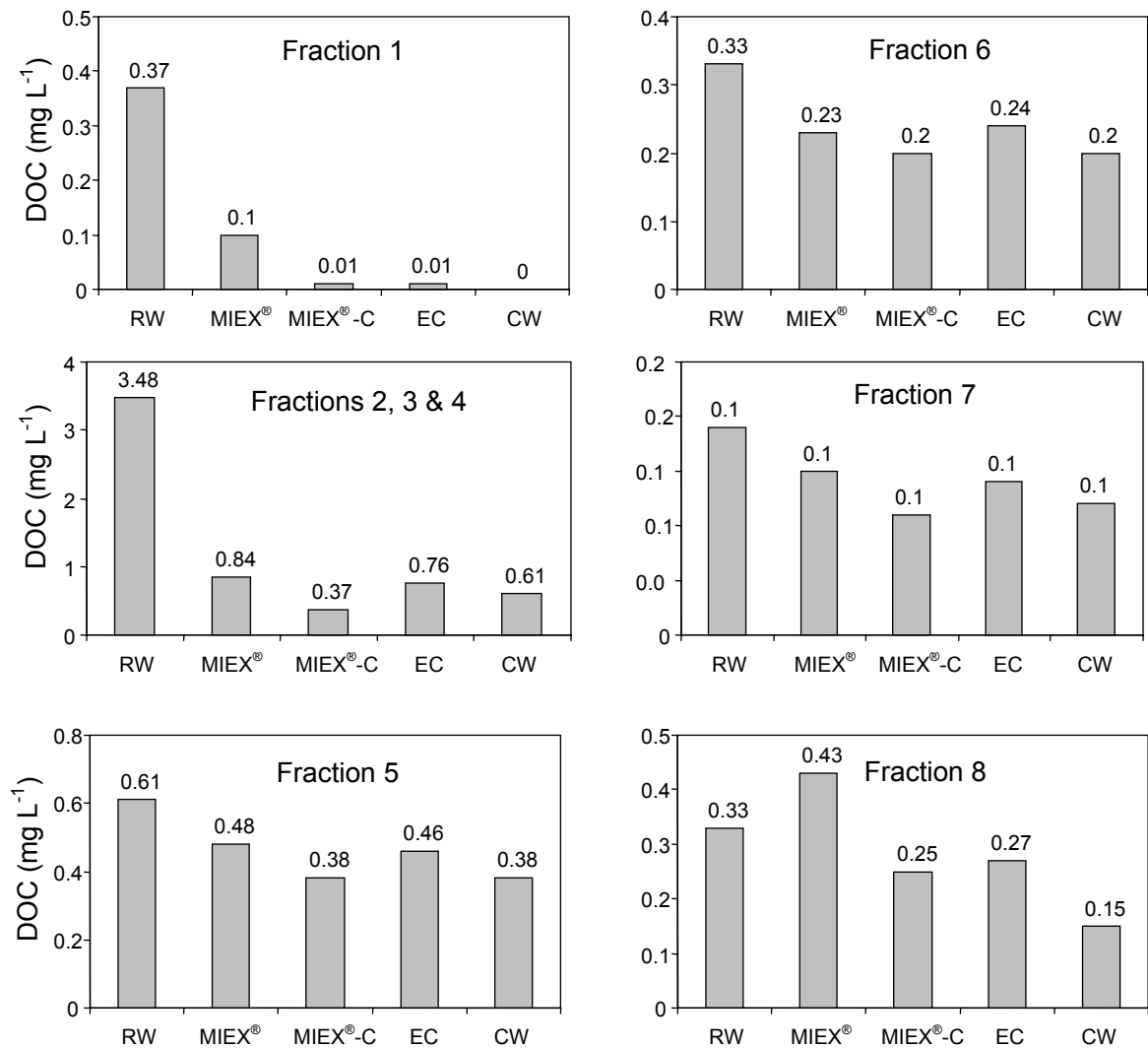


Figure 3.5 DOC concentrations (mg L^{-1}) in MW fractions from samples from the Wanneroo GWTP. Values above bars represent DOC concentrations in each fraction (mg L^{-1}).

The highest MW components (Peaks 1 and 2) were very effectively removed by coagulation processes: there was no trace of this material in water that was treated by either of the two coagulation processes (Figure 3.2c and d and Figure 3.3c and d); however, Peak 1 was poorly removed by the MIEX[®]-only step (Figure 3.2b and Figure 3.3b), and material in Peaks 2 and 3 was also more resistant to removal by the MIEX[®] process than by coagulation (Figure 3.2b and Figure 3.3b). The poor removal of Peak 1 by the MIEX[®] (Figure 3.2b and Figure 3.3b) process is consistent with suggestions that this fraction may be comprised of colloidal organic and

inorganic material, since colloids would not be removed by an anion exchange process, but are known to be very effectively removed by alum coagulation processes (Vrijenhoek *et al.*, 1998). The increase in SUVA observed after treatment of raw water in the MIEX[®] process (Table 3.1) was clearly due to the poor removal of Peak 1, and any effect from the other fractions was negligible in comparison. This study illustrates the application of HPSEC-UV₂₅₄-OCD to improved understanding of water treatment operations. For example, since Peak 1 is probably colloidal material, it could be removed by alternative processes, such as nanofiltration, which, when combined with MIEX[®], could give low SUVA values, comparable to MIEX[®]-C. However, aggregate parameters, such as total SUVA, do not provide sufficiently detailed information to offer such insights.

The observation that Peaks 2 and 3 were effectively removed by both coagulation processes, but poorly removed in the MIEX[®] only process, is also in agreement with the probable nature of the material within these fractions, i.e. DOC of intermediate MW (~5 000-7 000 Da), enriched in humic and fulvic hydrophobic material. Much of the NOM in groundwaters from this region is thought to consist largely of tannin-derived substances, probably from condensed tannins (Heitz, 2002), which are composed predominantly of phenolic moieties, with relatively minor carboxylic acid content. As well there could be significant lignin input from forested areas overlying the groundwater abstraction zone. Kazpard *et al.* (2006) have shown in a study of a model humic acid, that hydroxy aromatic moieties are preferentially removed by alum coagulation, supporting the above observation. Such phenolic moieties would not be amenable to removal via the MIEX[®] ion exchange mechanism because they are likely to be present in their protonated (uncharged) form at the pH of treatment (7.0-7.5; pK_a phenol = 9.8 (Schwarzenbach *et al.*, 1993 for example)), consistent with the poor removal of these fractions in the MIEX[®] only process. The hydrophobic, high SUVA, high MW material that probably comprises most of Peaks 2 and 3 is known to be well-suited to removal by alum coagulation, as was observed in the current study. These observations were confirmed by the SUVA profiles,

presented in Figure 3.6a. The SUVA profiles were constructed by taking the UV_{254} chromatograms and dividing the obtained signal by the signal obtained from the OCD chromatogram using Method C. These MW specific-SUVA profiles showed that coagulation treatment preferentially removed aromatic components, and that, while MIEX[®] treatment removed DOC, it did not remove aromatic compounds in preference to non-aromatic moieties. The SUVA profile of the MIEX[®]-treated water (Figure 3.6b) was lower than that of the raw water (Figure 3.6a) over the entire MW range, but the shapes of the two profiles were not markedly different. Indeed, in the MIEX[®] treatment process, the removal of UV absorbing moieties appeared to be lowest at high MW, in agreement with suggestions above that these high MW fractions (Peaks 2 and 3) are enriched in uncharged phenolic moieties, which would not be readily removed by the ion exchange process. However, as expected, both of the coagulation processes removed the UV absorbing species in the medium to high MW fractions much more effectively than the MIEX[®] only process. The SUVA profiles of both coagulation processes (Figure 3.6c and Figure 3.6d) were very similar, clearly demonstrating how these similar processes removed similar DOC species.

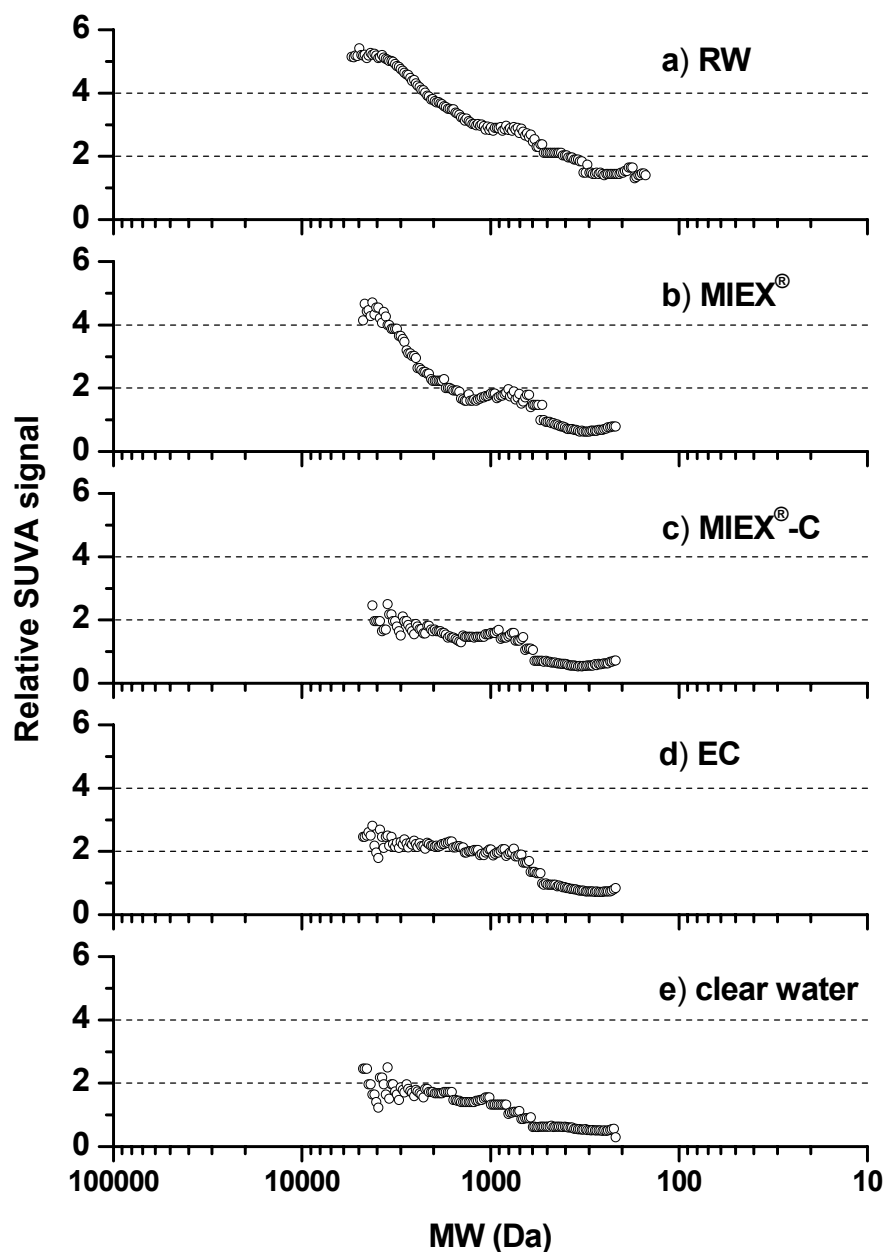


Figure 3.6 MW specific-SUVA chromatograms (Method C, 250 mm x 20 mm column) of water samples from the Wanneroo GWTP: a) RW, b) MIEX[®], c) MIEX[®]-C, d) EC, e) clear water.

Peak 4 appeared to be much more effectively removed by the MIEX[®] process than by EC (Figure 3.5), but since it was difficult to resolve this peak from Peak 3 using HPSEC-OCD (Method A), this fraction was not represented separately in Figure 3.5. Preferential removal with MIEX[®] treatment suggests that the material in Peak 4 contained anionic species. Material represented by Peaks 5-7 was removed to a similar extent by both

MIEX[®] and EC treatment (Figure 3.5). This suggests that these fractions are probably enriched in negatively charged species such as carboxylic acids, and accordingly these anionic species of relatively low MW (1 000 – 4 000 Da) should be readily removed by ion-exchange. These low MW fractions (peaks 5-7) were also readily removed by EC. Peak 8 was the only fraction that appeared to be poorly removed by both processes, and in fact the concentration of this fraction appeared to increase after MIEX[®] treatment (Figure 3.2 and Figure 3.3). However, quantification of this peak was not as reliable as for the other peaks, since the chromatographic resolution for this peak was very poor due to strong interactions of the analytes with the HPSEC stationary phase. If Peak 8 is indeed bioavailable, it would be significant in the water treatment context, and it would be beneficial to further develop the HPSEC analytical technique so that this material can be better resolved and detected. These techniques would need to utilize OCD detection, since the material has very low SUVA.

The MIEX[®]-only process outperformed EC in the removal of only one peak (i.e. Peak 4), but when MIEX[®] was followed with an alum coagulation stage (MIEX[®]-C), significantly lower DOC concentrations were obtained across all MW fractions compared with EC. The improved performance of MIEX[®] when combined with other processes is consistent with previous observations (Drikas *et al.*, 2003, Smith *et al.*, 2003). The application of alum coagulation after MIEX[®] treatment appeared to render the coagulation process more effective than when the latter process (such as EC) was used in isolation. For example, even the peaks that were preferentially removed by EC (e.g. Peaks 2 and 3) were removed more effectively when MIEX[®] treatment preceded the coagulation step (see Figure 3.5). Chromatograms obtained using the analytical HPSEC column, in which Peak 3 is clearly separated from peak 4 (Figure 3.2), show that the UV₂₅₄-active component of Peak 3 could not be removed by either process in isolation: the UV₂₅₄-active component of this peak was poorly removed by MIEX[®]-only and only marginally better removed by EC. However, Peak 3 was almost totally removed by the combined MIEX[®]-C process. Even though EC had been

optimised for maximum removal of DOC, the combined MIEX[®]-C process was still more effective at removing all fractions of DOC (including those that were preferentially removed by EC) than either the MIEX[®]-only or the EC process. MIEX[®], when combined with subsequent alum coagulation, proved to be by far the most effective treatment, removing the greatest amount of DOC over the greatest MW range, demonstrating the eminently complementary functions of these two processes.

The present study confirmed previous results which showed that DOC removal using MIEX[®]-C surpassed that achieved using EC by about 25 % (Smith *et al.*, 2003), but it also showed that most of the additional DOC removed by MIEX[®]-C comprised DOC of a surprisingly narrow MW distribution. DOC concentrations achieved after MIEX[®]-C and EC treatments were 1.59 and 2.14 mg L⁻¹, respectively, a difference of 0.55 mg L⁻¹. According to results shown in Figure 3.5, almost 70 % of this differential portion of DOC can be attributed to Peaks 2-4 (i.e. the amount of DOC in Peaks 2-4 that was removed by MIEX[®]-C was 0.39 mg L⁻¹ more than the amount of DOC in these fractions removed by EC). Examination of chromatograms in Figure 3.2 and Figure 3.3 shows that Peak 2 was equally well removed by both processes, so the most important fractions in the context of the present discussion are Peaks 3 and 4, which fit within a narrow MW range (4 000 – 7 000 Da).

3.3.4. HPSEC-Fluorescence Spectroscopy

Measurement of the fluorescence of MW fractions (HPSEC-Flu) of the raw and treated water samples was carried out using a multidetection system (UV₂₅₄, followed by fluorescence and finally OCD), as described by (Her *et al.*, 2003) (Method C). The chromatograms from measurement of the five samples taken from the Wanneroo GWTP were analysed by HPSEC-Flu using an excitation wavelength of 282 nm and emission wavelength of 353 nm to obtain a spectra representative of humic and fulvic acids and protein type structures (Her *et al.*, 2003) and presented in Figure 3.7.

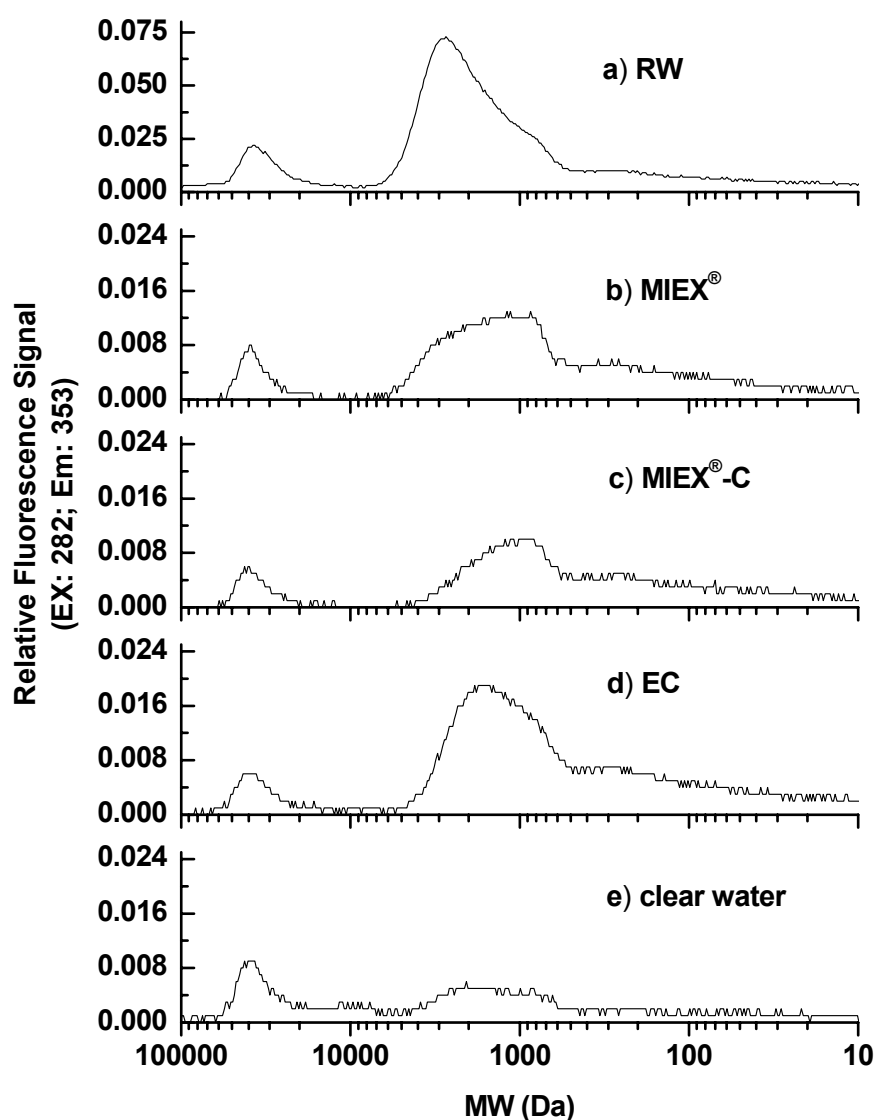


Figure 3.7 Chromatograms from HPSEC-Flu (Method C, 250 mm x 20 mm column, excitation wavelength of 282 nm and emission wavelength of 353 nm) of water samples from the Wanneroo GWTP: a) RW, b) MIEX[®], c) MIEX[®]-C, d) EC, e) clear water.

The specific fluorescence (S_{FLU}) in each sample was then calculated. S_{FLU} is the DOC-normalised fluorescence, obtained by dividing the fluorescence response (peak height) at a particular MW by the DOC response (peak height) at that MW in the HPSEC-OCD chromatogram. The MW profiles of S_{FLU} (Figure 3.8) were quite different to the SUVA profiles (Figure 3.6), demonstrating the distinction between the types of chemical sub-structures and functionalities that were detected by these two methods. Whereas SUVA tended to decrease with decreasing MW, especially in the raw and MIEX[®]-treated samples, in all samples, with the exception of the clear water,

the S_{FLU} increased with decreasing MW, to a maximum around 750 Da, and then decreased. The S_{Flu} in the raw water sample was relatively low at high MW (~5 000 Da), increasing rapidly to a broad maximum at 800 – 3 000 Da, and then decreasing steadily with decreasing MW from 750 Da (Figure 3.8a). The combination of low S_{FLU} and high SUVA at relatively high MW (5 000 Da) observed in this sample is consistent with similar observations in previous studies (Perminova *et al.*, 1998). Low S_{Flu} combined with high SUVA suggests the presence of aromatic substances with high structural rigidity, that is, high MW (Perminova *et al.*, 1998). The decrease in S_{Flu} at low MW (<750 Da) agrees with other findings in the current study that these fractions consist of compounds that contain lower relative amounts of aromatic or conjugated moieties than the higher MW fractions.

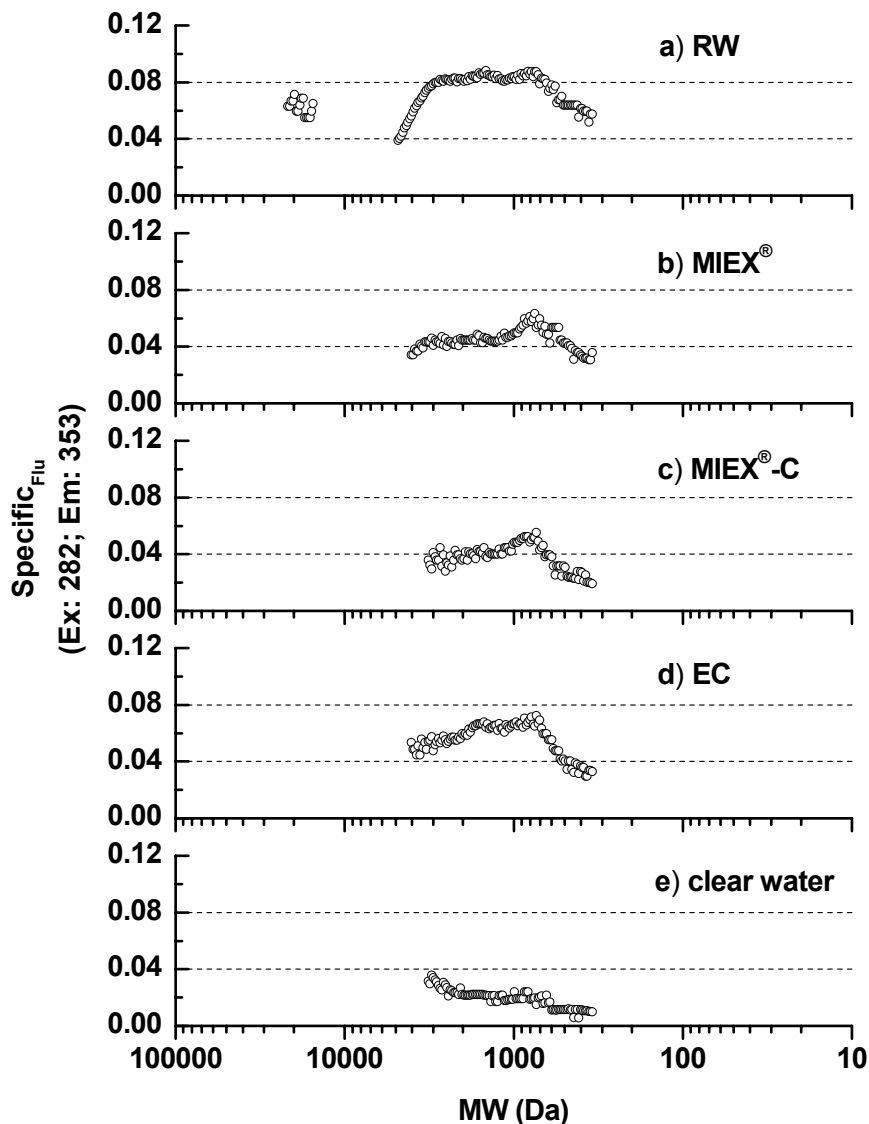


Figure 3.8 MW S_{Flu} chromatograms (Method C, 250 mm x 20 mm column) of water samples from the Wanneroo GWTP: a) RW, b) MIEX[®], c) MIEX[®]-C, d) EC, e) clear water.

While the MW profiles of DOC and UV_{254} -active substances in the clear water (CW) sample were an approximate average of those from the EC and MIEX[®]-C process, surprisingly, the S_{Flu} profile of the CW sample was much lower than the corresponding profiles from the coagulation processes. The CW sample essentially comprised equal proportions of water exiting the MIEX[®]-C and the EC processes, and it was therefore expected that the quality of this water would be approximately representative of the average of these two samples. Water exiting the coagulation processes (i.e. clarifiers) is filtered through conventional sand/anthracite filters and is then disinfected by

chlorination prior to distribution (chlorine dose = 4.4 mg L⁻¹). Values of DOC and UV₂₅₄ for the CW sample were close to the average of those in the samples from treatment by MIEX[®]-C and EC (Table 3.1), showing that the processes of filtration and chlorination did not significantly affect these aggregate water quality characteristics. However, chlorination can affect the fluorescence characteristics of DOC by altering the molecular structure of aromatic and/or other moieties, changes which would not necessarily be detectable by alternative methods such as SUVA or total DOC (Skoog, 1982). The substantial decrease in fluorescence observed in the CW sample probably occurred as a result of substitution of bromine or chlorine atoms onto aromatic or heterocyclic rings within the DOC. The SUVA profile for this sample was only marginally lower than that expected from equal mixing of water from MIEX[®]-C and EC, suggesting that only a minor loss of aromaticity occurred (i.e. substitution of halogens predominated over ring cleavage).

3.4. Conclusions

In this comparative study, the advantage of OC detection was highlighted, especially with regard to the very high MW peaks most likely comprised of inorganic colloids complexed to small concentrations of DOC. Here the overestimation by UV₂₅₄ detection of the relative amounts of DOC, likely due to light scattering in the UV detector from the colloidal material, highlighted the need for OCD detection. Also, when the aromatic content or degree of conjugation is low, UV₂₅₄ detection underestimated the contribution of certain peaks, particularly those in the mid MW range.

The advantage of smaller 'analytical' scale columns compared to 'preparative' scale columns was demonstrated for the MW determination of NOM of both raw and treated waters. Separation of MW components into eight semi-resolved peaks using analytical HPSEC columns was possible, while Peaks 2, 3 and 4 in the raw water and Peaks 3 and 4 in the treated waters were left unresolved using a preparative HPSEC column. This was particularly important for comparing the two treatment strategies at the

Wanneroo GWTP as Peaks 3 and 4 were the most important in the comparisons of the MIEX[®] and coagulation processes. Combining multiple detectors for HPSEC analysis was particularly useful as information on the structure of material in each MW component could be obtained.

Importantly, using OCD in combination with UV₂₅₄ detection for the evaluation of water treatment process at the Wanneroo GWTP demonstrated some key outcomes. The highest MW fraction, significantly overestimated by UV₂₅₄ detection, was shown to contribute a minor percentage of the total DOC when using OCD. Also, this fraction was relatively easily removed by both conventional and enhanced coagulation, but only partially removed after MIEX[®] treatment. The next largest MW DOC peaks (Peaks 2 and 3 in Figure 3.3) were also completely removed by both coagulation processes, but again were poorly removed after treatment by the MIEX[®] process. The DOC represented by peak 4 (Figure 3.3) was the MW fraction most effectively removed after MIEX[®] treatment, far more effectively than after enhanced coagulation treatment. Interestingly, treatment with conventional coagulation following MIEX[®] treatment further increased the removal of Peak 4 in the HPSEC-UV₂₅₄-OCD chromatogram (Figure 3.3), compared to enhanced coagulation, indicating MIEX[®] treatment somehow altered the nature of this material making it more amenable to removal by alum coagulation. The remaining DOC was removed to similar degrees by the combined MIEX[®]-coagulation process and the enhanced coagulation process. Treatment of the raw water with MIEX[®] resin followed by alum coagulation outperformed enhanced coagulation by approximately 25 % but, interestingly, the increased performance was confined to a relatively small MW range of 4 000 – 7 000 Da.

4. DEVELOPMENT OF A DISSOLVED ORGANIC CARBON DETECTOR FOR USE WITH HPSEC

The material in this chapter has been published in:

Allpike, B.P., Heitz, A., Joll, C.A. and Kagi R.I. (2007) A New Organic Carbon Detector for Size Exclusion Chromatography. *Journal of Chromatography A*, **1157**, pp 472-476

4.1. Introduction

A major limitation of many previous studies in which HPSEC has been used to investigate NOM is that UV absorbance was used to determine the concentration of DOC (e.g. Rausa *et al.*, 1991, Peuravuori and Pihlaja, 1997, Vuorio *et al.*, 1998, Myllykangas *et al.*, 2002) The response of these detectors is highly dependent on the chromophores present in the analytes; the signal strength of those analytes with chromophores is a product of the extinction coefficient of the chromophores as well as the amount of material present. Analytes without chromophores are simply not detected. Zhou and co-workers (2000) investigated the effect of increasing UV detector wavelength on the response of aquatic NOM in HPSEC-UV. They found that the calculated M_n and M_w values increased with increasing detector wavelength, illustrating further how MW determinations by this method are unreliable. For these reasons, organic carbon detectors (OCD) have been developed for use with HPSEC systems (Huber and Frimmel, 1991, Vogl and Heumann, 1998, Specht and Frimmel, 2000, Her *et al.*, 2002a, Her *et al.*, 2002b). The advantage of these methods is that the detector signal is directly proportional to the concentration of organic carbon (OC) and that, irrespective of functionality; any type of organic carbon species can be detected.

Several systems for detection of trace concentrations of OC using HPSEC have been described previously (Huber and Frimmel, 1991, Vogl and Heumann, 1998, Specht and Frimmel, 2000, Her *et al.*, 2002a, Her *et al.*,

2002b). The principle of operation of three of the four systems (Huber and Frimmel, 1991, Specht and Frimmel, 2000, Her *et al.*, 2002a, Her *et al.*, 2002b) involves removal of inorganic carbon (by acidification and removal of the CO₂ produced), followed by wet chemical (UV-persulfate) oxidation of the organic carbon to produce CO₂, which is then analysed using a non-dispersive infrared (NDIR) detector (Huber and Frimmel, 1991, Specht and Frimmel, 2000) or a conductivity detector (Her *et al.*, 2002a, Her *et al.*, 2002b). The fourth system used HPSEC followed by ICP for detection of organic carbon (Vogl and Heumann, 1998), but problems associated with CO₂ contamination in the argon used for inductively coupled plasma-mass spectrometry (ICP-MS) detection of organic components and the high capital cost of the equipment have prevented further uptake of this system. The most commonly used system, developed by Huber and Frimmel (1991), used an elegant thin-film reactor for very efficient conversion of OC to CO₂, followed by detection by NDIR spectroscopy. This system is well proven, but has not been widely adopted, possibly due to the high cost and complexity of the instrument. In this chapter, a new detector for use with high performance HPSEC, which is compatible with preparative scale and smaller scale columns, is described. The detector retains the simplicity of the design by Specht and Frimmel (2000), but uses a 'lightpipe' Fourier transform infrared (FTIR) cell. The lightpipe was chosen as the detector for CO₂ because of its small internal volume, and high sensitivity, minimising sample volumes and analysis time, while maintaining chromatographic integrity.

4.1.1. Oxidation of Dissolved Organic Carbon Using UV/Persulfate

Oxidation of DOC to CO₂ and subsequent measurement of the CO₂ in real time was the critical step in the design of the OCD in this study. In the analysis of water samples for DOC, oxidation is typically achieved by addition of the strong oxidant, persulfate, and exposure of the sample to a high power mercury discharge lamp. There are four subcategories of UV radiation; UV-A (400-315 nm), UV-B (315-280 nm), UV-C (280-200 nm) and vacuum UV (200-100 nm) (Backlund, 1992). Shorter wavelengths imply higher energies and thus higher potential to destroy NOM (Kulovaara *et al.*,

1996). The optimal germicidal effect has been found at ≤ 260 nm (Backlund, 1992, Frimmel, 1994, Kulovaara *et al.*, 1996, Frimmel, 1998) and for this reason mercury discharge lamps are effective sources of UV radiation for this application.

The most common lamp used for oxidation of aquatic NOM is a low pressure mercury discharge lamp. Low pressure mercury lamps produce a sharp emission line at 253.7 nm only when the pressure of gas inside the lamp is low (≤ 10 Torr); however, the output power of these lamps (~ 40 W) is also relatively low (Bolton, 2001). To increase the power of mercury discharge lamps (≥ 300 W) it is possible to increase the pressure of mercury inside the lamp (medium pressure), which produces a broader emission spectrum as shown in Figure 4.1.

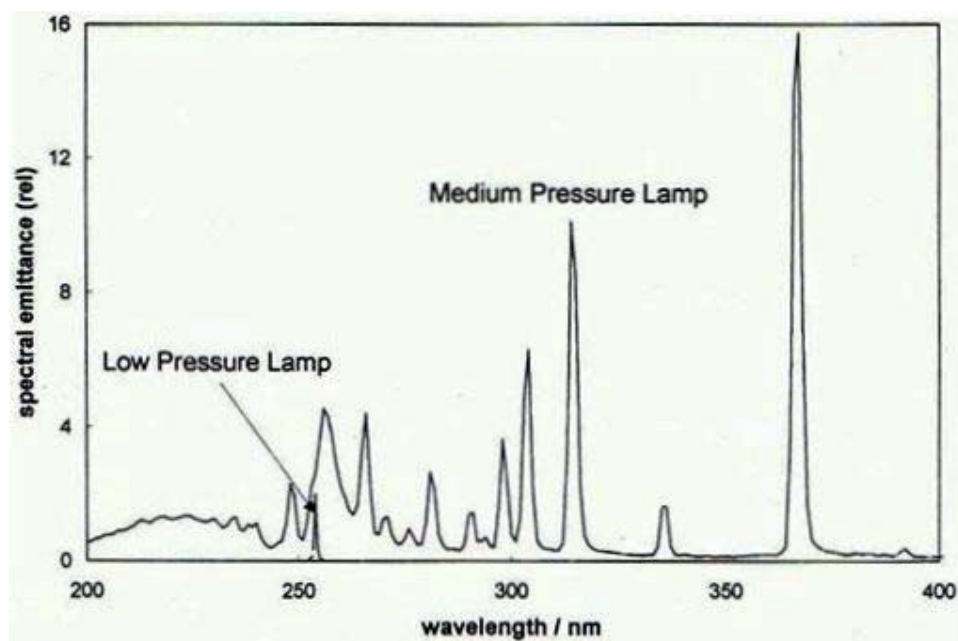


Figure 4.1 Relative Spectral emittance from low pressure and medium pressure lamps. (Taken from Bolton, 2001).

The consequence of increasing the pressure of mercury inside the lamp is that a high percentage of UV light is produced at higher wavelengths. Backlund (1992) states that the effective range of UV radiation for destruction of organic compounds is below 310 nm. Using a medium pressure mercury lamp results in a large amount of radiation being wasted in respect to destruction of organic bonds; however, compared to a low

pressure lamp there is considerably more UV radiation below 310 nm suggesting greater potential for oxidation of organic compounds. Another possibility for UV treatment of organic compounds is Excimer lamps. Excimer lamps operate similar to mercury discharge lamps except they are filled with a molecular dimer rather than mercury gas. These dimers produce an intense narrow band of UV light at a specific wavelength, for example Xenon Excimer lamps produce UV radiation at 172 nm (Osram, 2007).

Understanding the oxidation of aquatic NOM with UV light, however, is hampered by the poorly defined structure of the material. Aquatic NOM has strong spectral absorbance in the UV range. On a molecular level, this leads to electronically excited states and photochemical reactions. The main pathways of UV reactions or photoreactions involving NOM are transfers of energy to form reactive species and further reactions to form radicals. The multifunctional character of NOM leads to reactions with these radicals resulting in rearrangements and eventual degradation to CO₂ (Frimmel, 1994) (Figure 4.2)

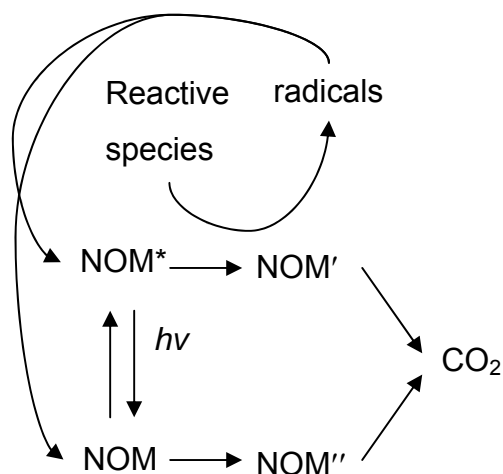
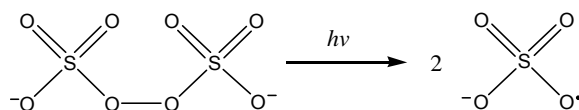


Figure 4.2 Pathway of photoreactions of NOM (NOM* = NOM at an excited state; $h\nu$ = UV irradiation; NOM' and NOM'' are NOM with slightly different structures) (Adapted from Frimmel, 1994).

The addition of persulfate to the system aids the oxidation of NOM through the formation of more radical species. Dogliotti and Hayon (1967) described the persulfate ion as an efficient oxidant of organic compounds due to the formation of free radical sulfate ions which have a higher redox potential ($\text{SO}_4^{\cdot-} + \text{e}^- \rightarrow \text{SO}_4^{2-}$, $E^\circ = 2.5\text{-}3.1\text{ V}$; (Anipsitakis and Dionysiou, 2004) than

the hydroxide radical ($\cdot\text{OH} + e^- \rightarrow \text{OH}^-$; $E^\circ = 1.985 \text{ V}$; (Anipsitakis and Dionysiou, 2004). The radical-forming reaction is shown in equation 4.1 below (Anipsitakis and Dionysiou, 2004). It is this combination of radical reactions that results in the oxidation of NOM to CO_2 .



4.1

4.1.2. Methods for Removal of Inorganic Carbon in HPSEC with Organic Carbon Detection

One of the biggest problems in high-sensitivity OC measurements is the quantitative removal of inorganic carbon (IC) (e.g. bicarbonate and carbonate) from the mobile phase stream exiting the HPSEC column (Huber and Frimmel, 1991). The addition of an acid to lower the pH to ≤ 2 shifts the equilibrium in favour of the formation of CO_2 , which is then removed. A number of methods have been developed to remove the resulting CO_2 from the aqueous stream. In the case of the thin film reactor developed by Huber and Frimmel (1991), the mobile phase stream is acidified with orthophosphoric acid prior to entering the oxidation chamber. In the chamber a shielded section of the reactor exists where no UV light is allowed to pass. Here the mobile phase is sparged with nitrogen gas, removing CO_2 from solution. The mobile phase stream then passes into the section of the reactor not shielded from UV light and oxidation of organic species occurs. Specht and Frimmel (2000) later developed an HPSEC-OCD detector which used an alternative technique for removing primary CO_2 and carbonaceous salts. Firstly the sample is acidified with orthophosphoric acid and then nitrogen gas introduced. The removal of the CO_2 and nitrogen is achieved in an open chamber, where the liquid sample falls under gravity. The gas mixture containing inorganic CO_2 and nitrogen is then able to exit to the atmosphere. The mobile phase stream is then transported to the remainder of the system using a peristaltic pump. Other methods for removing CO_2

from a liquid phase involved the use of hydrophobic membranes such as PTFE. Her and co-workers (2002a, 2002b) utilised hollow fibre membranes (HFM) which were used as a bundle containing approximately 50 individual HFM fibres in a polycarbonate housing. The housing had an opening at either end to allow the liquid to flow and also two openings at the top of the housing. A negative pressure was applied to one opening and CO₂ free dry gas passed through the other as a result of the negative pressure. The effect was that CO₂ dissolved in the liquid phase passed through the hydrophobic membrane due to equilibrium effects while the liquid phase flowed out of the other end of the unit.

4.1.3. Scope of Study

In the current study, an organic carbon detector for use with HPSEC was developed. Following separation of the NOM in various MW fractions and detection by UV₂₅₄, each section of the system was optimised. This included removal of inorganic species, oxidation of the organic component to CO₂, removal of produced CO₂ from solution and detection of CO₂ by an FTIR lightpipe detector. As well, statistical parameters were determined and calibration of the system for determining DOC concentrations was conducted.

4.2. Experimental

4.2.1. Samples

Glassware was cleaned according to the procedure outlined in Section 2.2.1.

A sample of water was taken after aeration at the Wanneroo GWTP (WGWTP) on the 2nd February 2004 and prepared as outlined in Section 2.2.1.

4.2.2. Materials and Methods

4.2.2.1. Ultra-pure Laboratory Water

Purified water was obtained as outlined in Section 2.2.2.1.

This water was then transferred to a 10 L glass UV reactor system to obtain “ultra-pure laboratory water”. The ultra-pure water system comprised a UV lamp (U-lamp, Australian UV Services, Australia), a nitrogen sparge and a PTFE coated magnetic stirrer bar. Water was left in the container for 24 hours to allow all organic material to be oxidised to CO₂. The container had a reflective coating to contain the UV radiation. This ultra-pure laboratory water was used for the preparation of all reagents and standards used for construction of the HPSEC-UV₂₅₄-OCD system.

4.2.2.2. Reagents

The HPSEC mobile phase consisted of phosphate buffer (10 mmol L⁻¹, 1.36 g L⁻¹ KH₂PO₄ (Sigma-Aldrich), and 10 mmol L⁻¹, 3.58 g L⁻¹ Na₂HPO₄ (Sigma-Aldrich)) at a pH of 6.85. The ‘semi-preparative’ column was used for the majority of testing due mainly to shorter analysis times but also for reasons that will be described in Section 4.3. Orthophosphoric acid (Univar) was added to the sample stream to convert inorganic carbon into CO₂. Sodium persulfate solution (Aldrich chemicals) was added to the sample stream before it entered the UV chamber to aid the oxidation of organic carbon to CO₂. High purity nitrogen (BOC) was used as the sparging gas for removal of CO₂ produced in the oxidation of OC. Industrial grade nitrogen (BOC) was used to cool the UV lamp and maintain an inert environment to eliminate the formation of ozone gas inside the chamber.

4.2.2.3. HPSEC Column Systems

Three different HPSEC columns were utilised during this investigation:

- an 'analytical' scale TSK G3000SW_{xl} column (7.8 mm internal diameter, 300 mm length, mean particle size 5 μm, pore size 250 Å, Tosoh BioSep, Japan),
- a 'preparative' scale HW 50s column (internal diameter 22 mm, 250 mm length, mean particle size 30 μm, pore size 125 Å, Toyopearl, Japan) and
- a 'semi-preparative' scale HW 50s column (internal diameter 10 mm, length 250 mm, mean particle size 30 μm, pore size 125 Å, Toyopearl, Japan).

An HP 1050 series II pump with a Rheodyne 7125i 6-port injection valve and a filter photodiode UV absorbance detector (FPD) with a 254 nm filter controlled with Chemstation software was used.

4.2.3. Organic Carbon Detector Development: Wet Chemistry System for Oxidation of Dissolved Organic Carbon and Carbon Dioxide Removal

Details of construction of the detection system will be given in Section 4.3; individual components are described in this section.

Sodium persulfate and orthophosphoric acid solutions were dosed into the eluent stream exiting the HPSEC column using a dual channel syringe pump (Harvard Instruments, USA) fitted with 50 mL gas tight syringes (SGE). Removal of CO₂ produced from inorganic carbon was accomplished using a hydrophobic hollow fibre membrane (HFM) bundle (Sievers Instruments Inc., USA). The HFM bundle consisted of about 50 individual membranes with an internal diameter of approximately 1 μm and a length of 100 mm housed in a polycarbonate compartment. A D-Lab diaphragm pump (BOC Edwards) was used to apply 75 Torr of vacuum inside the polycarbonate housing, but external to the HFM bundle, to encourage transport of CO₂ across the membrane while restricting transport of any liquid. Oxidation of organic carbon was achieved by UV radiation from either a 300 W medium pressure

UV lamp (1200 mm length, Wedeco, USA) or an 30 W vacuum UV lamp (300 mm length, Australia UV Services, Australia) when effect of UV light on oxidation efficiency was being tested. The lamp was encased in a PVC tube (1 200 mm x 150 mm diameter for medium pressure lamp and 300 mm x 150 mm diameter for vacuum UV lamp), as discussed in Section 4.3. CO₂ derived from oxidation of the DOC was recovered using a nitrogen sparge and subsequent separation using two Genie model 170 (Mott Pacific Pty Ltd, Australia) membrane separators in series fitted with a hydrophobic PTFE 0.45 µm membrane (Alltech, Australia). Detection of the CO₂ derived from the oxidation of DOC was achieved using an IFS-55 FTIR (Brüker, Germany) spectrometer fitted with a lightpipe GC accessory (Brüker, Germany). Opus software was used to control the IFS-55 and to collect data.

4.2.4. Standard HPSEC Operating Conditions

Throughout this study, the following standard operating conditions were applied except where indicated otherwise. The column system was a 'semi-preparative' scale HW 50s column (internal diameter 10 mm, length 250 mm, mean particle size 30 µm, pore size 125 Å, Toyopearl, Japan). The mobile phase consisted of a 20 mmol L⁻¹ phosphate buffer (10 mmol L⁻¹ Na₂HPO₄ + 10 mmol L⁻¹ K₂HPO₄) at a flow rate of 1 mL min⁻¹ and injection volume of 2 mL. The chromatographic signal was detected by UV₂₅₄ as well as an OCD system. The eluent from the UV₂₅₄ detector was acidified with orthophosphoric acid (20 mmol L⁻¹) at 10 µL min⁻¹ and then passed through a HFM bundle to remove IC. Following removal of IC, the sample stream was dosed with persulfate solution (0.84 mmol L⁻¹) at 10 µL min⁻¹. The sample stream then travelled through a 1 200 mm quartz capillary positioned directly alongside a 300 W medium pressure UV lamp. The sample stream was then purged with nitrogen (5 mL min⁻¹) and then passed through two Genie membrane separators. These Genie gas-liquid separators separated the CO₂ produced from the oxidised OC and the nitrogen purge gas from the aqueous stream. This gas mixture was then directed through the FTIR lightpipe, where the produced CO₂ was detected and quantified.

4.3. Results and Discussion

4.3.1. HPSEC-OCD System

The developed HPSEC-OCD system comprised the following components:

- separation of DOC on the HPSEC column,
- detection of DOC by non-destructive methods such as UV₂₅₄,
- removal of IC,
- online oxidation of OC to CO₂,
- separation of CO₂ from the liquid phase and
- detection of CO₂ derived from the OC, using an FTIR-lightpipe.

A flow diagram of the HPSEC-OCD system layout is shown in Figure 4.3.

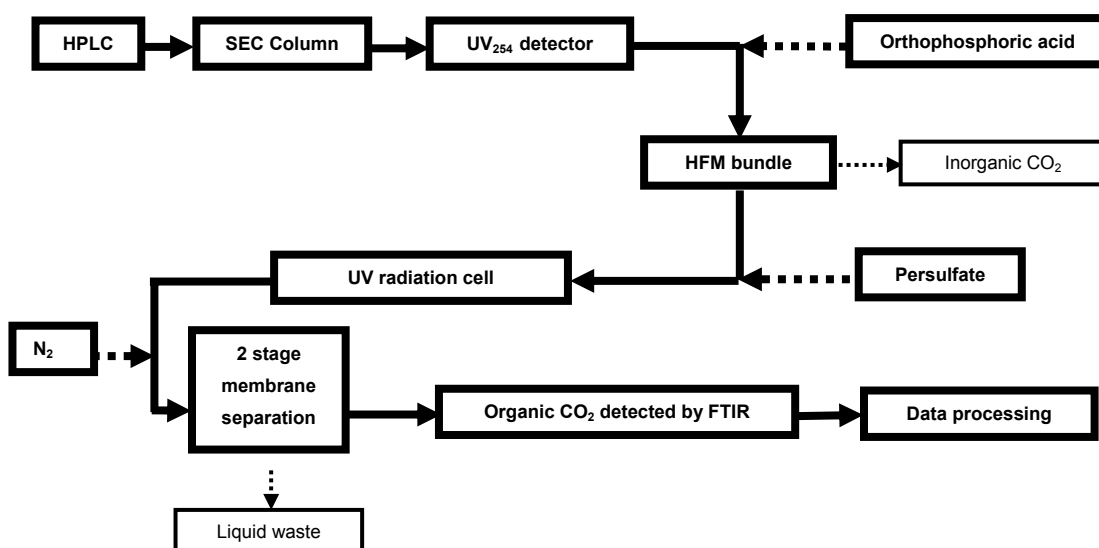


Figure 4.3 Layout of HPSEC-OCD system.

4.3.2. Removal of Inorganic Carbon

One of the biggest problems in high-sensitivity OC measurements is potential interference from CO₂, carbonate and bicarbonate in the sample (Huber and Frimmel, 1991). Using HPSEC, these species elute at longer retention times, partly co-eluting with the later eluting, lower MW organic material, as illustrated in Figure 4.4. If the IC is not effectively removed prior

to oxidation of the organic component, the concentration of organic matter eluting in this region will be overestimated, potentially leading to substantial errors.

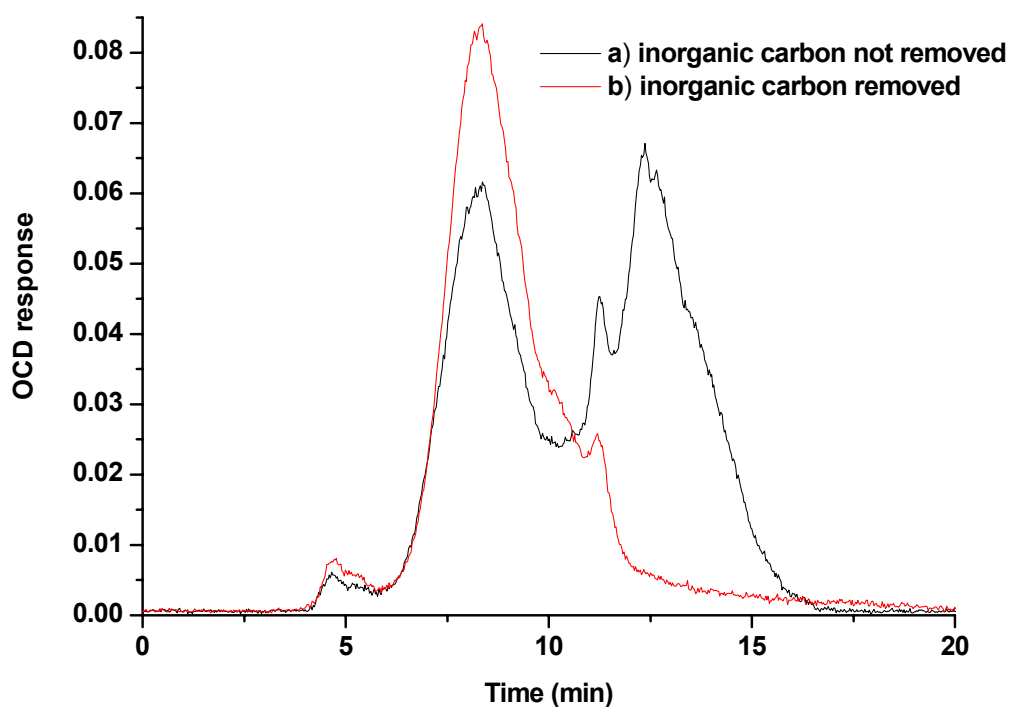


Figure 4.4 Interference in HPSEC-OCD caused by inorganic carbon species, a) inorganic carbon not removed, b) inorganic carbon removed. Chromatograms were obtained using a semi-preparative column and conditions as described in Section 4.2.4.

The method employed for removal of carbonaceous salts in the system described here was based on conversion of these salts to CO_2 , followed by transfer of the gas through a hollow fibre membrane (HFM) bundle. The method is similar to that used by Her and co-workers (2002b). The sample was first acidified to $\text{pH} \leq 2$ with orthophosphoric acid to convert all carbonates and bicarbonates to CO_2 and then passed through a HFM made from hydrophobic materials (PTFE) that do not allow the passage of bulk water. A schematic of an HFM bundle is shown in Figure 4.5.

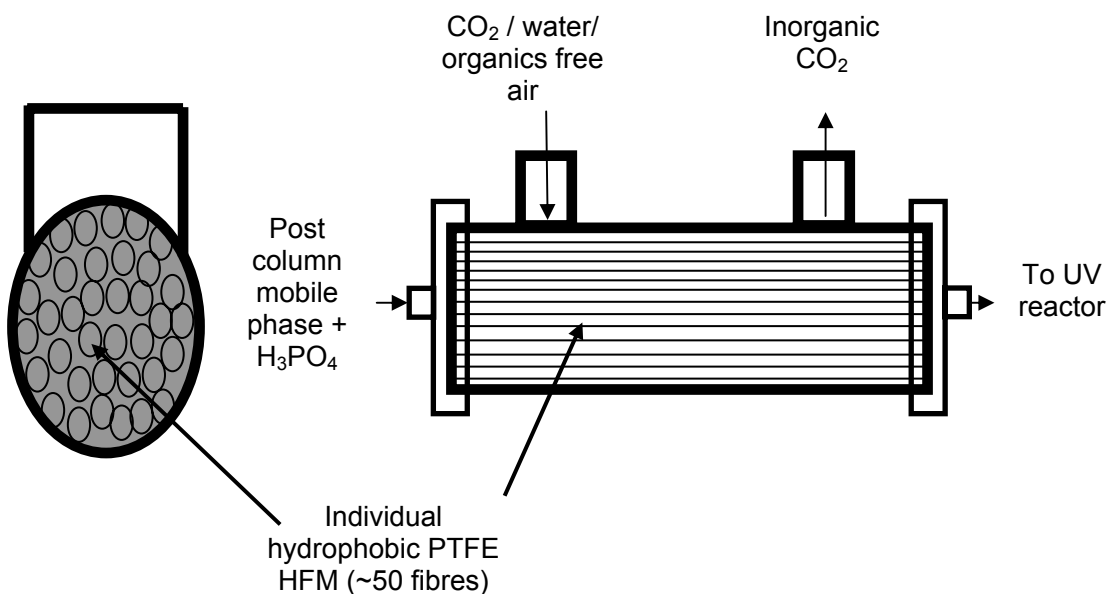


Figure 4.5 Scheme of HFM bundle used for removal of inorganic carbon.

The dose of orthophosphoric acid is a controlling factor in regard to the removal of carbonate and bicarbonate from the water sample. Figure 4.6 illustrates the effect of dosing orthophosphoric acid at a range of concentrations in a sample of aerated raw water from the WGWTP using the semi-preparative HW 50s column. The inorganic constituents eluted between approximately 12 and 18 minutes (shaded area of Figure 4.6): at low phosphoric acid concentrations the signal from the low MW organic compounds was completely overwhelmed by the interfering IC signal. In order to determine the optimal concentration for removal of IC, the mobile phase stream was dosed with a range of concentrations of orthophosphoric acid (0, 3.5, 8.5, 12.8, 17, 20, 25.5 and 29.8 % w/v). The acid was dosed at 1 mL min⁻¹ at a flow rate of 10 µL min⁻¹, resulting in concentrations in the sample stream of 0, 3.7, 8.6, 13.1, 17.4, 20.0, 26.0 and 30.4 mmol L⁻¹ respectively.

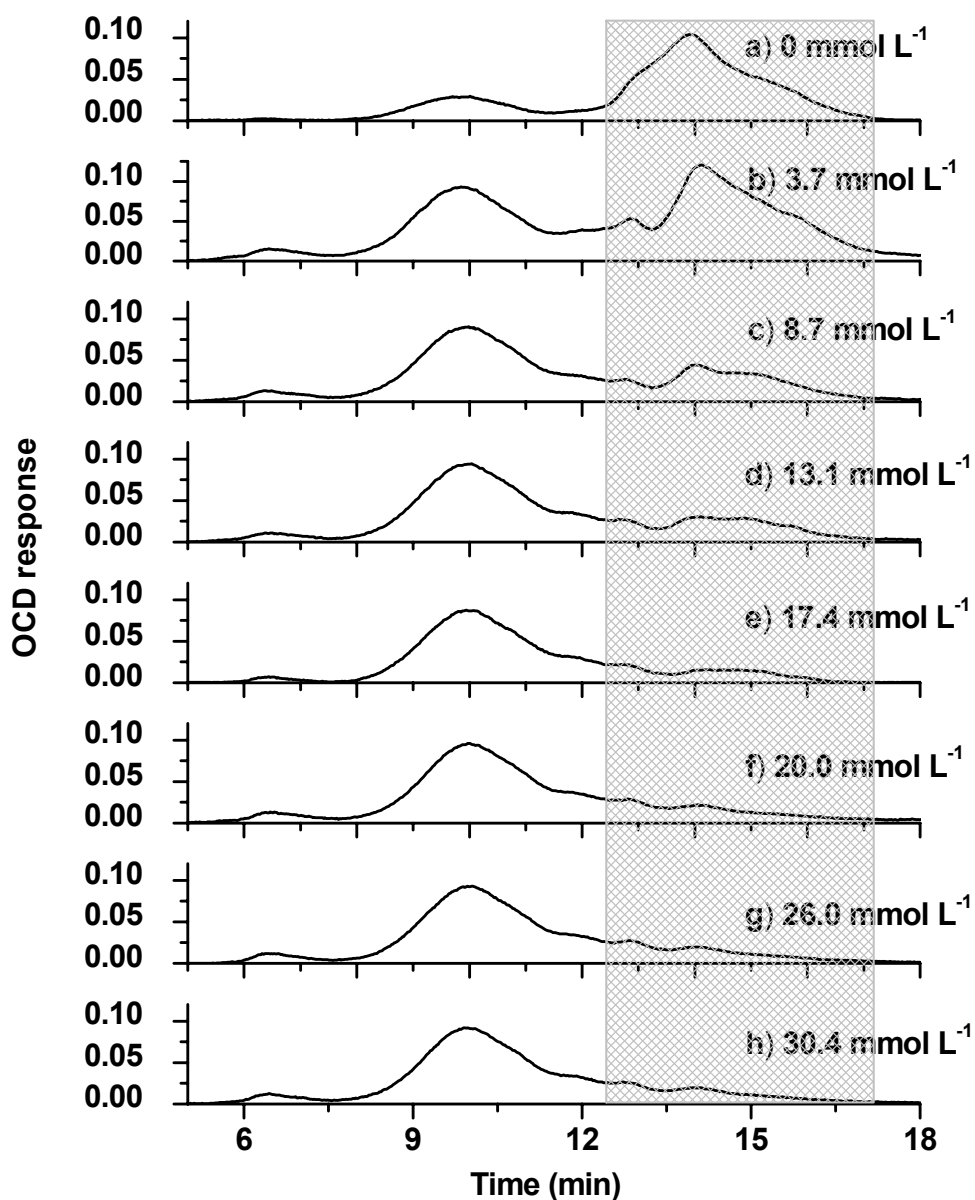


Figure 4.6 Influence of orthophosphoric acid concentration on removal of inorganic carbon species. Shaded area represents portion of chromatogram where IC eluted. Acid concentrations in solution: a) 0 mmol L⁻¹, b) 3.7 mmol L⁻¹, c) 8.7 mmol L⁻¹, d) 13.1 mmol L⁻¹, e) 17.4 mmol L⁻¹, f) 20.0 mmol L⁻¹, g) 26.0 mmol L⁻¹, h) 30.4 mmol L⁻¹. Chromatograms were obtained using a semi-preparative column and conditions as described in Section 4.2.4.

Increasing the concentration of orthophosphoric acid from 3.7 mmol L⁻¹ to 20.0 mmol L⁻¹ showed a progressive decrease in the IC signal (Figure 4.6). The improvement in removal of IC was considerable between 3.7 mmol L⁻¹ (Figure 4.6b) and 8.7 mmol L⁻¹ (Figure 4.6c) with further improvement when the concentration was increased to 13.1 mmol L⁻¹ (Figure 4.6d).

Further increases to 20.0 mmol L⁻¹ (Figure 4.6f) again increased the removal of inorganic carbon but no further improvement in removal of IC was observed at concentrations greater than 20 mmol L⁻¹ (i.e. at 26.0 mmol L⁻¹ (Figure 4.6g) and 30.4 mmol L⁻¹ (Figure 4.6h)). The improvement in removal of IC from the sample by increasing the concentration of orthophosphoric acid is further illustrated in Table 4.1 where each chromatogram has been integrated to give the area under each curve, an indication of detected carbon, either inorganic or organic. Orthophosphoric acid would not be expected to oxidise the organic component of the sample so any reduction in area is due to the removal of the IC.

Table 4.1 Influence of orthophosphoric acid concentration on integrated area of each chromatogram obtained in Figure 4.6.

Acid Concentration in sample stream (% w/v)	Acid Concentration in sample stream (mmol L⁻¹)	Integrated area (arbitrary units)
0.0	0.0	13.2
3.5	3.7	23.5
8.5	8.7	15.0
12.8	13.1	14.4
17.0	17.4	13.2
20.0	20.0	12.7
25.5	26.0	12.8
29.8	30.4	12.7

Table 4.1 confirms the above observation that there is a decrease in area up to a concentration of 20.0 mmol L⁻¹. Further increases in the concentration of orthophosphoric acid had no effect on the removal of IC from the sample.

An interesting observation from this experiment is the increase in area observed when the concentration of orthophosphoric acid in the sample stream was increased from 0 mmol L⁻¹ to 3.7 mmol L⁻¹. It might be expected that the initial addition of acid would lead to removal of IC and result in a lower integrated area. In fact, the integrated area almost doubled, increasing from 13 to 23 units, indicating the acid being added to the sample stream had some effect on the oxidation of OC inside the oxidation reactor. This

phenomenon was attributed to the acid catalysed formation of persulfate radicals in the oxidation cell, which will be discussed further in Section 4.3.3.

By passing the sample through a HFM bundle and utilising an orthophosphoric acid concentration of 20.0 mmol L^{-1} , greater than 99 % of the IC was removed from solution. Removal of IC at these levels enabled OC measurements to be determined with considerable accuracy. An orthophosphoric acid concentration of 20 % v/v or 20.0 mmol L^{-1} in the sample stream was therefore chosen for future analyses, because at this concentration, effectively all of the IC was removed from the sample. To confirm these observations, a further set of experiments was carried out using synthetic water samples where IC, in the form of carbonate and bicarbonate, were added to ultra-pure laboratory water. Figure 4.7 shows the effect of IC removal of a 100 mg L^{-1} and 5 mg L^{-1} solution of IC (50 % carbonate and 50 % bicarbonate). Both samples were passed through the HFM bundle and then the rest of the OCD system, both with and without the addition of 20 mmol L^{-1} orthophosphoric acid. The effect on peak area was used to evaluate the removal of IC. No column was used for these experiments. All other experimental conditions were as described in Section 4.2.4.

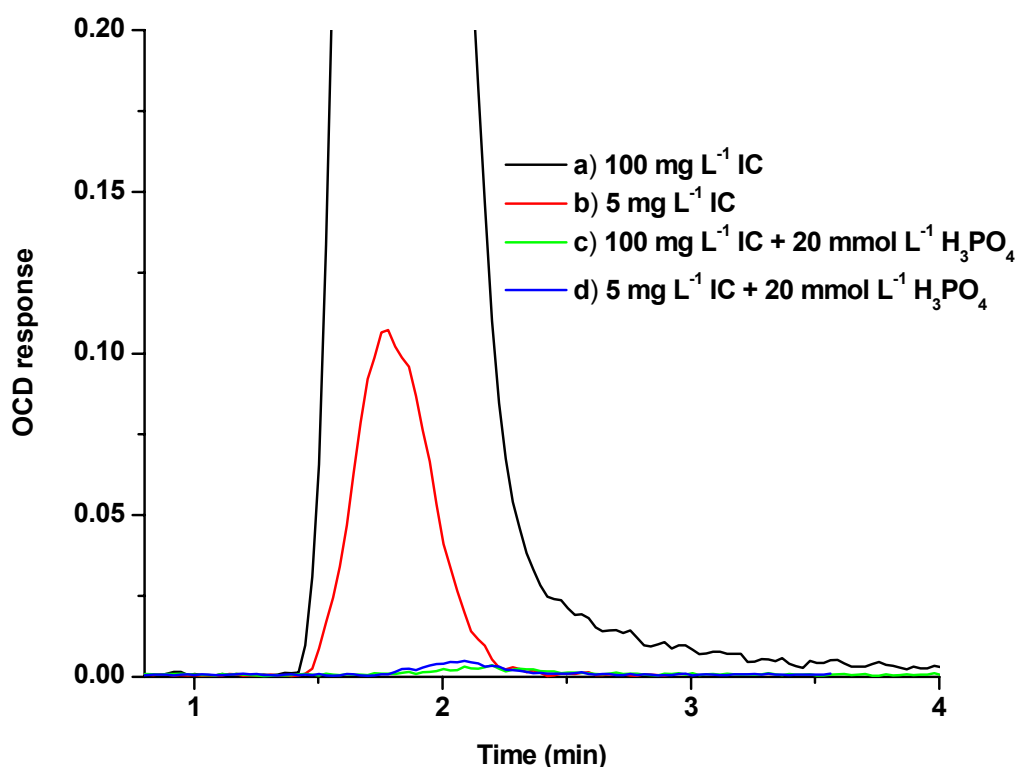


Figure 4.7 Removal of inorganic carbon using a orthophosphoric acid concentration of 20.0 mmol L^{-1} and a HFM bundle a) 100 mg L^{-1} inorganic carbon, b) 5 mg L^{-1} inorganic carbon, c) 100 mg L^{-1} inorganic carbon dosed with 20.0 mmol L^{-1} orthophosphoric acid and passed through HFM bundle, d) 5 mg L^{-1} inorganic carbon dosed with 20.0 mmol L^{-1} orthophosphoric acid and passed through HFM bundle. The signal was collected using conditions as described in Section 4.2.4.

From Figure 4.7 it is apparent that both 100 ppm (Figure 4.7a) and 5 ppm (Figure 4.7b) of IC were easily detected by the system. Following acidification and passage through the HFM, effectively all of the inorganic carbon was removed.

4.3.3. Oxidation of Organic Matter Using Persulfate and UV Treatment

The key process in the operation of the OCD in this study was oxidation of the OC in the mobile phase to CO_2 . This process occurs after the removal of the IC component from the mobile phase stream. The CO_2 produced in this way can then be detected using a suitable detection system, in this case an FTIR spectrometer with lightpipe accessory. This provides an indirect measurement of the concentration of OC in the mobile phase.

The critical factors in oxidation of OC by the UV/persulfate method are the amount and type of UV light to which the sample is exposed, the amount of persulfate present to assist in the oxidation process, and the pH.

Wavelengths below 260 nm (UVC and vacuum UV) are optimal for the destruction of organic bonds (Backlund, 1992, Frimmel, 1994, Kulovaara *et al.*, 1996).

4.3.3.1. UV Radiation

Two sources of UV radiation were compared for their ability to oxidise organic compounds containing various functional groups to CO₂. A 30 W vacuum UV source capable of producing UV radiation at both 254 nm and 182 nm (80 % at 254 nm and 20 % at 182 nm) was compared with a 300 W medium pressure UV source producing UV radiation over a wide range of wavelengths (Table 4.2). The compounds tested were those that were selected by Specht (2000) to test the oxidation capacity of a similarly designed HPSEC-OCD system. The capacity of each UV source to oxidise these compounds to CO₂ is shown in Table 4.2. In these experiments, the compounds were dissolved in the mobile phase at a concentration of 10 mg L⁻¹ DOC before direct injection into the OCD system (i.e. without first passing through an HPSEC column; flow rate: 1 mL min⁻¹, injection volume: 2 mL). The peak area of the selected model compound was calibrated against potassium hydrogen phthalate at a range of concentrations and the percentage of oxidation was calculated as the detected amount of DOC. The method used for calibration of the system is outlined in Section 4.3.7.

Table 4.2 Oxidation efficiency of the medium pressure UV lamp and the vacuum UV lamp measured on seven organic compounds (DOC = 10 mg L⁻¹. The signal was collected using conditions described in Section 4.2.4. Peak areas were calibrated against potassium hydrogen phthalate (Section 4.3.7).

Compound	Medium pressure UV lamp		Vacuum UV lamp	
	% oxidation	% RSD	% oxidation	% RSD
Oxalic acid	99.9	2.0	104.3	3.0
Dextran	90.0	3.0	88.0	7.0
Glucose	99.8	1.9	104.9	3.5
Tannic acid	73.5	7.7	54.4	10.6
Urea	98.3	1.1	86.5	5.6
Thiourea	58.4	3.0	28.6	3.2
EDTA	105.2	6.3	99.9	2.6

From Table 4.2 it is clear that oxalic acid, glucose and EDTA were all readily oxidised by both systems. These results agree with those observed by Specht *et al.* (2000) who also found that oxalic acid, glucose and EDTA were detected at recoveries of > 90 %. However, dextran, tannic acid and thiourea were not completely oxidised by either system, although the medium pressure UV source oxidised these compounds to a greater extent. Urea, while almost completely oxidised by the medium pressure UV source, was only partially oxidised by the vacuum UV lamp. Specht *et al.* (2000) also found that tannic acid and thiourea were not completely oxidised using a similarly designed HPSEC-OCD system, with 70 % and 48 % recovery respectively for these two compounds. However these authors found that when using a commercial DOC detector (Shimadzu TOC 5000) the recovery of tannic acid increased to 80 % and that of thiourea increased to >100 %.

As demonstrated in Table 4.2, the medium pressure UV lamp was superior to the vacuum UV lamp in terms of oxidation of the selected organic compounds, probably because of its higher power output (300 W vs. 30 W for the vacuum UV lamp). Although the vacuum UV lamp emits a high percentage of its radiation at or below 260 nm, considered ideal for oxidation of organic compounds (Backlund, 1992, Frimmel, 1994, Kulovaara *et al.*, 1996, Frimmel, 1998), the total amount of radiation emitted below this wavelength is substantially greater for the medium pressure UV lamp (see

Figure 4.1). In addition, the medium pressure lamp is 600 mm longer, resulting in a considerably longer exposure time. The effect of exposure time will be described later in this section. Previous work on the photolytic degradation of pharmaceutical compounds compared the performance of medium pressure and low-pressure UV sources (Pereira *et al.*, 2007). Although in this study it was acknowledged that UV radiation at 254 nm is optimal for oxidation of organic compounds (most of the UV light from the vacuum UV lamp is at this wavelength), the considerably greater UV intensity between 200 and 280 nm was shown to be more beneficial for the oxidation of the tested compounds (Pereira *et al.*, 2007). In a separate study Buchanan *et al.* (2005) investigated the performance of low pressure UV and vacuum UV treatment on the oxidation of fractionated NOM. While the study of these fractions did not provide data on individual organic compounds, certain trends were evident by comparing this study with the work on model compounds in the current research. In the work of Buchanan *et al.* (2005), NOM was separated into four fractions termed very hydrophobic acids (VHA), slightly hydrophobic acids (SHA), charged (CHA) and neutral (NEU) fractions. The fractions were irradiated in a batch process, which was not directly comparable to the on-line method in this thesis but still provided useful information. Only the VHA fraction was significantly oxidised after 15 minutes of contact, while the other three fractions were less unaffected by UV oxidation even after 300 minutes of contact (Buchanan *et al.*, 2005). From this study it would seem that organic compounds comprising NOM are not completely oxidised using vacuum UV treatment, even at extended contact times.

4.3.3.2. Effect of Persulfate on the Oxidation of Organic Compounds

The concentration of persulfate in the sample stream is another factor that can influence the efficiency of oxidation of organic compounds. A range of persulfate concentrations were tested to determine the optimal dose for oxidation of OC in a sample of raw aerated water from the WGWTP. Persulfate concentrations of 0, 5, 10, 20, 30, 50 and 60 g L⁻¹, representing 0, 0.21, 0.42, 0.84, 1.26, 2.1 and 2.52 mmol L⁻¹ of persulfate in the sample

stream, respectively, were tested on under the following experimental conditions:

- Injection volume: 2mL
- mobile phase: phosphate buffer, 20 mmol L⁻¹
- persulfate dose rate: 10 μL min⁻¹
- mobile phase flow rate: 1 mL min

No column was used to separate the sample into its various MW components. The results are shown in Figure 4.8.

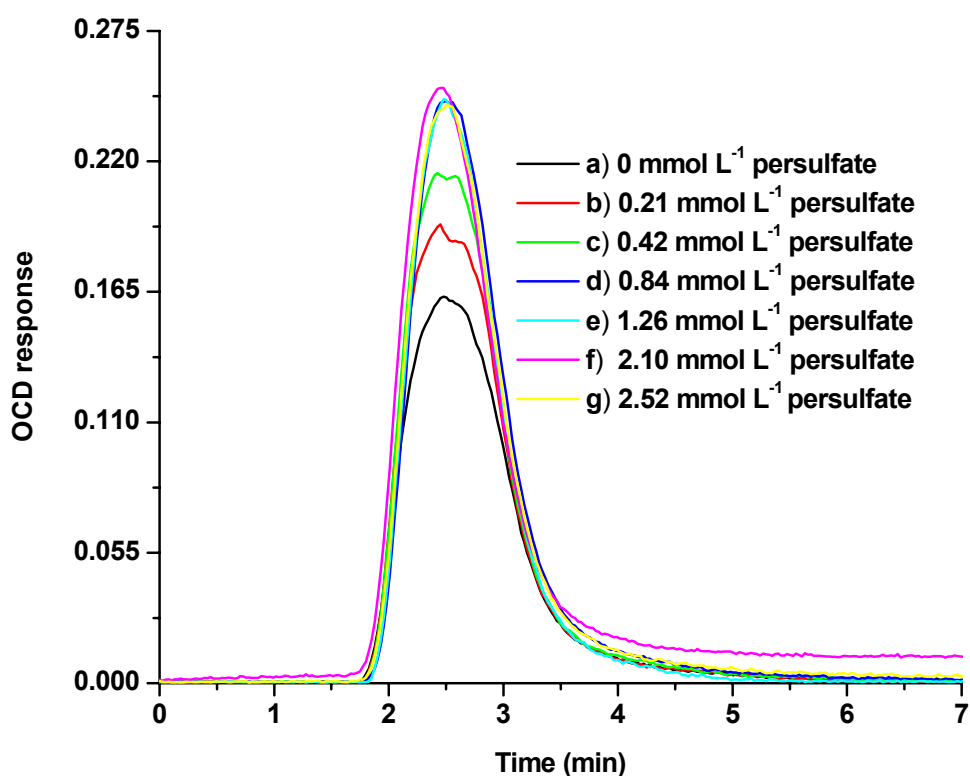


Figure 4.8 Influence of persulfate concentration on oxidation of organic carbon in a sample of RW. Persulfate concentrations, from 0 to 2.52 mmol L⁻¹ in solution, dosed at 10 μL min⁻¹, the signal was collected without using a chromatographic column, using conditions described in Section 4.2.4.

Results in Figure 4.8 demonstrate that increasing the concentration of persulfate in the sample stream increased the oxidation efficiency of OC and that the optimal concentration of persulfate was 0.84 mmol L⁻¹. At persulfate concentrations greater than 0.84 mmol L⁻¹ no further increase in oxidation of OC in this sample was observed. Oxidation of OC occurred even in the sample where persulfate had not been added, demonstrating that a portion

of the OC in the sample was oxidised by UV radiation without an added source of radicals. In the absence of persulphate the amount of OC oxidised was only 75 % of that oxidised at 0.84 mmol L⁻¹ persulfate. Addition of 0.21 mmol L⁻¹ of persulfate increased the percentage of the sample oxidised to 85 %. Thus, addition of only a small amount of additional persulfate resulted in an increase in oxidation efficiency of 10 %. A further increase of persulfate to 0.42 mmol L⁻¹ increased the oxidation of OC to 92 % of the maximum achieved at a persulfate concentration of 0.84 mmol L⁻¹. Thus doubling the persulfate dose increased the oxidation a further 7 %. It was concluded that the optimal dose of persulfate was 0.84 mmol L⁻¹ and this concentration was used for the remainder of the development work.

4.3.3.3. Influence of UV radiation Exposure Time on the Oxidation of Organic Compounds

The impact of UV radiation exposure time on OC oxidation efficiency was tested, as described in this section. The amount of time that the OC sample was exposed to UV radiation was determined by the length and diameter of the capillary in the UV cell and the rate of flow through the capillary. Since the flow rate of the mobile phase is controlled by chromatographic requirements, the time that the sample is exposed to UV radiation is determined by the length and diameter of the capillary. To investigate the effect of the exposure time on the oxidation of OC, sections of the quartz capillary were shielded from UV radiation by coating it with a reflective foil of various lengths, while all other conditions were kept constant. The maximum length that could be tested was 1200 mm, the overall length of the UV lamp. In this way lengths of 1200 mm, 900 mm, 600 mm and 300 mm were tested. The system comprised a mobile phase of 20 mmol L⁻¹ phosphate buffer at a flow of 1 mL min⁻¹ and an injection volume of 2 mL. Orthophosphoric acid was dosed to achieve a concentration of 20 mmol L⁻¹ and persulfate solution at a concentration of 0.84 mmol L⁻¹. No column was used to separate the sample OC into its MW components. Figure 4.9 shows the difference in oxidation efficiency between the different lengths of quartz capillary exposed to UV radiation.

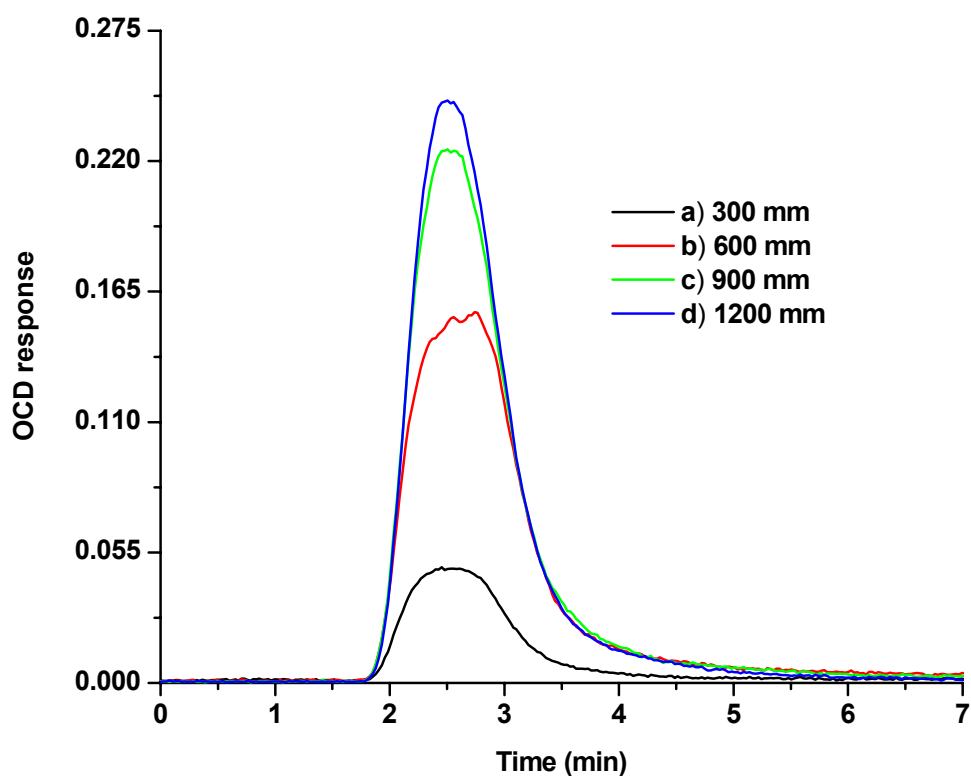


Figure 4.9 Oxidation efficiency of organic carbon subjected to a medium pressure UV lamp with quartz capillary of varying length. a) 300 mm, b) 600 mm, c) 900 mm, d) 1200 mm. The signal was collected without a chromatographic column, using conditions described in Section 4.2.4.

As shown in Figure 4.9 the length of capillary exposed to UV radiation, and thus the exposure time, had a pronounced affect on the ability of the system to oxidise OC to CO₂. When only 300 mm (Figure 4.9a) of the capillary was exposed to UV radiation the integrated peak area of the CO₂ detected was only 25 % of the maximum area obtained in this set of experiments (i.e. the area obtained when the exposed length was 1 200 mm (Figure 4.9d)). Increasing the exposure length to 600 mm (Figure 4.9b) increased the percentage of OC that was oxidised to 80 % of the maximum and a further increase of the exposed length of capillary to 900 mm (Figure 4.9c) increased this to 98 %. The improvement in oxidation efficiency with increased lamp length is shown in Figure 4.10.

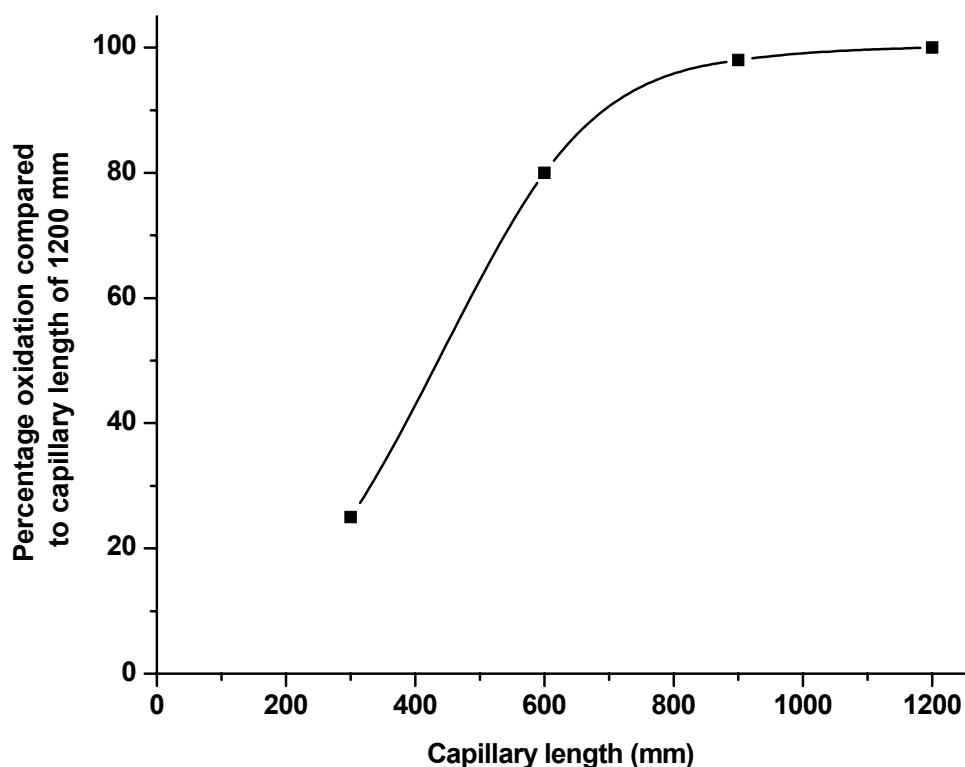


Figure 4.10 Conversion of the DOC component of post-aeration WGWTW water to CO₂ versus quartz capillary length.

From Figure 4.10 it would appear that maximum oxidation was achieved at or close to 1 200 mm and any further increases in the length of the exposed capillary beyond 1 200 mm, would not have provided significant improvements in oxidation efficiency.

The time taken for the separated sample to travel through the reactor capillary was considered to be important, not only because of the UV radiation exposure time, but also because increased dead volume may result in deterioration of chromatographic integrity. It was thought that excessive dead volume could increase sample dispersion within the reaction system, which would adversely affect the peak resolution observed at the detector. The effect of residence time in the OCD system was investigated by injecting 2 mL of a sample containing 20 mg L⁻¹ IC into the system without chromatographic separation. Other conditions were as described in Section 4.2.4. As shown in Figure 4.11 the HFM bundle was removed to allow the IC

sample to continue through the system and the 1 200 mm quartz capillary was interchanged to investigate the sample dispersion that it may cause.

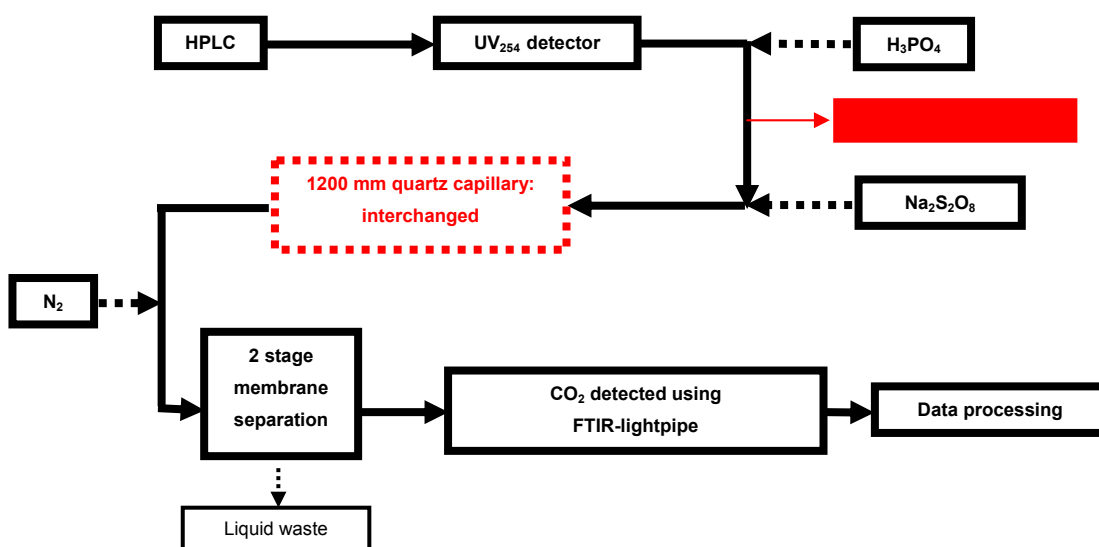


Figure 4.11 Schematic of HPSEC-UV₂₅₄-OCD system used to test effect of residence time (system volume) on peak resolution.

In this way the IC was converted into CO₂ but due to the absence of the ICR, it was not removed from the system. The effect of residence time was evaluated by comparing the peak areas and shapes obtained with and without the quartz capillary in the system. First, the quartz capillary was removed, a sample was injected, the quartz capillary was then reinserted and a second identical sample was injected. The internal diameter of the 1 200 mm quartz capillary was 0.6 mm, giving an internal volume of 1.3 mL. The effect of the quartz capillary on peak width and area is shown in Figure 4.11.

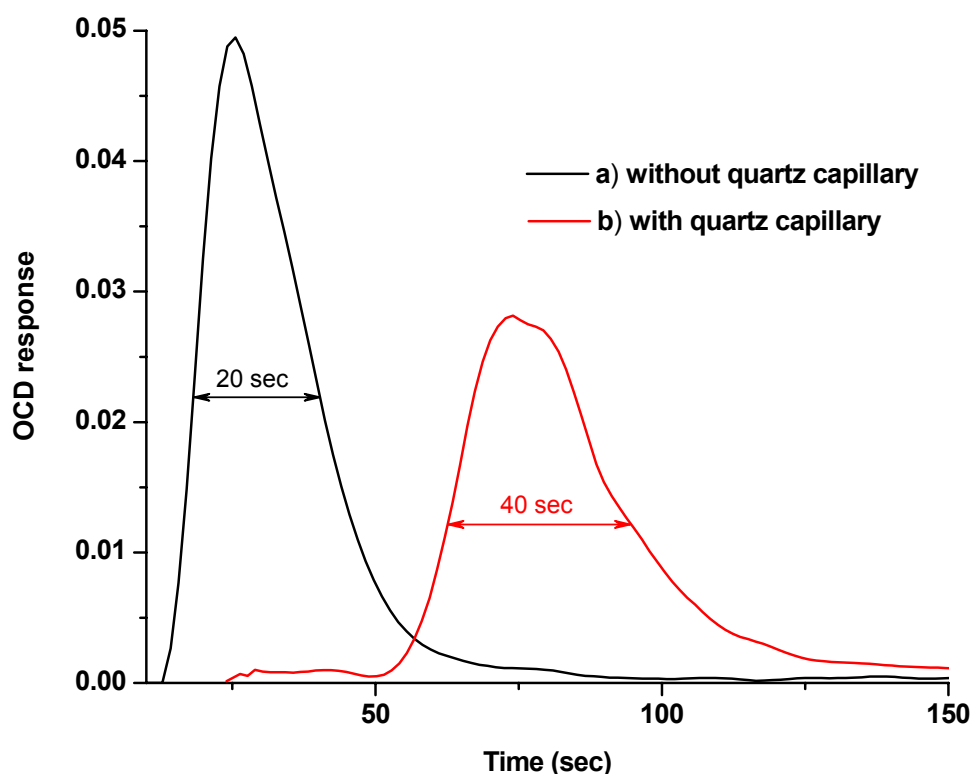


Figure 4.12 Influence of quartz capillary on peak width and residence time. a) black line = without quartz capillary present, b) red line = with quartz capillary present. Chromatograms were obtained without a chromatographic column using conditions described in Section 4.2.4.

A comparison of the two injections showed that the capillary had a substantial influence, both on the peak shape and on the time taken for the injected components to reach the detector. The effect of the capillary in the system resulted in an increase of 40 secs in the time taken to reach the detector (10 sec without capillary, 50 sec with capillary); an increase in peak width of 46 secs (72 sec versus 118 sec) and; an increase in peak width at half maximum height of 20 secs (20 sec versus 40 sec). This demonstrated the importance of the compromise between using a longer capillary for improved oxidation and shortening the capillary for reducing sample dispersion in the system. For the system that had been developed here, a capillary length of 1 200 mm was necessary due to the length of lamp and, as shown previously, this was the minimum length for optimal oxidation of OC. On the other hand, it would have been desirable to have as short a capillary as possible to minimise sample dispersion. A possibility for

reducing the internal volume of the 1 200 mm capillary was to reduce its internal diameter, but unfortunately a quartz capillary of smaller internal diameter could not be sourced. However, it was possible to obtain a PTFE capillary with an internal diameter of 0.5 mm, so a comparison was made between this PTFE capillary (length 1 200 mm, ID 0.5 mm) and the quartz capillary (length 1 200 mm; ID 0.6 mm). In this case a sample of Wanneroo raw water (post aeration) was used and all conditions were as described in Section 4.2.4, except that the chromatographic column was omitted. Results are shown in Figure 4.13.

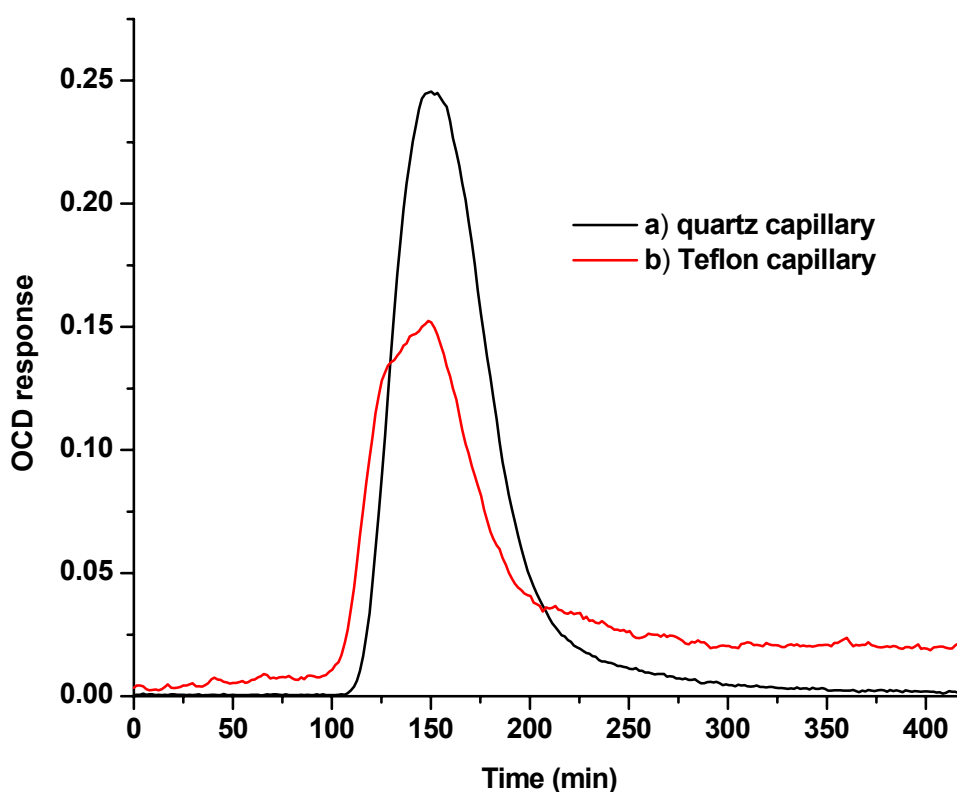


Figure 4.13 Comparison of a) black line = quartz capillary and b) red line = PTFE capillary on peak width. Signals were obtained without a chromatographic column using conditions described in Section 4.2.4.

Reducing the internal diameter of the capillary did have the desired effect, in that peak width was reduced and the sample moved more rapidly through the system. This was evidenced by the faster elution time of the sample in the case where the PTFE capillary was used. However, the combination of reducing the exposure time of the sample to UV radiation and changing the

capillary material reduced the peak area by approximately 18 %, reflecting a decrease in the oxidation efficiency of the system. Hence it was concluded that the quartz capillary was superior to the PTFE capillary and the former was used for the remainder of this study.

4.3.3.4. Effect of pH on the Oxidation of Organic Carbon

The effectiveness of oxidation of DOC by UV and persulfate is influenced by the pH. Kolthoff and Miller (1951) have demonstrated that the formation of sulfate radicals from persulfate is dependent on pH and is catalysed by hydrogen ions. To evaluate the effect of pH on the production of sulfate radicals and, hence, on the oxidation of OC, phosphoric acid solutions of 0 mmol L^{-1} and 3.7 mmol L^{-1} were compared (persulfate concentration was 0.84 mmol L^{-1} in the sample stream). The resultant chromatograms are shown in Figure 4.14.

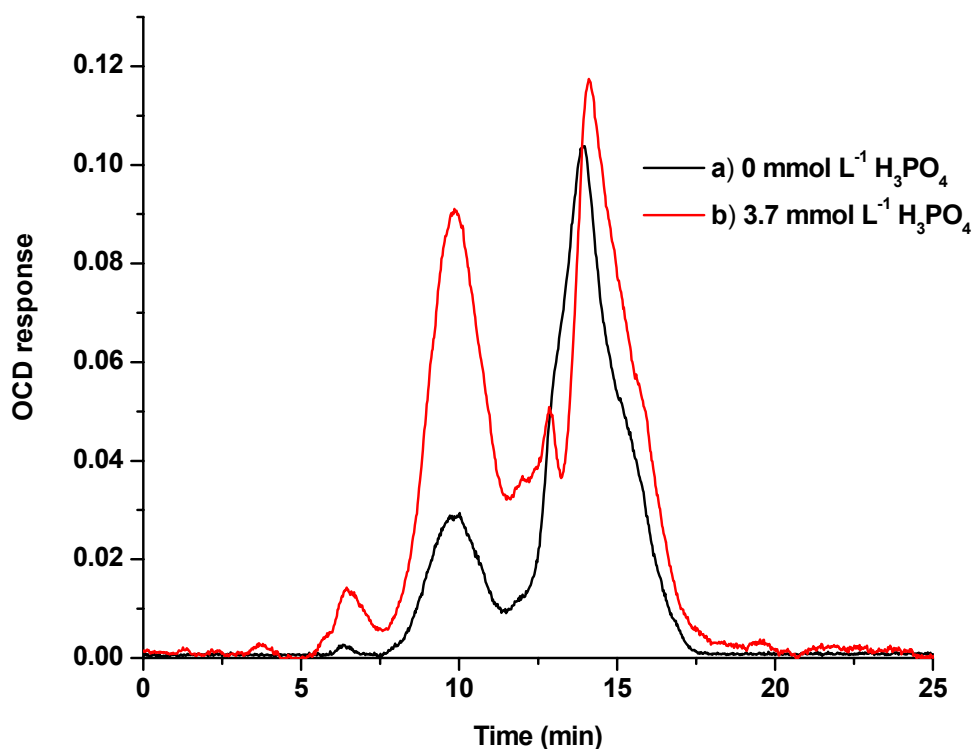


Figure 4.14 Influence of hydrogen ions on the oxidation of organic carbon by UV/persulfate. Black line a) 0 mmol L^{-1} orthophosphoric acid, red line b) 3.7 mmol L^{-1} orthophosphoric acid. Chromatograms were obtained with a semi-preparative chromatographic column using conditions described in Section 4.2.4.

The peaks between 5 and 11 minutes, representative of OC, were significantly less abundant when the sample stream contained no acid (Figure 4.14a). Addition of acid to the sample stream at 3.7 mmol L^{-1} substantially increased the areas of the OC peak (Figure 4.14b). This demonstrates the importance of acid, not only for removal of IC, but also for facilitating persulfate radical formation to assist in the oxidation of OC.

4.3.4. Dose Rate of Orthophosphoric Acid and Sodium Persulfate

Having determined the optimum effective concentrations of acid and persulfate, the next step was to optimise the rate at which these reagents were added to the sample stream. The acid and persulfate were dosed to the sample stream using a dual channel syringe pump capable of introducing reagents to the sample stream at flow rates below $1 \mu\text{L min}^{-1}$. Both reagents were dosed at the same rate due to limitations with the equipment. To evaluate the effect of dosing rate on the reactions of both OC and IC, orthophosphoric acid and sodium persulfate solutions were introduced to the sample stream at various rates. The concentrations of the dosed solutions were varied so that the concentrations in the eluent stream would remain at 20.0 mmol L^{-1} and 0.84 mmol L^{-1} respectively. The sample tested was a sample of raw water from the WGWTP. The effect of the seven dosing rates used is shown in Figure 4.15.

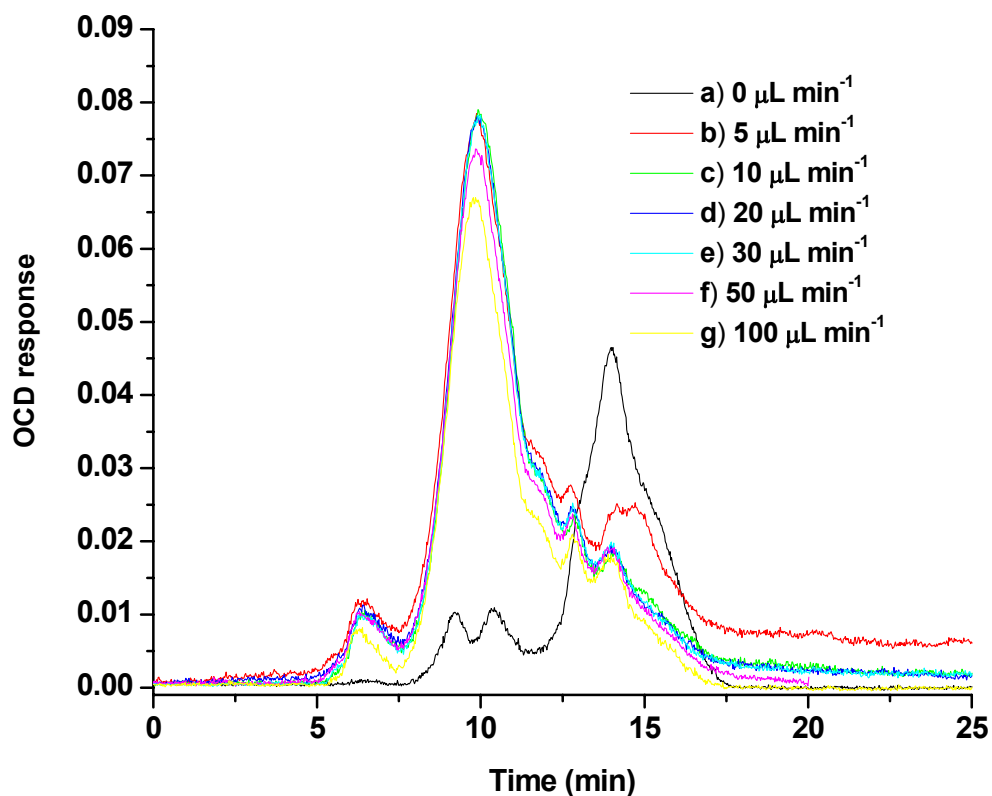


Figure 4.15 Influence of the concentration of persulfate and orthophosphoric acid dose on removal of inorganic carbon and oxidation of organic carbon. a) $0\ \mu\text{L min}^{-1}$, b) $5\ \mu\text{L min}^{-1}$, c) $10\ \mu\text{L min}^{-1}$, d) $20\ \mu\text{L min}^{-1}$, e) $30\ \mu\text{L min}^{-1}$, f) $50\ \mu\text{L min}^{-1}$, g) $100\ \mu\text{L min}^{-1}$. Chromatograms were obtained with a semi-preparative chromatographic column using conditions described in Section 4.2.4.

When acid and persulfate were not added to the eluent stream (Figure 4.15a) the oxidation of OC occurred solely due to the action of UV radiation and was therefore incomplete: in addition, IC was not removed from the eluent stream at all. When the dose of acid and persulfate was increased to $5\ \mu\text{L min}^{-1}$ (Figure 4.15b) a dramatic improvement in the oxidation of OC was observed and most of the IC was removed prior to oxidation in the UV reaction cell. While the oxidation of OC appeared to be optimal at this dose rate (compared to the higher dose rates) IC removal was incomplete. The dose of $5\ \mu\text{L min}^{-1}$ was not sufficient to convert all of the IC present to CO_2 , possibly because the contact time between the acid and sample stream was too short for adequate mixing (the concentration of acid was constant for all the dose rates tested). If the contact time between the dose point and the ICR was too short, the low flow may have resulted in a non-uniform

distribution of acid in the sample stream, with the result that some IC remained unreacted. Increasing the dose rate of acid and persulfate to $10 \mu\text{L min}^{-1}$ (Figure 4.15c) resulted in oxidation of OC similar to the $5 \mu\text{L min}^{-1}$ dose; however, the IC fraction appeared to be completely removed from the sample stream. Thus, while a dose of $5 \mu\text{L min}^{-1}$ would have been adequate for oxidation of OC, due to equipment constraints, a dose of $10 \mu\text{L min}^{-1}$ was required as a minimum for removal of IC. Increasing the dose rate to 20 and $30 \mu\text{L min}^{-1}$ (Figure 4.15d and Figure 4.15e) had no effect on the oxidation of OC and IC when compared to a dose of $10 \mu\text{L min}^{-1}$. Identical chromatograms were obtained for these three dose rates. This may have implications when samples of higher OC or IC concentrations are analysed. The dose rate could be increased to allow for greater oxidation without concern about the chromatographic. Conversely, increasing the dose rate to 50 and $100 \mu\text{L min}^{-1}$, (Figure 4.15f and Figure 4.15g) did have an adverse effect on the chromatogram. Peak intensity was reduced for dose rates of 50 and $100 \mu\text{L min}^{-1}$ due to dilution of the sample (by 5 and 10 % respectively), enough to reduce overall peak intensity.

4.3.5. Detection of Carbon Dioxide Produced from Organic Carbon Species

The final step in the organic carbon detection system was the transfer of CO_2 produced from oxidation of OC into the gas phase, followed by quantitation of the CO_2 by an infrared detector. Separation of CO_2 from the aqueous eluent phase was achieved using a hydrophobic PTFE membrane. Nitrogen was metered into the eluent stream directly prior to the hydrophobic membrane unit, as a 'carrier' gas to sparge CO_2 from the liquid phase. The CO_2 /nitrogen mixture passed through the membrane while the aqueous mobile phase was directed to waste. The critical variable in this process was the flow of nitrogen into the eluent stream. Figure 4.16 shows the effect of varying the nitrogen flow rate on the CO_2 signal.

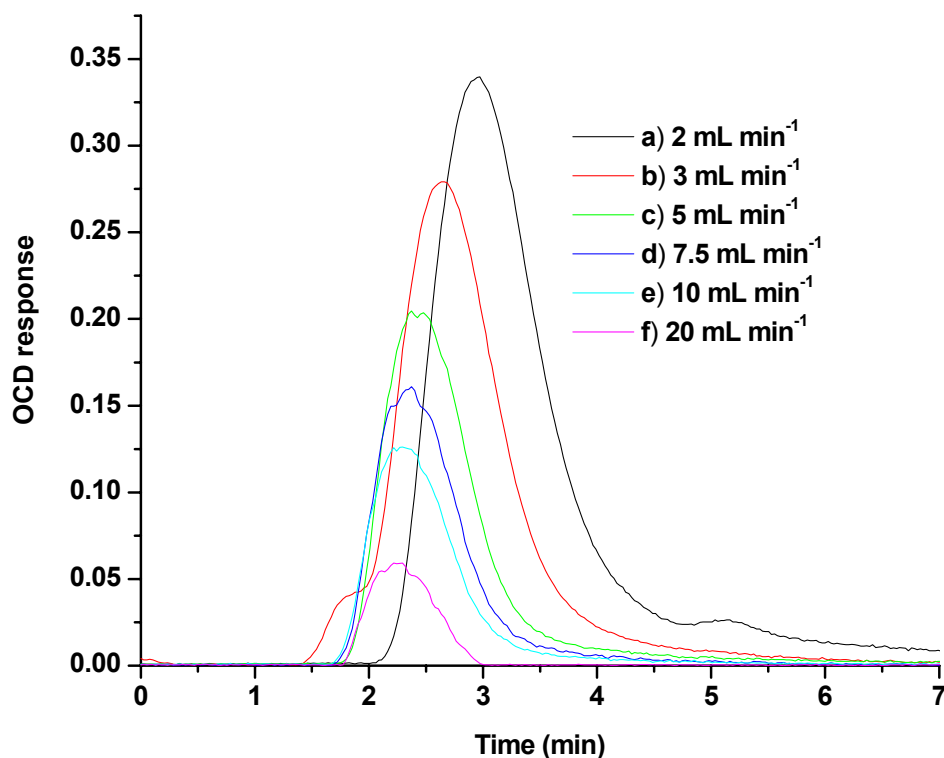


Figure 4.16 Recovery of CO₂ through the hydrophobic PTFE membrane with varying nitrogen flows, a) 2 mL min⁻¹, b) 3 mL min⁻¹, c) 5 mL min⁻¹, d) 7.5 mL min⁻¹, e) 10 mL min⁻¹ and f) 20 mL min⁻¹. Signals were obtained without a chromatographic column using conditions described in Section 4.2.4.

The peaks in Figure 4.16 represent the amount of CO₂ that passed through the hydrophobic membrane, as detected by the lightpipe FTIR detector. The area under the curve corresponds to the detector response for CO₂ reaching the detector. The response decreased substantially upon increasing the flow rate of nitrogen ‘carrier’ gas through the gas-liquid membrane separators. A nitrogen flow of 2 mL min⁻¹ gave an integrated peak area of 15.7 units (Figure 4.16a). This decreased to 12.1 units when the nitrogen flow rate was increased to 3 mL min⁻¹, to 7.2 units at 5 mL min⁻¹ (Figure 4.16c), 5.4 units at 7.5 mL min⁻¹ (Figure 4.16d), 4.2 units at 10 mL min⁻¹ (Figure 4.16e) and further to 1.6 units as the flow rate was increased to a maximum of 20 mL min⁻¹ (Figure 4.16f). It was assumed that increasing the nitrogen flow rate would not have decreased the transfer of CO₂ from the liquid to gas phase and therefore, the same amount of CO₂ would have reached the detector in every experiment. The decrease in detector response upon increasing flow

rate was probably due to the faster transfer of CO₂ through the detector cell. Higher flow rates would have resulted in fewer scans for the same mass of CO₂ in each peak, and therefore, resulted in decreased detector response per unit mass of CO₂. The detector scanning rate was 40 Hz, optimum for the mercury cadmium telluride (MCT) detector used in the lightpipe system, resulting in seven scans per second. For the lowest flow rate tested (33 μL sec⁻¹), a given molecule of CO₂ would have resided in the cell (volume = 160 μL) for 5 seconds, and hence would have been scanned 35 times. However at the highest flow rate (333 μL sec⁻¹) the CO₂ sample would have travelled through the detector 10 times faster and would therefore only have been scanned 3.5 times. This accounts for the lower signal to noise at higher flow rates.

The choice of carrier gas flow rate was a compromise between detector response and peak width, i.e. peak resolution: even though the lowest flow rate gave the highest peak area, with excellent signal to noise, the excessive peak broadening at this flow rate could adversely affect the chromatographic integrity of the sample. At the lowest flow rate (33 μL sec⁻¹), the detector cell (160 μL) would have taken 5 seconds to fill. Mixing of the sample within the cell during this time may not have preserved the chromatographic resolution obtained during the HPSEC separation, so a higher flow rate of 5 mL min⁻¹ was chosen. This flow rate still gave adequate sensitivity and was therefore chosen as the flow rate for use with subsequent experiments. As will be shown in Section 4.3.7 (Table 4.4), at this flow rate the detection limit of the instrument was 30 ng DOC per peak which was adequate, considering concentrations that would likely be analysed by this system.

4.3.6. Column Selection in HPSEC-DOC Analysis

While chromatographic performance is an extremely important factor to consider when selecting a column for use with OCD, there are other factors which need to be considered. Some of these are detection limits and analysis time, which will be discussed in later sections. A critical

requirement, when coupling a column and DOC detector, is the level of background carbon leached into the mobile phase from the column. Every part of the system will introduce some carbon, whether it is contamination from the mobile phase, introduction of carbonate and bicarbonate salts from the sample being analysed or contamination from the oxidants used. One of the most serious potential sources of carbon contamination is from the column stationary phase. The current detector setup using an FTIR spectrometer with lightpipe accessory for detection of CO₂, allowed for assessment of background CO₂ contamination. A background scan is necessary in FTIR to account for the instrumental and environmental contributions to the infrared signal (Smith, 1996).

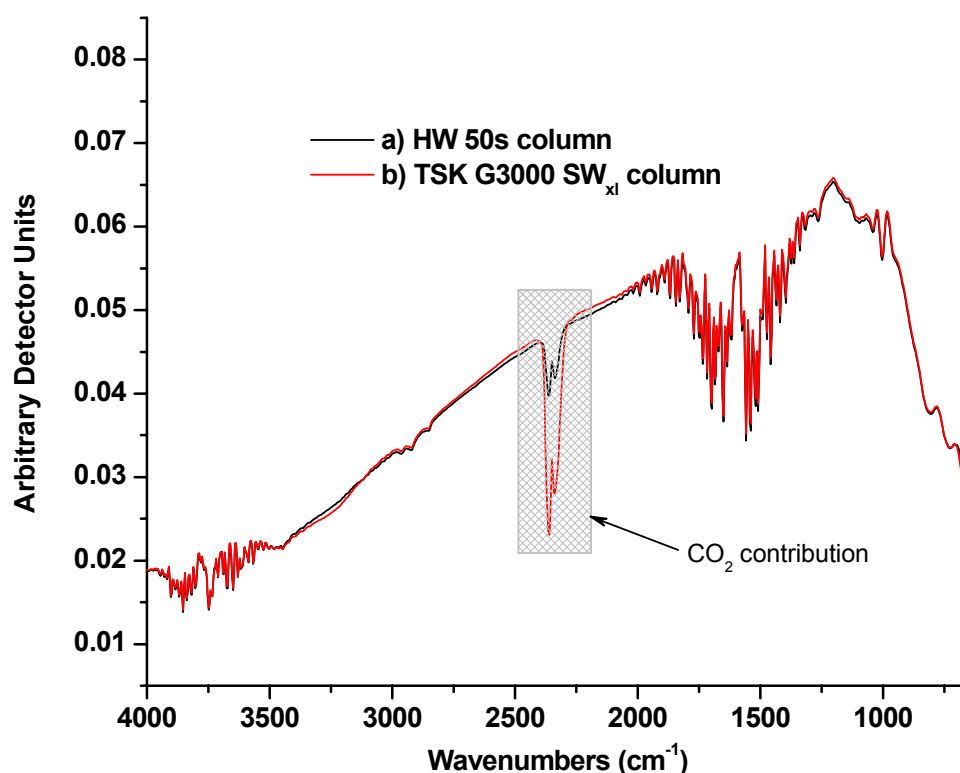


Figure 4.17 FTIR background signal of blank injection showing CO₂ contribution in HPSEC-OCD using a) HW-50s column (250 mm x 22 mm i.d.) and b) TSK G3000SW_{xl} (300 mm x 7.8 mm i.d.) column contribution. Chromatograms were obtained using conditions described in Section 4.2.4.

Figure 4.17 shows the contribution of CO₂ to the background signal when using a Tosoh HW-50s polymer based resin column (Figure 4.17a) and a Toyopearl TSK G3000SW_{xl} silica based resin column (Figure 4.17b). The

shaded area highlights the major peak representing the contribution from CO₂ (wavenumber 2350 cm⁻¹ (Smith, 1996)). It is apparent from Figure 4.17 that the CO₂ background is much greater for the TSK G3000SW_{xl} silica based resin analytical column (300 mm x 7.8 mm i.d) than for the Tosoh HW-50s resin (250 mm x 22 mm i.d.). The reasons for this increased contribution from the analytical column are unclear. One possible explanation is that residual organic carbon was continually leached from the stationary phase which in turn was oxidised in the UV reaction cell and detected by the FTIR lightpipe system. However this column was rinsed extensively before use and had been used for hundreds of analyses prior to these experiments, and the suggestion that OC continued to leach from the column is therefore curious. Other workers have also observed this problem with this column type: a group of collaborators at the Australian Water Quality Centre (South Australia) who were also working on developing an OCD noted that eluent from the column contained higher than expected residual OC (personal communication Chow, 2005).

The CO₂ background from the TSK G3000SW_{xl} column was of sufficient magnitude to render this column unsuitable for the use with HPSEC-OCD. As was established in Chapter 3, the 300 mm x 7.8 mm i.d. column containing TSK G3000SW_{xl}, was the best column for use in HPSEC-UV analysis of DOC in natural waters since it achieved the best separation of OC. The small scale of the column meant that lower sample volumes could be used and that analysis times were shorter than for preparative scale columns. However, the increased contribution of CO₂ from this column resulted in an unacceptably poor signal, severely compromising sensitivity and resolution in HPSEC-OCD, as shown in Figure 4.18 where the UV₂₅₄ and OCD signals are compared. It should be noted that only a very small amount (ng) of OC can have a severe effect on the system.

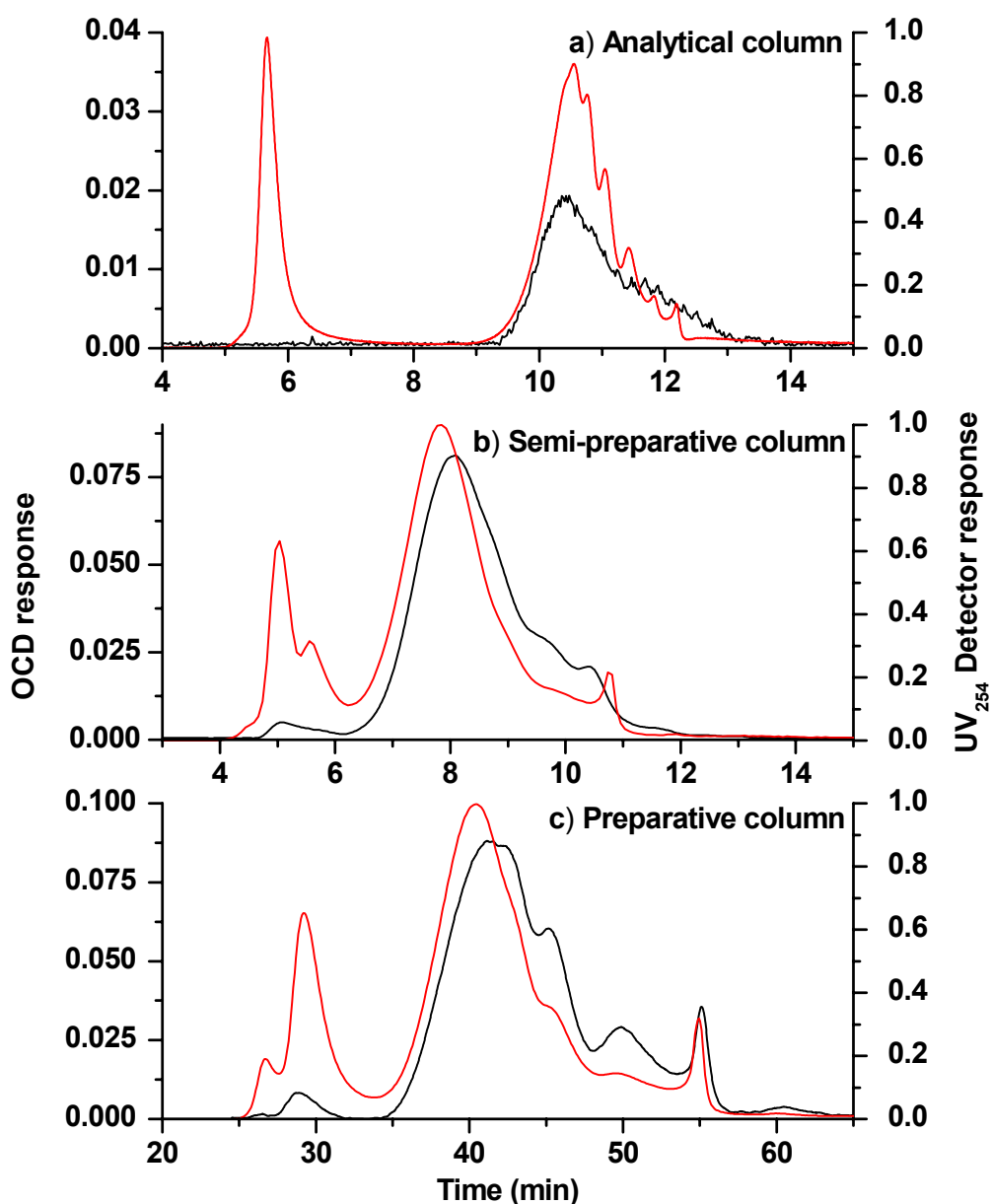


Figure 4.18 HPSEC UV₂₅₄ and OCD chromatograms of raw water on a) analytical column (300 mm x 7.8 mm i.d.) , b) semi-preparative column (250 mm x 10 mm i.d.) and c) preparative column (250 mm x 22 mm i.d.). Chromatograms were obtained using column system as mentioned above using conditions described in Section 4.2.4.

Figure 4.18a is the chromatogram obtained when a sample of raw aerated groundwater following aeration was subjected to HPSEC-UV₂₅₄-OCD with an analytical scale column packed with TSK G3000SW_{xl} silica based stationary phase. As can be seen, because of the high CO₂ background, signal intensity was significantly reduced and as a result peak resolution was poor when compared to the other two columns (HW-50s resin semi-preparative

column, 10 mm i.d., 250 mm length (Figure 4.18b); HW-50s resin preparative column, 22 mm i.d., 250 mm length (Figure 4.18c)). The overall shape of the chromatogram is broadly similar to those obtained from the other two columns, but resolution appears to be compromised. All chromatographic conditions, reagents and flow rates were identical for each of the three columns used. The separation of the sample using the TSK G3000SW_{xl} was excellent, as shown by the HPSEC chromatogram that was obtained using the UV₂₅₄ absorbance detector. Hence, the reason for the apparent poor resolution for the OCD using this column must have been caused by the poor signal quality due to the high CO₂ background. Therefore, at present, the use of analytical scale columns containing silica based stationary phases is not compatible for use with OCD.

As was shown in Figure 4.17, the background contribution of CO₂ from the HW-50s polymer based resin phase was considerably less and was in fact identical to that obtained when no column was connected (results not shown). The implication is that when compared to the TSK G3000WSW_{xl} resin, signal intensity is greater and resolution of peaks is superior. However, comparing the semi-preparative column (Figure 4.18b) and the preparative column (Figure 4.18c) demonstrate that there is also an improvement in peak separation with a move to larger column diameters. Peuravuori and Pihlaja (2004) have previously noted that peak resolution obtained with a preparative scale BioSep-SEC-S 3000 (600 x 21.2 mm i.d., particle size 5 µm pore size 250 Å) was identical to an analytical scale Tosoh TSK G3000SW_{xl} (300 x 7.5 mm i.d., particle size 10 µm pore size 250 Å). They stated that under similar chromatographic conditions chromatograms should be identical. Hence, the column of choice for use with OCD was an HW-50s polymer based resin preparative column, 22 mm i.d., 250 mm length.

4.3.7. Calibration of OCD and Statistical Parameters for Quantitative Analysis

A major advantage of organic carbon detection for HPSEC over alternative detector technologies is that signal intensity can be linked to the concentration of organic compounds present in a sample. As was demonstrated in Chapter 3, UV detection at 254 nm can both overestimate and underestimate the DOC concentration, as the signal intensity is dependant on the structure of the analytes rather than the absolute amount of carbon present. It is therefore possible to calibrate the HPSEC-OCD system so that the concentration of OC represented by each chromatographic peak, or portion of a peak, can be calculated.

The HPSEC-OCD system developed in this study was calibrated using potassium hydrogen phthalate (KHP) standards at the following concentrations: 1, 2, 3, 4, 5, 8, 10, 15, 20 and 30 mg L⁻¹. A maximum concentration of 30 mg L⁻¹ was chosen, as concentrations of DOC above this limit were not likely to be analysed without dilution. Since a small amount of material can be irreversibly sorbed onto the HPSEC column (Peuravuori and Pihlaja, 2004), these standards were analysed by direct injection into the OCD system, in the absence of an HPSEC column. Also as KHP has a relatively low MW (204 Da) it would permeate the pore space of the stationary phase, and integration of the resultant peak may be more difficult, due to the slight tailing of peaks that would result after passage through a column. The basis of the calibration process was to perform the calibration in the absence of a column and to use the line of best fit produced from the calibration curve to calculate the area of the analysed sample.

Due to the variety of columns and sample sizes utilised, calibration was carried out using three different injection volumes (100, 200 and 500 µL), which resulted in 100 ng to 7 500 ng of carbon being injected onto the column. The peak areas and standard deviations resulting from these experiments are listed in Table 4.3.

Table 4.3 Peak areas and RSD (n=5) of standards used to calibrate organic carbon concentrations.

Injection Volume (μL)	Concentration (mg L^{-1})	Mass (ng)	Peak Area	RSD
100	1	100	0.92	1.5
	2	200	1.3	1.3
	3	300	1.8	2.2
	4	400	2.0	0.4
	5	500	2.3	0.15
	8	800	3.6	0.3
	10	1 000	4.2	2.2
	15	1500	5.6	0.9
	20	2 000	7.3	0.8
	30	3 000	10.7	0.65
200	1	200	1.3	2.6
	2	400	2.1	1.2
	3	600	2.8	0.9
	4	800	3.6	0.12
	5	1 000	4.2	0.5
	8	1 600	6.2	3.6
	10	2 000	7.4	3.0
	15	3 000	10.7	1.0
	20	4 000	14.4	2.0
	500	1	5 00	2.3
2		1 000	4.2	3.1
3		1 500	5.7	3.1
4		2 000	7.6	1.1
5		2 500	9.4	0.65
8		4 000	14.3	3.3
10		5 000	17.8	0.2
	15	7 500	25.4	1.5

To enable a calibration curve to be constructed which would be valid for any of these injection volumes, the mass of carbon injected onto column was plotted against the resulting peak area. Five replicate injections of each standard were analysed to obtain a statistically significant result (Adams, 1995). The calibration curve, line of best fit and correlation coefficient are shown in Figure 4.19

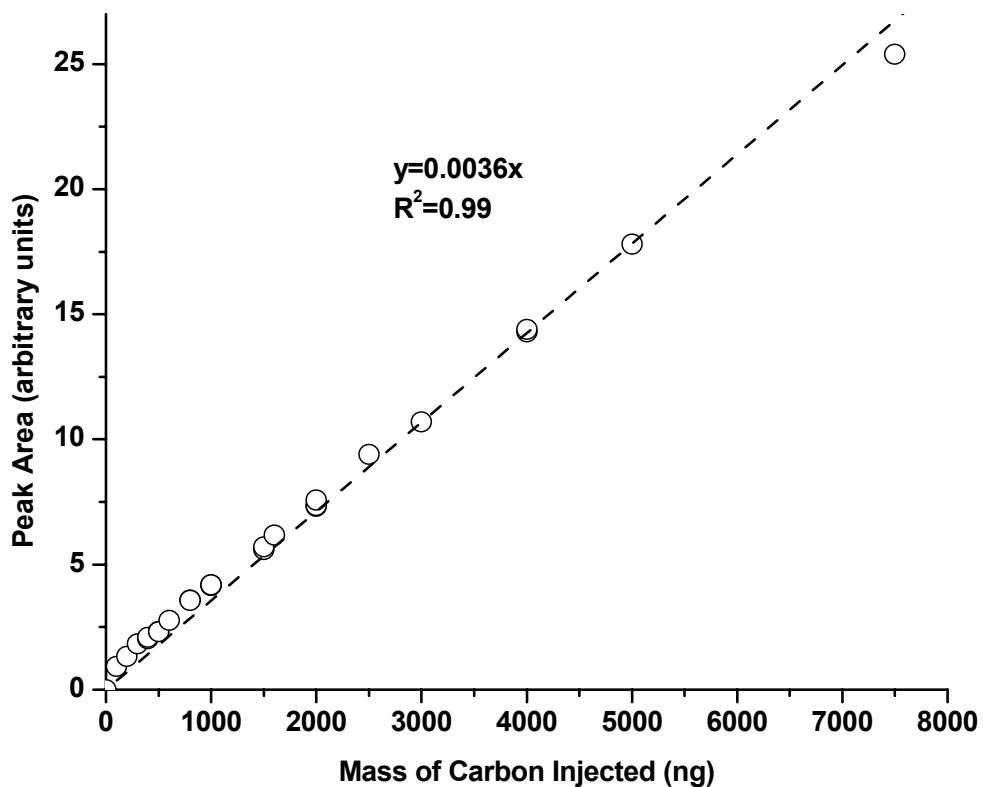


Figure 4.19 Calibration graph for organic carbon concentrations taken from Table 4.3.

From the calibration curve shown in Figure 4.19, the concentration of a sample can be determined by dividing peak area by the slope of the line of best fit. The correlation coefficient of 0.99 showed that a high degree of precision was obtained.

The limit of detection (LOD) and limit of quantitation (LOQ) provide a measure of the lower limits at which inferences relating to sample concentrations can be made with confidence. Adams (1995) defined LOD of an analyte as ‘the concentration at which a confident qualitative decision can be made about its presence in a sample’ and the LOQ as ‘the concentration at which a confident quantitative decision can be made about its presence in a sample’. The LOD is calculated by taking the mean of the area of the noise and adding it to three times the standard deviation of this noise and converting this peak area to concentration using the line of best fit

determined by calibration. The LOQ is calculated in a similar manner, except that ten times the standard deviation is used (Adams, 1995).

To calculate LOD and LOQ, ten blank injections were carried out. The blank samples consisted of ultra-pure laboratory water that had been used to prepare the OC standards for calibration. The area of the noise was determined by integrating the area under the curve where the peak from an OC standard would have eluted. LOD and LOQ are listed in Table 4.4 along with relevant statistical parameters.

Table 4.4 Limits of detection and determination for organic carbon detection.

Statistical Parameters	Value
Mean area	0.054
Std Dev (n=10)	0.019
LOD (ng)	31
LOQ (ng)	68

Results in Table 4.4, show that 30.8 ng of OC must be injected onto the column before a positive identification of a peak can be made and 68 ng of carbon needs to be injected before quantitation of peak area can be undertaken.

As stated previously Peuravuori and Pihlaja (2004) found that during HPSEC a small portion of material remains irreversibly sorbed onto the stationary phase, leading to underestimation of OC. The proportion of the unrecovered material was estimated by conducting a series of measurements where a sample was analysed both in the presence and in the absence of an HPSEC column. In the absence of a column (bypass mode), the peak area represented the total concentration of OC in the sample. The amount of OC that was irreversibly sorbed onto the column was estimated by subtracting the total peak area obtained with a column in place from the total peak area obtained in bypass mode. The unrecovered portion that was sorbed onto the stationary phase of the HPSEC column was termed the 'hydrophobic' material; i.e., the material that was sufficiently water insoluble to remain sorbed to the stationary phase at the pH and ionic strength of the mobile

phase. Table 4.5 shows the concentration calculated for the aerated water from the WGWTP, the same sample analysed in Figure 4.21. The results were obtained by taking the average of the peak areas of 10 replicate injections.

Table 4.5 Comparison of DOC concentration from Shimadzu TOC analyser and HPSEC-UV₂₅₄-OCD system, showing hydrophobic organic carbon content in raw water sample from WGWTP.

Experiment	DOC (mg L ⁻¹)
Organic carbon concentration OCD detector bypass(n=10)	6.88
RSD bypass	0.11
Organic carbon concentration Shimadzu TOC analyser	6.85
Organic carbon concentration HPSEC(n=10)	6.3
RSD HPSEC	0.35
Loss of organic carbon on Column	0.55

For the sample of raw water from WGWTP, 0.55 mg L⁻¹ of the total 6.88 mg L⁻¹ (8 %) was sufficiently hydrophobic that it remained sorbed to the stationary phase. The performance of the OCD developed in this study compared well with that of a commercially available dissolved organic carbon detector (Shimadzu TOC 5000). The concentration of OC obtained for the aerated Wanneroo GWTP raw water sample was 6.88 mg L⁻¹ using the OCD in this study and 6.85 mg L⁻¹ using the commercial DOC detector.

To investigate the repeatability of the system, 5 repeat injections of raw aerated WGWTP water were carried out using the semi-preparative column and conditions as outlined in Section 4.2.4. These five chromatograms are displayed in Figure 4.20.

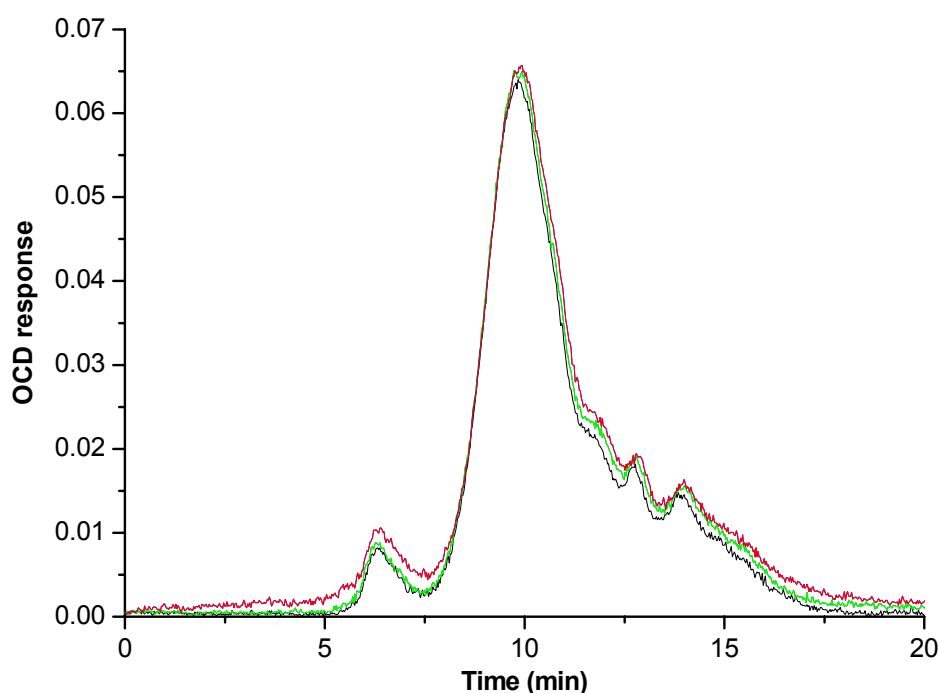


Figure 4.20 Repeatability investigation: different coloured curves represent the five different injections; HPSEC-OCD chromatogram of raw aerated water from WGWT, a) is the OCD signal and b) is the UV₂₅₄ signal. Chromatograms were obtained with a semi-preparative chromatographic column conditions described in Section 4.2.4.

The five chromatograms produced following five separate injections demonstrate the repeatability that is achieved using this system. To further demonstrate the quality of the data, the area under each curve was integrated and the data plotted in Table 4.6.

Table 4.6 Repeatability data of chromatograms plotted in Figure 4.20.

Repeat injection	Integrated area (units)
1	11.4
2	12.2
3	12.3
4	13.1
5	13.1
Average area (units)	12.4
5 std dev (%)	5.4

The integrated data from Table 4.6 suggests that variation in obtained signals using this detection system is minimal and results can be interpreted with a large degree of confidence.

4.3.8. Application of HPSEC-UV₂₅₄-OCD to Study the Molecular Weight Distribution of NOM

Following optimisation and calibration of the system, a feed water sample, collected at the WGWTP was analysed using both OCD and UV₂₅₄ as detectors, with a 250 mm x 22 mm i.d. column with HW-50s media. The chromatograms obtained are shown in Figure 4.21.

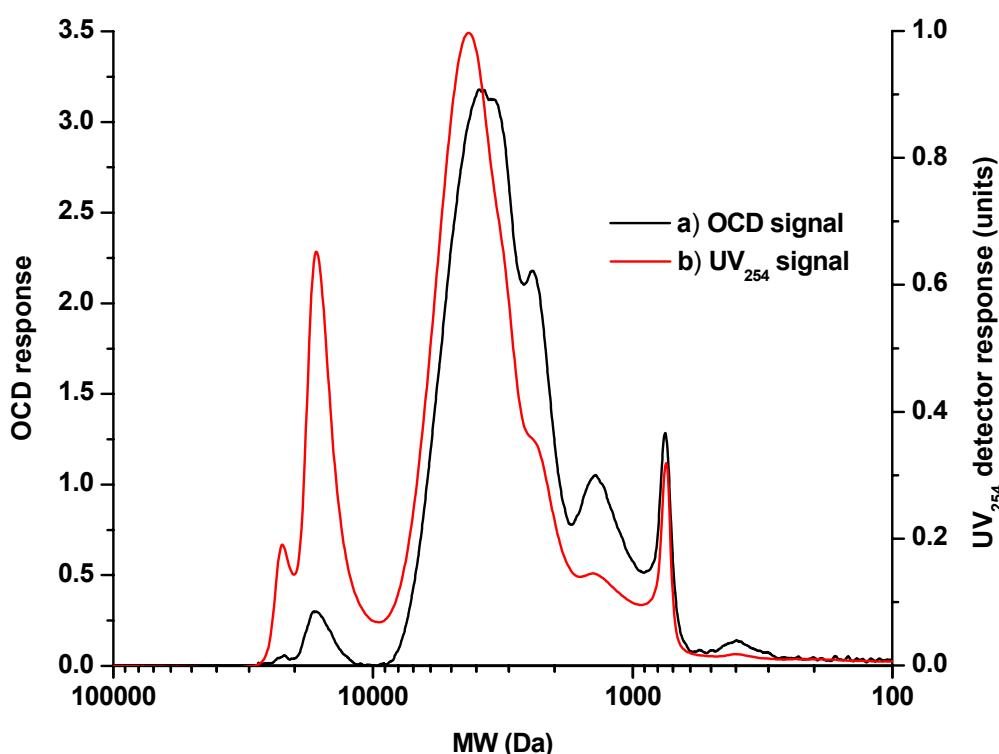


Figure 4.21 HPSEC-UV₂₅₄-OCD chromatogram of raw aerated water from WGWTP, a) is the OCD signal and b) is the UV₂₅₄ signal. Chromatograms were obtained with a preparative chromatographic column conditions described in Section 4.2.4.

There are obvious differences between the HPSEC-OCD and HPSEC-UV₂₅₄ chromatograms shown in Figure 4.21. The most noticeable difference is the peak intensity for material eluting at a MW of approximately 20 KDa (at the V_0 of the column). According to Huber and Frimmel (1996) this peak is likely to be comprised of colloidal material with a low organic content. Differences in the relative intensities of the HPSEC-OCD and HPSEC-UV₂₅₄ of this peak at V_0 demonstrate this colloidal nature. The intensity of the peak in the HPSEC-UV₂₅₄ chromatogram is likely due to light scattering of the colloidal

component, while the low intensity in the HPSEC-OCD chromatogram suggests that a small amount of organic material was associated with this colloidal fraction. The organic material with MW between 3 000 and 10 000 Da was also overestimated on the basis of the UV signal. Huber and Frimmel (1996) have suggested this material is likely to be comprised mainly of humic moieties and with a high aromatic content. Aromatic material strongly absorbs UV at 254 nm, which would account for the greater than expected signal intensity. Conversely, the organic material between 1000 and 3000 Da is underestimated by UV detection, compared to OCD. Huber and Frimmel (1996) and Specht and Frimmel (2000) suggested this peak likely comprised fulvic acids and keto acids. These types of compounds have a comparatively low UV absorbance at 254 nm, which would explain why their concentration, as shown by OCD, was underestimated by UV. There is a narrow band of organic material with a MW of approximately 600 - 700 Da where signal intensity for both the UV and DOC detectors appears very similar. Specht and Frimmel (2000) noted that small aromatic acids eluted at what appeared to be lower molecular weights than aliphatic compounds of similar MWs apparently due to interactions between the compounds and the stationary phase. Thus this narrow band may be comprised of small aromatic acids which would absorb UV at 254 nm and hence produce a signal comparable with OCD. The final portion of organic material eluted as a broad band at MWs below 500 Da. This material was underestimated by UV detection, which is not surprising as Huber and Frimmel (1996) suggested it likely contained hydrophilic organic material of aliphatic nature. The absence of any aromatic structural features and minimal conjugation would mean that signal intensity for this material is weak when using UV detection at 254 nm. It is evident that OCD is superior to UV in regard to providing an HPSEC chromatogram where signal intensity is related quantitatively to the actual concentration of organic material in a peak. The use of UV in combination with OCD is useful in that it provides an indication of the chemical structure of the eluting material.

4.4. Conclusion

The development of an organic carbon detection system for use with HPSEC was described. The system developed was similar to that of Specht and Frimmel (2000), apart from the use of an FTIR lightpipe detector equipped with a small detection cell for improving detection limits and reducing sample dispersion. The application of hollow fibre membranes and an optimised orthophosphoric acid dose (20 mmol L^{-1}) resulted in almost complete removal of inorganic carbon, this enabled HPSEC-OCD measurements to be conducted with a high degree of confidence. The combination of an optimised persulfate dose (0.84 mmol L^{-1}) and exposure of the sample stream to UV radiation through a quartz capillary (1200 mm in length) proved effective for the oxidation of organic carbon to CO_2 . A study of model organic compounds indicated in fact that the system developed in this study was superior to the system of Specht and Frimmel (2000) for the studied compounds. Hydrophobic PTFE membranes were an effective means for removing produced CO_2 from solution while the flow rate of nitrogen used as the sparge gas was an important parameter for detection of CO_2 in the lightpipe detector. The flow rate chosen (5 mL min^{-1}) was a compromise between lower detection limits and the considerable peak broadening achieved with low flow rates and greater peak resolution but higher detection limits when the flow rate was high.

The optimisation of each section of the OCD system resulted in HPSEC-OCD chromatograms which were noticeably different to those obtained using HPSEC-UV, particularly with respect to the highest and lowest MW peaks. Also, concentrations of DOC for each peak as well as the whole sample, both with and without separation on an HPSEC column could be determined with a high degree of accuracy.

5. DISINFECTION BEHAVIOUR OF MOLECULAR WEIGHT FRACTIONS ISOLATED BY PREPARATIVE HIGH PRESSURE SIZE EXCLUSION CHROMATOGRAPHY

5.1. Introduction

Chlorine is added to drinking water to control potentially harmful waterborne pathogens. However, the reaction between chlorine and aquatic NOM has the potential to form by-products which have their own health implications (Richardson, 2003). Rook (1974) and Bellar *et al.* (1974) first identified trihalomethanes (THMs) as the major product of drinking water disinfection with chlorine. Subsequent work identified that naturally occurring bromide present in chlorinated water was oxidised to hypobromous acid (HOBr) or hypobromite ion (OBr^-), depending on pH, species which are also able to undergo reactions with aquatic NOM to form brominated DBPs, among them THMs (Rook, 1976).

The formation of DBPs and the nature of DBP distribution are dependent on the presence and characteristics of DBP precursors, namely aquatic NOM, the concentration of bromide and iodide and the temperature and pH of the water being disinfected (Richardson, 1998). Variations in these parameters have resulted in more than 500 DBPs being reported in the literature for the chlorination of groundwaters and surface waters (Richardson, 2003). Reported DBPs, however, only account for a little under 50% of the total organic halogen (TOX) (Richardson, 2003). TOX represents a technique that has been used to measure the total halogenated component of treated drinking water. THMs are usually the largest group of chlorinated by-products, accounting for approximately 20% of the total TOX in chlorinated water (Richardson, 2003). They are also perhaps the easiest components to analyse and, for this reason, as well as having been identified as potential carcinogens (Bull *et al.*, 2001), are the class of compounds that have been most thoroughly investigated as an indicator of DBP formation (Richardson, 2003).

Due to the complexity of aquatic NOM, the mechanisms of THM formation have usually been studied in synthetic waters with model organic compounds. In many studies, *meta*-dihydroxybenzene structures have been shown to rapidly form high yields of THMs (e.g. Morris and Baum, 1978, Boyce and Hornig, 1983, Reckhow and Singer, 1985). The mechanism of THM formation from *meta*-dihydroxybenzene moieties was originally proposed by Rook (1976) and later amended by Boyce and Hornig (1983). The importance of these structures in the formation of THMs from humic substances was confirmed when 3,5-dihydroxybenzoic acid was found as a chemical degradation by-product of humic material (Norwood *et al.*, 1987). However, Gallard and von Gunten (2002a) demonstrated that the rate of formation of THMs from *meta*-dihydroxybenzene moieties was too fast to account for all THM precursors contained in aquatic NOM. The rate constant for formation of THMs from resorcinol (*meta*-dihydroxybenzene) was calculated as $k \geq 100 \text{ M}^{-1} \text{ s}^{-1}$ (Gallard and von Gunten, 2002b), while, in a separate study, rate constants for THM formation in surface waters ($k = 0.01\text{-}0.03 \text{ M}^{-1} \text{ s}^{-1}$) and groundwaters ($k \cong 0.12 \text{ M}^{-1} \text{ s}^{-1}$) were significantly less (Gallard and von Gunten, 2002a). The slower reacting THM precursors reportedly can account for greater than 70 % of precursors in aquatic NOM (Gallard and von Gunten, 2002a) and therefore other structures such as monohydroxybenzenes ($k = 2.49 \text{ M}^{-1} \text{ s}^{-1}$) and *para*-nitrophenol ($k = 0.026 \text{ M}^{-1} \text{ s}^{-1}$) may be important (Gallard and von Gunten, 2002b). Monohydroxy-benzenes gave a lower yield (0.004 moles of CH_3Cl per mole of compound) of THMs than resorcinol (0.7 moles of CH_3Cl per mole of resorcinol) (Reckhow and Singer, 1985), but they are reported to be more concentrated in aquatic NOM than dihydroxybenzene moieties (Norwood *et al.*, 1987), and could therefore be responsible for a large part of the slower reacting THM precursors (Gallard and von Gunten, 2002a).

Gallard and von Gunten (2002a) investigated possible structures of the fast and slow reacting fractions, through addition of model compounds to natural water samples, and measured chloroform formation upon chlorination. Resorcinol, phenol and methyl glyoxal were used as model compounds in

their study, representing known structural moieties of NOM. Only resorcinol was found to contribute to the formation of chloroform during the initial fast reacting stage, with $1\ \mu\text{mol L}^{-1}$ of chloroform produced for every $1\ \mu\text{mol L}^{-1}$ of resorcinol added. The addition of phenol did not change the amount of chloroform produced during the initial rapid reacting phase, but, after this initial phase, $0.2\ \mu\text{mol L}^{-1}$ of chloroform was produced from every $4\ \mu\text{mol L}^{-1}$ of phenol added. The high yield of THMs formed rapidly when *meta*-dihydroxybenzene structures are chlorinated was due to the formation of chlorinated keto-carboxylic acids, from breakdown of the aromatic ring, where the enol is stabilised by the carboxylic group (Gallard and von Gunten, 2002b). In the case of chlorinated ketones formed from monohydroxybenzene, such stabilisation is not possible and hence the rate and formation of THMs was lower (Gallard and von Gunten, 2002a). Addition of methylglyoxal did not affect chloroform production (Gallard and von Gunten, 2002a).

A number of authors (e.g., Rook, 1977, Larson and Rockwell, 1979, Reckhow and Singer, 1985, Westerhoff *et al.*, 1999, Westerhoff *et al.*, 2004, Bull *et al.*, 2006, Echigo and Minear, 2006) have identified *meta*-dihydroxy substituted benzene moieties (containing a carbon atom flanked by two carbons bearing hydroxy groups) to be particularly effective at rapid formation of THMs. Also, β -diketones and β -ketoacids have been shown to rapidly form THMs (Larson and Rockwell, 1979, Norwood *et al.*, 1980, Reckhow and Singer, 1985). Larson and Rockwell (1979) identified β -keto acids (or structures which could be converted to β -keto acids by simple reactions with chlorine) as structures capable of rapid THM formation. Citric acid and 3-ketoglutaric acid were two compounds that were particularly effective in forming THMs, although at a slower rate than *meta*-dihydroxybenzene, while in the same study isocitric acid, fumaric acid, maleic acid and oxaloacetic acid were ineffective in the formation of THMs in the presence of chlorine (Larson and Rockwell, 1979). Reckhow and Singer (1985) also demonstrated the effectiveness of compounds containing methyl ketone moieties for the formation of THMs upon chlorination. They found

that up to 96% of chlorine added to solutions of compounds containing methyl ketone moieties was incorporated into the THMs formed. Details of the chlorination of other aliphatic model compounds are limited when compared to the vast amount of literature on aromatic model compounds and modest number of reports on methylketones, β -diketones and β -ketoacids. Reckhow and Singer (1985) have published THM formation potential (THMFP) from chlorination experiments involving some simple aliphatic structures, including simple alcohols, aldehydes, ketones and carboxylic acids. Of the compounds tested, none produced significant quantities of THMs apart from the methyl ketone, 2-oxo-propionic acid.

Like the structural differences, changes in the MW of aquatic NOM can significantly influence the formation of THMs. Amy *et al.* (1991) provided evidence of the MW influence of NOM on THM formation by studying various MW fractions isolated by ultrafiltration and the THM concentrations measured after contact of these fractions with chlorine in the presence of natural bromide at a Cl_2/DOC ratio of 3:1. As the average MW of NOM was lowered for a Colorado River water, THM concentration, normalised against the DOC concentration, increased from 36 $\mu\text{g THM/mg DOC}$ for the $< 0.45 \mu\text{m}$ fraction to 46 $\mu\text{g THM/mg DOC}$ for the $< 1000 \text{ Da}$ fraction. Similarly for a California State water project water, the produced THM concentration increased from 48 $\mu\text{g THM/mg DOC}$ for the $< 0.45 \mu\text{m}$ fraction to 57 $\mu\text{g THM/mg DOC}$ for the $< 1000 \text{ Da}$ fraction (Amy *et al.*, 1991). In a more recent study on the effect of MW on THM formation, Gang *et al.* (2003) used ultrafiltration to collect four fractions of DOC of various apparent MWs. These fractions (0.2 μm -10 KDa, 10 KDa-1 KDa, 1 KDa-460 Da and $\leq 460 \text{ Da}$) were chlorinated and specific chlorine demand and THM formation determined. Significant differences in the chlorine demand of the fractions were found, with the highest MW fraction having the greatest chlorine demand and the lowest MW fraction having the lowest chlorine demand. This was suggested to be due to the larger MW material having a greater degree of conjugation. THM formation was calculated as a yield coefficient, where the mass of THM produced (μg) was normalised against the chlorine

consumed (mg) (*i.e.* $\mu\text{g-THM}/\text{mg-Cl}_2$ consumed) using identical DOC concentrations. Using this rationale, it was found that the larger the MW of a DOC component, the smaller the yield coefficient of THMs. This was proposed to be due to smaller halogenated intermediates being formed by the lower MW fractions, which are then able to decompose more readily to THMs, compared to the larger halogenated intermediates formed from higher MW DOC (Gang *et al.*, 2003).

Chow *et al.* (2005) published a comprehensive review of the reactivity of various NOM fractions in the formation of disinfection by-products (DBPs). In this review, no clear correlation between the MW of NOM fractions and the chlorine demand or formation of DBPs were identified. Conflicting data was in fact presented on the formation of DBPs from different MW fractions. Owen *et al.* (1993) presented data indicating the smallest MW fraction ($< 1\ 000$ Da), isolated by ultrafiltration, was the most significant producer of THMs, consistent with the results of Via and Dietrich (1996), who also used ultrafiltration to isolate MW fractions of NOM. However, Oliver and Thurman (1983) and Collins *et al.* (1985) reported specific THM yields increasing with increasing MW of fractions isolated by ultrafiltration, while Kitis *et al.* (2002) could find no clear trend in the study of chlorination of various MW fractions isolated by ultrafiltration from two surface waters from different origins.

These published studies utilised ultrafiltration to obtain MW fractions of NOM. This technique provides only broad MW ranges, based on the membranes used, and the largest MW material, approaching $0.2\ \mu\text{m}$, are grouped with intermediate MW material, at approximately $10\ 000$ Da. As has been shown previously in Section 3.3.2, the largest MW fraction can potentially contain inorganic colloidal species which may not be reactive to chlorine, lowering the observed chlorine demands for this fraction, and thus not provide a true indication of the chlorine reactivity of the organic fraction of the large MW material. Also, using the ultrafiltration approach, low MW inorganic species, such as nitrate and sulphate, will be concentrated in the lowest MW fraction. These species are known to have an appreciable oxidant demand (Jolley

and Carpenter, 1981), potentially biasing results for oxidation experiments. Newcombe *et al.* (1997), in a study of surface water from South Australia, explained the bias of ultrafiltration membranes against negatively charged components of NOM due to the residual negative charge on the surface of the membrane. This potentially can result in each fraction containing lower MW material than would be expected due to retention of charged lower MW material. It is possible that the lack of consistent correlation between the MW of NOM fractions and the chlorine demand or formation of DBPs from those fractions arises from these issues associated with ultrafiltration to prepare the fractions.

An alternative approach to collecting well resolved MW fractions of NOM has been reported by Piccolo *et al.* (2002) and Peuravuori and Pihlaja (2004), who used HPSEC in a preparative mode to collect up to eight MW fractions of NOM free from inorganic contaminants. Piccolo *et al.* (2002) used preparative HPSEC to collect MW fractions from a sample of humic acid isolated from a North Dakota lignite. Two samples were investigated: the humic acid sample without treatment and the humic acid sample treated with 0.05 M acetic acid, apparently used to disrupt the weak dispersion forces holding the humic molecules together. In both cases, eight MW fractions of the humic acid were collected and the mobile phase salts removed by dialysis. Using this method, Piccolo *et al.* (2002) were able to recover 98 % of the original humic acid samples after dialysis and lyophilisation. The solid isolates were then analysed by pyrolysis GC-MS (Py-GC-MS) and solution state ^1H NMR spectroscopy. These analyses showed distinct differences between the collected MW fractions, with a general trend from aromatic rich species of high MW to more hydrophilic oxygenated compounds in the lower MW fractions. In a similar study, Peuravuori and Pihlaja (2004) used HPSEC in a preparative mode to fractionate and isolate MW fractions of NOM from a surface water sample from Lake Savojärvi in southern Finland. By using a superior mobile phase to achieve greater chromatographic resolution, eight fractions were collected after preparative HPSEC. These fractions were subjected to dialysis to remove mobile phase salts and lyophilisation to obtain solid isolates and resulted in organic carbon recoveries of 92 % of the

injected NOM separated into eight distinct MW fractions. The solid isolates were then analysed by FTIR spectroscopy; however, unlike the results of Piccolo *et al.* (2002), the analytical methods used were not able to identify significant differences between at least six of the eight fractions, while only slight differences in FTIR peak intensities were observed.

5.1.1. Scope of Study

The disinfection behaviour of MW fractions collected by preparative HPSEC has not previously been investigated. In the current study, following the methods of Piccolo *et al.* (2002) and Peuravuori and Pihlaja (2004), nine MW fractions of NOM from a shallow bore in the Wanneroo borefield were isolated, inorganic contaminants removed and the fractions analysed by solid state ^{13}C NMR spectroscopy. Following structural characterisation, each of the fractions was treated with chlorine and the chlorine demand determined over seven days, and then, in the presence of a low concentration of bromide, THM concentrations were determined over a seven day period.

5.2. Experimental

5.2.1. Samples

A sample of groundwater for isolation and fractionation of NOM by preparative HPSEC was taken on the 8th February 2005 from Production Bore W300 (Figure 5.1), drawing water from the shallow unconfined aquifer in the Gnamara mound.

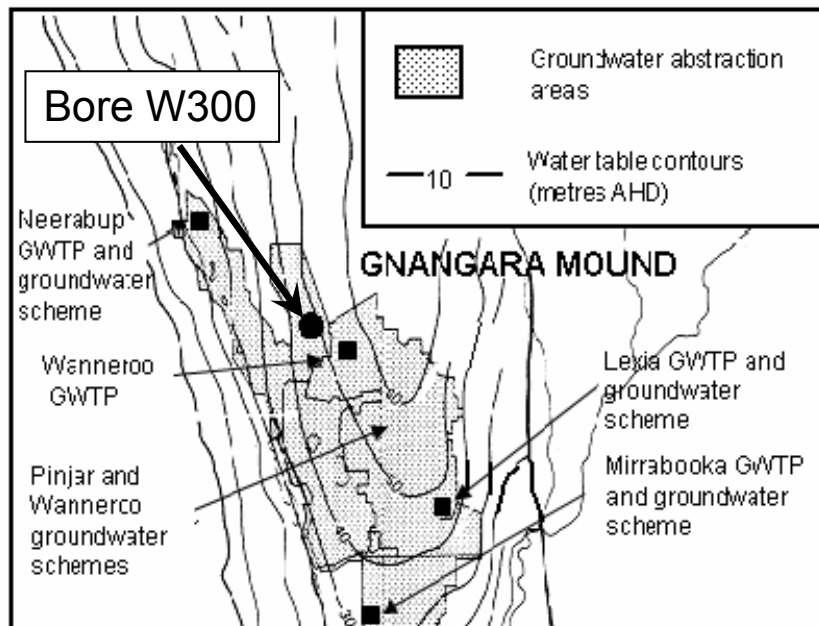


Figure 5.1 Location of production Bore W300.

Two stainless steel containers (75 L and 50 L) were rinsed with acetone, rinsed three times with purified laboratory water, once with dilute nitric acid (1 %), rinsed five times with purified laboratory water and finally three times with the sample. The sample (119 L) was collected after running the bore for 5 minutes prior to collection, then transported directly to the laboratory and filtered through a 0.45 μm membrane (Saehan high-clean polycarbonate membrane) to yield 117.8 L of sample (DOC concentration 31.9 mg L^{-1} , UV_{254} 1.03 cm^{-1}) which was then stored at 4 °C until required. A sub-sample of this water was sent to an external laboratory for a number of analyses on bulk water characteristics.

A portion of the sample (65.4 L) was concentrated approximately 13-fold using a tangential flow ultrafiltration (UF) system, comprising a Prep/Scale-TFF 6 foot² PLAC regenerated cellulose UF membrane (Millipore, USA) with a nominal MW cut-off of 1000 Da. The retentate (5 L) had a DOC

concentration of 385 mg L^{-1} which indicated a recovery of DOC of 92 %. This UF concentrated water was then fractionated by preparative HPSEC.

5.2.2. Materials and Methods

5.2.2.1. Purified Laboratory Water

Purified water was obtained as described in Section 2.2.2.1.

5.2.2.2. Reagents

Analytical grade methanol (ChromAR HPLC, Mallinckrodt), acetone (ChromAR HPLC, Mallinckrodt) and nitric acid (UNIVAR) were used without further purification. Potassium dihydrogenphosphate (BDH chemicals) and disodium hydrogenphosphate (BDH chemicals), used in the HPSEC mobile phase, were both of analytical grade. Standards used for MW calibration of the analytical HPSEC system, including polystyrene sulphonates (Polymer Scientific Services) and Dextran blue (Sigma-Aldrich), were all analytical grade. Analytical grade sodium bromide (Chem-Supply, AR) and sodium hypochlorite (Ajax chemicals) was used in the preparation of bromide and chlorine solutions, respectively, and analytical grade sodium thiosulfate (Ajax chemicals) was used to quench remaining free chlorine equivalents. For the calibration of the THM analysis, analytical grade bromoform, chloroform, dibromochloromethane and dichlorobromomethane (Sigma-Aldrich) were used with 1,2-dibromopropane (Sigma-Aldrich) as the surrogate standard. Analytical grade sodium carbonate (BDH chemicals) was used for ionic strength adjustment for the solid phase microextraction (SPME) analyses.

5.2.2.3. Preparative HPSEC Separation

Preparative fractionation of the sample was carried out following the method described by Peuravuori and Pihlaja (1997). The chromatographic system was comprised of a BioSep SEC-S 3000 (300 x 21.2 mm i.d., Phenomenex) column equipped with a BioSep SEC-S 3000 guard column (75 x 21.2 mm i.d., Phenomenex), a 20 mmol L^{-1} phosphate buffer (1.36 g L^{-1}

potassium dihydrogenphosphate and 3.58 g L⁻¹ disodium hydrogenphosphate) as the mobile phase, a flow rate of 2 mL min⁻¹ and an injection volume of 2 mL. The HPLC system was an Agilent 1100 equipped with a dual-loop autosampler, a diode array detector collecting data at 254 nm, and an automated fraction collector capable of collecting an infinite volume of individual fractions to enable the system to run without interruption for an extended period of time (the period for one preparative HPSEC run was approximately 1.2 hours). Nine individual MW fractions were collected along with the HPSEC mobile phase after each of the large number of sample injections. Elution volumes were used as selection criteria for each MW fraction, and the automated fraction collector was able to collect the same MW fraction eluting at this elution volume, combining with identical MW fractions collected in previous runs. The large volume of each separated MW fraction was concentrated by rotary evaporation to 500 mL, also containing the concentrated phosphate mobile phase used as the HPSEC mobile phase. As a result, each fraction was then dialysed against purified laboratory water until the conductivity remained constant (~5 mS m⁻¹). Bromide measurements were taken according to the procedure outlined in Section 5.2.2.6. A sub-sample of these retentates (20 mL) was taken and the DOC concentration determined by a commercial DOC analyser (Shimadzu TOC 5000). Depending on the DOC concentration of the fraction, a further sub-sample (~5-25 mL) was taken and diluted in 500 mL of purified laboratory water to obtain a DOC concentration of 2 mg L⁻¹. The remaining volume of each fraction was then freeze dried to obtain solid isolates of MW fractions for ¹³C NMR analysis. The total number of preparative HPSEC runs was 1038, equating to 800 mg of DOC and approximately 25 L of unconcentrated Bore W300 water.

5.2.2.4. Analytical HPSEC

Analytical scale HPSEC was carried out according to the method described in Chapter 3.2.2.4.

5.2.2.5. Chlorine Demand and Trihalomethane Formation Potential Measurements

A sub-sample of the dialysed, concentrated sample (~5-25 mL) was taken for each fraction depending on DOC concentration and diluted in purified laboratory water (500 mL) to obtain a DOC concentration of 2 mg L⁻¹. An exception was Fraction 3, where 1 L of purified laboratory water was used in the dilution step to obtain a 2 mg L⁻¹ DOC concentration solution. Chlorine demand and THMFP measurements were conducted using this diluted sample.

For chlorine demand experiments, three sub-samples (3 x 100 mL, apart from Fraction 3 where seven sub-samples, 7 x 100 mL, were required) were taken from the 2 mg L⁻¹ DOC concentration solutions and dosed with a concentrated hypochlorite solution (1 850 mg L⁻¹) to produce initial chlorine concentrations of 4, 6 and 8 mg L⁻¹ (except that Fraction 3 had initial chlorine concentrations of 4, 6, 8, 12, 14, 16 and 18 mg L⁻¹). Free chlorine measurements were conducted at regular time intervals (0, 0.5, 1, 4, 24, 72 and 168 hours) using the DPD colorimetric method (Clesceri *et al.*, 1998). Chlorine demand was calculated according to the method described by Warton *et al.* (2006), where the demand of chlorine by the water sample is calculated to give a chlorine residual of 0 mg L⁻¹ after 168 hours of contact.

For THMFP analyses, a further 100 mL sub-sample of each fraction (DOC concentration of 2 mg L⁻¹) was dosed with a concentrated hypochlorite solution (1 850 mg L⁻¹) and concentrated bromide solution (1 000 mg L⁻¹) to produce solutions with 8 mg L⁻¹ initial free chlorine and 0.2 mg L⁻¹ initial bromide (except that Fraction 3 had an initial free chlorine concentration of 18 mg L⁻¹ to account for its higher chlorine demand). At regular time intervals (0.5, 1, 4, 24, 72 and 168 hours), a 15 mL aliquot was taken and dosed with a concentrated sodium thiosulfate solution (50 µL, 2 000 mg L⁻¹) to quench any remaining free chlorine equivalents, and the samples stored in the dark at 4 °C until analysed for THMs. For analysis of THMs, aliquots

(10 mL) of each quenched fraction were added to sodium carbonate (1.67 g) for ionic strength adjustment, and an aliquot (10 μL) of a solution of dibromopropane, used as a surrogate standard for calibration of THMs. Calibration standards for quantitation of THM concentrations were prepared by dissolving bromoform, dibromochloromethane, dichlorobromomethane and chloroform (200 mg of each) in methanol (100 mL) to produce a combined stock solution (2 000 mg L^{-1} of each THM). Working solutions were prepared as required. Calibration was carried out by diluting the working solution (0, 2, 20, 26, 50, 76 and 100 μL) in purified laboratory water (10 mL) containing sodium carbonate (1.67g) and the surrogate standard solution (10 μL). From analysis of these calibration standards, concentrations of THMs in water samples could be calculated.

THM concentrations were determined using automated headspace solid-phase microextraction (SPME) coupled with gas chromatography-mass spectrometry (GC-MS), using a Gerstel Multi-Purpose Sampler 2 (MPS-2) for automated SPME and an Agilent 6890 GC and Agilent 5873 mass selective detector (MSD). Sample vials were added to the MPS-2 autosampler and heated to 40 $^{\circ}\text{C}$ and agitated at 300 rpm for 15 minutes prior to analysis. The SPME fibre (divinyl benzene/Carboxen/polydimethylsiloxane (50/30 μm)) was inserted into the headspace of the vial for 15 minutes for extraction of THMs. The SPME fibre was desorbed at 270 $^{\circ}\text{C}$ for 10 minutes in the injector port of the GC and a split ratio of 50:1 employed. Analytes were separated using a 30 m x 0.25 mm i.d., phase thickness 1 μm , fused silica column (ZB-5, Phenomenex). The helium carrier gas operated at a pressure of 7.3 psi and a flow rate of 1 mL min^{-1} . The following temperature program was used: initial temperature 40 $^{\circ}\text{C}$ (3 minutes), increased at 8 $^{\circ}\text{C min}^{-1}$ to 120 $^{\circ}\text{C}$ (0 minutes) then increased at 20 $^{\circ}\text{C min}^{-1}$ until the final temperature of 280 $^{\circ}\text{C}$ (5 minutes). The MS operated in electron impact mode at 70 eV, collecting in selected ion monitoring mode, monitoring ions m/z 83, 85, 96, 127, 129, 131, 173, 175.

¹³C Nuclear Magnetic Resonance Spectroscopy of Individual MW Fractions

The solid-state ¹³C cross polarization (CP) magic angle spinning (MAS) NMR spectra were obtained at a ¹³C frequency of 50.3 MHz on a Varian Unity 200 spectrometer at the University of Adelaide, Australia. The freeze-dried MW fractions were each packed in a 7 mm diameter cylindrical zirconia rotor with Kel-F end-caps and spun at 5000 ± 100 Hz in a Doty Scientific MAS probe. The spectra were acquired using a 1 msec contact time and a 1 sec recycle delay. Between 24 000 and 61 000 scans were collected, representing a total run time of 7 to 17 hours. The free induction decays (FID) were acquired with a sweep width of 40 kHz; 1216 data points were collected over an acquisition time of 15 msec. The FID was zero-filled to 32768 data points and processed with a 50 Hz Lorentzian line broadening and a 0.01 sec Gaussian broadening. The chemical shift was externally referenced to the methyl resonance of hexamethylbenzene at 17.36 ppm. Spectra were corrected for background signal by subtracting the spectrum acquired for an empty rotor under the same acquisition conditions.

5.2.2.7. Analysis of Bromide

Samples were filtered through a 0.45 µm membrane (Pall Acrodisc®) and analysed using an ICS90 ion chromatography system (Dionex Corporation). Samples were injected using an AS40 automated sampler (Dionex Corporation) with an injection volume of 100 µL. Analytes were separated using an Ionpak AS141A column (250 mm x 4 mm, Dionex Corporation), operating with an Ionpak AG14 guard column (50 mm x 4 mm, Dionex Corporation). The mobile phase was comprised of a 1.5 mmol L⁻¹ NaHCO₃ + 4.5 mmol L⁻¹ Na₂CO₃ solution operating at a flow rate of 1.5 mL min⁻¹. Detection was *via* a Dionex conductivity detector equipped with a DS5 detection stabiliser (Dionex Corporation) and an AMMS III 4MM suppressor (Dionex Corporation) with a 20 mmol L⁻¹ H₂SO₄ regenerant stream solution at a flow of 2 mL min⁻¹. Data was interpreted using Chromeleon V 6.7

software. The detection limit of the system for bromide was determined to be $10 \mu\text{g L}^{-1}$.

5.2.2.8. Measurement of Constituents and Water Quality Parameters in Water Samples

Water quality parameters including colour, turbidity, conductivity, pH and UV_{254} and the concentrations of total alkalinity, chloride, total dissolved solids, hardness and total filterable solids were determined as outlined in Section 3.2.2.1.

5.2.2.9. Measurement of Dissolved Organic Carbon Concentration

DOC concentrations were measured according to the procedure outlined in Section 3.2.2.3.

5.3. Results and Discussion

5.3.1. Isolation and Fractionation of Aquatic NOM by Preparative HPSEC

A large volume (119 L) of groundwater from a Wanneroo bore in the shallow unconfined aquifer was collected for isolation and fractionation of NOM by preparative HPSEC. Characteristics of the water sample are presented in Table 5.1. This particular bore was chosen because it is one of the Wanneroo bores which contains a very high concentration of DOC, allowing collection of significant quantities of DOC from a smaller volume of sample. The DOC concentration in the sample collected was 32 mg L^{-1} and the sample contained a moderate bromide concentration at 0.2 mg L^{-1} . The UV_{254} value, 1.03 cm^{-1} , was considerably high as was true colour at 220 Hazen units. The pH of 5.9 was low for this sample.

Table 5.1 Characteristics of Bore water W300

Parameter	units	Value
DOC	mg L ⁻¹	31.9
UV ₂₅₄	cm ⁻¹	1.03
True Colour	Hazen Units	220
Bromide	mg L ⁻¹	0.2
pH	units	5.9
Chloride	mg L ⁻¹	76
Total Alkalinity as CaCO ₃	mg L ⁻¹	15
Conductivity	μS cm ⁻¹	310
Total Dissolved Solids	mg L ⁻¹	210
Hardness	mg L ⁻¹	45
Turbidity	NTU	8
Total filtered solids	mg L ⁻¹	175.7

The sample was first filtered through a 0.45 μm membrane. A portion (65.4 L) of this filtered sample was then subjected to ultrafiltration using a 1 000 Da membrane and concentrated to 5 L. The DOC concentration of the retentate was 385 mg L⁻¹, representing a recovery of DOC of 92%, following ultrafiltration concentration, compared with a 97 % recovery in the study by Peuravuori and Pihlaja (2004), using preparative HPSEC to investigate humic material isolated from Lake Savojärvi in southern Finland. The loss of sample following ultrafiltration indicates that only approximately 8 % of NOM was of MW < 1 000 Da. Significantly HPSEC chromatograms (Figure 5.2 and Figure 5.3) indicated that material with a MW < 1 000Da was in fact removed during the process.

Preparative fractionation of a portion (2.07 L) of the ultrafiltration retentate was carried out, using a preparative-scale BioSep SEC-S 3000 (300 x 21.2 mm i.d.) column and UV₂₅₄ detection, following the method described by Peuravuori and Pihlaja (1997). The procedure was automated by use of an autosampler and an automated fraction collector, allowing repeated injections (1038 × 2 mL) of sample and combined collection of nine fractions from the repeat analyses. A typical preparative HPSEC chromatogram obtained using this system is shown in Figure 5.2, which also shows the

elution volume cut-offs of the nine fractions collected. The total volume, after 1038 injections, of each of the nine fractions collected depended upon the peak width over which it was collected. For example, the largest volume of sample was collected for Fraction 3, while the smallest volume of sample was collected for Fraction 5 and Fraction 8. The amount of organic material collected, however, was a function of the volume of each fraction collected, as well as the amount of organic material in each individual peak. Using this rationale, the greatest amount of organic material was collected in Fraction 3, followed by Fraction 4, while Fraction 2 contained the least overall amount of organic matter.

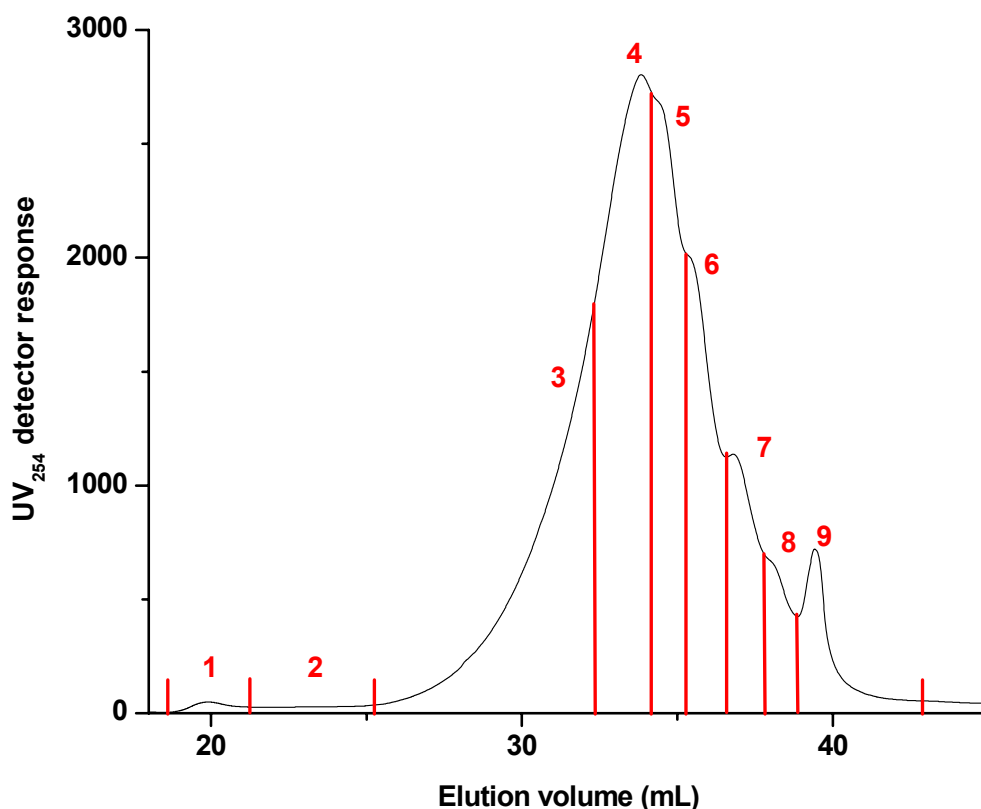


Figure 5.2 Preparative HPSEC-UV₂₅₄ chromatogram of UF treated W300 bore water, indicating positions of nine collected fractions. Numbers in red are the number attributed in the text to each fraction. The column was a BioSep SEC-S 3000 (300 mm x 21.2 mm i.d.) silica base HPSEC column and the mobile phase was a 20 mmol L⁻¹ phosphate buffer. The flow rate was 2 mL min⁻¹ and the injection volume was 2 mL.

Each of the nine fractions were concentrated by rotary evaporation and then dialysed in a 1 000 Da dialysis bag to remove mobile phase salts, and

analysed, as well as the original UF concentrated sample, on an analytical-scale HPSEC column with a similar phase (TSK G3000SW_{xl}) to that of the preparative HPSEC column. Figure 5.3 illustrates the HPSEC chromatogram of the ultrafiltration retentate of W300 borewater analysed on the analytical TSK G3000SW_{xl} column, as well as chromatograms of the nine fractions collected by preparative HPSEC (BioSep-SEC-S 3000 column), after dialysis.

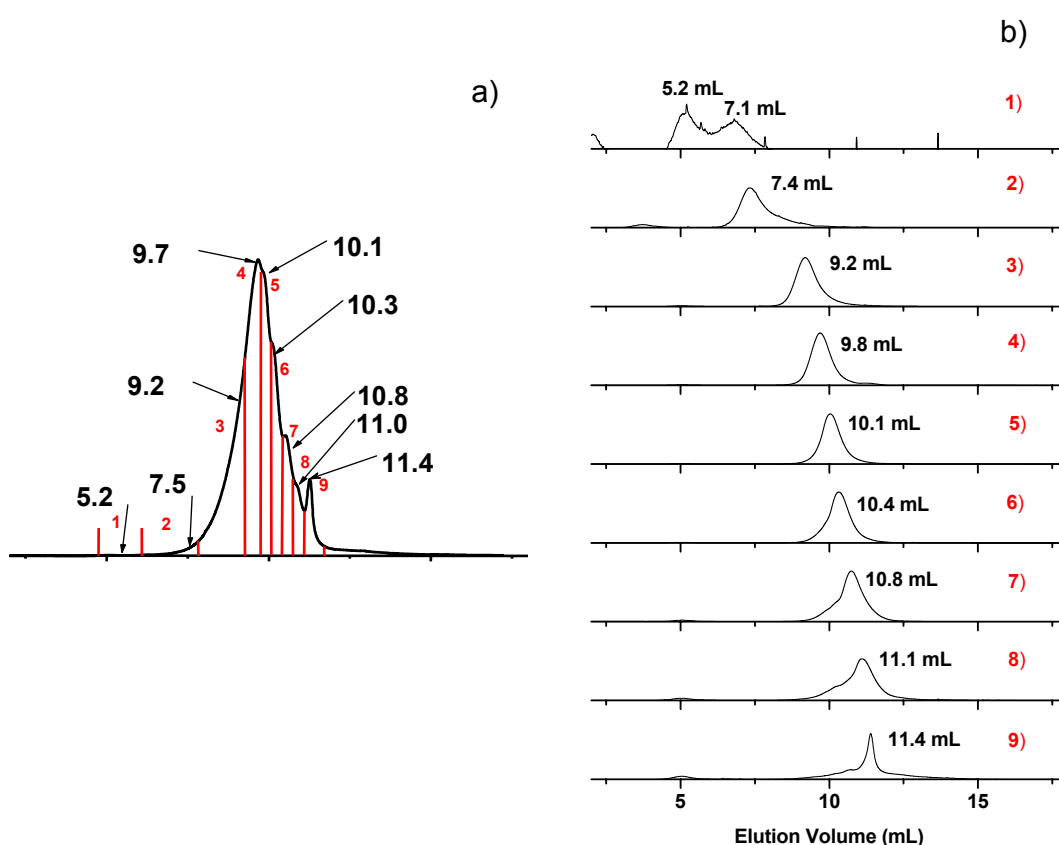


Figure 5.3 a) Analytical HPSEC-UV₂₅₄ chromatogram (TSK G3000SW_{xl} 300 mm x 7.8 mm column) of UF treated W300 water. Numbers above chromatogram represent the elution volume at which fractions were collected. Numbers in red are the number attributed to each fraction in the text. Red lines mark intervals where fractions were collected; b) HPSEC-UV₂₅₄ chromatograms of individual fractions after analysis on the analytical column. Volume above represents elution volume of individual fractions. Numbers in red are numbers attributed to fractions in text.

Comparison of analytical scale HPSEC (Figure 5.3a) and preparative scale HPSEC (Figure 5.2) on two similar silica-based phases produced chromatograms that were practically identical. Apart from Fraction 1, for each isolated MW fraction, a single peak was observed upon re-injection on

the analytical HPSEC column (Figure 5.3b). For Fraction 1, two semi-resolved peaks were obtained upon re-injection. The reasons for this will be discussed below. This indicates that, with the chromatographic system used, true MW fractions were likely to have been obtained. Figure 5.3 illustrates the homogeneity of the nine separated fractions was excellent, and retention volumes of individual peaks were almost identical to those obtained in the HPSEC chromatogram of the whole water sample. Peuravuori and Pihlaja (2004) found similar results in their study using preparative HPSEC to fractionate a lake humic material. From Figure 5.3, the nine fractions collected by preparative HPSEC eluted at 5.2, 7.4, 9.2, 9.8, 10.1, 10.4, 10.8, 11.1 and 11.4 mL when subjected to analytical scale HPSEC. These elution volumes correspond to apparent MW values of > 72 000 (although the apparent MW of this fraction was outside the calibration range of the system), 16 500, 4 900, 3 250, 2 650, 2 150, 1 650, 1 350 and 1 100 Da. The first peak at an elution volume of 5.2 mL is situated at the void volume of the column, and therefore is comprised of material of greater molecular size than is able to be separated by the column system. The elution volume of the last peak, which eluted as a sharp peak at 11.4 mL, is likely to be at the permeation volume of the column. As was stated previously (Section 2.2.2.2), the permeation volume of the column was measured with acetone. Specht and Frimmel (2000) have demonstrated that using standards such as acetone and methanol for measuring the permeation volume overestimates the actual value due to interactions with the stationary phase. Instead, they have shown that measuring the conductivity of the mobile phase, while injecting water as a MW standard, gives a more accurate value for the permeation volume. They have also noted that the sharp peak which occurs at higher elution volumes is at the permeation volume (Specht and Frimmel, 2000). Taking this into account, it is likely that the sharpness of the peak at 11.4 mL is at the permeation volume, due to a lowering of the mobile phase ionic strength, as a result of a mismatch between the sample and mobile phase ionic strengths (Figure 5.3b, Fraction 9). The 1 100 Da MW value of this last-eluting peak is further confirmation that ultrafiltration with a 1 000 Da membrane did successfully provide the fraction of NOM of MW > 1 000 Da.

The chromatograms of individual MW fractions in Figure 5.3b illustrate that peaks 3-6 were comprised of organic material of a homogeneous and uniform nature, i.e., the MW of components making up these fractions was very similar. These four fractions account for approximately 80 % of the total detected organic material (based on UV_{254} -absorptive capacity). Also, each of these fractions eluted at the elution volume corresponding to their elution volume in the chromatogram of the whole sample. Fractions 2, 7 and 8 also contained material that was relatively homogeneous and uniform with regard to MW, although the MW distribution was greater than for Fractions 3-6. Fractions 2, 7 and 8 accounted for approximately 12% of the total detected organic material (based on UV_{254} -absorptive capacity), again each eluting at the same elution volume as shown in the chromatogram of the whole sample. Fraction 1 shows two peaks, with the first at an elution volume of 5.2 mL equal to that in the original mixture, accounting for approximately 60 % of the UV_{254} area of this fraction, and a peak at 7.1 mL, accounting for the remaining 40 % of the fraction. In the original mixture, this fraction accounted for only 1.4 % of the UV_{254} area and thus the total amount collected of this fraction was extremely low. Possibly the presence of the second peak at 7.1 mL is a result of partial mixing with Fraction 2 during the fraction collection stage. These two fractions contain the least amount of DOC and would thus be particularly susceptible to small amounts of mixing during the collection of fractions. Fraction 9 is unlike any of the others, with an extremely sharp peak produced at exactly the same elution volume as in the original mixture (11.4 mL). Approximately 90 % of the material eluted as a sharp band centered at 11.4 mL, which is likely due to the 'salt boundary' effect. It is possible this fraction will contain material with a range of MWs centred around this elution volume, but due to the lowering of the ionic strength at this point of the chromatogram, charged and very hydrophilic molecules will elute in this sharp band as they have been restricted in the volume of the stationary phase they can sample due to charge exclusion. Based on UV_{254} -absorptive capacity, this material accounted for only approximately 6 % of the total organic matter in the sample.

5.3.2. Recovery of Dissolved Organic Carbon from Preparative HPSEC Separation

The total amount of organic carbon (measured as a DOC concentration) subjected to preparative HPSEC was 800 mg in 1038 runs. After collection of fractions, concentration by rotary evaporation and removal of mobile phase salts by dialysis, analysis of bromide and DOC concentrations for each fraction were conducted. This resulted in 751.5 mg (94 %) of organic carbon recovered in total in the nine fractions, and no bromide was detected in any of the nine fractions after dialysis. This preparative HPSEC recovery compares favourably to the 92 % recovery achieved by Peuravuori and Pihlaja (2004) who, using preparative HPSEC, collected eight fractions which were then de-salted using an identical procedure to that described in this research, and 98 % recovery achieved by Piccolo *et al.* (2002) who collected six fractions also using preparative HPSEC and an identical procedure to desalt obtained fractions. Piccolo *et al.* (2002) and Peuravuori and Pihlaja (2004) attributed the small loss of organic matter to adsorption onto the stationary phase. Table 5.2 shows the mass of organic matter measured as DOC for each of the nine preparative SEC fractions collected after dialysis, as well as the total amount of material injected in 1038 chromatographic runs, the percentage of the UV₂₅₄ absorbing material contained in each fraction (determined by the integrated area of each peak in the UV₂₅₄ chromatogram), the M_w of material in each peak and the polydispersity of material in each peak.

From Table 5.2, 57 % of the DOC was collected in Fractions 3 and 4. This compares closely with the integrated area of the HPSEC-UV₂₅₄ chromatogram (54 %). Fractions 5-9, representing the lower MW components of the sample, accounted for 41 % of the total DOC, with Fractions 1 and 2 contributing only 2 % of the total DOC. The areas from the HPSEC-UV₂₅₄ chromatogram and DOC measurements of the dialysed fractions produced very similar results for the amount of material in each fraction.

Table 5.2 Distribution of DOC by Preparative HPSEC-UV₂₅₄ and Nominal MWs of the Separated Size Fractions. ^a calculated from measured DOC concentration of solution.

sample	mass of DOC (mg) ^a	% DOC in fraction	% of total HPSEC-UV ₂₅₄ peak area	polydispersity (ρ)
original water (UF treated)	800	-	-	1.65
Fraction 1	3	0.5	1	8
Fraction 2	10.5	1.5	1	1.3
Fraction 3	231	31	29.5	1.2
Fraction 4	199	26	24.5	1.1
Fraction 5	98	13	14	1.1
Fraction 6	75	10	12	1.1
Fraction 7	68	9	8	1.2
Fraction 8	24	3	3.5	1.3
Fraction 9	43	6	6.5	1.6
Σ (Fractions 1-9)	751.5	100	-	-

The polydispersity (MW spread) of the nine fractions (Table 5.2) is of particular interest and was calculated according to equations 1.1-1.3. Apart from Fraction 1, the remaining eight fractions have values all relatively close to 1. A value of 1 represents a polymer with a monodispersed MW (Mori and Barth, 1999), i.e. all molecules in the polymer have the same average MW. Polymers with a polydispersity of close to one have narrow MW distributions, and polymers with polydispersities further away from unity have wider ranges

of average MWs for the molecules in that polymer (Mori and Barth, 1999). As was shown in Figure 5.3 b, Fraction 1 contained material with a wide range of MWs, so its high value of ρ is not surprising. In particular, Fractions 3-7, accounting for 90 % of the organic matter in the sample, had values of ρ between 1.1 and 1.2. Fractions 2, 8 and 9 had moderate values of ρ of 1.3, 1.3 and 1.6, indicating that these fractions are all still relatively monodispersed in regard to MW distribution. These polydispersity values compare favourably to many commercially available polymer standards used as calibration standards for MW.

5.3.3. Solid State ^{13}C NMR Spectroscopy of Individual MW Fractions

NMR spectroscopy is one of the most useful spectroscopic methods for investigation of NOM structure because qualitative and quantitative organic structural information for certain organic moieties can be generated in both solution and solid states under nondegradative conditions (Knicker and Nanny, 1997). Quantification under certain conditions can, however, be difficult due to incomplete cross polarisation of certain atoms, typically aromatic carbon atoms (Alamany *et al.*, 1983, Wilson, 1987, Knicker and Nanny, 1997). With this in mind, solid state ^{13}C NMR spectroscopic analysis was conducted for the first time on MW fractions of NOM isolated by preparative HPSEC chromatography. Due to limitations in collected sample sizes (see Table 5.2), Fractions 1 and 2 could not be analysed by NMR spectroscopy. Also, Fractions 5 and 6 and Fractions 7-9 were combined to obtain two samples with sufficient material for analysis. Fractions 5 and 6 eluted adjacent to each other in the HPSEC chromatogram (Figure 5.2) and, thus, it is not unreasonable to assume that they will contain organic material of a similar nature. Similarly, Fractions 7, 8 and 9 eluted adjacent to each other in the HPSEC chromatogram (Figure 5.2) and most likely contain organic matter of a similar nature. The solid state ^{13}C NMR spectra of Fraction 3, Fraction 4, Fractions 5 and 6 and Fractions 7-9 are shown in Figure 5.4.

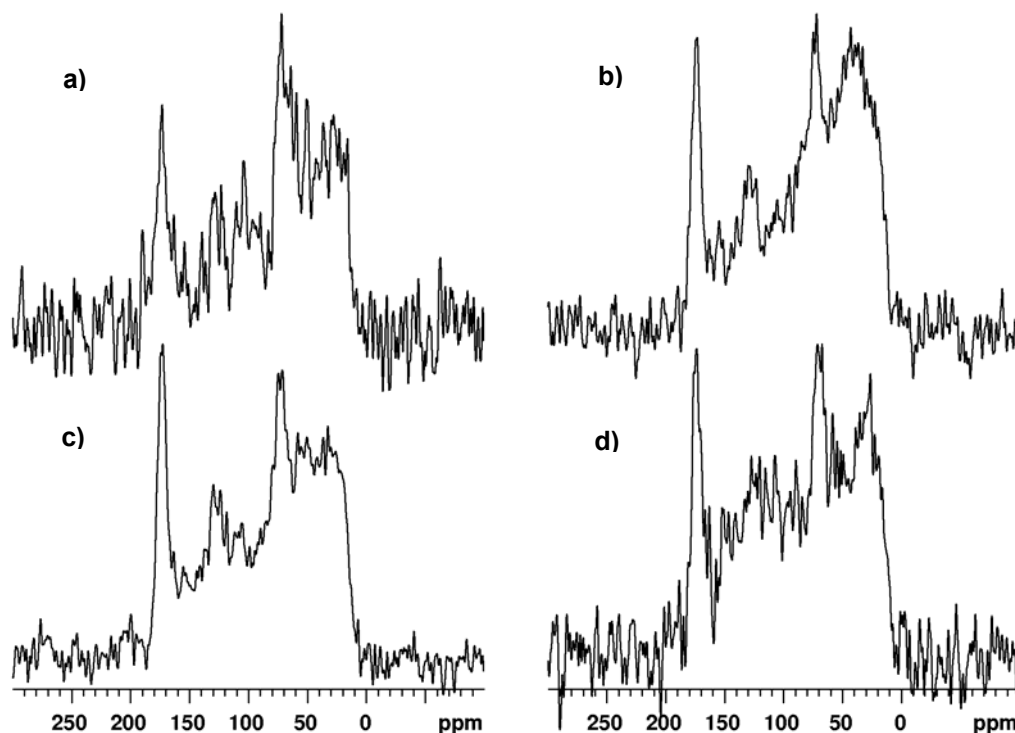


Figure 5.4 Solid state ^{13}C NMR spectra of isolated samples. a) Fractions 7-9, b) Fractions 5 & 6, c) Fraction 4, d) Fraction 3.

To compare the four spectra in Figure 5.4, functional group types were assigned to various chemical shift ranges, based on the previous work of Croue *et al.* (2000), Hatcher *et al.* (2001), Bianchi *et al.* (2004) and Keeler *et al.* (2006), where solid state ^{13}C NMR spectroscopy was used for the characterisation of aquatic NOM. The four spectra obtained were relatively noisy due to the limited sample sizes available for analysis and, as a result, the spectra were only integrated over four broad regions: 0 - 60, 60 - 110, 110 - 165 and 160 - 190 ppm. These spectral regions are then attributed to the following functionalities: 0 - 60 ppm to aliphatic carbons, 60 - 100 ppm to O-aliphatic carbons, 100 - 160 ppm to aromatic carbons and 160 - 190 ppm to carbonyl carbons (Croué *et al.*, 2000, Hatcher *et al.*, 2001, Bianchi *et al.*, 2004, Keeler *et al.*, 2006). Results from integration of the four spectra are shown in Figure 5.5.

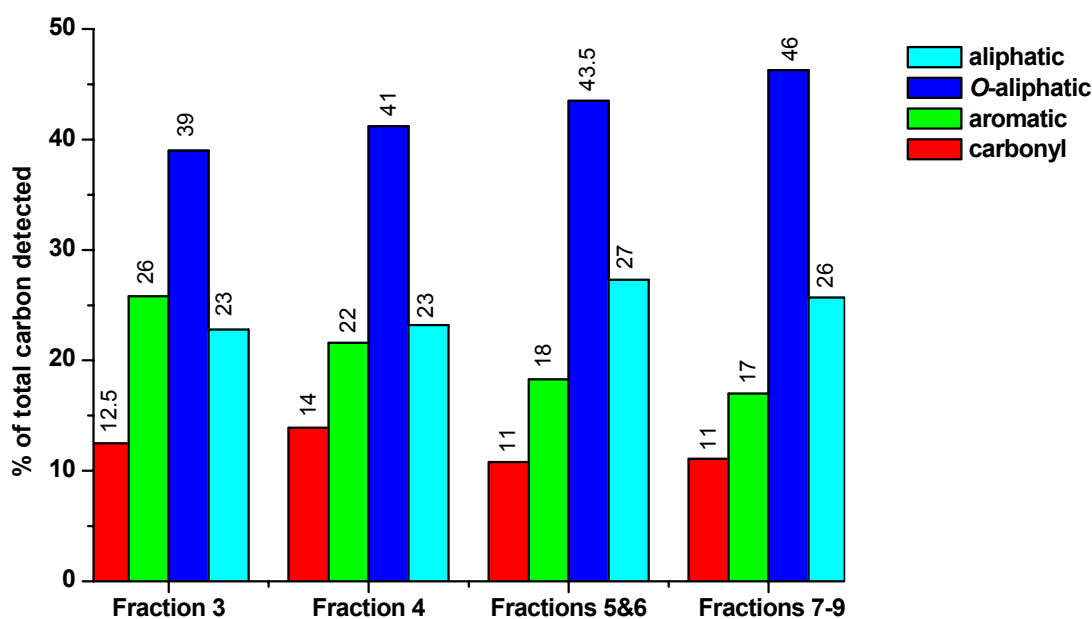


Figure 5.5 Relative proportions of carbon types in the solid state ^{13}C NMR spectra of the isolated NOM samples: Fraction 3 only, Fraction 4 only, Fractions 5 and 6 combined and Fractions 7-9 combined. The relative percentage of the four different carbon types in each sample is listed above the corresponding bar.

Overall, the distributions of types of carbons from solid state ^{13}C NMR spectroscopy were similar for the four samples. The major carbon type in Fraction 3, Fraction 4, Fractions 5 and 6 and Fractions 7-9 was O-aliphatic carbon (39 %, 41 %, 43.5 % and 46 %, respectively). For Fraction 3, aromatic carbon was the second most abundant carbon type, responsible for 26 % of the detectable carbon. Fraction 4, Fractions 5 and 6 and Fractions 7-9 had an aromatic carbon content of 22 %, 18 % and 17 %, respectively. For these three fractions, aliphatic carbon was the second most dominant carbon type, with 23 % for Fraction 4, 27 % for Fractions 5 and 6 and 26 % for Fractions 7-9, while Fraction 3 had an aliphatic carbon content of 23 %. Carbonyl carbon was the least abundant carbon type in all four isolated fractions: Fraction 3 had a carbonyl carbon content of 12.5 %, Fraction 4 was comprised of 14 % carbonyl carbon, while fractions 5 and 6 and Fractions 7-9 both had 11 % of their total detectable carbon present as carbonyl carbon.

In their study of fractionated NOM collected after preparative HPSEC, Piccolo *et al.* (2002) used solution state ^1H NMR spectroscopy to investigate structural trends of isolated fractions. By using this technique on isolated fractions of NOM, an intense water signal was observed, effectively eliminating any detail in the 3 to 5 ppm range. As explained above, due to inferior chromatographic resolution, only six MW fractions were obtained in their study, however, valid comparisons can still be made to the four samples analysed in this research. Piccolo *et al.* (2002) found that the smallest MW fraction was depleted in aromatic protons, while the large MW fractions had a strong aromatic proton signal, similar to ^{13}C NMR spectroscopy of samples in this study. Piccolo *et al.* (2002) also observed that the intermediate MW fraction (Fraction 3) had a small signal for aromatic protons, conflicting with the pyrolysis data obtained in the same study. This was explained by suggesting material in this fraction contained significantly substituted aromatic groups (Piccolo *et al.*, 2002). In the context of the current study, the intermediate fraction of Piccolo and co-workers corresponds to Fraction 4, and perhaps, to a lesser degree, Fraction 5, both of which showed reduced aromatic content compared to Fraction 3, but did still show aromatic carbon was present. The higher aliphatic carbon signal observed from Fraction 4 and 5 may possibly have resulted from aliphatic groups in these fractions being bonded predominantly to aromatic carbon. Interestingly, the largest MW material in the study by Piccolo *et al.* (2002) also showed a strong olefinic proton signal. A similarly strong olefinic contribution may also partially explain the high abundance of aliphatic carbon in the ^{13}C NMR studies of Fractions 3 and 4 in the current study. The smallest MW material isolated by Piccolo *et al.* (2002) was identified as the most polar, likely containing more oxygenated structures, similar to the results obtained in the current study.

Analysis by ^{13}C NMR spectroscopy suggested that the samples had some similarities in terms of the observed NMR signals, however, it was apparent that, as the MW of the fractions decreased, carbons bonded to oxygenated groups (as indicated by carbonyl and O-aliphatic signals) increased, while aromatic carbon content decreased. In terms of structural features of the

material in each of the studied samples, this suggests that the functional groups predominating in the lower MW fractions, specifically Fractions 7-9 but also Fractions 5 and 6, were likely to be carbohydrate type groups, low MW aliphatic acids, ether and ester linkages, aliphatic alcohols or methylketone type structures. For the larger MW material in Fractions 3 and 4, there was less oxygenated functionality and a shift towards more aromatic species. Interestingly, the carbonyl signal of Fractions 3 and 4 was higher than for the other fractions analysed. This could be, for example, due to quinone structures, which are known to exist in NOM (Thurman, 1985) as well as dihydroxybenzene moieties, and could be partly responsible for the large UV₂₅₄ signal observed in the HPSEC chromatograms of these fractions.

Newcombe *et al.* (1997), in a study of a highly coloured surface water from South Australia, used ultrafiltration to isolate NOM into five MW fractions and study the structural characteristics by solid state ¹³C NMR spectroscopy. As in the current study, Newcombe *et al.* (1997) found that O-aliphatic carbon was the dominant signal; however, unlike the MW fractions isolated in this Thesis, the relative amount of O-aliphatic carbon decreased as the MW decreased. Newcombe *et al.* (1997) described this trend as a decrease in carbohydrate type material as MW decreased. It was also noted that as the carbohydrate content decreased, aromatic carbon was enriched, an opposite trend to that found in the current research. Levels of carbonyl carbon in each ultrafiltration MW fraction were similar to the carbonyl content of MW fractions obtained here by preparative HPSEC, and the carbonyl carbon abundance displayed a similar trend with regard to MW in both studies (Newcombe *et al.*, 1997). Li *et al.* (2004) used solid state ¹³C NMR spectroscopy to study the structural characteristics of MW fractions isolated by ultrafiltration of a Pahokee peat HA sample. Unlike the MW fractions isolated in the current research, or those isolated by Newcombe *et al.* (1997), aliphatic and aromatic carbon were the dominant carbon types, accounting for, on average, about 35 % for each carbon type in all ultrafiltration fractions from the peat sample. This is, perhaps, more a feature of the sample nature, as Norwood *et al.* (1987) have shown humic acids to contain a higher proportion of aromatic groups and less oxygenated functionality. Similar to

the trends observed in the current research, aliphatic carbon levels were fairly constant, increasing slightly as MW decreased, while the aromatic carbon content was also relatively stable, with a slight decrease in abundance as MW increased (Norwood *et al.*, 1987).

These comparisons indicate the diverse results that have been obtained when using either solution state ^1H or solid state ^{13}C NMR spectroscopy to study differences in isolated MW fractions. This is, perhaps, a result of the diverse nature of samples studied; indicating sample nature is highly dependent on the surrounding environment with regard to structural characteristics. With this in mind, chlorination experiments were conducted on each of the isolated MW fractions to study the disinfection behaviour of the NOM in these fractions. The results from the chlorine demand and THM formation experiments were then correlated with the NOM characteristics as determined by solid state ^{13}C NMR spectroscopy and HPSEC analysis.

5.3.4. Effects of Chlorine on Individual MW Fractions

5.3.4.1. Chlorine Demand of Individual MW Fractions

The 7 day chlorine demand was determined for each of the MW fractions obtained from preparative HPSEC. Aqueous solutions of each fraction at a DOC concentration of 2 mg L^{-1} were prepared. For this experiment, three initial chlorine doses ($4, 6$ and 8 mg L^{-1}) were used, apart from experiments involving the more reactive Fraction 3, where $4, 6, 8, 12, 14, 16$ and 18 mg L^{-1} doses were required, and the chlorine decay monitored over 7 days. The chlorine demand of each aqueous solution containing a MW fraction was calculated, according to the method of Warton *et al.* (2006), as the dose required to yield a chlorine concentration of exactly 0 mg L^{-1} after 7 days, extrapolated from the results of multiple chlorine dosing experiments.

In these experiments, the chlorine demands of the individual fractions are almost exclusively due to reactions of chlorine with NOM, since the majority of inorganic species would have been removed in the isolation process used to collect the fractions. Dialysis (nominal MW $1\ 000\text{ Da}$) was performed after

preparative HPSEC separation to removed the phosphate mobile phase used in the HPSEC analysis and this process would have also removed other inorganic components in the fractions. The conductivity of each fraction was measured throughout the dialysis process, with measurements decreasing until values of $\sim 5 \mu\text{S m}^{-1}$ were obtained, indicating that the majority of inorganic species with MWs below 1000 Da were removed from the fractions. Ion chromatography was used to measure the bromide concentration of these fractions, with all fractions having values below the detection limit of the method ($< 0.01 \text{ mg L}^{-1}$).

Table 5.3 Chlorine demands of the nine fractions obtained by preparative HPSEC. All fractions had a DOC concentration of 2 mg L^{-1} . Chlorine demand values are chlorine concentrations required to obtain a chlorine residual of 0 mg L^{-1} after 168 hours of contact.

Fraction	Chlorine demand (mg L^{-1})
1	0.12
2	3.4
3	10.4
4	4.85
5	1.5
6	2.27
7	2.47
8	2.50
9	0.44

The nine individual fractions had significantly different chlorine demands, as evident in Table 5.3. Of all nine fractions, Fraction 1 had the lowest chlorine demand. This fraction was comprised of NOM with the highest MW and also most likely to contain colloidal components, as established in Chapter 3.3.2. The possible association of NOM with colloid species may have resulted in a reduction in reactivity of the NOM in this fraction with chlorine. Fraction 3 had the highest chlorine demand of the nine fractions. According to Huber and Frimmel (1996), this fraction is likely to contain mainly humic-type material with a large aromatic content, and possibly include significant quantities of phenols and dihydroxybenzenes, which have been shown to be highly reactive with chlorine (Gallard and von Gunten, 2002a). This is consistent with the results of NMR spectroscopy of this fraction (Figure 5.4d

and Figure 5.5), where the aromatic carbon signal for this fraction was more abundant relative to the aromatic carbon signal in other fractions. Krasner *et al.* (1996a) established that aromatic compounds, particularly those found in humic material, undergo a number of reactions with chlorine, accounting for the high chlorine demand of this material. In addition, Owen and co-workers (1993) found that the humic fraction in fact was more reactive with chlorine compared to non-humic material from the same source. Krasner *et al.* (1996a) studied the effect of chlorine on NOM fractions isolated by resin fractionation from the Apremont reservoir in France and found that the humic fraction of NOM had twice the chlorine demand of the fulvic acid fraction and three times the demand of the hydrophilic acid fraction. The hydrophilic acid fraction appeared to have a low aromatic content as shown by its low SUVA value and NMR spectroscopic data (Krasner *et al.*, 1996a).

Fractions 2 and 4 produced chlorine demands of 3.41 and 4.85 mg L⁻¹, respectively. Fraction 2 was likely to be composed of a mixture of the material characteristic of Fraction 1 and Fraction 3 and its intermediate chlorine demand reflected this. Fraction 2 was comprised of relatively high MW NOM, with molecular size approaching the exclusion limit of the column. Hence, like Fraction 1, Fraction 2 may have included some NOM associated with inorganic colloidal material lowering its availability for reactions with chlorine. However, some of the NOM in Fraction 2 may have been similar to that found in Fraction 3, which was shown to be very reactive with chlorine. Fraction 4 also had a lower chlorine demand than Fraction 3. Fraction 4 had a lower average MW than Fraction 3 and, according to Huber and Frimmel (1996), is reportedly less humic, and more fulvic, in nature than Fraction 3. Croué *et al.* (2000) showed that this material had increasing amounts of aliphatic carbon compared with the highly aromatic humic material found in Fraction 3. Comparison of the NMR spectra of Fraction 4 with that of Fraction 3 (Figure 5.4c and 5.4d and Figure 5.5) also showed a reduction in aromatic carbon content, while aliphatic carbon remained constant and O-aliphatic carbon content increased, with the decreasing MW. Thus, there appeared to be a progression towards lower MW material containing less aromatic (phenolic) components and a greater concentration of aliphatic

oxygenated functional groups in this sample. Norwood *et al.* (1987) found that, although phenolic moieties are present in fulvic acids, they account for a significantly lower percentage of the total organic matter than in higher MW humic acids. This gradual progression towards lower proportions of reactive aromatic moieties may account for the lower chlorine demand of Fraction 4.

Fractions 5-8 have similar, lower chlorine demands (1.5, 2.27, 2.47 and 2.5 mg L⁻¹, respectively) compared to Fraction 3. As was the case for Fraction 4, NMR analysis of Fractions 5 and 6 (Figure 5.4b and Figure 5.5) showed a lower proportion of aromatic carbon compared to Fraction 3. Accordingly, as a result of the lower amounts of the reactive aromatic (phenolic) moieties, the chlorine demand of these fractions was lower. Since the NOM in Fraction 5 is less aromatic, compared with Fraction 3, there would be fewer sites available in the organic material for attack by chlorine resulting in a lower chlorine demand. Previous studies by Huber and Frimmel (1996) and Schmitt *et al.* (Schmitt *et al.*, 2003) suggested that the intermediate MW range (Fractions 5-8 of the HPSEC chromatogram in this study), was comprised of NOM with highly substituted aromatic or conjugated acid or keto acid functionality. NMR analysis illustrated that Fractions 5 and 6 (Figure 5.4b and Figure 5.5) and Fractions 7 - 9 (Figure 5.4a and Figure 5.5) did in fact have less aromatic and carbonyl carbon, with increased aliphatic and O-aliphatic functional groups. Morris and Baum (1978) reported that, in addition to aromatic compounds, methyl ketones or compounds oxidisable to methyl ketones are also reactive towards free chlorine. Analysis of Fractions 5 and 6 (Figure 5.4b and Figure 5.1) and Fractions 7-9 (Figure 5.4a and Figure 5.5) using NMR spectroscopy found that while aromatic carbon was reduced, compared to Fraction 3 and 4, the carbonyl carbon and aliphatic carbon concentrations increased, possibly indicating increased methyl ketone functionality. Furthermore, the increase in O-aliphatic carbon may indicate greater carbohydrate, aliphatic alcohols, ether and ester moieties, possibly accounting for the chlorine demand of these fractions. However, these structures have lower chlorine demands compared to phenolic structures (Reckhow and Singer, 1985) and may explain the lower chlorine demands of Fractions 5 – 9.

Fraction 9 had a chlorine demand of 0.44 mg L^{-1} , which was considerably lower than all other fractions, except Fraction 1. Fraction 9 had the lowest apparent MW, $1\ 100 \text{ Da}$. Also, this fraction eluted at the salt boundary of the HPSEC system, indicating the content of hydrophilic moieties was higher than in other fractions, suggesting lower concentrations of reactive aromatic species. The potential absence of some of the most reactive moieties within the organic structure may account for its lower reactivity with chlorine.

5.3.4.2. Trihalomethane Formation Potential of Individual MW Fractions

5.3.4.2.1. 7 Day Total Trihalomethane Formation

Chlorine was added to each of the nine fractions (DOC concentrations normalised to 2 mg L^{-1}) at a concentration of 8 mg L^{-1} (18 mg L^{-1} for Fraction 3), together with bromide at a concentration of 0.2 mg L^{-1} , corresponding to the bromide concentration in the Wanneroo bore W300 unfractionated water sample. If all bromide is oxidised to HOBr/OBr^- in these experiments, 0.13 mmol L^{-1} of HOCl/OCl^- (0.25 mmol L^{-1} HOCl/OCl^- for Fraction 3) and $0.0025 \text{ mmol L}^{-1}$ of HOBr/OBr^- will be available for reaction with the DOC resulting in a molar ratio of 50:1 HOCl/OCl^- to HOBr/OBr^- (100:1 HOCl/OCl^- to HOBr/OBr^- for Fraction 3). The formation of THMs was monitored over 168 hours, with measurements conducted after 0.5, 1, 4, 24, 72 and 168 hours. Aliquots of an aqueous solution of sodium thiosulfate were added at the specified times to reduce chlorine concentrations and bromine to bromide ions, stopping their reaction with NOM. In Figure 5.6, the total THM (TTHM) molar concentrations, i.e., the sum of the molar concentrations of chloroform, bromodichloromethane, dibromochloromethane and bromoform, are plotted against time for the nine fractions. TTHM data, as well as individual THM speciation, is presented in Appendix 3.

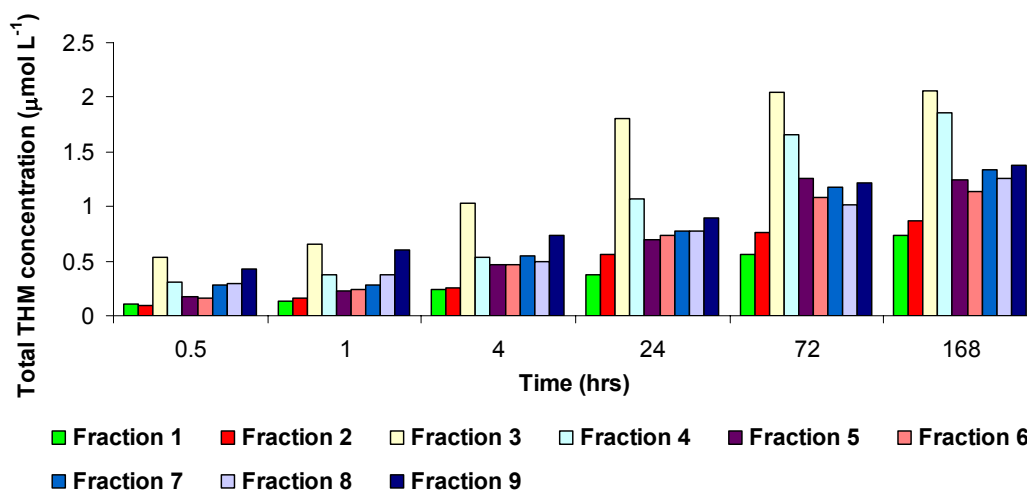


Figure 5.6 Total THM concentration plotted against time for each of the nine individual MW fractions. Colours refer to individual fractions as stated in the legend.

As illustrated in Figure 5.6, Fraction 1 had the lowest 7 day total THM formation potential (THMFP) ($0.74 \mu\text{mol L}^{-1}$), followed by Fraction 2 ($0.87 \mu\text{mol L}^{-1}$). The THMFP of Fractions 3 and 4 after 168 hours of contact showed similar, very high concentrations, with $2.1 \mu\text{mol L}^{-1}$ and $1.85 \mu\text{mol L}^{-1}$ of total THMs formed. Interestingly, Fractions 5 - 9 all had similar, moderate THMFPs after 168 hours ($1.24 \mu\text{mol L}^{-1}$, $1.14 \mu\text{mol L}^{-1}$, $1.34 \mu\text{mol L}^{-1}$, $1.25 \mu\text{mol L}^{-1}$ and $1.4 \mu\text{mol L}^{-1}$, respectively), which were 33 % - 46 % lower than the concentration of THMs formed from Fractions 3. A difference in the rate of formation of THMs was also observed. For instance, Fractions 1, 2, 4, 5 and 6 formed THMs slowly with 14 %, 11 %, 16 %, 14 % and 15 %, respectively, formed in the first 30 minutes of contact with chlorine, while Fractions 3, 7, 8 and 9 formed THMs faster with 26 %, 21 %, 24 % and 31 %, respectively, of their total THMs in the first 30 minutes of contact with chlorine.

As with differences in the chlorine demand of the nine fractions, the variation observed in THMFP suggests structural differences in the organic material in the isolated MW fractions. Similarly, the disparity between rates of THM formation may provide some evidence for the likely structural features of the organic material in these fractions. Fractions 3 and 4 had the greatest yield of THMs after 168 hours of contact with chlorine, indicating structures with

the greatest propensities for undergoing chlorine and bromine substitution or addition reactions leading to the subsequent formation of THMs. However, the difference in reaction kinetics of THM formation possibly infers differences in the structures of these two fractions, since Fraction 3 formed THMs faster than Fraction 4. When lake water from the Limmat River was chlorinated, Gallard and von Gunten (2002a) found 28% of THMs produced were formed during the initial fast reacting phase, i.e. within 30 minutes. It was also found that resorcinol (dihydroxy) and phenol (monohydroxy) could both produce THMs, but only resorcinol contributed to THM production during the initial fast reacting phase (Gallard and von Gunten, 2002a). Therefore, Fraction 3 may have a greater *meta*-dihydroxybenzene content than Fraction 4, while Fraction 4 may have a higher monohydroxybenzene content than Fraction 3. It is also important to note that, due to its high chlorine demand, Fraction 3 had a greater initial chlorine concentration which would likely have influenced the kinetics of the formation of THMs. The aromatic carbon content of Fractions 3 was slightly higher than Fraction 4, as determined by NMR spectroscopic analysis (Figure 5.4c and 5.4d and Figure 5.5). The aromatic carbon content in Fractions 3 and 4 was also the highest of any fraction or group of fractions, consistent with the highest THM concentrations being formed from these two fractions. However, there was insufficient NMR spectroscopic information available to compare the specific *O*-aromatic carbon contents of the two fractions and yield information regarding the likely distribution of phenolic groups.

Similar concentrations of THMs were formed from Fractions 5 – 9 after 168 hours of contact with chlorine, albeit in lower concentrations than Fractions 3 and 4. However, the rates of formation of THMs from Fractions 5 and 6 and Fractions 7 – 9 were appreciably different. For example, Fractions 5 and 6 formed 14 % and 15 % of their THMs in the first 30 minutes of contact, while Fractions 7 - 9 formed 21 %, 24 % and 31 %, respectively, in the first 30 minutes of contact. NMR spectroscopic analysis (Figure 5.4a and 5.4b and Figure 5.5) of these fractions showed elevated aliphatic and *O*-aliphatic carbon contributions compared to Fractions 3 and 4 (Figure 5.4c and 5.4d and Figure 5.5), with Fractions 5 and 6 having a greater aliphatic carbon

input and Fractions 7 - 9 having greater O-aliphatic carbon content. The aromatic and carbonyl carbon contributions were similar for Fractions 5 - 9. The lower TTHM formation for Fractions 5 – 9 compared to Fractions 3 and 4 may be explained by a reduction in the relative aromatic and carbonyl carbon content in these fractions.

An explanation of the difference in THM formation kinetics between Fractions 5 and 6 and Fractions 7 – 9 may lie in nature of aliphatic groups in these low MW fractions. Larson and Rockwell (1979), Norwood *et al.* (1980), Reckhow and Singer (1985) and Gallard and von Gunten (2002a) identified methyl ketones, or moieties oxidisable to that structure, as potential aliphatic compounds that can form THMs rapidly and produce high yields. Hence, Fractions 7 – 9 may contain a greater percentage of these structures or groups that can be oxidised to methyl ketones in the presence of chlorine than Fractions 5 and 6, resulting in faster THM formation for Fractions 7 – 9. Alternatively, as suggested by Gang and co-workers (2003), the difference in kinetics may be a function of MW. The larger MW species of Fractions 5 and 6 may require additional reactions to form precursors suitable for THM formation before THM formation can occur. The lower MW fractions, Fractions 7 – 9, may contain a higher proportion of precursors that readily directly participate in THM formation, compared to Fractions 5 and 6, resulting in the observed faster THMFP.

Fractions 1 and 2 produced the lowest yields of THMs and also produced THMs at the slowest rate. As with Fractions 5 and 6 when compared to Fractions 7 - 9, a possible explanation for the lower yield of THMs and slower haloform reaction kinetics may be a result of MW. Fractions 1 and 2 were comprised of organic matter with the highest MW, and, hence, release of THMs upon chlorination is likely to be a more involved reaction pathway. Also, it has been suggested (Huber and Frimmel, 1996, Allpike *et al.*, 2005) that the organic matter in the larger MW fractions is associated with colloidal material which may mean active sites otherwise involved in reactions with chlorine are not available for attack. It was not possible to conduct NMR

spectroscopic analyses on these two high MW fractions, so no NMR data was available for comparison.

5.3.4.2.2. Trihalomethane Speciation

Final (7 day) concentrations of the four THM analogues are plotted after 168 hours of contact with 0.13 mmol L⁻¹ chlorine (0.25 mmol L⁻¹ chlorine for Fraction 3) and 0.0025 mmol L⁻¹ bromine in Figure 5.7. Differences in the relative molar amounts of the four THM analogues for all nine fractions after 168 hours contact with chlorine and bromine are evident in Figure 5.7. Fractions 3 and 4 produced much greater concentrations of chloroform than the other seven fractions, with lower concentrations of the dibromo and tribromo THMs. Fractions 1 and 2 produced similar THM distributions, with low TTHM concentrations but distributed similarly between chlorinated and brominated species. The distribution of THMs in Fractions 5-8 appear to favour the more chlorinated species compared with Fractions 1 and 2, but less so than Fractions 3 and 4. Fraction 9 had a greater proportion of bromodichloromethane compared to the other three THM analogues than the other fractions.

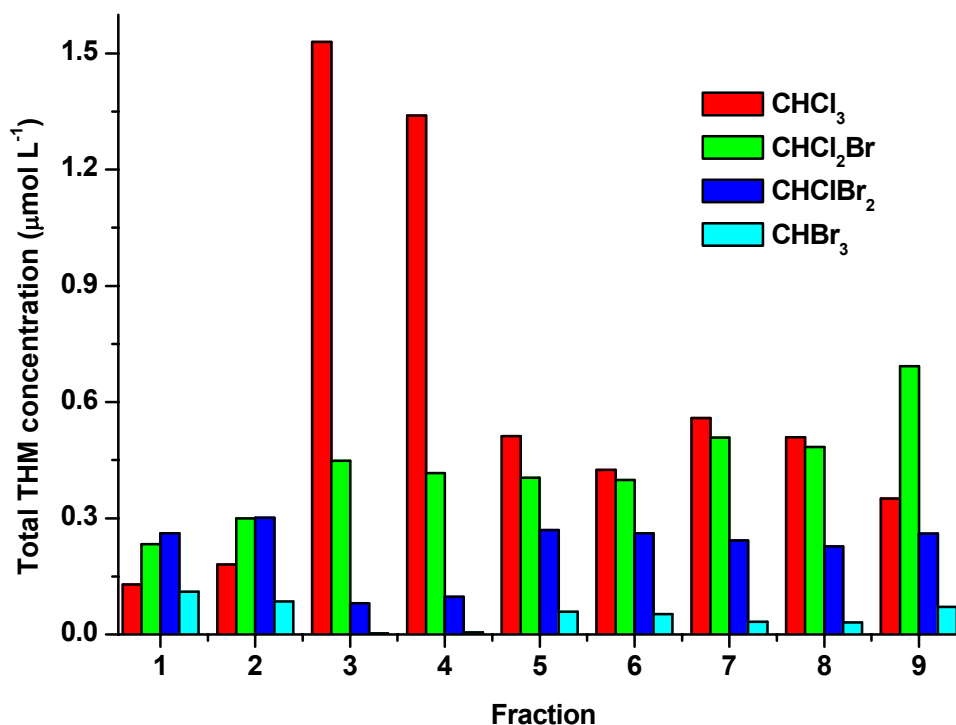


Figure 5.7 Relative molar concentrations of individual THMs found after exposure to chlorine and bromine for 168 hours for the nine MW fractions collected from preparative HPSEC. CHCl₃ = chloroform, CHCl₂Br = bromodichloromethane, CHClBr₂ = dibromochloromethane, CHBr₃ = bromoform.

The considerably higher formation of chlorinated THMs, particularly chloroform, for Fractions 3 and 4 may result, in part, from the higher ratio of reactive chlorine to bromine (50:1 for Fraction 4 and 100:1 for Fraction 3). Several authors (e.g. Amy *et al.*, 1985, Heller-Grossman *et al.*, 1993, Krasner *et al.*, 1996b, Ichihashi *et al.*, 1999b) have identified that the speciation of DBPs is dependent on the ratio of chlorine to bromine. However, the ratio of chlorine to bromine does not account for the discrepancies between THM speciation of the remaining seven fractions, indicating that structural differences in the organic material played a major role in THM speciation. Westerhoff and co-workers (2004) treated seven model aromatic compounds (including resorcinol, phenol, aniline, benzoic acid, vanillic acid, syringic acid and 3,5-dimethoxybenzoic acid) and maleic acid with equal concentrations of chlorine and bromine in separate experiments. This study showed that for these model compounds, apart from resorcinol, the highest yield of THMs occurred from the addition of

bromine, while for resorcinol, chlorine addition resulted in an approximate 40 % increase in THM formation compared to addition of bromine. Norwood *et al* (1980) also investigated THMFP after chlorinating the same set of model compounds and found that chloroform formation was highest from resorcinol; bromination experiments were not conducted in this research. In a similar study by Ichihashi *et al* (1999a), 21 phenolic model compounds were studied in relation to THM formation when chlorine and bromine were added in separate experiments. In this work, only 2,4-dihydroxytoluene, and to a lesser degree 3,5-dihydroxytoluene, resulted in an increased proportion of chloroform compared with bromoform when chlorine and bromine were added in equimolar concentrations. In the current study, higher concentrations of chlorinated THMs in Fractions 3 and 4 may be a result of increased concentrations of *meta*-dihydroxybenzene (resorcinol type) moieties present, also suggested by NMR data obtained for these fractions (Figure 5.4 and Figure 5.5), as indicated by the rate of THM formation (discussed in Section 5.3.4.2).

In the study by Westerhoff *et al.* (2004), separate oxidation experiments using chlorine and bromine were conducted on coagulation treated water. Increasing the coagulant dose resulted in greater incorporation of bromine into the organic matrix, in effect “coagulation preferentially removed organic materials capable of forming haloforms in the presence of chlorine”. Since previous work (e.g. Chow *et al.*, 1999, Allpike *et al.*, 2005) has shown that coagulation removes the larger MW fractions of NOM, leaving smaller MW material in the water, this provided evidence for the greater production of chlorinated THMs from higher MW material. The greater propensity of the higher MW fractions, Fractions 3 and 4, to form chlorinated THMs (Figure 5.7) is consistent with the conclusions of Westerhoff *et al.* (2004).

To more closely examine the distribution of DBPs, the bromine incorporation factor (BIF) was applied. The BIF indicates the extent of bromine substitution in a class of DBPs, characterised by the bromine fraction of the total molar halogen in the class of DBPs (Gould *et al.*, 1981). Since this development, Obolensky and Singer (2005) have refined the formula to

provide an equation producing a value between 0 (indicating 100 % of DBPs present as the chlorinated analogue) and 1 (indicating 100 % of THMs present as brominated analogue) for bromine incorporation. The formula for the refined BIF (THMs) is given below:

$$BIF(THMs) = \frac{[BrCl_2CH] + 2 \times [Br_2ClCH] + 3 \times [Br_3CH]}{3 \times \{[Cl_3CH] + [BrCl_2CH] + [Br_2ClCH] + [Br_3CH]\}} \quad 5.1$$

Using BIFs, straightforward interclass comparisons of the extents of bromine substitution are possible. The BIF (THMs) for each of the nine fractions are listed in Table 5.4.

Table 5.4 Bromine incorporation factors for THMs (BIF (THMs)) for each of the nine fractions collected by preparative HPSEC. BIF (THMs) calculated using Equation 5.1.

Fraction	BIF
1	0.49
2	0.45
3	0.1
4	0.11
5	0.3
6	0.32
7	0.27
8	0.27
9	0.35

Interestingly, the largest MW fractions, Fractions 1 and 2, which also produced the least amount of THMs, incorporated the greatest amount of bromine in produced THMs. Fractions 3 and 4, with the greatest THMFPs, had the lowest BIFs, while Fractions 5-9 had similar BIFs, which showed greater bromine incorporation compared to Fractions 3 and 4, but slightly less bromine incorporation into formed THMs than Fractions 1 and 2.

In this current work, the molar ratio of reactive chlorine to bromine was constant (50:1, apart from Fraction 3, where the ratio was 100:1), where chlorine was in large excess compared to bromine. The different THMFPs produced from the constant molar ratio of halogens appear to suggest structural differences between the fractions were responsible for the variations in the individual THM molar concentrations. The formation of significant concentrations of brominated THMs (BIFs 0.27 – 0.49) from

Fractions 1, 2 and 5 – 9 in the presence of such a large excess of chlorine indicates: a) that the THM precursors in these fractions were more reactive towards bromine; b) the lower reactivity of these fractions allowed more selectivity with the halogenating agent, resulting in more reaction with bromine, the more electrophilic reagent; c) the formation was a result of the combination of both of these effects. Previous studies of chlorination of some natural water sources containing bromide ion have suggested that bromine is more reactive towards aliphatic precursors compared to aromatic precursors (Heller-Grossman *et al.*, 1993, Liang and Singer, 2003). The higher BIFs observed for Fractions 5 – 9 (0.3, 0.32, 0.27, 0.27 and 0.35, respectively) compared to Fractions 3 and 4 (0.1 and 0.11, respectively) potentially indicates a greater aliphatic carbon content of the lower MW fractions, Fractions 5 – 9. This idea is supported by the ^{13}C NMR spectra in Figure 5.4 and Figure 5.5. However, Fractions 1 and 2 had even higher bromine incorporation (BIFs of 0.49 and 0.45, respectively) but ^{13}C NMR spectroscopy was not available for these fractions. In their study of competing chlorination and bromination reactions, Westerhoff *et al.* (2004) demonstrated the greater redox potential of the active chlorine species, HOCl ($E_{\text{red}}^0 = +1.63\text{V}$) compared with the active bromine species, HOBr ($E_{\text{red}}^0 = +1.331\text{V}$). Potentially, due to the complex nature of organic material in Fractions 1 and 2 (Section 3.3.2), chlorine may have participated in oxidation reactions, producing active sites for reaction with electrophilic bromine, which has a higher electron density and smaller bond strength and hence is a stronger electrophile than chlorine (March, 1992).

Further evidence for the incorporation of varying degrees of chlorine and bromine into produced THMs for each fraction was investigated through the use of percentage halogen incorporation. The percentage of the total chlorine and bromine added to the fractions which was incorporated into THMs is provided in Table 5.5. The % chlorine and bromine incorporation values were calculated according to Equations 5.2 and 5.3. The data for % chlorine and bromine incorporation into THMs for each separate time period (i.e., 0.5, 1, 4, 24, 72 and 168 hours) is given in Appendix 4.

$$\% \text{ Cl incorporation} = \left(\frac{\sum (3 \times n\text{Cl}_3\text{CH}) + (2 \times n\text{Cl}_2\text{BrCH}) + (n\text{ClBr}_2\text{CH})}{n(\text{Cl}_2 \text{ dosed})} \right) \times 100 \quad 5.2$$

$$\% \text{ Br incorporation} = \left(\frac{\sum (3 \times n\text{Br}_3\text{CH}) + (2 \times n\text{Br}_2\text{ClCH}) + (n\text{BrCl}_2\text{CH})}{n(\text{initial Br})} \right) \times 100 \quad 5.3$$

Where n = number of moles

Table 5.5 Chlorine and bromine incorporation into THMs as a percentage of the total chlorine and bromine dosed to fractions.

Fraction	% Cl incorporated	% Br incorporated
1	1.0	44
2	1.3	46
3	2.2	25
4	4.5	25
5	2.4	45
6	2.1	43
7	2.7	44
8	2.5	41
9	2.3	57

For all fractions analysed, significantly greater amounts of bromine were incorporated into THMs than chlorine. Similar results for chlorine incorporation were observed by Luong *et al.* (1982), who found, in their study of a slow sand filtered surface water in central London, that chlorine incorporation never exceeded 4 %, while bromine incorporation reached a maximum value of 30 %. Consistent with these results, in the current study, chlorine incorporation was below 5 % and bromine incorporation reached a maximum of 57 %. Cooper *et al.* (1983) found bromine incorporation in natural surface waters could be as high as 60 % of initial bromide dose, with chlorine incorporation in the order of 10 – 20 %. Furthermore, Symons *et al.* (1996) showed bromine incorporation in river waters of up to 30 %, with only ~1 % of chlorine incorporated into THMs. Higher percentage bromine incorporation than chlorine incorporation into DBPs is therefore well established (also Stevens, 1979, Luong *et al.*, 1982, Amy *et al.*, 1985, Pourmoghaddas *et al.*, 1993, Symons *et al.*, 1996).

The difference in incorporation of chlorine and bromine into produced THMs can be rationalised by a review of the rate constants for appropriate reactions between chlorine, bromide/bromine and NOM. Upon addition of chlorine (HOCl) to a solution containing bromide, bromide is oxidised to HOBr ($k = 1550 \text{ M}^{-1} \text{ s}^{-1}$) (Kumar and Margerum, 1987), which typically occurs much faster than reactions between HOCl and NOM ($k = 0.7 - 5 \text{ M}^{-1} \text{ s}^{-1}$) (Westerhoff *et al.*, 2004). The reaction between HOCl and bromide occurs within the first few seconds of contact (Echigo and Minear, 2006) and thus a portion of HOCl may be consumed in the oxidation of bromide, increasing the HOBr/DOC ratio. This effect is compounded due to the cycling of bromide during chlorination. Westerhoff *et al.* (1998) reported that only approximately 10 % of the bromine initially reacted with NOM forming brominated organic compounds, while the remaining 90 % was reduced to bromide. Subsequently, the reduced bromide can be re-oxidised with available chlorine to bromine and participate in further reactions with NOM. Through this process, 1 mol of bromide can potentially consume much more than 1 mole of chlorine and this process of bromide cycling can, in part, account for the greater bromine incorporation observed (Westerhoff *et al.*, 2004). However, reactions between HOCl and *meta*-dihydroxybenzene moieties have been shown to occur an order of magnitude more quickly ($k = >100 \text{ M}^{-1} \text{ s}^{-1}$) (Gallard and von Gunten, 2002b) than reactions between HOCl and NOM in general. The relatively high incorporation of chlorine and relatively low incorporation of bromine into THMs for Fractions 3 and 4 may be a result of higher concentrations of *meta*-dihydroxybenzene moieties, as possibly indicated by the relatively higher content of aromatic carbon in these fractions shown in their ^{13}C NMR spectra, although the higher initial chlorine dose of Fraction 3 is the likely cause of the lower percentage chlorine incorporation for this fraction.

The varied THM formation resulting from the addition of chlorine and bromine to each of the nine isolated MW fractions strongly indicates that variations in the structure of NOM in each fraction played a role in the observed speciation changes. While ^{13}C NMR spectroscopy was only able to highlight slight structural changes between the nine fractions, the significant

differences in behaviour following disinfection suggest more pronounced variations. Some clear trends were evident, particularly with similarities between adjacent MW fractions. Fraction 1, the largest MW fraction, had a low chlorine demand and moderate THMFP. Along with data presented in Section 3.3.2, it was suggested that this fraction was perhaps complexed with inorganic colloidal material, resulting in a lower concentration of precursors available for participation in THM forming reactions. Also, Fraction 2, while having a greater chlorine demand than Fraction 1, did not produce significant quantities of THMs, perhaps also due to the complexed nature and large MW of this material or, alternatively, indicating organic material in this fraction supported formation of DBPs other than THMs. Fractions 3 and 4 had the highest chlorine demands of all the fractions, likely due to the high aromatic (potentially phenolic) content of these fractions. Disinfection behaviour, as well as NMR data, suggested that these fractions may contain *meta*-dihydroxybenzene moieties which could explain the high chlorine demand and high THMFP, as well as the greater formation of chlorinated THMs. Fractions 5 – 9 all behaved similarly in the presence of chlorine (apart from the lower chlorine demand of Fraction 9) and had similar THMFPs. A difference was observed between Fractions 5 and 6 and Fractions 7 – 9, with a slightly higher rate of THM formation for the lower MW Fractions 7 – 9, most likely due to the simplicity of formation pathways of THMs from lower MW material.

From a treatment perspective, these results pose some interesting questions with regard to disinfection of treated waters. Previous work has suggested that, for some water sources, the < 1 000 Da MW fraction, isolated by ultrafiltration, can be responsible for the greatest production of THMs per mg of DOC (Owen *et al.*, 1993, Via and Dietrich, 1996, Kitis *et al.*, 2002). This conclusion has, however, been contradicted in other studies. For example, Schnoor *et al.* (1979) identified the MW fraction < 3 000 Da of water taken from the Iowa River as the most significant THM precursor accounting for 75 % of THMFP, while the < 1 000 Da fraction contributed only 25 % of THMFP. In addition, Joyce *et al.* (1984) suggested that the < 1 000 Da MW fraction was responsible for a very small percentage of THM precursors based on

chlorination experiments of ultrafiltered fractions of a surface water sample. In any event, it was shown in Chapter 3 of this Thesis and in the work of Chow *et al.* (1999) that coagulation effectively removes the mid to high MW fractions of NOM, leaving the low to mid MW fractions of NOM in coagulation treated water. The current disinfection studies show that, if complete removal of the four highest MW fractions (accounting for 59 % of the organic matter in the sample analysed) is achieved in coagulation treatment, only approximately 46 % of the THMFP of the water would be removed. The low MW NOM fractions are therefore an important concern for water utilities as they are a significant source of THMs upon chlorination of treated water.

Trihalomethanes in drinking water are regulated by public health authorities at various concentrations. In Australia, the TTHM guideline values are set at $250 \mu\text{g L}^{-1}$ (NH&MRC, 1996), while in Canada, TTHM concentrations are calculated on a local running annual average which should not exceed $100 \mu\text{g L}^{-1}$ (Canada, 2006). Also, the Canadian guidelines stipulate that bromodichloromethane concentrations should not exceed $16 \mu\text{g L}^{-1}$ for the local running annual average, as this compound has been shown to have an increased potential to form cancer in laboratory animals (Canada, 2006). The US Environmental Protection Agency (USEPA) regulates TTHM levels according to a maximum contaminant level (MCL), currently set at $80 \mu\text{g L}^{-1}$ (USEPA, 2007). While reducing total THMs is the first area of concern for drinking water authorities, the speciation of THMs may also be an issue, as DBPs containing bromine may be more toxic than chlorinated species (LaLonde *et al.*, 1997, Richardson *et al.*, 2003, Plewa *et al.*, 2004). The speciation may become more of an issue in the drying climate in Australia as waters of more marginal quality, and often containing higher bromide concentrations, must be utilised. For these reasons, the lower MW fractions appear to be an even greater concern for water utilities, since they have incorporated higher levels of bromine into produced THMs, and, in particular, bromodichloromethane was the most abundant THM from Fraction 9. It is, therefore, increasingly important to utilise treatment methods with some

capability to remove low MW NOM (e.g. MIEX[®]) and to develop new treatment methods for this purpose.

5.4. Conclusions

For the first time, disinfection behaviour of NOM MW fractions isolated by HPSEC in a preparative mode has been applied. This technique allows the collection of MW fractions of NOM which can then be directly characterised by techniques such as solid state ¹³C NMR spectroscopy and disinfection behaviour. Using preparative HPSEC, greater than 90% of the organic matter could be obtained and separated into nine discrete MW fractions. The recovery of DOC from the entire isolation procedure of preparative HPSEC, concentration by rotary evaporation, dialysis and lyophilisation was 87 %. The nine fractions collected represented distinct MW fractions of NOM with apparent MW values > 72 000, 16 500, 4 900, 3 250, 2 650, 2 150, 1 650, 1 350 and 1 100 Da, calibrated against PSS standards. Reinjection of these fractions onto an analytical scale HPSEC column, with a similar phase to that of the preparative column, showed MW fractions with small polydispersities, indicating fractions containing similar sized MW species.

It was found that the mid to high MW fractions exerted high chlorine demands (i.e., were very reactive with chlorine), likely due to the large humic component of these fractions. Resorcinol type moieties within humic structures are very reactive with chlorine, and the high chlorine demand and more aromatic nature of these fractions indicated that resorcinol type moieties may be abundant in these fractions. The smaller MW material had a moderate to low chlorine demand and a more aliphatic and less aromatic character than the mid to high MW fractions. In these smaller MW fractions, methyl ketones, or structures oxidisable to those structures, may play a greater role in the observed chlorine demand. The very largest MW fraction was shown to have a very low chlorine demand. This is likely due to the possible colloidal nature of the fraction, where organic material may be

associated with colloidal structures and not readily available for reactions with chlorine.

The THM formation potential of the individual MW fractions was also measured, as an indicator to the formation of disinfection by-products and to provide the first direct information on the relative propensity of different MW fractions to produce THMs upon disinfection. The fractions with the highest chlorine demands, the more aromatic Fractions 3 and 4, also produced the highest concentrations of THMs, consistent with the idea that aromatic moieties, such as *meta*-dihydroxybenzenes, are significant THM precursors. While the highly aromatic larger MW fractions had a greater chlorine demand, not all of the by-products produced were in the form of THMs. This is presumably due to the larger MW components requiring more reaction steps during attack by halogen to form the small THM compounds, with some intermediate oxidised and halogenated compounds formed. In future work, adsorbable organic halogen (AOX) measurements on the halogenated MW fractions would allow study of the relative amounts of these intermediate halogenated compounds.

The distribution of the four THMs was also investigated for the fractions, with apparent MWs above 3 200 Da forming greater amounts of chloroform than the smaller MW fractions, where the formation of brominated THMs was more favoured. The high reactivity of the highly aromatic larger MW fractions is likely the reason for the greater incorporation of chlorine in the THMs formed from these large MW fractions. For the smaller fractions, where reactivity with halogen is lower, bromine incorporation became a more dominant mechanism, despite the large excess of chlorine in the system.

While the mid to high MW humic fractions (Fractions 3 and 4) contained the most relative amounts of DOC (57%) in the W300 water sample, these fractions are well-removed by conventional coagulation processes and, therefore, may play a minor role in THM formation in coagulation treated waters. The lower MW fractions (Fractions 7 – 9), totalling 18 % of the DOC in the raw water sample, are poorly removed by coagulation treatment, but

still form significant quantities of THMs (approximately one third of the TTHMs of all the MW fractions) upon disinfection. These lower MW fractions are likely to be significant contributors to THM formation in treated waters and application of treatment methods, such as MIEX[®] resin or biological treatment, or development of alternative processes for their removal is vital for control of THM formation in these water types.

6. ISOLATION AND CHARACTERISATION OF NOM FROM VARIOUS STAGES AT THE WANNEROO GWTP FOR EVALUATION OF THE PERFORMANCE OF TREATMENT PROCESSES FOR NOM REMOVAL

6.1. Introduction

This work was conducted in parallel with the much larger study carried out by Warton *et al.* (2007), who compared the effect of treatment with MIEX[®] resin and coagulation at the Wanneroo Groundwater treatment Plant (WGWTP). In their research, Warton and co-workers (2007) investigated what Croué *et al.* (2000) termed Tier 3 and Tier 4 characterisation techniques to investigate the effect on product water quality of three treatment processes, namely MIEX[®] resin treatment, MIEX[®] resin treatment followed by coagulation with aluminium sulfate (alum) and coagulation with alum operating in an enhanced mode. The Tier 3 and Tier 4 characterisation techniques were outlined in Section 1.4.2 and provide information related to chemical behaviour of NOM (Tier 3) and a spectral signature of NOM *in-situ*, such as UV absorbance (Tier 4).

There have been numerous published papers on the performance of MIEX[®] resin at a pilot or bench scale level (e.g. Morran *et al.*, 1996, Nguyen *et al.*, 1997, Chow *et al.*, 2001, Pelekani *et al.*, 2001, Singer and Bilyk, 2002, Drikas *et al.*, 2003, Fearing *et al.*, 2004), but work on full scale applications of the MIEX[®] process has, until recently, been limited (Allpike *et al.*, 2005). The study by Warton *et al.* (2007) was the first of its kind describing the behaviour of the MIEX[®] process on a full scale plant level using several parameters to assess its performance. Briefly, the combined MIEX[®] and coagulation process (MIEX[®]-C) was found to produce higher quality water than simply coagulation in an enhanced mode (EC), as measured by DOC concentration, UV₂₅₄ absorbance, chlorine demand, THMFP, turbidity and colour. Also, the MIEX[®] only process (not combined with coagulation) removed DOC with a greater range of MW than the enhanced coagulation process, which preferentially removed the large MW fraction. Significantly, THMFP was

appreciably lower in water from the combined MIEX[®] and coagulation process compared with water from enhanced coagulation treatment.

After an extensive literature search, there does not appear to be any previous studies using Tier 2 characterisation techniques to investigate NOM in water following treatment with MIEX[®] resin. Tier 2 characterisation techniques investigate the nature and abundance of structural units in the NOM molecules. For example, Chow *et al.* (1999) used pyrolysis-GC-MS (Py-GC-MS) and Fourier transform infrared (FTIR) spectroscopy, as well as HPSEC, to characterise NOM isolated from raw water as well as remaining after alum coagulation treatment from the Myponga and Hope Valley reservoirs located in South Australia. It was observed that the mid to high MW fraction of NOM (> 1000 Da) was removed after alum treatment. FTIR data was inconclusive in this study due to contamination from residual aluminium sulfate which had not been removed prior to analysis, but Py-GC-MS indicated that the NOM remaining after treatment was enriched in carbohydrate type material (Chow *et al.*, 1999). In a similar study, Page *et al.* (2003) used Py-GC-MS to investigate NOM from raw water as well as remaining after alum coagulation treatment in water from the Mt. Bold, Myponga and Warren reservoirs in South Australia, as well as the Moorabool and West Gellibrand reservoirs in Victoria. Similar to the study of Chow *et al.* (1999), carbohydrate derived products were enriched in samples following treatment with alum coagulation (Page *et al.*, 2003).

Kazpard *et al.* (2006) investigated the effect of alum coagulation on a model humic acid using ¹³C and ²⁷Al NMR spectroscopy. At low alum concentration, phenolic groups were preferentially associated with the alum coagulant and hence appeared to be the easiest moieties removed by this process. As the alum dose was increased, carboxylic acid groups then appeared to be associated with alum, suggesting initially hydroxy aromatic moieties within NOM were preferentially removed, followed by negatively charged species such as carboxylic acids (Kazpard *et al.*, 2006). This is consistent with the suggestion in Section 3.3.3 that hydroxy aromatic

material in the large MW HPSEC fractions was preferentially removed during the coagulation process.

6.1.1. Scope of Study

The work described in this Chapter focussed on characterisation of the nature and abundance of functional groups (Tier 2 characterisation techniques) in NOM isolated by ultrafiltration from water samples collected from four points within the WGWTP. Samples were taken at points following aeration of the raw inlet water, following treatment with MIEX[®] resin, following treatment with MIEX[®] resin and coagulation, and following treatment by coagulation operating in an enhanced mode, at the same time as those described in the work of Warton *et al.* (2007). The samples of isolated NOM in solution were analysed for some water quality parameters, as well as HPSEC-UV₂₅₄-OCD, while the solid NOM isolates were characterised by Py-GC-MS, FTIR and ¹³C NMR spectroscopy.

6.2. Experimental

6.2.1. Samples

The water treatment process streams at the WGWTP have been described in detail in Section 1.4.1. The water treatment process streams and sampling points (*) at the WGWTP are shown schematically in Figure 6.1.

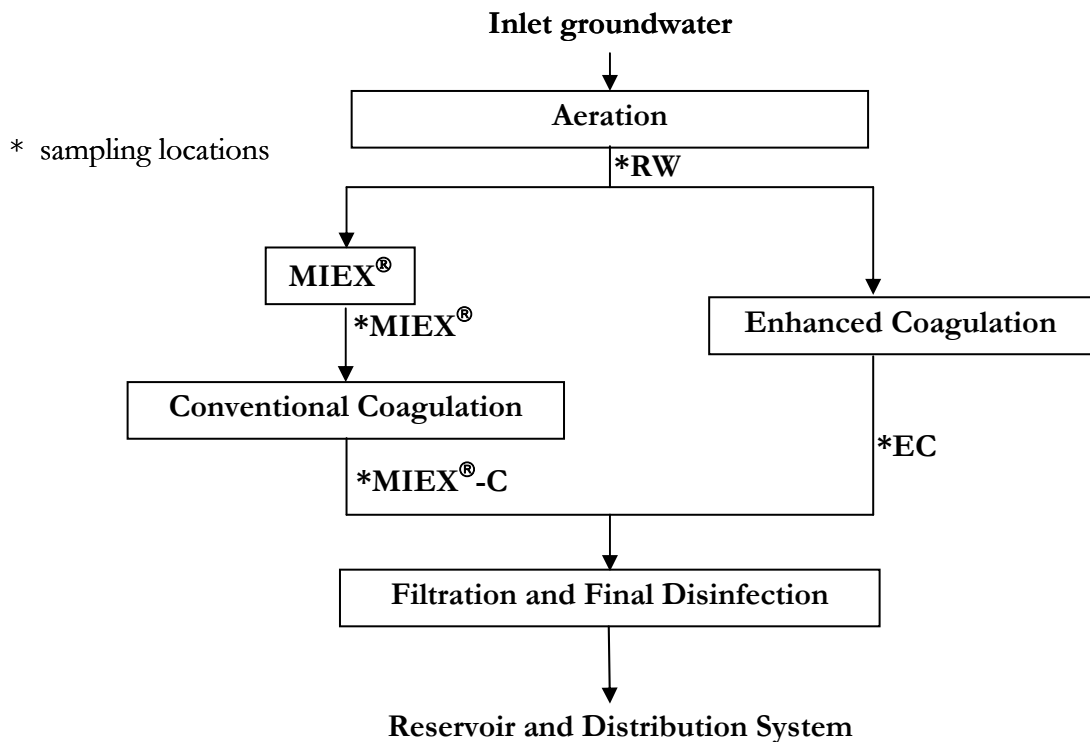


Figure 6.1 Schematic of the WGWTP showing sampling locations (*) and sample names.

Water from the four points of the WGWTP was sampled on 24th February 2003, and taken at an identical time to the samples described in the work of Warton *et al.* (2007). Four 1 000 L stainless steel containers were cleaned with high pressure steam, rinsed 5 times with the particular sample, then filled to the brim and sealed. Following collection of 1 000 L of water sample from each of the four sampling locations at the WGWTP, the sealed samples were transported immediately to air conditioned storage (20-25 °C). Sub-samples (8 L) were filtered through a 0.45 µm membrane (Saehan high-clean polycarbonate membrane) and stored in the dark at 4 °C until required.

6.2.1.1. Ultrafiltration Treatment for Sample Isolation

Samples were concentrated using a custom designed tangential flow ultrafiltration (UF) system. The setup comprised four Prep/Scale-TFF 6 feet² membranes (PLAC, regenerated cellulose, Millipore, USA) with a nominal MW (NMW) cut-off of 1 000 Da. Two of the membranes were connected in parallel, with each of those membranes then connected to a second

membrane in series. Membranes connected in series allowed flow rates to be increased, while maintaining the appropriate pressure inside the membranes (75 psi), and thus enabled twice the amount of sample to be processed than would otherwise have been possible. The setup of the UF system is shown schematically in Figure 6.2.

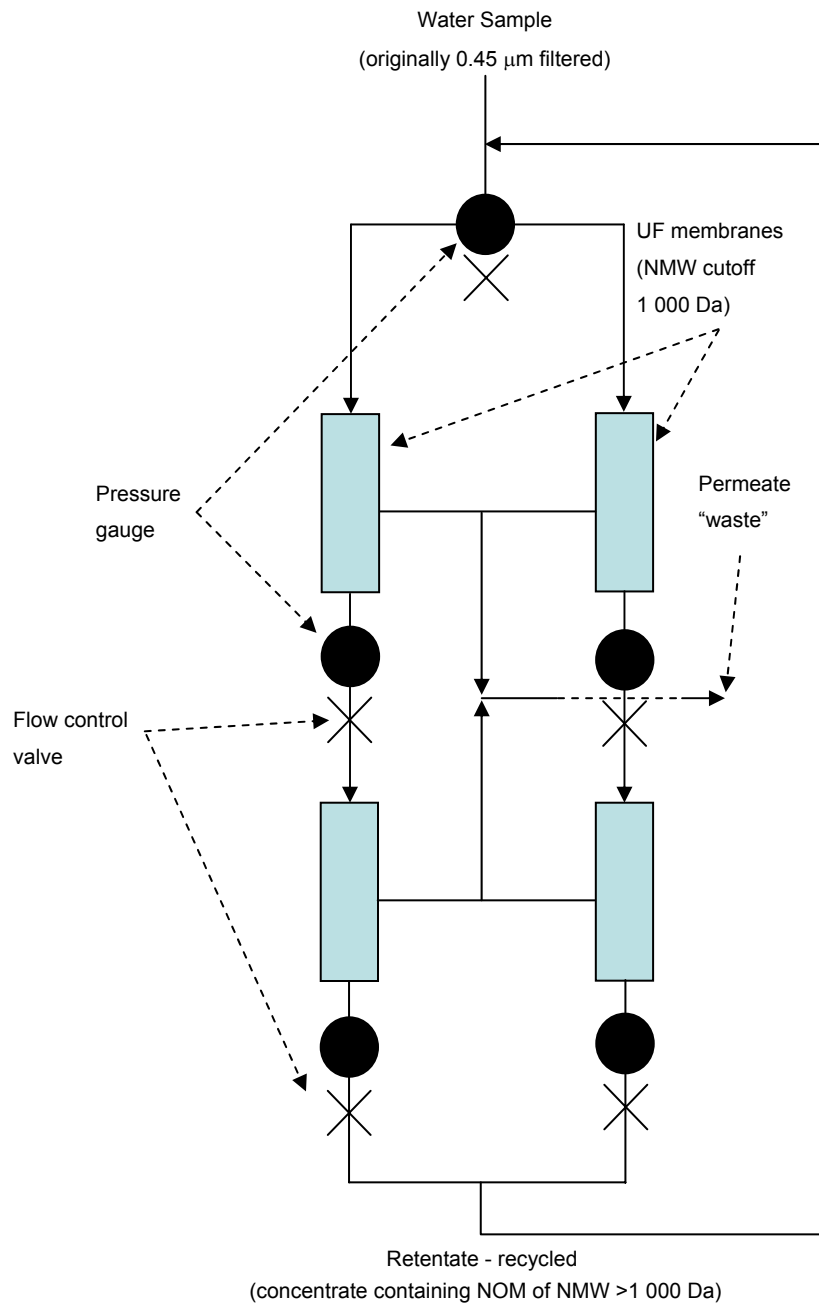


Figure 6.2 Schematic of ultrafiltration system.

Approximately 1 000 L of the MIEX[®]-C and EC samples, 750 L of the MIEX[®] sample and 600 L of the raw water (RW) sample were each concentrated to

approximately 75 L by collecting the UF retentate and continually recycling this through the system until the required volume was reached while the permeate was directed to waste. Following this approximate 10-fold concentration step, the four samples were each further concentrated to about 15 L using another ultrafiltration step with a single membrane (NMW 1 000 Da) to reduce the amount of organic material potentially lost during the process. Finally, the UF concentrates were freeze dried to obtain solid isolates of 150 - 350 mg. Elemental analysis, as outlined in Section 6.2.2.7, revealed a high inorganic salt content (approximately 50 % ash) still remained in each solid isolate. To remove the salts, samples were treated as follows. A small portion of each freeze dried sample (~50 mg) was dissolved in purified laboratory water (400 mL) and added to a 400 mL UF cell (stirred UF cell, Amicon) fitted with a UF membrane (YM1, regenerated cellulose, Millipore, USA) with a nominal MW cut-off of 1 000 Da. The volume was reduced to approximately 100 mL, and then made up to 400 mL again with purified laboratory water. This procedure was repeated until the conductivity of the retentate decreased to approximately $5 \mu\text{S M}^{-1}$. The whole process was repeated on the entire amount of each sample to obtain isolates free from inorganic contaminants. Finally, desalted retentates for each of the four samples were freeze dried to obtain solid NOM isolates of 50 - 150 mg.

6.2.2. Materials and Methods

6.2.2.1. Purified Laboratory Water

Purified water was obtained as outlined in Section 2.2.2.1.

6.2.2.2. Measurement of Constituents and Water Quality Parameters in Water Samples

Water quality parameters including pH, alkalinity, turbidity, UV_{254} , colour, conductivity and the concentrations of bromide, chloride, total filterable solids, aluminium, calcium, iron, hardness, potassium, magnesium,

manganese, sodium, sulfate, nitrate, silicon and total anions were determined as outlined in Section 3.2.2.2.

6.2.2.3. Measurement of Dissolved Organic Carbon Concentration

DOC concentrations were measured according to the procedure outlined in Section 3.2.2.3.

6.2.2.4. Biodegradable Organic Carbon Concentration

Biodegradable organic carbon (BDOC) concentrations were measured as outlined by Zappia *et al.* (2007), a method based on the method developed by Joret and Levy (1986), except that the biomass used to inoculate the flasks was grown on sintered glass Siran[®] beads in a biofilter fed with water from a production bore (W257) in the Wanneroo borefield.

Briefly, inoculum (200 g) was added to the water sample (600 mL) in an annealed 1 L flask. Filtered (0.2 μm) medical grade air was delivered to the flask (70 mL min^{-1}) covered with a protective foil to ensure no UV light entered the flask. Aliquots of the test water (40 mL) were taken from the sample vessel over a seven day period (after 0, 1, 4, 24, 48, 72, and 168 hours) and the DOC concentrations determined. The BDOC concentration was determined by the difference between the initial DOC concentration and the DOC concentration after the specified contact time. The maximum concentration difference achieved over this 7 day period was the reported BDOC concentration.

6.2.2.5. Assimilable Organic Carbon Concentration

Assimilable organic carbon (AOC) concentration measurements were performed by researchers at CSIRO Land and Water, Floreat, Western Australia. Water samples (1 L; stored on ice at ~ 0 °C) were transported to the CSIRO laboratory directly after collection. The AOC concentration of the

MIEX[®] treated sample was not determined due to contamination during sample transportation. AOC concentrations were determined according to the method of van der Kooij (1982) where a culture of *Pseudomonas fluorescens* PI7 and *Aquaspirillum* NOX were grown in the presence of sodium acetate and maximum counts determined and used to calibrate the AOC concentration of samples supplied.

6.2.2.6. HPSEC Analysis

HPSEC-UV₂₅₄-OCD analysis was carried out according to the procedure outlined in Section 4.2.4 using a TSK HW-50s gel column (length 25 cm, inner diameter 2 cm, particle size 30 µm, pore size 125 Å).

6.2.2.7. Elemental Analysis

Elemental analysis was conducted on solid isolates of the four samples obtained after ultrafiltration and lyophilisation by Chemical and Micro Analytical Services Pty. Ltd, Victoria, Australia. The percentage of carbon, hydrogen, nitrogen, oxygen and sulphur, as well as the percentage of ash (representing the inorganic component), were determined.

6.2.2.8. Fourier Transform Infrared Spectroscopy of Solid NOM Isolates

Fourier transform infrared (FTIR) spectra of the four solid NOM isolates were collected in the transmission mode using a Bruker IFS-66 spectrometer. Detector resolution was maintained at 4 cm⁻¹ for all analyses. Approximately 1 mg of freeze dried material was ground and 250 mg of potassium bromide (dried at 100 °C) was mixed with the ground material, and the mixture was pressed into a small disc. FTIR analyses were carried out by collecting 4 background scans followed by 4 scans of the sample. All FTIR spectra were scanned between 4 000 and 700 cm⁻¹ and data analysis performed with OPUS software.

6.2.2.9. Pyrolysis-Gas Chromatography-Mass Spectrometry of Solid NOM Isolates

Pyrolysis-gas chromatography-mass spectrometry (Py-GC-MS) was carried out using a Chemical Data Systems 160 Pyroprobe. The freeze dried solid NOM isolates (~1 mg) were introduced into a quartz capillary with a plug of pre-annealed glass wool at one end and the capillary was placed inside the NiChrome coil of the Pyroprobe which was inserted into the Pyroprobe housing. The coil was heated at 650 °C for 20 secs. The pyroprobe/GC interface temperature was maintained at 250 °C. Pyrolysis products were cryofocussed at – 196 °C at the front of the GC column for 2 minutes prior to elution. Analysis was performed by GC-MS on a Hewlett Packard HP 5890 GC and 5971 mass selective detector (MSD) operating in the EI mode and scanning from 50 to 550 m/z with an ionisation energy of 70 eV. Separation of pyrolysis products was achieved using a fused silica capillary column: 30 m x 0.25 mm i.d. and column phase thickness of 0.25 µm (ZB-5, Phenomenex). Helium was used as the carrier gas at a pressure of 8 psi, flow rate of 1 mL min⁻¹ and 30:1 split ratio. The following temperature program was applied: 40 °C (2 minutes) to 310 °C (15 minutes) at a rate of 4 °C. The transfer line temperature was 300 °C, with the quadrupole at 106 °C and the source maintained at 230 °C. Data was collected using Chemstation software and mass spectra obtained compared to those in the Wiley 275 database for peak identification.

6.2.2.10. Solid State ¹³C Nuclear Magnetic Resonance Spectroscopy of Solid NOM Isolates

All solid state ¹³C nuclear magnetic resonance (NMR) spectra were recorded at the School of Natural Sciences, University of Western Sydney, New South Wales, Australia, using a Bruker DPX 200 W Avance 200 MHz spectrometer operating at 50.3 MHz (for ¹³C) using the cross-polarization and magic angle spinning (CPMAS) method. For the four samples analysed, 250 000 scans were collected, with a contact time of 0.5 milliseconds and an experimental

recycle time of 1 second. The sample spinning rate was maintained at 6 000 Hz, except for sample 1 where a spinning rate of 8 000 Hz was also tested to check for the presence of spinning side bands. The NMR data were Fourier transformed with a line broadening between 50 - 200 Hz to obtain the frequency domain spectra. The chemical shifts were internally referenced to adamantane and corrected relative to external tetramethylsilane (0 ppm).

6.3. Results and Discussion

6.3.1. Analysis of Water Samples Prior To Ultrafiltration

6.3.1.1. Water Quality Parameters of Water Samples

The WGWTP is novel in that it is configured to enable raw water to be directed into either or both treatment streams (Figure 6.1). Following aeration, raw water can be diverted to the train employing both MIEX[®] resin and coagulation treatment, or to the train employing only enhanced coagulation treatment, or both treatment trains. This enables both treatment trains to be compared simultaneously with water of identical quality. A detailed description of the process has been given previously as described in Section 1.4.1. Large (1000 L) water samples after aeration (RW), following treatment with MIEX[®] resin (MIEX[®]), following MIEX[®] resin and coagulation treatment (MIEX[®]-C) and following enhanced coagulation (EC) were collected in February 2004 and some water quality parameters are given in Table 6.1.

Table 6.1 Water quality parameters of samples from the WGWTP: raw water following aeration (RW), following MIEX[®] treatment (MIEX[®]), following MIEX[®] and coagulation treatment (MIEX[®]-C), and following enhanced coagulation treatment only (EC). n.d. = not determined.

Parameter	units	RW	MIEX [®]	MIEX [®] -C	EC
DOC	mg L ⁻¹	6.85	3.5	1.7	2.25
BDOC	mg L ⁻¹	3.2	1.6	1.4	1.1
AOC	µg L ⁻¹	208	n.d.	62	35
Total Alkalinity as CaCO ₃	mg L ⁻¹	90	75	55	35
Alkalinity	milliequiv. L ⁻¹	1.6	1.6	1.1	0.7
Alkalinity as HCO ₃	mg L ⁻¹	99	91	84	42
Bromide	mg L ⁻¹	0.5	0.45	0.45	0.45
Chloride	mg L ⁻¹	170	190	215	170
UV ₂₅₄	cm ⁻¹	0.43	0.25	0.07	0.09
Colour (@ 400 nm)	TCU	55	27	2	5
Conductivity at 25°C	mS m ⁻¹	78	83	91	81
Total Filterable Solids - CO ₂	mg L ⁻¹	419	431	476	425
Total Filterable Solids by Summation	mg L ⁻¹	468	476	508	446
Aluminum - Unfiltered ICP	mg L ⁻¹	0.45	0.4	0.05	0.15
Calcium ICP	mg L ⁻¹	2.4	2.4	2.4	2.4
Iron - Unfiltered ICP	mg L ⁻¹	1.8	1.6	0.015	0.1
Hardness as CaCO ₃	mg L ⁻¹	90	89	90	89
Potassium ICP	mg L ⁻¹	6.5	7	7	7
Magnesium - Unfiltered ICP	mg L ⁻¹	7.5	7	7	7
Manganese - Unfiltered ICP	mg L ⁻¹	0.045	0.045	0.04	0.04
Sodium ICP	mg L ⁻¹	110	115	135	110
Sulfate ICP	mg L ⁻¹	16	14	39	63
Nitrate + nitrite as nitrogen	mg L ⁻¹	< 0.05	0.55	0.07	< 0.05
pH	units	7.1	7.05	6.7	6.3
Silicon (as SiO ₂)	mg L ⁻¹	16	15	13	14
Total Anions	milliequiv. L ⁻¹	5.15	6.7	6.8	6.2
Turbidity	NTU	2.8	3.8	0.2	0.5

The DOC concentration varies significantly between each of the four samples; DOC decreased from the RW value of 6.85 mg L⁻¹ to 3.5 mg L⁻¹ for the MIEX[®] sample (49 %), 1.7 mg L⁻¹ for the MIEX[®]-C sample (75 % relative

to the RW) and 2.25 mg L^{-1} for the EC sample (67 % relative to the RW). Removal of this level of DOC after the various treatment processes is consistent with previously reported data on lab-scale, pilot-scale and full treatment facility scale experiments. In a lab-scale study using virgin MIEX[®] resin, Boyer and Singer (2005) compared MIEX[®], MIEX[®]-C and alum only treatment on four samples taken from drinking water sources in California, USA. DOC removal varied depending on the sample, with MIEX[®] treatment able to remove 36 - 72 % of DOC from the four samples. Alum coagulation performed poorly compared to MIEX[®] treatment, with alum treatment able to remove only between 14 – 33 % of DOC from the same four samples. Combining the two treatment strategies did not significantly improve DOC removal, with on average only a further 5% improvement using MIEX[®]-C compared to only MIEX[®] treatment (Boyer and Singer, 2005). A pilot-scale study of a Wanneroo raw water blend with an initial DOC concentration of 12.1 mg L^{-1} found that MIEX[®] treatment reduced DOC levels by 58%, while EC reduced DOC concentrations by 66% and combined MIEX[®]-C treatment reduced DOC concentrations by 82 % (Cadee *et al.*, 2000). In the study by Warton *et al.* (2007), as well as the ‘summer blend’ samples analysed (identical to the samples studied in the current work), a typical ‘winter blend’ set of samples was also investigated. The initial DOC concentration of the raw water in this sample set was 4.2 mg L^{-1} . For these samples, it was found that MIEX[®] treatment removed 54 % of the raw water DOC, while MIEX[®]-C and EC removed 61 % and 48 %, respectively (Warton *et al.*, 2007). In general, the performances of the various treatment strategies investigated in the current study are consistent with previous studies, particularly with pilot and full scale studies where initial DOC concentrations were high as in the current study.

Biodegradable organic carbon (BDOC), the portion of DOC that is both mineralised and assimilated by heterotrophic flora, is determined as the difference between the initial DOC concentration and the minimum DOC concentration observed during the incubation period (Escobar and Randall, 2001). The RW BDOC (3.2 mg/L) decreased to 1.6 mg L^{-1} (50 % removal) for the MIEX[®] sample, 1.4 mg L^{-1} (56 % relative to the RW) for the MIEX[®]-C

sample and 1.1 mg L^{-1} (66 % relative to the RW) for the EC treated sample. Unlike DOC removal, the BDOC fraction of organic matter was more effectively removed by EC treatment compared to MIEX[®]-C, while MIEX[®]-C treatment outperformed MIEX[®] treatment. Volk *et al.* (2000) investigated the removal of both DOC and BDOC from 10 surface water samples following coagulation treatment and found their removal was linked. It was shown that waters with high DOC concentrations (10.7 mg L^{-1}) typically had high BDOC levels (2.4 mg L^{-1}), while waters containing low DOC concentrations (2.5 mg L^{-1}) typically had low BDOC concentrations (0.39 mg L^{-1}). Treatment of these samples with alum resulted in a 56 % DOC and 40 % BDOC reduction for the high DOC water and a 10 % DOC and 5% BDOC reduction of the low DOC water. Volk *et al.* (2000) concluded that the majority of BDOC may be humic material of large MW or materials bound to humic substances; these materials are easily removed by coagulation (Chow *et al.*, 1999 and results in Section 3.3.3). In the current study, while the good removal (66 %) of BDOC by EC sample is consistent with these reports, it would be expected that MIEX[®]-C would at least equal this performance. Rather, the BDOC removal after MIEX[®]-C (56 %) was lower than EC treatment (66 %). In the parallel study of identical water samples, Warton *et al.* (2007) identified that during the coagulation process after MIEX[®] treatment, the polyacrylamide polyelectrolyte dose, added to aid flocculation, was, in fact, disproportionately high compared with the EC process. Kay-Shoemaker (1998) reported that polyacrylamide flocculants were biodegradable *via* degradation of the pendant side chain, leaving the backbone chain [-CH₂-] intact. Residual polyacrylamide in the MIEX[®]-C water sample, resulting from the high dose, could potentially have contributed to the higher than expected BDOC of this sample. If, in fact, the BDOC component is predominantly comprised of larger humic material, as proposed by Volk *et al.* (2000), this could potentially explain its lower removal by MIEX[®] treatment. As was demonstrated in Section 3.3.1, MIEX[®] treatment appears to be less effective in removal of this fraction EC or MIEX[®]-C treatment, hence the greater BDOC concentration after MIEX[®] treatment compared to the other two treatment methods.

Assimilable organic carbon (AOC) is the fraction of DOC which can be utilised by specific strains or defined mixtures of bacteria, resulting in an increase of biomass concentration (Escobar and Randall, 2001). AOC represents the most readily degradable fraction of biodegradable organic matter (Escobar and Randall, 2001). Again, the AOC decreased with treatment from the RW AOC of $208 \mu\text{g L}^{-1}$ to the MIEX[®]-C value of $62 \mu\text{g L}^{-1}$ (70 % removal) and $25 \mu\text{g L}^{-1}$ (83 % removal) for EC. The AOC concentration of the MIEX[®] sample was not determined. In the study by Volk *et al.* (2000), AOC concentrations of the 10 surface water samples were also determined, and it was found that the AOC fraction was more difficult to remove during coagulation. It was proposed that this fraction was comprised of smaller non-humic or hydrophilic material (Volk *et al.*, 2000). If this is the case, the MIEX[®]-C treatment would be expected to outperform EC treatment with respect to AOC removal; however, this was not observed and may again be a result of overdosing of polyelectrolyte in the MIEX[®]-C stream leading to a higher AOC concentration than expected after this process.

According to Clesceri *et al.* (1998), UV_{254} can be used as a surrogate measure for selected organic constituents, such as lignin, tannin, humic substances and various aromatic compounds. The UV_{254} values for the four samples correlated reasonably well with their respective DOC concentrations, with the RW having the highest UV_{254} value (0.43 cm^{-1}), with a reduction of almost 50 % for the MIEX[®] sample (0.24 cm^{-1}) and significant reductions for the MIEX[®]-C (0.07 cm^{-1} , 84 % relative to the RW) and EC (0.09 cm^{-1} , 79 % relative to the RW) samples. The high removal of this material by MIEX[®]-C and EC treatment are consistent with coagulation treatment effectively removing the aromatic high MW fraction of NOM (Chow *et al.*, 1999 and Section 3.3.1). Colour refers to the 'true' colour; i.e., the colour of the sample with the turbidity removed. The colour may result from the presence of natural metallic ions (e.g. iron and manganese), humus and peat materials, plankton, weeds and industrial contamination (Clesceri *et al.*, 1998). The colour values were strongly correlated with the respective UV_{254} and DOC concentrations, with the RW colour (55 TCU) reduced by almost

50 % after MIEX[®] resin treatment (27 TCU) and even greater removal by MIEX[®]-C (2 TCU, 96 % relative to the RW) and EC (5 TCU, 91 % relative to the RW) treatment.

6.3.1.2. HPSEC-UV₂₅₄-OCD Analysis of Water Samples

Using the method described in Section 4.2.4, HPSEC-UV₂₅₄-OCD analysis of the four collected water samples was conducted, and the chromatograms from OCD are displayed in Figure 6.3.

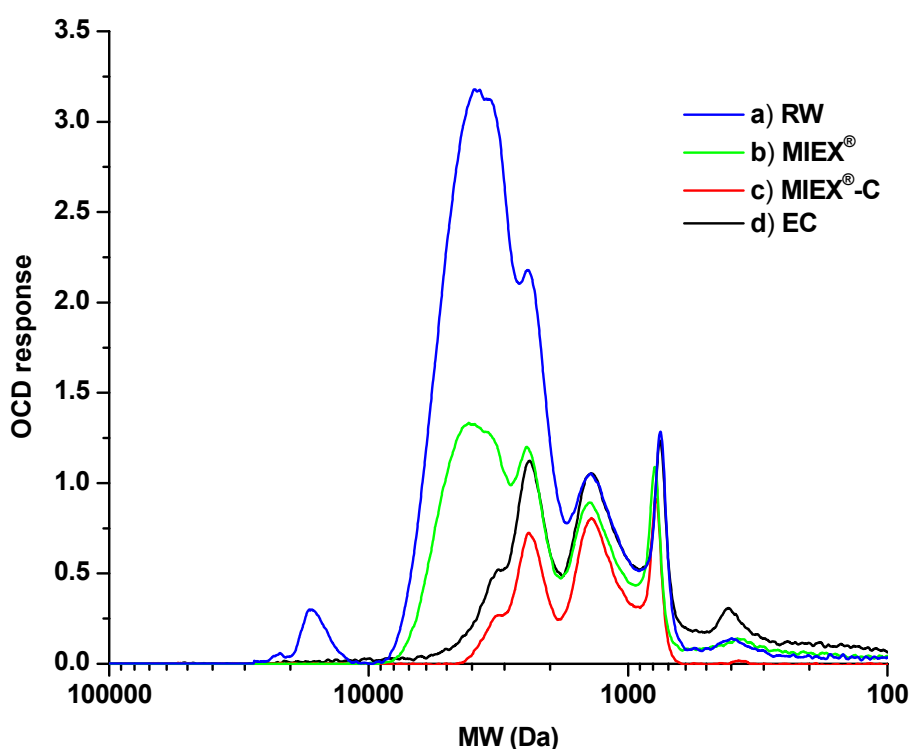


Figure 6.3 HPSEC-OCD chromatograms of water samples: a) RW, b) MIEX[®], c) MIEX[®]-C and d) EC.

The RW sample contained organic carbon distributed over the largest range of MWs (100 - 30 000 Da). The MIEX[®] sample had the next largest MW range (100 – 9 000 Da) of organic carbon, while the MIEX[®]-C (100 – 5 000 Da) and EC (100 – 6 000 Da) samples had a similar MW range of detected organic carbon. This is consistent with literature reports (Vrijenhoek *et al.*, 1998, Drikas *et al.*, 2003) as well as results obtained in this Thesis (Section 3.3.1), where it has been shown that coagulation is

particularly effective in removing the large MW components of NOM, whereas MIEX[®] treatment removes NOM over a wider MW range but is not as effective as coagulation at removing the very high MW material (> 10 000 Da) or the intermediate MW material (4 000 – 10 000 Da).

Comparison of the four HPSEC-OCD chromatograms showed the majority of DOC in the RW sample had a MW of between 2 000 – 8 000 Da. After treatment with MIEX[®] resin, more than half of this material was removed, while MIEX[®]-C and EC treatment removed virtually all organic carbon > 4 000 Da and more than half the organic carbon of MW between 2 000 - 4 000 Da which was present in the raw water. Organic carbon with a MW less than 2 000 Da was present in similar amounts in all four samples. Material with MW from 1 000 – 2 000 Da was present in approximately equal amounts for the RW and EC samples, but MIEX[®] treatment removed some of this material, and MIEX[®]-C treatment removed even more of this material. Again, the RW and EC samples showed similar amounts of organic material with MW between 600 and 1 000 Da, but MIEX[®] treatment removed a small amount of this material, and MIEX[®]-C removed more of it. The lowest MW organic carbon (with a MW range less than 600 Da) was again removed most effectively by MIEX[®]-C treatment, and MIEX[®] and EC treatments removed about half of this material.

Including HPSEC-UV₂₅₄ chromatograms along with HPSEC-OCD chromatograms provides insights into the composition of the eluted organic material. Figure 6.4 shows the HPSEC-UV₂₅₄-OCD chromatograms of the RW, MIEX[®], MIEX[®]-C and EC water samples.

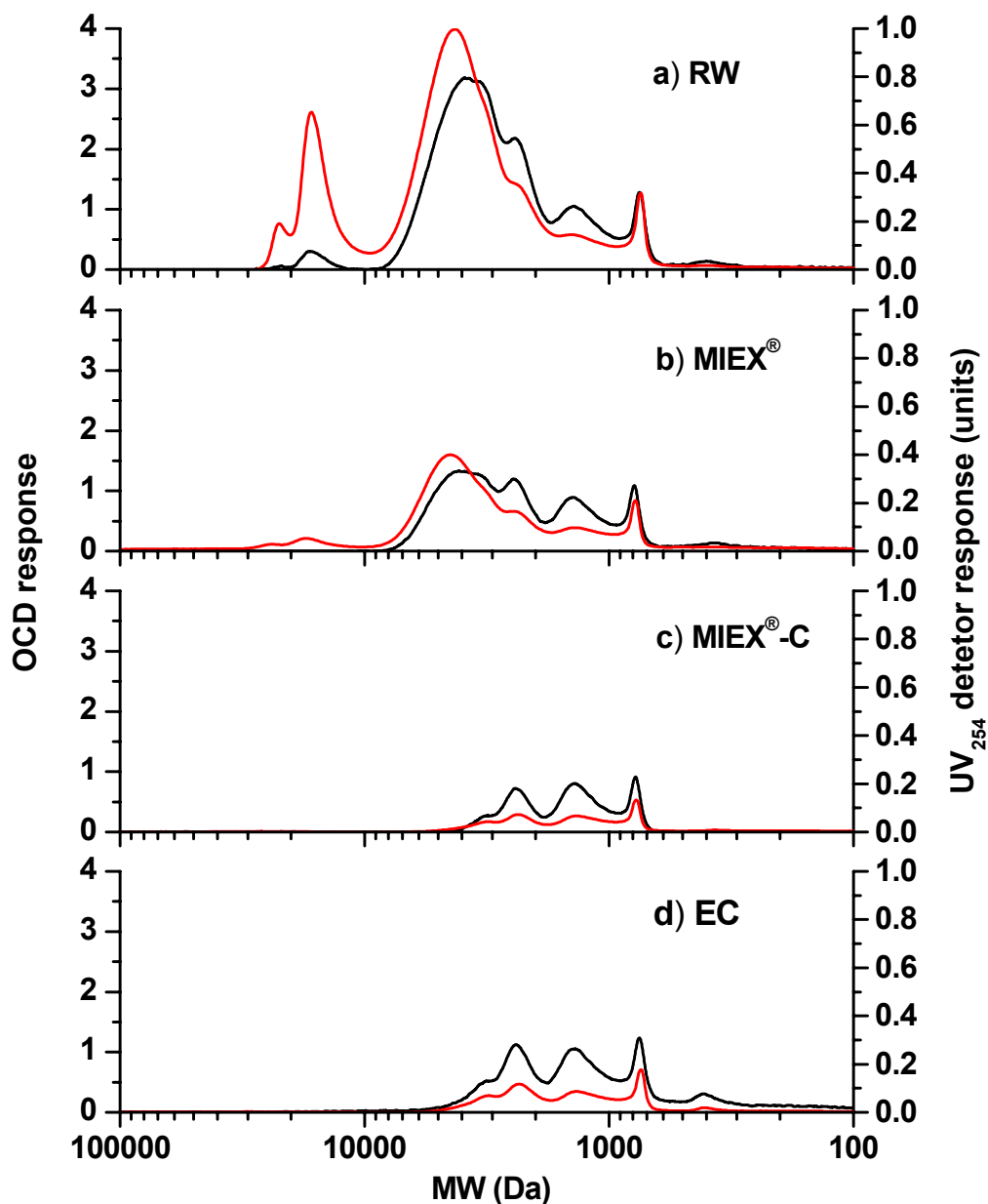


Figure 6.4 HPSEC-UV₂₅₄-OCD chromatograms of water samples: a) RW, b) MIEX[®], c) MIEX[®]-C and d) EC. The black line represents the OCD signal and the red line represents the UV₂₅₄ signal.

The most noticeable feature in Figure 6.4 is the significant overestimation of the largest MW material (> 10 000 Da) for the RW sample by HPSEC-UV₂₅₄ compared to HPSEC-OCD. Similarly, it appears that low MW fractions (< 2 000 Da) are underestimated by UV₂₅₄ detection compared to OCD. This is consistent with the material in the high MW region > 10 000 Da containing highly aromatic or colloidal material and the lower MW fraction being

depleted in aromatic species and containing more hydrophilic aliphatic species. The chromatograms shown in Figures 6.3 and 6.4 are almost identical to those observed in the study of the WGWTP reported in Chapter 3 of this Thesis. The raw water was characterised by a large peak at very high MW (V_o) in the UV₂₅₄ chromatogram which does not correspond with the OCD signal. In Chapter 3, this phenomenon was described as likely due to the presence of inorganic colloidal species which will induce light scattering in the UV detector and account for the observed signal. Schmitt *et al.* (2003), in their study of surface water from southern Germany, found that inorganic colloids eluted at the void volume of the same HPSEC column. Similarly, Huber & Frimmel (1996) identified colloidal material at high MWs in their study of a surface water sample from Southern Germany. With regard to the complete removal of this fraction by coagulation treatment, this corresponds with the results in Section 3.3.1 on similar water samples. If, in fact, as suggested, the largest MW material contained colloidal species, it would be effectively removed by coagulation (Vrijennoek *et al.*, 1998), while the MIEX[®] anion exchange process would likely be ineffective in its removal, as observed in Figure 6.4.

Typically, other reported raw water samples display the same broad MW distribution as that observed in the raw water sample in the current study. Peuravuori and Pihlaja (1997) investigated the HPSEC-UV₂₅₄ MW profiles of four samples, two lake and two river water samples from Finland. All samples displayed a large high MW component approaching the void volume of the column, with decreasing amounts of lower MW species. Using OCD, Huber and Frimmel (1996) classified various MW regions of the HPSEC chromatogram of a surface water sample from southern Germany. Similar to the sample in the current research, there was a large humic portion at high MW, with the intermediate MW fraction classified as fulvic acids, progressing through to low MW hydrophilic compounds. Apart from the absence of a peak representative of the colloidal component, the raw water in the current study had a similar MW distribution to the raw water in a study by Myllykangas *et al.* (2002) of alum coagulation of surface water from Lake Kallavesi in Finland. Treating Lake Kallavesi water with alum effectively

removed the mid to high MW species (> 2 000 Da in that study) similar to alum treatment in the current research. However, the low MW fraction (< 1 000 Da) was poorly removed in the work of Myllykangas *et al.* (2002), as found in the chromatograms in Figure 6.4 and the study of a similar set of samples from the WGWTP discussed in Chapter 3. Fabris *et al.* (2007) investigated, by HPSEC-UV, the effect of MIEX[®] combined with alum coagulation on water from the Myponga reservoir in South Australia. In this work, the material of MW 1 000 - 10 000 Da was totally removed, and chromatograms of treated waters were similar to chromatograms shown in Figure 6.3 and 6.4, as well as results discussed in Chapter 3. Similar studies using HPSEC-UV₂₅₄-OCD on surface water used at the Villejean treatment plant, France, showed that coagulation was able to remove the high MW fraction very effectively, while MIEX[®] treatment was responsible for NOM removal across a wider MW range and not as effective as coagulation for removal of the highest MW species (Humbert *et al.*, 2007).

Overall, HPSEC-UV₂₅₄-OCD demonstrated that the MIEX[®]-C treatment removed the greatest amount of organic material over the largest range of MWs. The removal was greatest at MWs above 4 000 Da, with smaller but significant removal below this MW value. EC treatment showed the second highest removal of organic material. However, this occurred almost exclusively above 2 000 Da. Below 2 000 Da, the DOC content in the EC sample was very similar to that in the RW sample. MIEX[®] treatment of the water removed organic material across the entire MW range. Removal was not as effective as EC above 2 000 Da, however, below this value, MIEX[®] outperformed EC, while removing slightly less medium to high MW material than MIEX[®] combined with coagulation (MIEX[®]-C) treatment.

6.3.2. Analysis of Ultrafiltration Isolated NOM Samples

6.3.2.1. Elemental Analysis of NOM Isolates

The samples collected from four points of the WGWTP were subjected to UF (membrane with NMW 1 000 Da) to concentrate the NOM. Following UF, the retentates were subjected to lyophilisation and the solid isolates obtained

were analysed by elemental analysis at a commercial laboratory. Results of the percentage ash (an indication of inorganic content) were approximately 50% for each sample. As a result, small subsamples (50 mg) of the lyophilised samples were redissolved in purified laboratory water (400 mL) and subjected to a second UF treatment using a stirred UF cell and concentrated to 100 mL. This process was repeated until the conductivity of the retentate was $\sim 5 \mu\text{S m}^{-1}$. The whole process was repeated for the remainder of the sample and the UF retentates combined and freeze dried to obtain solid NOM isolates free from inorganic contamination. The yields of solid NOM obtained (RW = 150 mg, MIEX[®] = 140 mg, MIEX[®]-C = 50 mg and EC = 70 mg) were sufficient for a variety of analyses. While Croué *et al.* (2000) stated that characterisation of NOM isolates that had not previously been fractionated into some sort of sub-groups might make results difficult to interpret due to the complexity of NOM, these fractionation steps are extremely time consuming and the procedures involved are complicated. Due to time constraints in the current study, it was not possible to further fractionate the isolated samples and characterisation techniques were carried out on the material which was retained by a 1000 Da UF membrane. From previous work in our laboratory, we have found that, by using this isolation technique, approximately 65-70 % of the DOC from a Wanneroo groundwater sample from the Gnangara mound was retained. Recoveries of NOM in the four treatment plant samples were 62 %, 65 %, 60 % and 71 % for the RW, MIEX[®], MIEX[®]-C and EC samples, respectively, consistent with our earlier study. A sub-sample of each of the four NOM isolates was again analysed for elemental composition at a commercial laboratory and the results are presented in Table 6.2.

Table 6.2 Elemental composition of the four NOM isolates. (n.d. = not detected).

Element (% w/w)	RW	MIEX[®]	MIEX[®]-C	EC
N	n.d.	n.d.	1.26	1.16
C	43.2	44.4	43	42.5
H	4.12	4.55	4.85	5.23
S	1.95	3.57	2.07	1.87
O	43.4	43.6	43	42.3
Ash @ 650 °C	8.0	8.5	8.2	4.5
C/H	10.5	9.76	8.85	8.12
C/O	0.99	1.02	0.99	1.01
C/N	-	-	34.1	36.6

From the values in Table 6.2, it is apparent that the isolation procedure was relatively successful in removing inorganic components from the four samples. This is represented by low ash values for the RW (8 %), MIEX[®] (8.8 %), MIEX[®]-C (8.2 %) and EC (4.5 %) isolates. In a study of surface water NOM isolated by UF from a bog lake in southern Germany, Abbt-Braun *et al.* (2004) observed ash values of 3.4 %, while values as low as 0.7 % were found for samples isolated by adsorption onto XAD resin. However, Croué *et al.* (2000) reported ash content as high as 34 % for reverse osmosis isolated NOM from the Blavet River in France, while nanofiltration isolated NOM contained 20 % ash from the identical source. Isolation of NOM from the same source by XAD resins resulted in ash values of 3 %, which was apparently low enough for accurate determination of elemental composition in the samples (Croué *et al.*, 2000). The elemental compositions of the four samples in this study were all quite similar. According to Abbt-Braun and Frimmel (1999), the C/H ratio is an indication of the aromatic/aliphatic character of the sample. A high C/H ratio indicates greater aromatic content, while lower C/H ratios indicate greater aliphatic character (Abbt-Braun and Frimmel, 1999). On this basis, aromaticity decreased in the order RW, MIEX[®], MIEX[®]-C and EC, while aliphatic nature increased through in this order. The UV₂₅₄ data from Table 6.1 supports this observation, with the RW sample having the highest UV₂₅₄ absorbance (0.43 cm⁻¹), indicating greater aromaticity or conjugated double bonds, followed by MIEX[®] (0.25 cm⁻¹), EC (0.09) and MIEX[®]-C (0.07). In a study of the

Suwannee River in the USA, Croué *et al.* (2000) separated NOM into 11 fractions using various resins on the basis of polarity. Using this approach, hydrophobic (acids and bases), transphilic (acids and neutrals), hydrophilic (acids (x2), neutrals and bases) and ultrahydrophilic (acids, humic acids and neutrals) materials were isolated. It was observed that, as the material became less hydrophobic, the C/H ratio generally decreased. In relation to the current study, MIEX[®] treatment reduced the C/H ratio, indicating more hydrophilic NOM compared to the RW while MIEX[®]-C and EC treatment resulted in an even lower C/H ratio, indicative of a greater hydrophilic content. Croué *et al.* (2000) observed that C/O and C/N ratios remained similar for all samples analysed. The C/O ratios of the four samples in this study were very similar and the C/N ratios, while only available for the MIEX[®]-C and EC samples, were again very similar.

6.3.3. Pyrolysis-GC-MS Analysis of Solid NOM Isolates

The four NOM isolates were subjected to pyrolysis at 560 °C in a Pyroprobe, followed by GC-MS analysis of the pyrolysis products (Py-GC-MS). In Py-GC-MS, some specific degradation fragments (products) are known to be produced from macromolecular class types, such as carbohydrates, proteins or amino sugars and polyhydroxyaromatic compounds (van der Kaaden *et al.*, 1983, Gadel and Bruchet, 1987, Bruchet *et al.*, 1990, Saiz-Jimenez, 1995, Croué *et al.*, 2000, Garcette-Lepecq *et al.*, 2000, Gobé *et al.*, 2000). Figure 6.5 and Figure 6.6 show the pyrograms of the four NOM isolates: RW, MIEX[®], MIEX[®]-C and EC. More than 100 pyrolysis products were detected in the four samples analysed, although only the 41 most abundant are displayed in Figure 6.5 and Figure 6.6. These are identified by number and listed in Table 6.4.

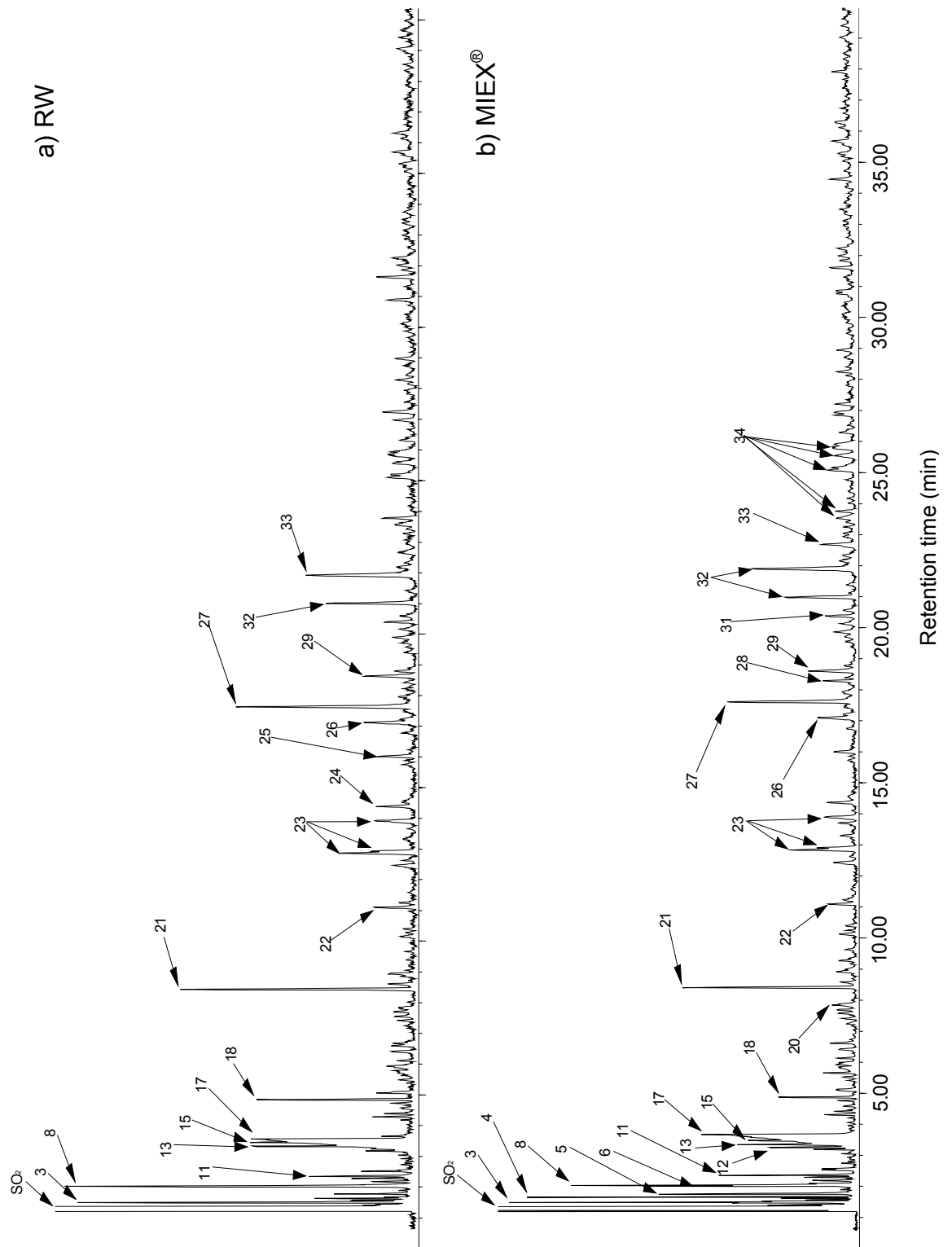


Figure 6.5 Pyrograms obtained by Py-GC-MS of NOM isolates from a) RW and b) MIEX[®]. Numbers above chromatograms refer to identification key in Table 6.4.

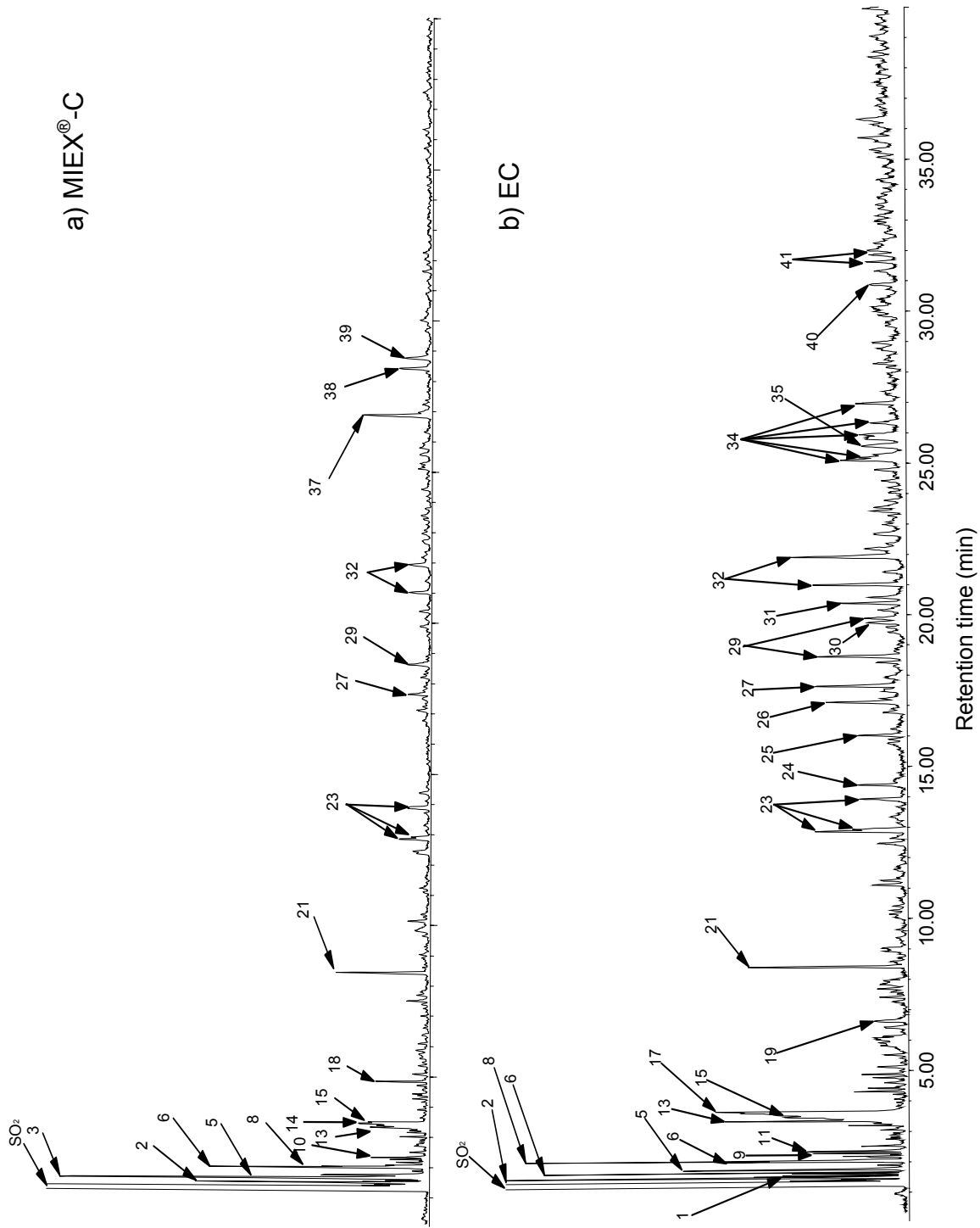


Figure 6.6 Pyrograms obtained by Py-GC-MS of NOM isolates from a) MIEX[®]-C and b) EC. Numbers above chromatograms refer to identification key in Table 6.4.

Table 6.3 Most abundant compounds identified in pyrograms of four NOM isolates. Category of compound type relates to Figure 6.5 and 6.6.

Peak number	Compound	Category (as in Figure 6.5 & 6.6)
1	chloromethane	halomethane
2	methylpropene	aliphatic hydrocarbon
3	butene	aliphatic hydrocarbon
4	bromomethane	halomethane
5	isocyanic acid	carbohydrate
6	acetonitrile	protein
7	nitroethane	protein
8	propanone	carbohydrate
9	dimethylcyclopropane	aliphatic hydrocarbon
10	propenenitrile	protein
11	iodomethane	halomethane
12	hexene	aliphatic hydrocarbon
13	butanone	carbohydrate
14	butenenitrile	protein
15	methylfuran	carbohydrate
17	acetic acid	carbohydrate
18	benzene	BTEX
19	dimethylfuran	protein
20	thioglycolic acid	organosulfur
21	toluene	BTEX
22	methylpyrazole	protein
23	xylene	BTEX
24	methylcyclopentenone	carbohydrate
25	methylfurandione	carbohydrate
26	methylcyclopentenone	carbohydrate
27	phenol	phenol
28	decene	aliphatic hydrocarbon
29	trimethylbenzene	BTEX
30	methylcyclopentadiene	aliphatic hydrocarbon
31	dimethylcyclopentenone	aliphatic hydrocarbon
32	methylphenol	phenol
33	cyclopropylpentane	aliphatic hydrocarbon
34	dimethylphenol	phenol
35	methylindene	protein
36	ethylphenol	phenol
34	dimethylphenol	phenol
37	piperidinedione	protein
38	methylpiperidinedione	proteins
39	dimethylpyrroledione	protein
40	methylbenzofuran	carbohydrate
41	dimethylnaphthalene	PAH

Py-GC-MS can provide a 'fingerprint' of the NOM that is quite specific. In order to simplify the results, the more than 100 detected pyrolysis products were allocated to one of nine categories based on the probable origin of the fragment. The categories were BTEX (benzene, toluene, ethylbenzenes and xylenes), carbohydrates, proteins, phenols, polyaromatic hydrocarbons (PAHs), organosulfur, aliphatic hydrocarbons, halomethanes and an unidentified category representing products which could not be positively identified by comparison of their mass spectra to the Wiley275 mass spectral database. These classifications are based on work by Croué *et al.* (2000), Garcette-Lepecq *et al.* (2000), Gobé, *et al.* (2000), Gadel and Bruchet (1987, and references therein), Saiz-Jimenez (1995), Bruchet *et al.* (1990) and van der Kaaden *et al.* (1983). The proportion of species within these categories was determined by summing the areas of each peak and calculating the ratio of this total category peak area to the total area of detected peaks as a percentage. This process was carried out in an identical manner for all of the four samples providing a consistent method for comparison of individual peaks and an estimate of the relative proportion of each biopolymer type in the sample. These ratios are presented as pie charts in Figure 6.7. The peak areas, as well as associated category of the individual identified pyrolysis products are listed in Appendices 5 and 6.

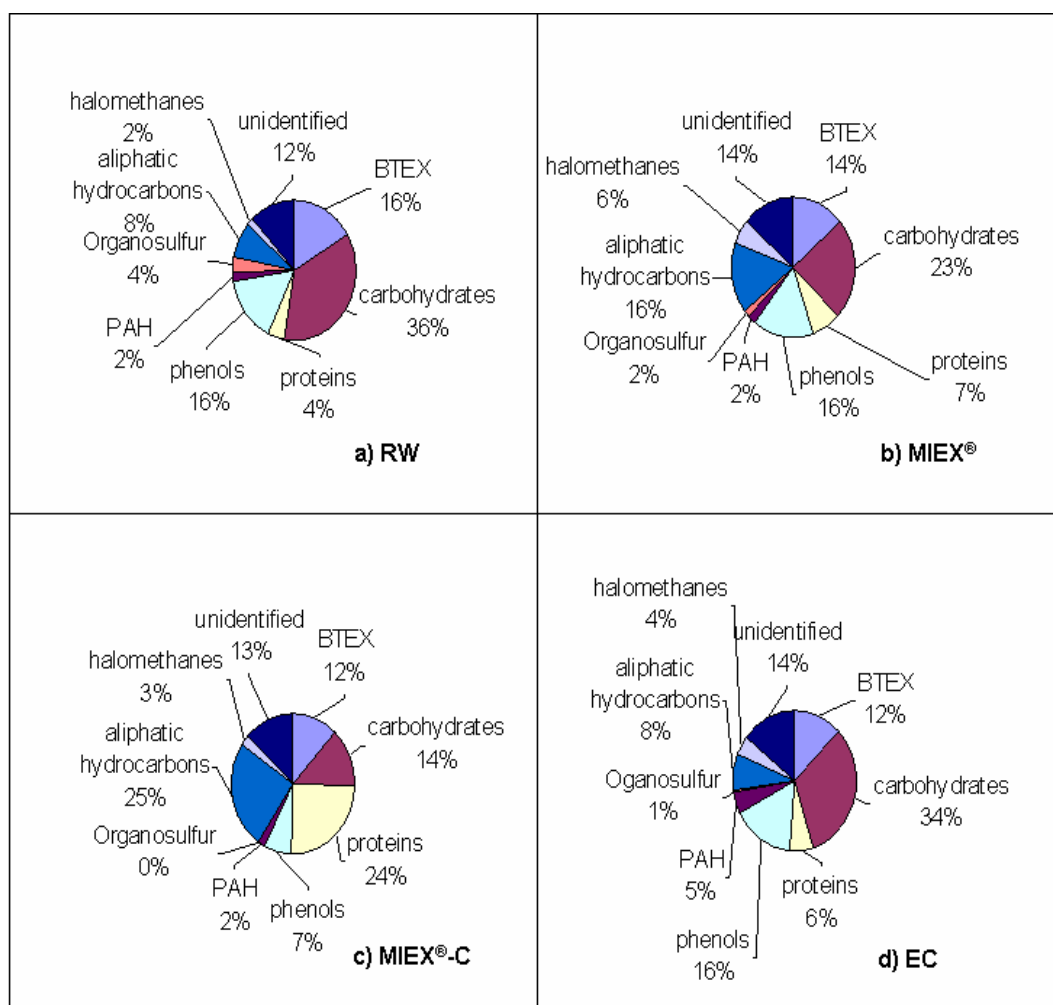


Figure 6.7 Relative yield of pyrolysis products of various biopolymer origin from NOM isolated from a) RW, b) MIEX®, c) MIEX®-C and d) EC.

Comparisons of the four samples showed similarities and also some interesting differences. Firstly, the contribution of the BTEX compounds was quite consistent throughout the four samples (12-16 %), however, it is difficult to assign these compounds to any biogenic precursor as they have diverse origins, and, in most cases, are probably secondary pyrolysis products (Sihombing *et al.*, 1996). There were also a number of peaks (12 % - 14 % of the total peak area) that could not be positively identified in each of the four chromatograms. While a number of these peaks had mass spectra that gave an indication of the likely structure, positive identifications still could not be made. These relatively low values meant that between 86 % - 88 % of the total pyrolysis peak area could be positively identified as specific pyrolysis products. Croué *et al.* (2000), in their study of hydrophilic and hydrophobic fractions of the Suwannee river NOM, reported between 79 % –

98 % of the total peak area representing pyrolysis products could be identified, while Page *et al.* (2003) found between 86 % - 94 % of the pyrolysis product peak area could be identified in their study of pyrolysis of NOM samples isolated from four alum treated surface waters. One of the biggest differences amongst the four samples was the contribution of carbohydrate derived compounds. The proportion of carbohydrate derived species for the RW was 36 %, compared with 23 % for the MIEX[®] sample, 14 % for the MIEX[®]-C sample and 34% for the EC sample. In a study of four surface water samples taken from South Australia (3) and Victoria (1), Page *et al.* (2003) used Py-GC-MS to characterise the raw waters, as well as the remaining NOM after treatment with alum. All four samples in this study showed alum coagulation was ineffective for the removal of carbohydrate derived material, as shown by an increased relative percentage after treatment. The EC sample analysed in this research similarly showed that enhanced alum coagulation appeared to be ineffective for removal of carbohydrate derived material. While carbohydrate derived compounds may still have been removed during coagulation, the relative concentration compared to material from other biopolymer sources was enriched. HPSEC-UV₂₅₄-OCD (Figure 6.3d and Figure 6.4d) indicated that EC was particularly effective in removing the high MW portion of NOM. Combining HPSEC data with results from Py-GC-MS analysis may indicate that the large MW fraction preferentially removed by EC treatment was comprised of structures deficient in carbohydrate derived material. This is consistent with the hypothesis proposed in Section 3.3.3 that this high MW material contained mainly humic type material deficient in oxygenated moieties. Chow *et al.* (1999), in a similar study of three surface waters from South Australia, found coagulation treatment removed the high MW species and the remaining NOM was enriched in carbohydrate derived material.

The protein derived material demonstrated a different trend, with EC (6 %) and MIEX[®] (7 %) samples containing a similar proportion of protein markers to the RW (4 %), while MIEX[®]-C (24 %) had an elevated proportion of these protein markers. Possibly this could be due to MIEX[®]-C treatment simply removing material from other categories to a greater extent compared to

protein derived substances, while MIEX[®] and EC, as a fraction of the total NOM, removed the protein markers to a similar extent. It could be expected that the anion exchange removal mechanism of the MIEX[®] resin may not be conducive to removal of such material; as well, the alum coagulant used may also be ineffective in removing positively charged species in the protein category. In a study of various fractions isolated by XAD type resins, Croué *et al.* (2000) found that the most hydrophilic fractions included up to 40 % of the identified pyrolysis product area as protein derived material. Similarly, according to the HPSEC results in Section 6.3.1.2, the MIEX[®]-C sample contained the most low MW hydrophilic material, as well as producing the greatest proportion of protein derived markers upon pyrolysis.

The phenols, possibly representative of tannin or lignin inputs (Sihombing *et al.*, 1996), showed similar proportions in three of the four samples, with only the MIEX[®]-C process having a reduction in the contribution of phenolic compounds. Also, van Heemst *et al.* (1999) reported phenolic compounds could be derived from several sources, including lignins and tannins, as well as proteins, making identification of the source of phenols difficult. It would appear from the pyrolysis data in Figure 6.7 that MIEX[®] and EC treatment were able to remove the biopolymers responsible for the phenolic contribution to an equal extent relative to the total amount of organic material in each sample. Possibly the different removal mechanisms of the two treatment processes remove material of different origins and the combination of the two techniques is able to remove a wider range of material responsible for the derivation of phenols, accounting for the lower percentage of phenol in the MIEX[®]-C treated sample.

The presence of higher relative amounts of aliphatic hydrocarbons possibly represents a greater aliphatic content of NOM in the MIEX[®]-C treated sample. The combination of coagulation, which effectively removes large MW, hydrophobic material (Chow *et al.*, 1999 and work described in Section 3.3.3), and MIEX[®] treatment, which targets NOM over a wider MW region (Section 3.3.3), has resulted in an increased proportion of material responsible for producing aliphatic compounds upon pyrolysis. This possibly

represents the material recalcitrant to both treatment methods. The lower percentage amounts of aliphatic compounds after only MIEX[®] or EC treatment possibly represents the lower relative removals of other compound classes, resulting in the aliphatic markers accounting for a lower overall percentage of identified pyrolysis products. The proportions of PAH, organosulfur and halomethane markers were relatively similar for all of the four samples.

6.3.4. Fourier Transform Infrared Spectroscopy of Solid NOM Isolates

FTIR spectroscopy is useful for identification of functional groups. Various functional groups can be assigned to certain infrared bands, based on the detailed work of Stevenson and Goh (1971), who investigated the wavelengths of absorbances of functional groups in various humic acid samples, and the major treatises in IR spectroscopy by Nakanishi and Solomon (1977) and Silverstein and Webster (1997). Typically, comprehensive interpretation of pure compounds is complex due to the generation of many absorbance bands. Paradoxically, the complexity of NOM makes the interpretation of spectra simpler, because only the strongest bands can be identified and associated with structural moieties (Croué *et al.*, 1999). Figure 6.8 shows the FTIR spectra of the RW, MIEX[®], MIEX[®]-C and EC solid NOM isolates.

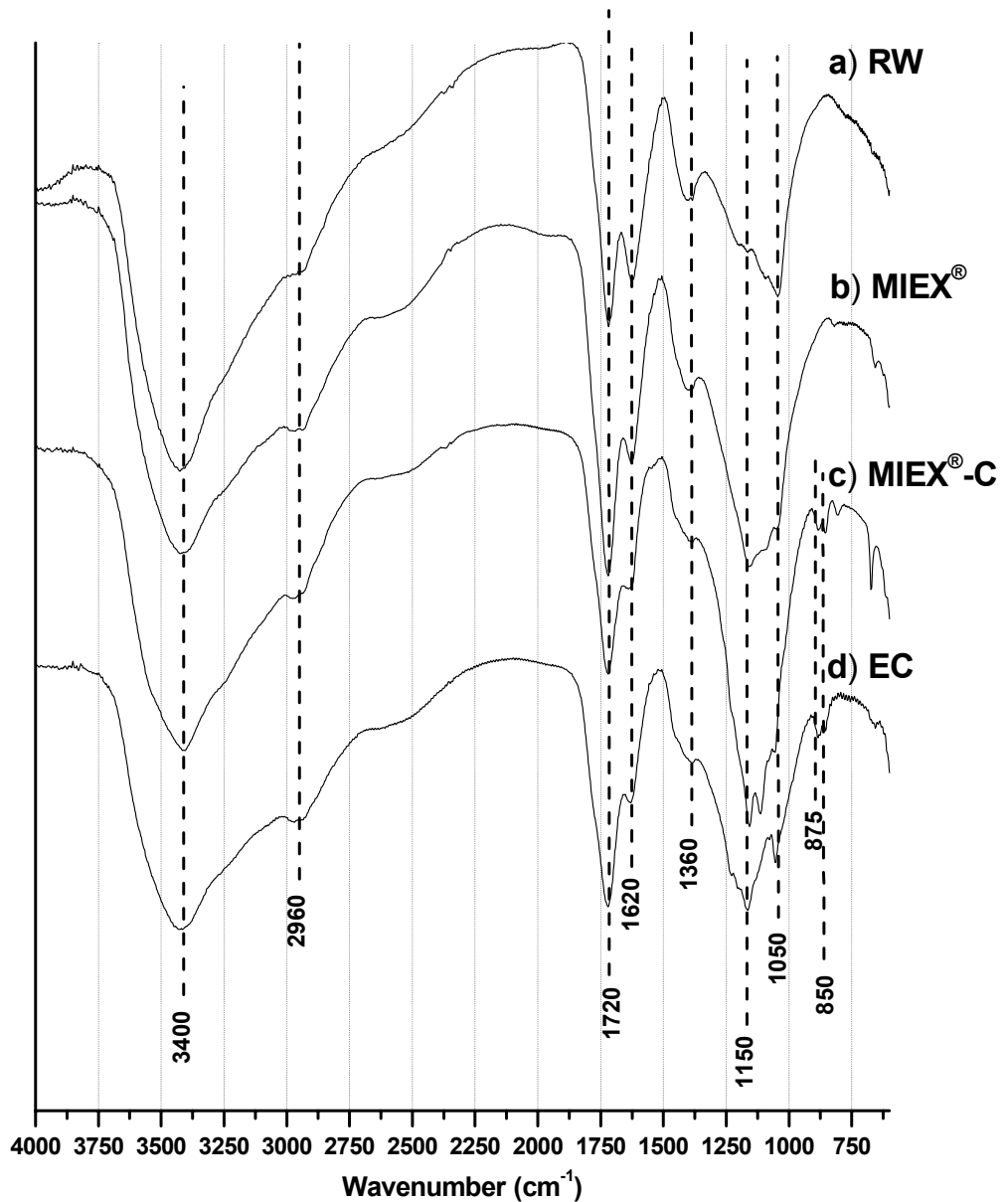


Figure 6.8 FTIR spectra of four solid NOM isolates: a) RW, b) MIEX[®], c) MIEX[®]-C, d) EC.

The FTIR spectra of the four samples in Figure 6.8 are all relatively similar. Interpretation of the spectrum produced from the RW NOM isolate (Figure 6.8a) illustrated a significant, very broad absorption band at 3 600 – 2 500 cm⁻¹, due to hydrogen bonded hydroxyl groups of carboxylic acids, as well as of phenols and alcohols (Nakanishi and Solomon, 1977, Silverstein and Webster, 1997). Broad bands at 3 000 – 2 800 cm⁻¹ are representative of C-H stretching from methyl (2 960 cm⁻¹ and 2 872 cm⁻¹) and methylene carbon (2 920 cm⁻¹ and 2 850 cm⁻¹) and the broad band centered at

$\sim 1720\text{ cm}^{-1}$ is indicative of C=O stretching. This could be due to the presence of carboxylic ($\sim 1720\text{ cm}^{-1}$), ketonic (1715 cm^{-1}), aldehydic ($1740 - 1720\text{ cm}^{-1}$) or ester ($1750 - 1720\text{ cm}^{-1}$) carbonyl groups, which all have a strong absorbance at this wavelength. The strong band at $\sim 1620\text{ cm}^{-1}$ was possibly the combined contribution of the amide I stretch (C=O, 1640 cm^{-1}) and amide II bend (N-H, $1655 - 1620\text{ cm}^{-1}$) and N-H bending vibrations of amines ($1650 - 1580\text{ cm}^{-1}$). Aromatic carbon stretches (1600 cm^{-1} and 1580 cm^{-1}) also produce moderate to strong bands in this region. The moderate to strong band at $\sim 1360\text{ cm}^{-1}$ is characteristic of asymmetric and symmetric bending of CH_3 and CH_2 groups associated with carbonyl moieties, such as those of ketones, esters and carboxylic acids. A significant feature of the FTIR spectra was absorbance bands centred at $\sim 1100-1200\text{ cm}^{-1}$. Several functional groups give signals in this region, including bands due to C-O stretching of alcohols ($1000 - 1200\text{ cm}^{-1}$), C-O stretching and O-H deformations of carboxylic acids at $\sim 1200\text{ cm}^{-1}$, C-O stretching of esters ($\sim 1100\text{ cm}^{-1}$) and C-O-C stretching of ethers ($\sim 1100\text{ cm}^{-1}$) (Nakanishi and Solomon, 1977, Silverstein and Webster, 1997).

Treatment of the RW sample, however, did show some variations in the FTIR spectra of the NOM isolates. Most noticeably, the MIEX[®]-C (Figure 6.8c) and EC (Figure 6.8d) treated samples displayed a significant absorbance in the $1000 - 1200\text{ cm}^{-1}$ region, possibly representing C-O stretching of various functional groups. Also, the S-O stretching of the sulfate group has a broad band in this region ($\sim 1150\text{ cm}^{-1}$), as well as minor bands at $\sim 850\text{ cm}^{-1}$ (Nakanishi and Solomon, 1977, Silverstein and Webster, 1997). This may be particularly significant in the MIEX[®]-C (Figure 6.8c) and EC (Figure 6.8d) samples, as these waters are high in sulfate ion during the coagulation process, and the large peak in the $1000 - 1200\text{ cm}^{-1}$ region of the IR spectra may indicate that residual sulfate may not have been completely removed during the desalting process.

A reduction in the relative proportion of the band at $\sim 1620\text{ cm}^{-1}$ compared to other bands in the spectrum of the MIEX[®]-C and EC samples compared to

the RW sample possibly indicates a reduction in the amount of aromatic carbon in the MIEX[®]-C and EC samples. HPSEC results showed effective removal of the high MW, highly aromatic fraction for the EC (Figure 6.4d) and MIEX[®]-C (Figure 6.4c) samples, while MIEX[®] treatment (Figure 6.4b) removed a lesser amount of this material. The FTIR spectra in Figure 6.8 also support the idea that the MIEX[®]-C and EC samples had the lowest proportion of aromatic species relative to other signals observed. A significant feature of the RW FTIR spectrum (Figure 6.8a) was a strong absorbance band at $\sim 1\ 050\ \text{cm}^{-1}$. For the MIEX[®] treated sample (Figure 6.8b), the relative proportion of the band at this position had been reduced, possibly indicating a preferential removal of alcohol moieties. The nature of MIEX[®] treatment, i.e. anion exchange, suggests that hydroxy groups may be particularly susceptible to removal by MIEX[®]. The increase in the relative proportion of the signal at $\sim 1\ 150\ \text{cm}^{-1}$ for the NOM isolate from MIEX[®] treatment may be due to an increased proportion of ether or ester moieties. For the MIEX[®]-C (Figure 6.8c) and EC (Figure 6.8d) samples, the band possibly due to residual sulfate make interpretation of the region around $1\ 100\ \text{cm}^{-1}$ of the spectrum impossible. The other region of the FTIR spectra that indicates some difference in remaining NOM is at $\sim 1\ 360\ \text{cm}^{-1}$, indicative of methyl groups associated with carbonyl carbon. The contribution in this region of the spectra of the treated samples is reduced compared to that of the RW sample.

Generally, treatment of the RW appears to have resulted in preferential removal of aromatic species, as indicated by the reduction of the signal at $\sim 1\ 620\ \text{cm}^{-1}$ relative to other signals in the spectra. Significantly, the removal of residual sulfate during the desalting process may not have been complete. For the MIEX[®] treated water, it would appear that alcoholic hydroxy groups may have been removed in preference to other species such as ester and ether moieties, as indicated by the greater contribution at $\sim 1\ 150\ \text{cm}^{-1}$ in the spectrum of the NOM isolate after MIEX[®] treatment (Figure 6.8b).

6.3.5. Solid State ^{13}C Nuclear Magnetic Resonance Spectroscopy of Solid NOM Isolates

NMR spectroscopy is an attractive method to investigate NOM structure because qualitative and quantitative organic structural information can be generated in both solution and solid states under nondegradative conditions (Wilson, 1987). However, NMR spectroscopy is not as sensitive as FTIR spectroscopy, requiring sample sizes at least 50 times greater and quantification under certain conditions is difficult (Nanny *et al.*, 1997). With this in mind, solid state ^{13}C NMR analysis of the four NOM isolates was performed to further characterise the structure of each sample. The ^{13}C NMR spectra of the four NOM isolates are presented in Figure 6.9.

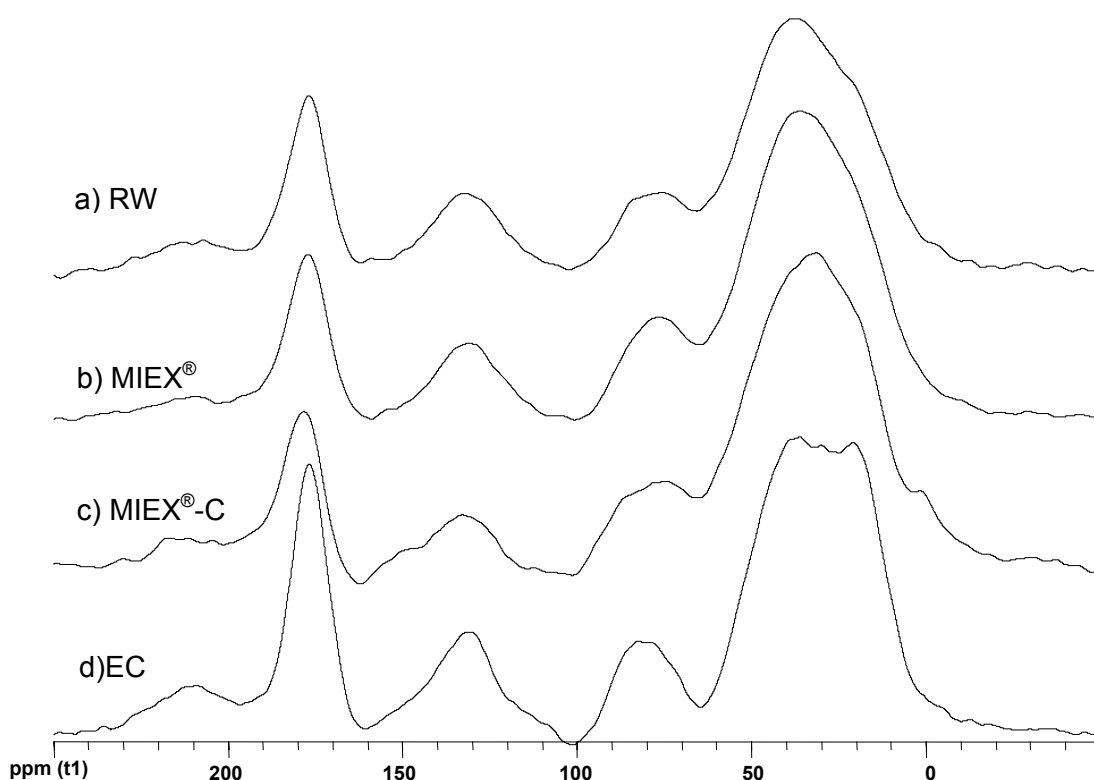


Figure 6.9 Solid state ^{13}C CPMAS NMR spectra of NOM isolates: a) RW, b) MIEX[®], c) MIEX[®]-C, d) EC.

Due to the increased sample size obtained in this study, the ^{13}C NMR spectra were of superior quality to the spectra obtained in Chapter 5 of this Thesis. Spectra of the four samples were integrated over five spectral

regions. These spectral regions can be attributed to the following functionalities: 0 - 60 ppm to aliphatic carbon, 60 - 100 ppm to carbohydrates or O-aliphatic carbons, e.g. carbohydrates, 100 - 165 ppm to aromatic carbon, 165 - 190 ppm to carboxyl carbon, and 190 - 230 ppm to carbonyl groups (Croué *et al.*, 2000, Hatcher *et al.*, 2001, Bianchi *et al.*, 2004, Keeler *et al.*, 2006). The aliphatic region includes the cumulative areas between 0 and 100 ppm and the area between 100 - 165 ppm is assigned to aromatic carbons (Malcolm, 1990). The superior spectra obtained in this study allowed the integration of a fifth group (190 – 230 ppm) classified as carbonyl carbon which was not possible in Chapter 5 due to the signal to noise ratio of these earlier spectra. Table 6.4 shows the results from integration of the four spectra over these regions.

Table 6.4 Relative proportions of carbon types in the solid state ^{13}C NMR spectra of the NOM isolates: Integration results from solid state ^{13}C NMR analysis of RW, MIEX[®], MIEX[®]-C and EC (Figure 6.9). % = percentage of peak area of total spectrum, ppm is chemical shift of peak in parts per million.

Chemical linkages	Chemical shift range (ppm)	RW	MIEX [®]	MIEX [®] -C	EC
Aliphatic carbon	0 - 60	61.5 %	66 %	70 %	59 %
O-aliphatic carbon	60 – 100	9.5 %	10.5 %	10 %	8 %
Aromatic carbon	100 – 165	11 %	8.5 %	5 %	10 %
Carboxyl carbon	165 – 190	15 %	13 %	12.5 %	18 %
Carbonyl carbon	190 - 230	3 %	2 %	2.5 %	5 %

Similar NMR spectra of the four isolated NOM samples were obtained (Figure 6.9), dominated by a strong, broad aliphatic carbon signal and a similarly strong, but narrower and better resolved, carboxyl carbon signal. While aliphatic carbon appears to be the most abundant type in all four spectra, it should be noted that aliphatic carbon can be overestimated using CPDAS with ^{13}C NMR spectroscopy. This is apparently due to a higher efficiency of magnetisation transfer from hydrogen to carbon in CH_2 groups compared with other carbon types (Wilson, 1987, Templier *et al.*, 2005). This may explain a possible overestimation of aliphatic carbon content, and underestimation of the aromatic component, in the four samples, as suggested by comparison with the HPSEC data in Section 6.3.1.2, where the

intermediate MW range material was thought to contain significant aromatic structures. The four ^{13}C NMR spectra appear similar to the spectrum from a hydrophobic fraction of surface water collected from the Gartempe River in France in the study by Templier *et al.* (2005). In the study of Templier *et al.* (2005), it was proposed that the hydrophobic fraction had significant lignin and carbohydrate input. This would support the hypothesis proposed in Section 3.3.3 where inlet water from the WGWTP, sampled at a different time period, had a significant hydrophobic content, suggesting a large aromatic contribution from the polyphenolic structures of lignin and tannin type material. Similar spectra were also observed for soil humic material (Garcette-Lepecq *et al.*, 2000) and kerogen-like organic matter from recent sediments (Gonzalez *et al.*, 2003).

Treatment of the RW with MIEX[®] resulted in removal of approximately half of the DOC (Table 6.1). It would appear from the relative proportions of carbon types by NMR (Table 6.4) that MIEX[®] treatment was slightly more effective in removing the aromatic fraction (RW 11 % compared with MIEX[®] 8.5 %), as opposed to other carbon types, but the absolute difference between the integrated areas of the spectra from the RW (Figure 6.9a) and MIEX[®] (Figure 6.9b) NOM isolates was small. The HPSEC data for these two samples (Figure 6.3a and b) indicated that the intermediate to high MW fraction (1 000 – 20 000 Da) was preferentially removed by this treatment method, possibly resulting in the relative reduction of this carbon type in relation to the other carbon species detected in the MIEX[®] sample compared to the RW sample. The higher proportion of aliphatic carbon in the spectrum of the MIEX[®] sample suggests MIEX[®] is less effective in the removal of aliphatic species.

Treatment with the MIEX[®]-C process removed 75% of the DOC, but, similar to MIEX[®] treatment, MIEX[®]-C did not significantly alter the distribution of carbon types compared to the RW sample. Again, aromatic carbon was slightly depleted, indicating the preferential removal of aromatic moieties, while the aliphatic signal was higher relative to the RW value (Table 6.4), possibly indicating that material represented by this carbon type is more

recalcitrant for MIEX[®]-C treatment. EC treatment removed 67% of the DOC and resulted in NOM with a similar NMR distribution (Figure 6.9d). The relative integrated proportion for aliphatic carbon (59 %) was slightly lower compared with the RW (61.5 %), while the proportions of remaining carbon types were not significantly different to those in the RW. This appears to indicate that EC treatment removed each of the measured carbon types without particular preference.

In a study of NOM isolated from three Australia sources (two from Victoria and one from the Wanneroo GWTP), Wong *et al.* (2002) used solid state ¹³C NMR spectroscopy to obtain structural characteristics of these samples. In the study by Wong *et al.* (2002), the ¹³C NMR spectrum of isolated material from the WGTP was similar to the RW NMR spectrum in the current research (Figure 6.9a), dominated by aliphatic carbon with the remaining signal distributed relatively evenly over the spectra. Unfortunately in the previous research, integrated areas of each spectral region were not reported, making a direct comparison difficult. Fractionation of the sample using XAD resins into a strongly hydrophobic, slightly hydrophobic and hydrophilic fraction resulted in a more intense aromatic carbon signal in the more hydrophobic fraction, while the slightly hydrophobic fraction had a greater proportion of aliphatic and O-aliphatic carbon. The hydrophilic fraction produced a poor quality spectrum, due to lack of sample, but it appeared that the majority of the NMR signal was in the aliphatic and O-aliphatic range (Wong *et al.*, 2002). This would support the likely nature of the hydrophobic component, removed by coagulation, containing a greater amount of aromatic material, while the hydrophilic fraction remaining after coagulation treatment being enriched in aliphatic and O-aliphatic carbon.

Overall, in terms of characteristics of NOM remaining after the various treatments, NMR revealed some interesting trends. Treatment of the RW with MIEX[®] resin showed increases in the relative amounts of aliphatic carbon and O-aliphatic carbon, with small decreases in the relative amounts of aromatic carbon, carboxyl carbon and carbonyl carbon. The ion-exchange properties of the MIEX[®] resin mean that it is likely to remove the negatively

charged fraction of aquatic NOM. With regard to NMR analysis, this is shown as the carboxyl carbon type. Properties of the water after further treatment with coagulation (MIEX[®]-C) showed similar trends to the MIEX[®] treatment. In that coagulation step, the primary change was that the relative aliphatic content became slightly higher and the aromatic content slightly lower. This is consistent with the idea that the high molecular weight, aromatic humic material is easily removed by coagulation processes (Chow *et al.*, 1999 and results in Chapter 3). EC treatment of the RW sample only very slightly changed the functional group content of the NOM. Interestingly, the carboxyl carbon and ketone and carbonyl carbon content increased, while there were very slight decreases in the aliphatic, O-aliphatic and aromatic carbon content, after the enhanced coagulation stage.

6.4. Conclusions

Ultrafiltration with a NMW 1 000 Da membrane was successfully used to isolate and desalt sufficient NOM from four samples from the Wanneroo GWTP to allow detailed characterisation. The Wanneroo RW had a relatively high DOC concentration distributed over a wide range of MWs. The characteristics of this water were similar to those observed in surface reservoirs in South Australia (Fabris *et al.*, 2007), however, the Wanneroo sample had the additional presence of colloidal material at very high MWs. A similar very high MW fraction has been previously reported in samples taken from a bog Lake in the Black Forest of southern Germany (Huber and Frimmel, 1996, Schmitt *et al.*, 2003). NMR and FTIR data suggested the RW NOM was similar to the hydrophobic fraction of surface waters taken from a number of European sources (Huber and Frimmel, 1996, Peuravuori and Pihlaja, 1997, Myllykangas *et al.*, 2002, Schmitt *et al.*, 2003). The RW sample contained the highest DOC content of all four samples, with a greater UV₂₅₄ value, i.e. SUVA, indicating a greater degree of aromaticity and conjugation. The organic carbon in the RW sample had a wide range of MWs (100 - 30 000 Da) and greater aromatic content compared to the three treated water samples, as illustrated by the more abundant HPSEC-UV₂₅₄ profile. Analysis by FTIR spectroscopy also indicated a greater proportion of

aromatic carbon in this sample. NMR analysis further confirmed these characteristics, with the RW sample having the lowest proportion of carbon present as aliphatic carbon and the greatest aromatic carbon content. Analysis of this sample by Py-GC-MS interestingly showed a significant contribution from both aromatic moieties (BTEX, phenols and PAHs) and carbohydrates, slightly more significant than in the other samples. The relative contribution of aliphatic precursors in this sample was lower than in the MIEX[®] and MIEX[®]-C samples, but the same as in the EC sample, according to the Py-GC-MS analysis.

Treatment of the RW with the MIEX[®] resin process significantly altered the composition of the NOM. DOC was reduced by 49 %, while 50 % of the BDOC fraction was removed, colour was reduced by 51 % and UV₂₅₄ lowered by 42 %. MIEX[®] treatment was only moderately effective at removing intermediate to high MW DOC (>2 000 Da), with removal below 2 000 Da more effective than EC treatment, but not as efficient as MIEX[®]-C treatment. The character of the organic matter after treatment showed significant alteration, with FTIR and NMR analysis demonstrating some preferential removal of the aromatic component of the NOM. Interestingly, Py-GC-MS showed a lesser proportion of carbohydrate markers present after this treatment, appearing to indicate that the MIEX[®] resin was effective at removing this oxygenated component of NOM.

Treatment of the RW by MIEX[®] followed by coagulation (MIEX[®]-C) removed more than 75 % of the DOC, 85 % of the UV₂₅₄ component and 97 % of the colour, showing some preferential removal of the UV₂₅₄-active and coloured species by this method. Also, the MW range of the DOC in this treated water was significantly reduced. The majority of removal was above 2000 Da, although DOC removal across the entire MW range was observed. The character of the organic matter after treatment was also significantly altered. Structural characterisation studies using Py-GC-MS, FTIR and NMR spectroscopy revealed that the organic matter was more aliphatic than the organic matter in the RW, consistent with the reduction of the SUVA and reduction in the HPSEC-UV₂₅₄ signal. Py-GC-MS showed a lower relative

contribution from aromatic moieties, and a higher relative contribution from aliphatic species, than in the RW or MIEX[®] treated NOM isolates. NMR spectroscopy further highlighted the lower aromatic content, but higher aliphatic content, of this sample compared to the RW and MIEX[®] NOM isolates.

Enhanced coagulation (EC) treatment of the raw water removed a significant portion of DOC (70 %), UV₂₅₄ (80 %) and colour (90 %), also showing some preferential removal of the UV₂₅₄-active and coloured species by this method. The MW range of the DOC remaining after EC treatment was comparable to that remaining after MIEX[®]-C treatment, although EC removal at the lower MW range (< 2 000 Da) was not as efficient as either MIEX[®]-C or MIEX[®] treatment. Py-GC-MS and NMR analysis indicated that the organic matter in the EC sample had similar characteristics to the RW, with the relative aromatic, aliphatic, carbohydrate and protein precursor content being similar to that of the RW NOM by Py-GC-MS and aromatic and aliphatic contributions being similar to that of the RW NOM by NMR spectroscopy.

Generally, it was found that treatment removed proportionally more aromatic material, leaving organic matter with a lower average MW and a greater proportion of aliphatic material. In terms of the character of the organic matter remaining after the treatment processes, the MIEX[®] and MIEX[®]-C processes appeared to show a slight preference for removal of aromatic organic matter, whereas EC did not appear to show this preference. In regard to the treatment of water for distribution at a drinking water treatment plant, MIEX[®] only treatment was able to remove a significant portion of DOC, colour and UV₂₅₄ absorbing species, but, for this water source, MIEX[®] only treatment was not as effective as enhanced coagulation treatment, although the recalcitrant fraction of NOM after MIEX[®] treatment appeared to be the intermediate to high MW fraction which may be effectively removed by other processes such as coagulation or membrane filtration. Combining MIEX[®] with coagulation or a membrane filtration technique would effectively control the turbidity issues that arise after MIEX[®] treatment due to minor breakdown and carryover of the resin. The current study has shown the combination of

MIEX[®] followed by coagulation to be an effective method for removal of DOC. This combined treatment removed DOC across a broad MW range, leaving material that was more aliphatic with lower colour and UV₂₅₄ absorbance. The lower DOC concentrations, especially in the lower MW NOM, from MIEX[®] followed by coagulation treatment should improve downstream parameters, including lower chlorine demands, lower DBP formation and less biofilm formation in the distribution system.

7. THESIS CONCLUSIONS

High pressure size exclusion chromatography is the method of choice used by water researchers for determination of the MW distribution of NOM. The various treatment processes utilised for removal of NOM have been reported to be more effective in removing certain MW fractions and, hence, a detailed knowledge of the MW distribution of NOM in water samples is required.

During this research, trihalomethanes, used as an indicator for disinfection by-product formation, were shown to form from all MW fractions of NOM collected by preparative HPSEC. This is particularly important from a treatment perspective as traditional treatment technologies (i.e. coagulation, flocculation, sedimentation and filtration) specifically target the mid to high MW fractions. Consequently, THM formation from smaller MW material is an issue that will routinely affect water quality, particularly at the Wanneroo GWTP, the study site used in this Thesis.

A study of the treatment streams at the Wanneroo GWTP using HPSEC with OCD, UV_{254} and fluorescence detection demonstrated the preferential removal of the intermediate to high MW species in NOM by coagulation and flocculation even at an elevated coagulant dose. The combination of various detection systems during this study highlighted the importance of a multidetection approach. As such, a system was constructed that built on previously developed systems, with the use of a small detector cell enabling detection limits capable of measuring even the most dilute natural and treated water samples. The multidetection system indicated that organic matter removed during treatment contained material enriched in aromatic species, as indicated by a reduction of the SUVA values obtained after treatment, and the remaining NOM was likely comprised of a greater proportion of low MW aliphatic compounds. Comparatively, combining coagulation (at a reduced dose) and flocculation with MIEX[®] resin treatment removed the entire high MW fraction of NOM (similar to coagulation only treatment), while improving the removal of the intermediate MW material. The lowest MW fractions of NOM were not significantly removed by either of these treatment options; however, MIEX[®] treatment was more effective than

coagulation treatment. The HPSEC chromatogram of MIEX[®] treated water showed the largest MW fraction was removed to a lesser extent after treatment, while similar levels of the intermediate and low MW species were removed, compared to coagulation and combined MIEX[®] and coagulation treated samples. Ineffective removal of the largest MW fraction of NOM is not entirely unexpected when the anion exchange mechanism of the resin is considered, as the high MW fraction had previously been shown to possibly be comprised of inorganic colloidal species unable to participate in ion exchange reactions. This finding demonstrates, however, the potential attraction of combining MIEX[®] treatment with a treatment process, such as membrane filtration, which can effectively remove high MW NOM, while reducing chemical usage and still effectively removing the intermediate and low MW species.

Structural characterisation studies of NOM remaining after various treatment stages were conducted. NMR data revealed relatively similar percentages of aliphatic, *O*-aliphatic, aromatic, carboxyl and carbonyl carbon remained in each sample. The aliphatic carbon was the most abundant species in each of the samples confirming HPSEC observations that the material recalcitrant to treatment was more aliphatic than that removed during treatment. Also, oxygenated species accounted for a greater proportion of the remaining NOM than in the Raw Water. FTIR analyses also suggested that the proportion of aromatic carbon was reduced after treatment and that MIEX[®]-C and EC treatment were more effective than MIEX[®] only treatment at removing this carbon type. The remaining NOM, according to FTIR data, appeared to contain a greater proportion of carbonyl functionality. The results from Py-GC-MS were largely consistent with these trends, and additionally suggested that MIEX[®] treatment was more effective in the removal of carbohydrate derived carbon.

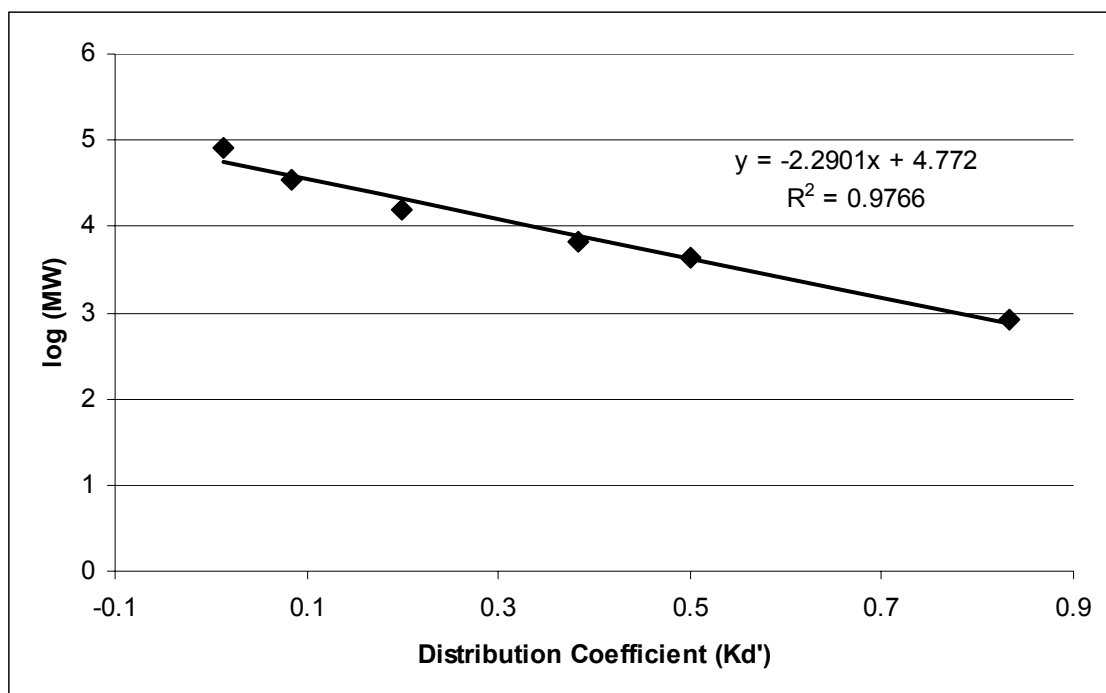
Chlorination studies of fractions isolated by preparative HPSEC indicated that THMs formed from all MW fractions. The largest MW fraction, eluting at the void volume of the column, had the lowest THMFP, possibly due to the presence of inorganic colloids. Fractions 3 and 4, containing the most

aromatic material, produced the highest specific yields of THMs. It was identified that the aromatic nature of these fractions likely meant that THMs were formed from *meta*-dihydroxybenzene moieties, known to produce THMs rapidly and in high concentration upon reaction with chlorine or bromine. However, it was established that this material was the easiest to remove during coagulation treatment and therefore would not significantly contribute to THM formation in distribution systems after coagulation treatment. The lowest MW fractions, Fractions 7 – 9, also produced significant concentrations of THMs, although lower specific yields than Fractions 3 and 4. Significantly, however, the rate of formation from Fractions 7 – 9 was similar to that from the large MW material in Fractions 3 and 4. Structural characterisation studies suggested that the material in Fractions 7 – 9 was more likely to contain low MW aliphatic hydrophilic compounds and possibly methyl ketones, or moieties potentially oxidisable to methyl ketones, a functional group known to result in THM formation, were compounds identified as possible THM precursors in these fractions. The lower MW of material in these fractions was also identified as a contributing factor to the fast kinetics of THMFP as a less complicated reaction pathway would be needed for THM release upon contact with chlorine or bromine. An important issue from this study was the increased bromine incorporation into THMs for the lower MW fractions, as brominated DBPs have been identified as potentially more harmful than chlorinated analogues.

In summary, HPSEC provides an effective tool for determining the MW distribution of aquatic NOM both before and after treatment. Preferential removal of the large MW material was demonstrated after coagulation, while MIEX[®] treatment targeted the intermediate MW fraction. Combining the two treatment options provided removal of NOM across a wide MW range and the combined method was more effective than the enhanced coagulation process. However, the inability of MIEX[®], coagulation or a combination of the two methods to effectively remove the lowest MW fractions of NOM will result in THM formation will be a significant issue for chlorinated water, with a more problematic contribution of brominated THMs in the treated water. Development of improved treatment methods, such as membrane filtration

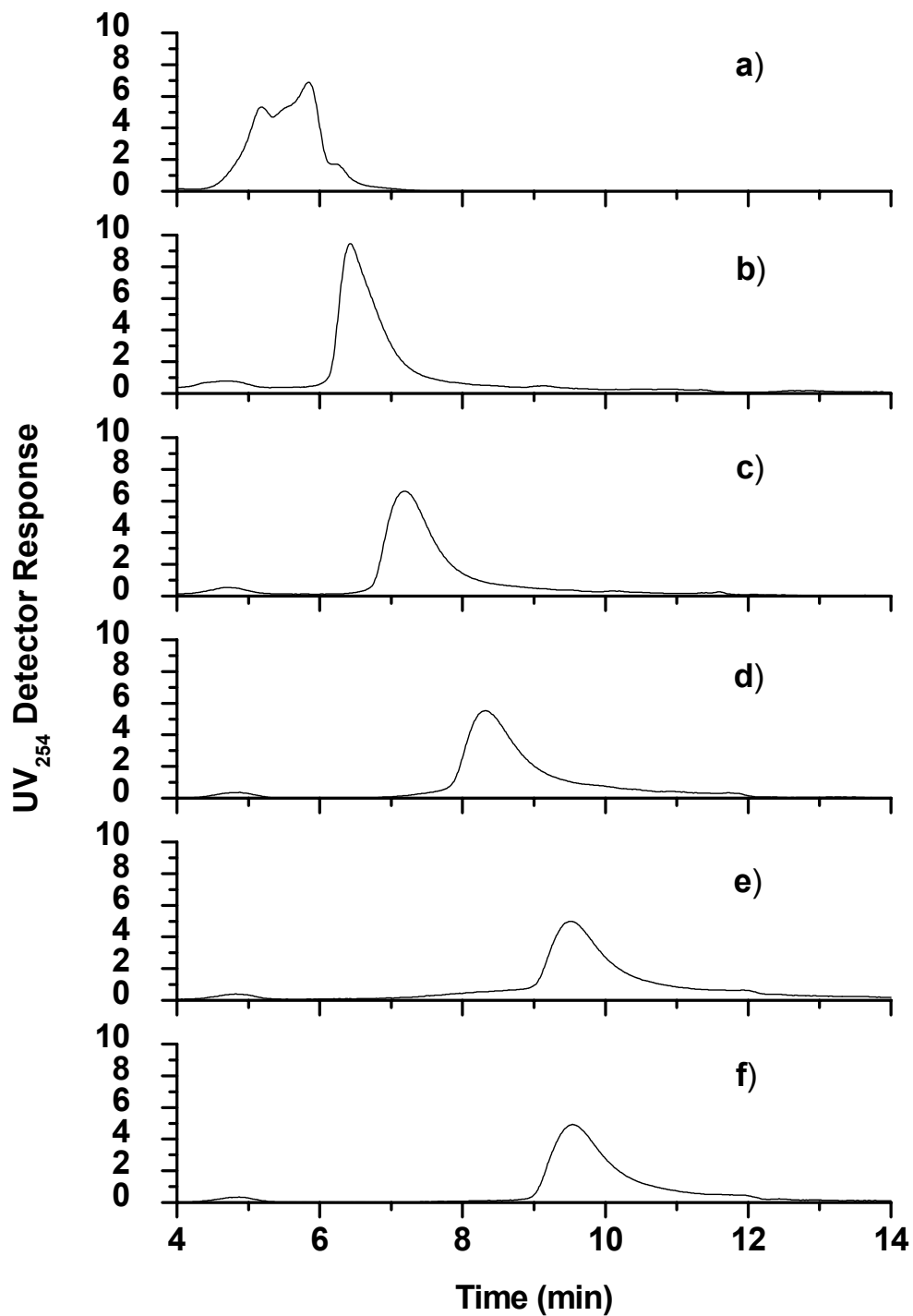
and biological treatment, for removal of these low MW fractions of NOM is vital for control of THM formation.

Appendix 1 Calibration curve and raw data of polystyrene sulphonate (PSS) standards used for calibration of the Tosoh TSK G3000SW_{x1} (7.8 x 300 mm, particle size = 5 μm, pore size = 250 Å) HPSEC column. * acetone and dextran are used in the calculation of Kd'.



Compound	MW (Da)	V _e	Kd'	Log (MW)
Acetone	58.1	13.3	*	-
Dextran	200 000	5.5	*	-
PSS	840	12.0	0.83	2.9
PSS	4 400	9.4	0.50	3.6
PSS	6 530	8.5	0.38	3.8
PSS	15 200	7.1	0.20	4.2
PSS	35 300	6.2	0.08	4.5
PSS	81 800	5.6	0.01	4.9

Appendix 2 HPSEC-UV₂₅₄ chromatograms of PSS with MW = 6 530 Da using the six eluents tested. a) MQ water, b) 10 mmol L⁻¹ sodium acetate, c) 10 mmol L⁻¹ phosphate buffer, d) 20 mmol L⁻¹ phosphate buffer, e) 10 mmol L⁻¹ phosphate buffer + 26 mmol L⁻¹ Na₂SO₄, f) 20 mmol L⁻¹ phosphate buffer + 20 mmol L⁻¹ Na₂SO₄.



Appendix 3 THM concentrations of Fractions 1-9 for each sampling time. Fractions (2mg L^{-1}) were treated with bromine (0.2 mg L^{-1}) and chlorine (8 mg L^{-1} apart from fraction 3, 18 mg L^{-1}). Concentrations shown in both $\mu\text{g/L}$ as well as $\mu\text{mol/L}$ for each individual THM species, as well as TTHM (sum of four THM analogues).

Fraction ; time	CHCl ₃	BrCl ₂ CH	Br ₂ CICH	CHBr ₃	TTHMs	CHCl ₃	BrCl ₂ CH	Br ₂ CICH	CHBr ₃	TTHMs
	$\mu\text{g L}^{-1}$					$\mu\text{mol L}^{-1}$				
1; 0.5hr	2.2	5.9	7.1	4.5	20	0.02	0.04	0.03	0.02	0.11
1; 1hr	2.4	6.8	9.2	6.0	24	0.02	0.04	0.04	0.02	0.13
1; 4hr	3.9	11.7	18.9	12.5	47	0.03	0.07	0.09	0.05	0.24
1; 24hr	6.2	18.1	28.7	18.0	71	0.05	0.11	0.14	0.07	0.37
1, 72hr	9.4	27.9	43.6	25.5	106	0.08	0.17	0.21	0.10	0.56
1; 168hr	15.5	38.2	54.4	28.0	136	0.13	0.23	0.26	0.11	0.73
2; 0.5hr	2.0	4.8	7.5	4.0	18	0.02	0.03	0.04	0.02	0.10
2; 1hr	2.7	7.6	13.4	7.6	31	0.02	0.05	0.06	0.03	0.16
2; 4hr	3.6	12.2	22.4	11.5	50	0.03	0.07	0.11	0.05	0.26
2; 24hr	15.2	30.7	39.4	13.7	99	0.13	0.19	0.19	0.05	0.56
2; 72hr	16.7	43.6	57.6	21.6	140	0.14	0.27	0.28	0.09	0.77
2; 168hr	21.5	49.1	62.8	21.6	155	0.18	0.30	0.30	0.09	0.87
3; 0.5hr	46.9	18.6	6.4	0.3	72	0.39	0.11	0.03	0.00	0.54
3; 1hr	54.9	26.2	7.7	0.4	89	0.46	0.16	0.04	0.00	0.66
3; 4hr	88.1	39.0	10.6	0.4	138	0.74	0.24	0.05	0.00	1.03
3; 24hr	160.2	62.7	14.8	0.6	238	1.34	0.38	0.07	0.00	1.80
3; 72hr	179.0	73.8	19.9	1.1	274	1.50	0.45	0.10	0.00	2.05
3; 168hr	182.6	73.5	16.8	0.6	274	1.53	0.45	0.08	0.00	2.06
4; 0.5hr	24.0	12.1	5.1	0.7	42	0.20	0.07	0.02	0.00	0.30
4; 1hr	28.5	16.7	7.0	0.8	53	0.24	0.10	0.03	0.00	0.38
4; 4hr	39.5	25.4	10.2	1.0	76	0.33	0.16	0.05	0.00	0.54
4; 24hr	86.4	43.6	15.0	1.2	146	0.72	0.27	0.07	0.00	1.07
4; 72hr	116.4	81.0	36.2	3.0	237	0.98	0.49	0.17	0.01	1.66
4; 168hr	159.9	68.3	20.2	1.4	250	1.34	0.42	0.10	0.01	1.86
5; 0.5hrs	7.8	9.0	7.9	2.6	27	0.07	0.05	0.04	0.01	0.17
5; 1hr	9.2	12.5	11.7	3.8	37	0.08	0.08	0.06	0.02	0.22
5; 4hr	15.7	25.9	28.1	9.6	79	0.13	0.16	0.13	0.04	0.46
5; 24hr	23.4	39.2	41.8	14.1	118	0.20	0.24	0.20	0.06	0.69
5; 72hr	64.9	67.1	52.7	13.1	198	0.54	0.41	0.25	0.05	1.26
5; 168hr	61.1	66.2	56.1	15.0	198	0.51	0.40	0.27	0.06	1.24
6; 0.5hrs	8.3	8.8	7.2	2.2	26	0.07	0.05	0.03	0.01	0.17
6; 1hr	9.3	13.2	13.3	4.8	41	0.08	0.08	0.06	0.02	0.24
6; 4hr	16.1	26.8	28.3	9.0	80	0.13	0.16	0.14	0.04	0.47
6; 24hr	27.9	42.5	40.1	10.9	122	0.23	0.26	0.19	0.04	0.73
6; 72hr	50.7	62.4	49.4	11.2	174	0.42	0.38	0.24	0.04	1.09
6; 168hr	50.7	65.3	54.4	13.3	184	0.42	0.40	0.26	0.05	1.14
7; 0.5hrs	10.3	23.9	8.9	2.2	45	0.09	0.15	0.04	0.01	0.28
7; 1hr	10.6	19.9	12.4	3.2	46	0.09	0.12	0.06	0.01	0.28
7; 14hr	19.6	40.3	23.8	5.1	89	0.16	0.25	0.11	0.02	0.54
7; 24hr	34.3	49.3	33.0	6.1	123	0.29	0.30	0.16	0.02	0.77

7; 72hr	61.5	70.0	43.4	7.5	182	0.52	0.43	0.21	0.03	1.18
7; 168hr	66.7	83.3	50.5	8.4	209	0.56	0.51	0.24	0.03	1.34
8; 0.5hrs	8.8	27.5	9.4	2.1	48	0.07	0.17	0.05	0.01	0.29
8; 1hr	10.7	34.6	12.7	2.8	61	0.09	0.21	0.06	0.01	0.37
8; 4hr	13.7	39.0	24.3	5.9	83	0.11	0.24	0.12	0.02	0.49
8; 24hr	22.8	59.5	37.8	9.1	129	0.19	0.36	0.18	0.04	0.77
8; 72hr	38.1	72.7	44.5	8.2	164	0.32	0.44	0.21	0.03	1.01
8; 168hr	60.8	79.4	47.4	7.9	196	0.51	0.48	0.23	0.03	1.25
9; 0.5hrs	8.9	49.1	9.6	2.9	70	0.07	0.30	0.05	0.01	0.43
9; 1hr	10.2	71.0	12.3	4.7	98	0.09	0.43	0.06	0.02	0.60
9; 4hr	14.3	77.4	22.8	9.4	124	0.12	0.47	0.11	0.04	0.74
9; 24hr	20.8	81.2	35.7	13.7	152	0.17	0.50	0.17	0.05	0.90
9; 72hr	38.3	99.9	47.9	14.8	200	0.32	0.61	0.23	0.06	1.22
9; 168hr	41.9	113.6	54.2	18.0	228	0.35	0.69	0.26	0.07	1.38

Appendix 4 THM data from Fractions 1-9 (DOC concentration 2 mg L⁻¹) for each sampling time. Percentage of TTHMs formed in first 30 minutes after chlorine addition (8 mg L⁻¹ apart from Fraction 3 18 mg L⁻¹), percentage of chlorine incorporated into TTHMs formed, percentage of bromine incorporated in TTHMs formed, percentage of chlorine incorporated in TTHMs formed in first 30 minutes after chlorine addition and percentage of bromine incorporated in TTHMs formed in first 30 minutes after chlorine addition (bromine was added at 0.2 mg L⁻¹).

Fraction ;time	% TTHMs formed in first 30 mins	%Cl Incorporation TTHMs	%Br Incorporation TTHMs	%Cl incorporated in TTHMs in first 30 mins	%Br incorporated in TTHMs in first 30 mins
1;0.5hr	14	0.1	6.3	14	14
1;1h r		0.2	8.1		
1; 4hr		0.3	16.0		
1; 24hr		0.5	24.0		
1; 72hr		0.7	35.7		
1; 168hr		1.0	43.5		
2; 0.5hr	11	0.1	5.9	10	13
2; 1hr		0.2	10.6		
2; 4hr		0.3	17.1		
2; 24hr		0.9	29.1		
2; 72hr		1.1	43.0		
2; 168hr		1.3	46.4		
3; 0.5hr	26	0.6	7.2	26	29
3; 1hr		0.7	9.5		
3; 4hr		1.1	13.8		
3; 24hr		1.9	21.3		
3; 72hr		2.2	26.2		
3; 168hr		2.2	24.7		
4; 0.5hr	16	0.7	5.2	16	21
4; 1hr		0.9	7.1		
4; 4hr		1.2	10.6		
4; 24hr		2.5	17.0		
4; 72hr		3.7	35.1		
4; 168hr		4.5	25.1		
5; 0.5hrs	14	0.3	6.4	13	14
5; 1hr		0.4	9.3		
5; 4hr		0.8	21.7		
5; 24hr		1.2	32.3		
5; 72hr		2.5	42.9		
5; 168hr		2.4	44.8		
6; 0.5hrs	15	0.3	6.0	15	14
6; 1hr		0.4	10.6		
6; 4hr		0.8	21.7		
6; 24hr		1.3	31.0		
6; 72hr		2.1	39.5		
6; 168hr		2.1	43.2		

7; 0.5hrs	21	0.5	10.3	20	23
7; 1hr		0.5	11.2		
7; 14hr		1.0	21.4		
7; 24hr		1.5	27.6		
7; 72hr		2.4	37.3		
7; 168hr		2.7	43.7		
8; 0.5hrs	24	0.5	11.3	22	27
8; 1hr		0.7	14.7		
8; 4hr		0.9	21.7		
8; 24hr		1.3	33.3		
8; 72hr		1.9	38.8		
8; 168hr		2.5	41.3		
9; 0.5hrs	31	0.8	17.0	32	30
9; 1hr		1.1	24.3		
9; 4hr		1.3	32.1		
9; 24hr		1.5	40.1		
9; 72hr		2.2	49.8		
9; 168hr		2.5	57.1		

Appendix 5 Peak areas of products obtained from flash pyrolysis-GC-MS analysis of solid aquatic NOM samples from the WGWTP.

Pyrolysis products	Category in Table 6.3	Peak areas			
		Sample Name			
		Raw	MIEX [®]	MIEX [®] -C	EC
acetic acid	carbohydrates	435 746	9 857 407	773 924	6 142 321
acetonitrile	proteins	0	0	4 222 166	2 767 925
aniline	proteins	0	0	228409	0
benzene	BTEX	1 692 971	1 708 688	1 328 679	664 918
benzofuran	carbohydrates	402 945	587 049	0	0
benzofuranone	carbohydrates	493 889	0	0	781 747
bromomethane	halomethane	0	3 032 627	0	2 785 537
butadiene	hydrocarbon	0	647 284	0	0
butanone	carbohydrates	2 705 173	2 142 097	1 648 402	0
butene	hydrocarbon	4215374	5 252 885	1 346 591	743 834
butenenitrile	proteins	0	0	2 007 421	0
butenoic acid	carbohydrates	0	0	0	640 634
butenone	carbohydrates	414 943	0	424525	3 318 739
carbon disulfide	organosulfur	0	433 729	0	0
chloroethane	halomethane	0	0	569 499	0
chloromethane	halomethane	0	1 566 769	1 534 500	1 217 462
cyanobenzene	proteins	0	0	362054	0
cyanopropane	proteins	0	0	256844	0
cyclobutane	alkane/alkene	0	582 804	0	0
cyclopentadiene	carbohydrates	490 473	616 376	488 758	702 807
cyclopropylpentane	hydrocarbon	0	1 638 040	0	0
decene	hydrocarbon	0	1 599 158	0	0
dihydroxy-dimethylbenzaldehyde	carbohydrates	295 555	0	0	0
dimethyl maleic anhydride	carbohydrates	0	0	0	641 136
dimethylbenzofuran	carbohydrates	448 673	632 920	237 307	771 132
dimethylcyclopentadiene	hydrocarbon	0	0	230771	589748
dimethylcyclopentenone	carbohydrates	700 030	1 053 466	532 149	2 277 983
dimethylcyclopropane	hydrocarbon	0	653 099	452 618	1 079 173
dimethylfuran	carbohydrates	688 967	604 444	301 081	770 924
dimethylindazole	proteins	222714	0	0	0
dimethylindene	carbohydrates	0	0	0	608 958
dimethylnapthalene	PAH	0	749 706	292 578	2 502 219
dimethylphenol	phenols	1 751 993	5 770 789	2 180 234	7 017 685
dimethylpyrroledione	proteins	0	0	1572909	0
dimethylthiophene	organosulfur	222 566	0	0	0
ethylbenzene	BTEX	580 369	750 137	550 394	961 714
ethylphenol	BTEX	0	996013	0	0
furan	carbohydrates	276 957	0	398 913	0
furfural	carbohydrates	0	0	796 679	0

heptadecene	alkane/alkene	0	701 618	0	0
heptanol	carbohydrates	0	442 961	0	0
heptene	hydrocarbon	0	751 390	0	0
hexadecene	hydrocarbon	0	561 758		0
hexene	hydrocarbon	0	1 305 934	363 302	0
Indanone	proteins	686 863	0	0	0
indene	proteins	703 612	0	0	0
iodomethane	halomethane	1 124 116	2 298 567	0	1 477 393
Isobenzofurandione	carbohydrates	0	0	262 266	840 737
isobutene	hydrocarbon	501 974	0	0	0
isocyanic acid	proteins	0	2 873 069	2 807 905	3 347 347
isopropylbenzene	BTEX	300 975	426 825	607 751	472 321
methanthiol	organosulfur	671 233	872 814	0	893 515
methyl(methylethyl)benzene	BTEX	0	0	0	509 392
methylbenzofuran	carbohydrates	752 714	811 583	259 170	1 764 112
methylbenzotrile	proteins	0	505 073	411 601	0
methylbutanone	carbohydrates	0	439 652	0	1 342 416
methylbutene	alkane/alkene	404 008	0	0	0
methylcyclohexadiene	carbohydrates	257 225	0	0	0
methylcyclopentadiene	hydrocarbon	856 076	659 864	1 002 602	827 119
methylcyclopentanedione	carbohydrates	0	899 023	0	1 115 957
methylcyclopentenone	carbohydrates	2 605 714	1 743 811	417 174	3 862 011
methylfuran	carbohydrates	422 6121	1 132 308	2 316 730	4 589 296
methylfurandione	carbohydrates	751 177	888 939	0	1 342 628
methylfuranone	carbohydrates	234 592	0	0	953 699
methylfurfural	carbohydrates	0	0	250 301	0
methylheptadecene	hydrocarbon	0	434 478	0	0
methylindanone	carbohydrates	0	0	0	545273
methylindene	carbohydrates	0	798 399	0	1 777 960
methylIsobenzofurandione	carbohydrates	470 571	0	0	748 786
methylmethoxynaphthalene	PAH	0	0	0	1051906
methylnaphthalene	PAH	1 255 648	852 460	718 691	738 367
methylnonadecene	hydrocarbon	0	462 027	0	0
methyloctadecene	hydrocarbon	0	622 477	0	0
methylphenol	phenols	4 895 275	7 975 281	2 372 022	6 989 309
methylpentene	hydrocarbon	0	0	4 779 367	0
methylpiperidonedione	proteins	0	0	1 532 477	0
methylpropene	hydrocarbon	0	0	0	5 027 634
methylpyrazole	proteins	0	963 211	0	0
methylpyridine	proteins	203 951	419 953	755 302	0
methylpyrrole	proteins	0	0	392 321	504 956
methylpyrrolidinedione	proteins	0	0	291 817	642 494
methylthiophene	organosulfur	976 570	1 271 064		
m-xylene	BTEX	643 086	1 022 440	593 844	12 21 851
naphthalenol	phenols	0	0	0	502 880
naphthol	phenols	322 669	490 022	0	0
naphthalene	PAH	851 390	823 816	450 004	0

nitroethane	proteins	0	2 632 646	0	0
nonadecene	hydrocarbon	0	634 788	0	0
nonene	hydrocarbon	0	527 547	0	0
octadecene	alkane/alkene	0	625 612	0	0
o-xylene	BTEX	986 444	1 561 957	706561	1 541 576
pentadiene	hydrocarbon	401 276	709 908	596 445	796 071
pentanone	carbohydrates	241 013	0	0	0
phenol	phenols	3 515 838	4 804 370	897 327	2 437 306
piperidinedione	proteins	0	0	3 629 358	627 825
propanone	carbohydrates	5 075 950	4 086 109	173 4497	410 1230
propenenitrile	proteins	0	0	1 222 364	
propanoic acid	carbohydrates	488 455	422 555	401 385	476 547
p-xylene	BTEX	1 493 875	2 294 551	1 186 593	2 276 743
pyridine	proteins	309 442	426 747	693 773	0
pyrrole	proteins	0	472 681	424 159	0
pyrrolidinedione	proteins	0	0	566 300	0
styrene	carbohydrates	0	0	686 464	0
tetradecane	hydrocarbon	0	906 101	0	0
thiophene	Organosulfur	574 138	0	0	0
toluene	BTEX	3 612 582	4 652 951	2 992 502	3 215 319
trimethylbenzene	BTEX	1 567 793	3 177 859	1 652 618	4 585 481
trimethylfuran	carbohydrates	180 814	419 515	0	0
trimethylnaphthalene	PAH	0	0	0	2 928 635
trimethylphenol	phenols	0	0	351 340	2 199 109
urea	proteins	548 778	0	0	0

Note:

- 0 = not detected
- BTEX = benzene, toluene and xylenes
- PAH = polyaromatic hydrocarbons
- Individual isomers were combined to give one value, e.g. all methylphenol isomers were combined and listed as methylphenol

Appendix 6 Total of all peak areas in each category as used to construct pie chart in Figure 7.5

	RW	MIEX[®]	MIEX[®]-C	EC
Total of all peaks	66623 666	120 240 053	8 1974 362	124 197 224
BTEX	10 659 787	16 833 607	9 836 923	14 903 667
carbohydrates	23 984 520	27 655 212	11 476 411	42 227 056
proteins	2 664 947	8 416 804	19 673 847	7 451 833
phenols	10 659 787	19 238 408	5 738 205	19 871 556
PAH	1 332 473	2 404 801	1 639 487	6 209 861
organosulfur	2 664 947	2 404 801	0	1 241 972
hydrocarbons	5 329 893	19 238 408	20 493 591	9 935 778
halomethanes	1 332 473	7 214 403	2 459 231	4 967 889
unidentified	7 994 840	16 833 607	10 656 667	17 387 611

- Abbt-Braun, G. and Frimmel, F.H. (1999) Basic characterisation of Norwegian NOM samples - Similarities and differences. *Environment International*, **25**, 161-180.
- Abbt-Braun, G., Lankes, U. and Frimmel, F.H. (2004) Structural characterisation of aquatic humic substances – The need for a multiple method approach. *Aquatic Sciences – Research Across Boundaries*, **66**, 151-170.
- Adams, M.J. (1995) Chemometrics in analytical spectroscopy, The Royal Society of Chemistry, Cambridge, United Kingdom.
- Aiken, G.R., McKnight, D.M., Wershaw, R.L. and MacCarthy, P. (1985) Humic substances in soil, sediment, and water, John Wiley, New York.
- Alamany, L.B., Grant, D.M., Pugmire, R.J., Alger, T.D. and Zilm, K.W. (1983) Cross polarisation and magic angle spinning NMR spectra of model organic compounds. 2. Molecules of low or remote protonation. *Journal of the American Chemical Society*, **105**, 2142-2147.
- Alessandrino, M., Garbin, S. and Pringle, P. (2006) Leaching of DOC from membrane filters, unpublished results, Curtin University of Technology.
- Allpike, B.P., Heitz, A., Joll, C.A., Kagi, R.I., Abbt-Braun, G., Frimmel, F.H., Brinkmann, T., Her, N. and Amy, G. (2005) Size exclusion chromatography to characterise DOC removal in drinking water treatment. *Environmental Science and Technology*, **39**, 2334-2342.
- Amy, G.L., Tan, L. and Davis M.K. (1991) The effects of ozonation and activated carbon adsorption on trihalomethane speciation. *Water Research*, **25**, 191-202.

Amy, G. (1993) Using NOM characterisation for the evaluation of treatment, in *Proceedings of Workshop on NOM in Drinking Water: Origin, Characterisation and Removal Conference*, Chamonix, France, September 19-22.

Amy, G. and Cho, J. (1999) Interactions between natural organic matter (NOM) and membranes: Rejection and fouling. *Water Science and Technology*, **40**, 131-139.

Amy, G., Collins, M.R., Kuo, C.J. and King, P.H. (1992) Molecular size distribution of dissolved organic matter. *Journal of the American Water Works Association*, **84**, 67-75.

Amy, G.L., Chadik, P.A., Chowdhury, Z.K., King, P.H. and Cooper, W.J. (1985) Water chlorination: chemistry, Environmental impact and health effects, pp. 907-922, Lewis Publishers, Chelsea, Michigan.

Amy, G.L., Tan, L. and Davis, M.K. (1991) The effects of ozonation and activated carbon adsorption on trihalomethane speciation. *Water Research*, **25**, 191-202.

Anipsitakis, G.P. and Dionysiou, D.D. (2004) Transition metal/UV-based advanced oxidation technologies for water decontamination. *Applied Catalysis B: Environmental*, **54**, 155-163.

Aoustin, E., Schafer, A.I., Fane, A.G. and Waite, D.T. (2001) Ultrafiltration of natural organic matter. *Separation and Purification Technology*, **22-23**, 63-78.

Backlund, P. (1992) Degradation of aquatic humic material by ultraviolet light. *Chemosphere*, **25**, 1869-1878.

Barlow, A., Wild, L. and Roberts, T. (1971) Structural evaluation of copolymers using preparative gel permeation chromatography. *Journal of Chromatography A*, **55**, 155-164.

Barth, H.G. (1980) A practical approach to steric exclusion chromatography of water-soluble polymers. *Journal of Chromatographic Science*, **30**, 135-143.

Becher, G., Carlberg, G.E., Gjessing, E.T., Hongslo, J.K. and Monarca, S. (1985) High-performance size exclusion chromatography of chlorinated natural humic water and mutagenicity studies using the microscale fluctuation assay. *Environmental Science and Technology*, **19**, 422-426.

Beckett, R., Jue, Z. and Giddings, C. (1987) Determination of molecular weight distributions of fulvic and humic acids using flow field-flow fractionation. *Environmental Science and Technology*, **21**, 289-295.

Bellar, T.A., Lichtenberg, J.J. and Kroner, R.C. (1974) Occurrence of organohalides in chlorinated drinking water. *Journal of the American Water Works Association*, **66**, 703-706.

Berdén, M. and Berggren, D. (1990) Gel filtration of humic substances in soil solutions using HPLC-determinations of the molecular weight distribution. *Journal of Soil Science*, **41**, 61-72.

Bianchi, T.S., Filley, T., Dria, K. and Hatcher, P.G. (2004) Temporal variability in sources of dissolved organic carbon in the lower Mississippi river. *Geochimica et Cosmochimica Acta*, **68**, 959-967.

Bloom, P.R. and Leenheer, J.A. (1989) Humic Substances II. In search of structure. Hayes, M.H.B., MacCarthy, P., Malcolm, R.L. and Swift, R.S. (eds), John Wiley and Sons, Chichester.

Bolton, J.R. (ed) (2001) Ultraviolet applications handbook, Bolton Photoscience Inc., Edmonton, Canada.

Bourke, M., Harrison, S., Long, B. and Lebeau, T. (2001) MIEX[®] resin pretreatment followed by microfiltration as an alternative to nanofiltration for

DBP precursor removal, *in Proceedings of AWWA Membrane Technology Conference*.

Bourke, M., Slunjski, M., O'Leary, B. and Smith, P. (1999) Scale-up of the MIEX[®] DOC process for full scale water treatment plants, *in Proceedings of 18th Federal Convention, Australia Water and Wastewater Association*, Adelaide Australia, on CD

Boyce, S.D. and Hornig, J.F. (1983) Reaction pathways of trihalomethane formation from the halogenation of dihydroxyaromatic model compounds for humic acid. *Environmental Science and Technology*, **17**, 202-211.

Boyer, T.H. and Singer, P.C. (2005) Bench-scale testing of a magnetic ion exchange resin for removal of disinfection by-product precursors. *Water Research*, **39**, 1265-1276.

Bracewell, J.M., Haider, K., Larter, S.R. and Schulten, H.-R. (1989) Humic substances II. In search of structure. Hayes, M.H.B., MacCarthy, P., Malcolm, R.L. and Swift, R.S. (eds), John Wiley and Sons, Chichester.

Bruchet, A., Rousseau, C. and Mallevalle, J. (1990) Pyrolysis-GC-MS for investigating high-molecular weight THM precursors and other refractory organics. *Journal of the American Water Works Association*, **82**, 66-74.

Buchanan, W., Roddick, F.A., Porter, N. and Drikas, M. (2005) Fractionation of UV and VUV pretreated natural organic matter from drinking water. *Environmental Science and Technology*, **39**, 4647-4654.

Buesseler, K.O., Bauer, J.E., Chen, R.F., Eglinton, T.I., Gustafsson, O., Landing, W., Mopper, K., Moran, S.B., Santschi, P.H., Vernon-Clark, R. and Wells, M.L. (1996) An intercomparison of cross-flow filtration techniques used for sampling marine colloids: Overview and organic carbon results. *Marine Chemistry*, **55**, 1-31.

Buffle, J., Deladoey, P. and Haerdi, W. (1978) The use of ultrafiltration for the separation and fractionation of organic ligands in fresh waters. *Analytica Chimica Acta*, **101**, 339-357.

Bull, R.J., Krasner, S.W., Daniel, P.A. and Bull, R.D. (2001) Health effects of disinfectants and disinfection by-products, Project #501, American Water Works Association Research Foundation, Denver..

Bull, R.J., Reckhow, D.A., Rotello, V., Bull, O.M. and Kim, J. (2006) Use of toxicological and chemical models to prioritize DBP research, Project #2867, American Water Works Association Research Foundation, Denver.

Bursill, D., Hine, P.T. and Morran, J.Y. (1985) The effect of natural organics on water treatment processes, in *Proceedings of Australian Water and Wastewater 11th Federal Convention*, pp. 197-204.

Cabaniss, S.E. and Shuman, M.S. (1988) Copper binding by dissolved organic matter: I. Suwannee River fulvic acid equilibria. *Geochimica et Cosmochimica Acta*, **52**, 185-193.

Cabaniss, S.E., Zhou, Q., Maurice, P.A., Chin, Y. and Aiken, G. (2000) A log-normal distribution model for the molecular weight of aquatic fulvic acids. *Environmental Science and Technology*, **34**, 1103-1109.

Cadee, K., O'Leary, B., Smith, P., Slunjski, M. and Bourke, M. (2000) World's first magnetic ion exchange (MIEX[®]) water treatment plant to be installed in Western Australia, in *Proceedings of American Water Works Association Conference*, Denver, USA, on CD.

Casassa, E. (1967) Equilibrium distribution of flexible polymer chains between a macroscopic solution phase and small voids. *Journal of Polymer Science Part B: Polymer Letters*, **5**, 773-778.

Casassa, E. (1971) Theoretical models for peak migration in gel permeation chromatography. *Journal of Physical Chemistry*, **75**, 3929-3939.

- Ceccanti, B., Calcinai, M., Bonmati-Pont, M., Ciardi, C. and Tarsitano, R. (1989) Molecular size distribution of soil humic substances with ionic strength. *The Science of the Total Environment*, **81-82**, 471-479.
- Chang, T.-L. (1968) On the separation mechanism of gel permeation chromatography. *Analytica Chimica Acta*, **42**, 51-57.
- Chang, Y. and Benjamin, M.M. (1996) Iron oxide adsorption and UF to remove NOM and control fouling. *Journal of the American Water Works Association*, **88**, 74-88.
- Chang, Y., Choo, K.H., Benjamin, M.M. and Reiber, S. (1998) Combined adsorption-UF process increases TOC removal. *Journal of the American Water Works Association*, **90**, 90-102.
- Chen, Y., Senesi, N. and Schnitzer, M. (1977) Information provided on humic substances by E_4/E_6 ratios. *Soil Science Society of America Journal*, **41**, 352-358.
- Cheng, W. (1986) Surface exclusion and geometrical exclusion. *Journal of Chromatography*, **362**, 309-324.
- Cheng, W. and Hollis, D. (1987) Flow-rate effect on elution volume in size-exclusion chromatography. *Journal of Chromatography A*, **408**, 9-19.
- Chin, Y., Aiken, G. and O'Loughlin, E. (1994) Molecular weight, polydispersity, and spectroscopic properties of aquatic humic substances. *Environmental Science and Technology*, **28**, 1853-1858.
- Chin, Y. and Gschwend, P.M. (1991) The abundance, distribution, and configuration of porewater organic colloids in recent sediments. *Geochimica Cosmochimica Acta*, **55**, 1309-1317.

Cho, J., Amy, G. and Pellegrino, J. (1999) Membrane filtration of natural organic matter: initial comparison of rejection and flux decline characteristics with ultrafiltration and nanofiltration membranes. *Water Research*, **33**, 2517-2526.

Chow, A.T., Gao, S. and Dahlgren, R.A. (2005) Physical and chemical fractionation of dissolved organic matter and trihalomethane precursors: A review. *Journal of Water Supply Research and Technology-Aqua*, **54**, 475-507.

Chow, C. (2005) Personal Communication, Leaching of organic contaminants from analytical silica base stationary phases 15-6-2004

Chow, C., Cook, D. and Drikas, M. (2001) Laboratory study of conventional alum treatment versus MIEX[®] treatment for removal of natural organic matter, in *Proceedings of 19th Federal AWA Convention, Canberra, on CD*.

Chow, C., van Leeuwen, J.A., Drikas, M., Fabris, R., Spark, K.M. and Page, D.W. (1999) The impact of the character of natural organic matter in conventional treatment with alum. *Water Science and Technology*, **40**, 97-104.

Christman, R.F., Norwood, D.L., Seo, Y. and Frimmel, F.H. (1989) Humic substances II: In search of structure. Hayes, M.H.B., MacCarthy, P., Malcolm, R.L. and Swift, R.S. (eds), John Wiley and Sons, New York.

Clesceri, L.S., Greener, A.E. and Eaton, A.D. (eds) (1998) Standard methods for the examination of water and wastewater, American Public Health Association, Washington D.C.

Collins, M.R., Amy, G. and King, P.H. (1985) Removal of organic matter in water treatment. *Journal of Environmental Engineering*, **19**, 422-426.

Collins, M.R., Amy, G.L. and Steelink, C. (1986) Molecular weight distribution, carboxylic acidity, and humic substances content of aquatic

organic matter: Implications for removal during water treatment.

Environmental Science and Technology, **20**, 1028-1032.

Conte, P. and Piccolo, A. (1999) High pressure size exclusion chromatography (HPSEC) of humic substances: Molecular sizes, analytical parameters, and column performance. *Chemosphere*, **38**, 517-528.

Cooper, A.R., Johnson, J.F. and Bruzzone, A.R. (1973) Gel permeation chromatography-I. The effect of flow rate and molecular weight on separation efficiency. *European Polymer Journal*, **9**, 1381-1391.

Cooper, W.J., Meyer, L.M., Bofill, C.C. and Cordal, E. (1983) Water chlorination: Environmental impact and health effects. Jolley, R.L., Brungs, W.A., Cotruvo, J.A., Cumming, R.B., Mattice, J.S. and Jacobs, V.A. (eds), pp. 285-296, Ann Arbor Science, Michigan.

Cornel, P.K., Summers, R.S. and Roberts, P.V. (1986) Diffusion of humic acid in dilute aqueous solution. *Journal of Colloid and Interface Science*, **110**, 149-164.

Croué, J.P. (2004) Isolation and humic and non-humic NOM fractions: Structural characterisation. *Environmental Monitoring and Assessment*, **92**, 193-207.

Croué, J.P., Debroux, J., Aiken, G., Leenheer, J.A. and Amy, G. (1999) Natural organic matter: Structural characteristics and reactive properties in formation and control of disinfection by-products in drinking water. Singer, P.C. (ed), American Water Works Association, Denver.

Croué, J.P., Korshin, G.V. and Benjamin, M. (2000) Characterisation of natural organic matter in drinking water, American Water Works Association Research Foundation, Denver.

Croué, J.P., Martin, B., Simon, P. and Legube, B. (1993) Les matières hydrophobes et hydrophiles des eaux de retenues: Extraction, caractérisation et quantification. *Water Supply*, **11**, 51-62.

Davidson, W.A. (1995) Hydrogeology and groundwater resources of the Perth region, Western Australia, Geological Survey of Western Australia, Perth, Australia, Bulletin 142.

Davis, J.A. and Gloor, R. (1981) Adsorption of dissolved organics in lake water by aluminium oxide. Effect of Molecular Weight. *Environmental Science and Technology*, **15**, 1223-1229.

Dawkins, J.V. (1976) Thermodynamic interpretation of polystyrene retention on crosslinked polystyrene gels in GPC with poor and theta solvents. *Journal of Polymer Science: Polymer Physics Edition*, **14**, 569-571.

DeHaan, H., Jones, R.I. and Salonen, K. (1987) Does ionic strength affect the configuration of aquatic humic substances, as indicated by gel filtration? *Freshwater Biology*, **17**, 453-459.

Department of Water (2007) Department of Water home page. Retrieved 10/08/2007 from <http://portal.water.wa.gov.au/portal/page/portal/home>

DiGiano, F.A., Brahhetta, B., Utne, B. and Nilson, J. (1993) Nanofiltration fouling by natural organic matter and the role of particles in flux enhancement, in *Proceedings of AWWA Membrane Technology Conference*, Baltimore, 273-291.

DiMarzio, E.A. and Guttman, C.M. (1969) Separation by flow. *Journal of Polymer Science Part B: Polymer Letters*, **7**, 267-272.

Department of Water (2007) Department of Water home page. Retrieved 10/08/2007 from <http://portal.water.wa.gov.au/portal/page/portal/home>

Dogliotti, L. and Hayon, E. (1967) Flash photolysis of persulfate ions in aqueous solutions; Study of the sulfate and ozonide radical anions. *Journal of Physical Chemistry*, **71**, 2511-2516.

Drikas, M., Chow, C. and Cook, D. (2003) The impact of recalcitrant organic character on disinfection stability, trihalomethane formation and bacterial regrowth: An evaluation of magnetic ion exchange (MIEX[®]) and alum coagulation. *Journal of Water Supply: Research and Technology-AQUA*, **52**, 475-487.

Dzombak, D.A. and Morel, F.M.M. (1990) Surface complexation modelling. hydrous ferric oxide, John Wiley and Sons, New York.

Echigo, S. and Minear, R.A. (2006) Kinetics of the reaction of hypobromous acid and organic matters in water treatment processes. *Water Science and Technology*, **53**, 235-243.

Edzwald, J.K. and Tobiason, J.E. (1999) Enhanced coagulation: US requirements and a broader view. *Water Science and Technology*, **40**, 63-70.

Engelhardt, H. and Mathes, D. (1977) Chemically bonded stationary phases for aqueous high-performance exclusion chromatography. *Journal of Chromatographic Science*, **142**, 311-320.

Ernst, R.R. and Anderson, W.A. (1966) Application of Fourier transform spectroscopy to magnetic resonance. *Review of Scientific Instruments*, **37**, 93-102.

Escobar, I.C. and Randall, A.A. (2001) Assimilable organic carbon (AOC) and biodegradable dissolved organic carbon (BDOC): complementary measurements. *Water Research*, **35**, 4444-4454.

Fabris, R., Lee, E.K., Chow, C.W.K., Chen, V. and Drikas, M. (2007) Pre-treatments to reduce fouling of low pressure micro-filtration (MF) membranes. *Journal of membrane Science*, **289**, 231-240.

Fearing, D.A., Banks, J., Guyetand, S., Monfort Eroles, C., Jefferson, B., Wilson, D., Hillis, P., Campbell, A.T. and Parsons, S.A.S.A. (2004) Combination of ferric and MIEX[®] for the treatment of a humic rich water. *Water Research*, **38**, 2551-2558.

Figini, R.V. and Marx-Figini, M. (1981) On the molecular weight determination by vapour pressure osmometry, relationship between diffusion coefficient of the solute and non-colligative behaviour. *Makromolekulare Chemie*, **182**, 437-443.

Franzmann, P.D., Heitz, A., Zappia, L.R., Wajon, J.E. and Xanthis, K. (2001) The formation of malodorous oligosulphides in treated groundwater. The role of biofilms and potential precursors. *Water Research*, **35**, 1730-1738.

Frimmel, F.H. (1994) Photochemical aspects related to humic substances. *Environment International*, **20**, 373-385.

Frimmel, F.H. (1998) Impact of light on the properties of aquatic natural organic matter. *Environment International*, **24**, 559-571.

Gadel, F. and Bruchet, A. (1987) Application of pyrolysis-GC-MS to the characterisation of humic substances resulting from decay of aquatic plants in sediments and waters. *Water Research*, **21**, 1195-1206.

Gaffney, J.S., Marley, N.A. and Clark, S.B. (1996) Humic and fulvic acids: Isolation, structure and environmental role. Gaffney, J.S., Marley, N.A. and Clark, S.B. (eds), pp. 2-15, American Chemical Society, Washington, D.C.

Gallard, H. and von Gunten, U. (2002a) Chlorination of natural organic matter: Kinetics of chlorination and of THM formation. *Water Research*, **36**, 65-74.

Gallard, H. and von Gunten, U. (2002b) Chlorination of phenols: Kinetics and formation of chloroform. *Environmental Science and Technology*, **36**, 884-890.

Gang, D., Clevenger, T.E. and Banerji, S.K. (2003) Relationship of chlorine decay and THMs formation to size. *Journal of Hazardous Materials*, **96**, 1-12.

Gao, H. and Zepp, R.G. (1998) Factors influencing photoreactions of dissolved organic matter in a coastal river of the south eastern United States. *Environmental Science and Technology*, **32**, 2940-2946.

Garcette-Lepecq, A., Derenne, S., Largeau, C., Bouloubassi, I. and Saliot, A. (2000) Origin and formation pathways of kerogen-like organic matter in recent sediments off the Danube Delta (Northwestern Black Sea). *Organic Geochemistry*, **31**, 1663-1683.

Gelotte, B. (1960) Studies on gel filtration: Sorption properties of the bed material Sephadex. *Journal of Chromatography*, **3**, 330-342.

Ghassemi, M. and Christman, R.F. (1968) Properties of yellow organic acids of natural waters. *Limnology and Oceanography*, **13**, 583-597.

Giddings, J.C., Kucera, E., Russel, C.P. and Myres, M.N. (1968) Statistical theory for the equilibrium distribution of rigid molecules in inert porous networks. exclusion chromatography. *Journal of Physical Chemistry*, **79**, 4397-4408.

Giddings, J.C., Williams, S.P. and Beckett, R. (1987) Fractionating power in programmed field-flow fractionation: Exponential sedimentation field decay. *Analytical Chemistry*, **59**, 28-37.

Gjessing, E.T. (1965) Use of Sephadex gel for the estimation of MW of humic substances in natural waters. *Nature*, **208**, 1091-1092.

Gjessing, E.T. and Lee, G.F. (1967) Fractionation of organic matter in natural waters on Sephadex columns. *Environmental Science and Technology*, **1**, 631-638.

Gobé, V., Lemée, L. and Amblè, A. (2000) Structure elucidation of soil macromolecular lipids by preparative pyrolysis and thermochemolysis. *Organic Geochemistry*, **31**, 409-419.

Gonzalez, J.A., Gonzalez-Vila, F.J., Almendros, G., Zancada, M.C., Polvillo, O. and Martin, F. (2003) Preferential accumulation of selectively preserved biomacromolecules in the humus fractions from a peat deposit as seen by analytical pyrolysis and spectroscopic techniques. *Journal of Analytical and Applied Pyrolysis*, **68-69**, 287-298.

Gonzalez-Vila, F.J., Lentz, H. and Ludemann, H.-D. (1976) FT-13C Nuclear magnetic resonance spectra of natural humic substances. *Biochemical and Biophysical Research Communications*, **72**, 1063-1070.

Gosh, R. and Schnitzer, M. (1980) Macromolecular structure of humic substances. *Soil Science*, **129**, 266-276.

Gould, J.P., Fitchhorn, L.E. and Urheim, E. (1981) Water chlorination: Environmental impacts and health effects. Jolley, R.L. (ed), pp. 297-310, Ann Arbor Science, Missouri.

Hager, D. (1980) Theoretical considerations of molecular sieve effects. *Journal of Chromatography*, **187**, 285-295.

Hashimoto, T., Sasaki, H., Aiura, M. and Kato, Y. (1978) High-speed gel-permeation chromatography of proteins. *Journal of Chromatography*, **160**, 301-305.

Hatcher, P.G., Breger, I.A. and Mattingly, M.A. (1980) Structural characteristics of fulvic acids from continental shelf sediments. *Nature*, **185**, 560-562.

Hatcher, P.G. and Clifford, D.J. (1994) Flash pyrolysis and in-situ methylation of humic acids from soil. *Organic Geochemistry*, **21**, 1081-1092.

Hatcher, P.G., Dria, K.J., Kim, S. and Frazier, S.W. (2001) Modern analytical studies of humic substances. *Soil Science*, **166**, 770-794.

Hatcher, P.G., Schnitzer, M. and Dennis, L.W. (1981) Aromaticity of humic substances in soils. *Soil Science Society of America Journal*, **45**, 1089-1094.

Health Canada. (2006) Environmental and workplace health; water quality, Retrieved 10/7/2007 from <http://www.healthcanada.gc.ca/waterquality>

Heitz, A. (2002) Malodorous dimethylpolysulfides in Perth drinking water. Ph.D. Dissertation, Curtin University of Technology, Perth, Western Australia.

Heitz, A., Blythe, J., Allpike, B.P., Joll, C.A. and Kagi, R.I. (2002) Plastic tastes in drinking water: Factors affecting the chemistry of bromophenol formation. *Water Science and Technology*, **2**, 179-184.

Heitz, A., Kagi, R.I. and Alexander, R. (2000) Polysulfide sulfur in pipewall biofilms: Its role in the formation of swampy odour in distribution systems. *Water Science and Technology*, **41**, 271-278.

Heller-Grossman, L., Manka, J., Limoni-Relis, B. and Rebhun, M. (1993) Formation and distribution of haloacetic acids, THM and TOX in chlorination of bromide-rich lake water. *Water Research*, **27**, 1323-1331.

Hem, L. and Efraimsson, H. (2001) Assimilable carbon in molecular weight fraction of natural organic matter. *Water Research*, **35**, 1106-1110.

Her, N., Amy, G., Foss, D. and Cho, J. (2002a) Variations of molecular weight estimation by HP-size exclusion chromatography with UVA versus online DOC detection. *Environmental Science and Technology*, **36**, 3393-3399.

Her, N., Amy, G., Foss, D., Cho, J., Yoon, Y. and Kosenka, P. (2002b) Optimization of method for detecting and characterizing NOM by HPLC-size exclusion chromatography with UV and on-line DOC detection. *Environmental Science and Technology*, **36**, 1069-1076.

Her, N., Amy, G., McKnight, D., Sohn, J. and Yoon, Y. (2003) Characterisation of DOM as a function of MW by fluorescence EEM and HPLC-SEC using UVA, DOC and Fluorescence detection. *Water Research*, **37**, 4295-4303.

Heumann, K.G. (2003) Personal Communication, Institute of Inorganic and Analytical Chemistry, Johannes Gutenberg University, 14th October.

Hine, P.T. and Bursill, D. (1987) Seasonal trends of natural organics in S.A. waters and their effects on water treatment, AWRC Research Report, 84/167.

Hirschberg, K.-J.B. (1989) Groundwater contamination in the perth metropolitan region., in *Proceedings of Swan Coastal Plain Management Conference*, ed. Lowe, G., Western Australian Water Research Council, Perth, pp. 121-134.

Hongve, D., Baann, J., Becher, G. and Lomo, S. (1996) Characterization of humic substances by means of high-performance size exclusion chromatography. *Environment International*, **22**, 489-494.

Huber, S.A. and Frimmel, F.H. (1991) Flow injection analysis of organic and inorganic carbon in the low-ppb range. *Analytical Chemistry*, **63**, 2122-2130.

Huber, S.A. and Frimmel, F.H. (1994) Direct gel chromatographic characterization and quantification of marine dissolved organic carbon using high-sensitivity DOC detection. *Environmental Science and Technology*, **28**, 1194-1197.

Huber, S.A. and Frimmel, F.H. (1996) Gelchromatographie mit kohlenstoffdetektion (LC-OCD): Ein rasches und aussagekräftiges verfahren zur charakterisierung hydrophiler organischer wasserinhaltsstoffe. *Vom Wasser*, **86**, 277-290.

Humbert, H., Gallard, H., Jacquemet, V. and Croué, J.-P. (2007) Combination of coagulation and ion exchange for the reduction of UF fouling properties of a high DOC content surface water. *Water Research*, **41**, 3803-3811.

Hunt, A.P., Parry, J.D. and Hamilton-Taylor, J. (2000) Further evidence of elemental composition as an indicator of the bioavailability of humic substances to bacteria. *Limnology and Oceanography*, **45**, 237-241.

Ichihashi, K., Teranishi, K. and Ichimura, A. (1999a) Brominated-trihalomethane formation from phenolic derivatives as a model of humic materials by the reaction with hypochlorite and hypobromite ions. *Chemistry Letters*, **33**, 957-958.

Ichihashi, K., Teranishi, K. and Ichimura, A. (1999b) Brominated trihalomethane formation in halogenation of humic acid in the coexistence of hypochlorite and hypobromite ions. *Water Research*, **33**, 477-483.

Ishiwatari, R., Hamana, H. and Machihara, T. (1980) Isolation and characterisation of polymeric organic materials in a polluted river water. *Water Research*, **14**, 1257-1262.

Jolley, R.L. and Carpenter, J.H. (1981) A review of the chemistry and environmental fate of reactive oxidant species in chlorinated water, *in Proceedings of Water Chlorination: Environmental Impact and Health Effects*, eds. Jolley, R.L., Brungs, W.A., Cotruvo, J.A., Cumming, R.B., Mattice, J.S. and Jacobs, V.A., Ann Arbor Science, Pacific Grove, California.

Joret, J.C. and Levy, Y. (1986) Méthode d'évaluation du carboné éliminable des eaux par voie biologique. *Tribune Cebedeau*, **510**, 3-9.

Joyce, W.S., Digiano, F.A. and Uden, P.C. (1984) THM precursors in the environment. *Journal of the American Water Works Association*, **76**, 102-106.

Kay-Shoemake, J.L., Watwood, M.E., Lentz, R.D. and Sojka, R.E. (1998) Polyacrylamide as an organic nitrogen source for soil microorganisms with potential effects on inorganic soil nitrogen in agricultural soil, *Soil Biology and Biochemistry*, **30**, 1045-1052.

Kazpard, V., Lartiges, B.S., Frochot, C., d'Espinose de la Caillerie, J.B., Viriot, M.L., portal, J.M., Gorner, T. and Bersillon, J.L. (2006) Fate of coagulant species and conformational effects during the aggregation of a model of a humic substance with Al¹³ polycations, *Water Research*, **40**, 1965-1974,

Keeler, C., Kelly, E.F. and Maciel, G.E. (2006) Chemical-structural information from solid-state ¹³C NMR studies of a suite of humic materials from a lower montane forest soil, Colorado, USA. *Geoderma*, **130**, 124-140.

Kemp, A.L.W. and Wong, H.K.T. (1974) Molecular-weight distribution of humic substances from lakes Ontario and Erie sediments. *Chemical Geology*, **14**, 15-22.

Kitis, M., Karanfil, T., Wigton, A. and Kilduff, J.E. (2002) Probing reactivity of dissolved organic matter for disinfection by-product formation using XAD-8 resin adsorption and ultrafiltration fractionation. *Water Research*, **36**, 3834-3848.

Knicker, H. and Nanny, M.A. (1997) Nuclear magnetic resonance spectroscopy in environmental chemistry. Nanny, M.A., Minear, R. and Leenheer, J.A. (eds), Oxford University Press, Oxford.

Kolthoff, I.M. and Miller, I.K. (1951) The Chemistry of Persulfate. I. The kinetics and mechanism of the decomposition of the persulfate ion in aqueous medium. *Journal of the American Chemical Society*, **73**, 3055-3059.

Kopaciewicz, W. and Regnier, F.E. (1982) Nonideal size-exclusion chromatography of proteins: Effects of pH at low ionic strength. *Analytical Biochemistry*, **126**, 8-16.

Korshin, G.V., Benjamin, M.M. and Sletten, R.S. (1997a) Adsorption of Natural Organic Matter (NOM) on Iron Oxides. Effects on NOM composition and formation of organo-halide compounds during chlorination. *Water Research*, **31**, 1643-1650.

Korshin, G.V., Li, C.W. and Benjamin, M.M. (1997b) Monitoring the properties of natural organic matter through UV spectroscopy: A consistent theory. *Water Research*, **31**, 1787-1795.

Korshin, G.V., Li, C.W. and Benjamin, M.M. (1996) Water disinfection and natural organic matter. Minear, R. and Amy, G. (eds), American Chemical Society, Washington DC.

Krasner, S.W., Croue, J.P., Buffle, J. and Perdue, E.M. (1996a) Three approaches for characterising NOM. *Journal of the American Water Works Association*, **88**, 66-78.

Krasner, S.W., Scilimenti, M.J., Chinn, R., Chowdhury, Z.K. and Owen, D.M. (1996b) Disinfection by-products in water treatment. Minear, R. and Amy, G. (eds), Lewis Publishers, Boca Raton.

Kubin, M. and Vozka, S. (1980) Wall effect in cylindrical pores and the shape of GPC calibration curves. *Journal of Polymer Science, Polymer Symposium*, **68**, 209-213.

Kulovaara, M., Corin, N., Backlund, P. and Tervo, J. (1996) Impact of UV₂₅₄-radiation on aquatic humic substances. *Chemosphere*, **33**, 783-790.

Kumar, K. and Margerum, D.W. (1987) Kinetics and mechanism of general-acid-assisted oxidation of bromide by hypochlorite and hypochlorous acid. *Inorganic Chemistry*, **26**, 2706-2711.

LaLonde, R.T., Bu, L., Henwood, A., Fiumano, J. and Zhang, L. (1997) Bromine-, chlorine-, and mixed halogen-substituted 4-methyl-2(5H)-furanones: Synthesis and mutagenic effects of halogen and hydroxyl group replacements. *Chemical Research in Toxicology*, **10**, 1427-1436.

Larson, R.A. and Rockwell, A.L. (1979) Chloroform and chlorophenol production by decarboxylation of natural acids during aqueous chlorination. *Environmental Science and Technology*, **13**, 325-329.

Laurent, T.C. and Killander, J. (1964) A theory of gel filtration and its experimental verification. *Journal of Chromatography*, **14**, 317-330.

Law, R.D. (1969) Application of preparative gel-permeation chromatography to studies of low molecular weight carboxy-polybutadienes. *Journal of Polymer Science Part A-1: Polymer Chemistry*, **7**, 2097-2116.

Leenheer, J.A. (1981) Comprehensive approach to preparative isolation and fractionation of dissolved organic carbon from natural waters and wastewaters. *Environmental Science and Technology*, **15**, 578-587.

Leenheer, J.A. (1984) Treatise on water analysis. Minear, R. (ed), Academic Press, New York.

Leenheer, J.A. (1997) Fractionation, isolation and characterisation of hydrophilic constituents of dissolved organic matter in water, *in Proceedings of Natural Organic Matter Workshop*, Poitiers, France.

Leenheer, J.A. and Huffman, E.W.D. (1976) Classification of organic solutes in water using macroreticular resins. *Journal of Research of the U.S. Geological Survey*, **4**, 737-751.

Leenheer, J.A. and Noyes, T.L. (1984) A filtration and column adsorption system for on-site concentration and fractionation of organic substances from large volumes of water, US Geological Survey Water Supply Paper 2230.

Levashkevich, G.A. (1966) Interaction of humic acids with iron and aluminium hydroxides. *Soviet Soil Science*, **April**, 422-427.

Li, L., Zhao, Z., Huang, W., Peng, P., Sheng, G. and Fu, J. (2004) Characterization of humic acids fractionated by ultrafiltration. *Organic Geochemistry*, **35**, 1025-1037.

Liang, L. and Morgan, J.J. (1990) Chemical modelling of aqueous systems II. Melchoir, D.C. and Bassett, R.L. (eds), pp. 293-308, American Chemical Society, Washington, D.C.

Liang, L. and Singer, P.C. (2003) Factors influencing the formation and relative distribution of haloacetic acids and trihalomethanes in drinking water. *Environmental Science and Technology*, **37**, 2920-2928.

Luong, T.V., Peters, C.J. and Perry, R. (1982) Influence of bromide and ammonia upon the formation of trihalomethanes under water-treatment conditions. *Environmental Science and Technology*, **16**, 473-479.

Malcolm, R.L. (1989) Humic Substances II. In search of structure. Hayes, M.H.B., MacCarthy, P., Malcolm, R.L. and Swift, R.S. (eds), John Wiley and Sons, Chichester.

Malcolm, R.L. (1990) The uniqueness of humic substances in each of soil, stream and marine environments. *Analytica Chimica Acta*, **232**, 19-30.

Malcolm, R.L. and MacCarthy, P. (1992) Quantitative evaluation of XAD-8 and XAD-4 resins used in tandem for removing organic solutes from water. *Environment International*, **18**, 597-607.

March, J. (1992) *Advanced organic chemistry*. John Wiley and Sons, New York.

Marinsky, J.A. (1986) A unified physiochemical description of the protonation and metal ion complexation equilibria of natural organic acids (humic and fulvic acids). Analysis of the influence of polyelectrolyte properties on protonation equilibria in ionic media: Fundamental concepts. *Environmental Science and Technology*, **20**, 349-354.

Matilainen, A., Lindqvist, N., Korhonen, S. and Tuhkanen, T. (2002) Removal of NOM in the different stages of the water treatment process. *Environment International*, **28**, 457-465.

McCreary, J.J. and Snoeyink, V.L. (1980) Characterization and activated carbon adsorption of several humic substances. *Water Research*, **14**, 151-160.

Mori, S. (1977) High-speed gel permeation chromatography. A study of operational variables. *Journal of Polymer Science*, **21**, 1921-1932.

Mori, S. and Barth, H.G. (1999) *Size exclusion chromatography*, Springer-Verlag, Berlin, Germany.

Mori, S., Hiraide, M. and Mizuike, A. (1987) Aqueous size-exclusion chromatography of humic acids on A Sephadex gel column with diluted phosphate buffers as eluents. *Analytica Chimica Acta*, **193**, 231-238.

Morran, J., Bursill, D., Drikas, M. and Nguyen, H. (1996) A new technique for the removal of natural organic matter, *in Proceedings of AWWA Watertech Convention*, Sydney.

Morran, J., Bursill, D., Drikas, M. and Nguyen, H. (1997) A simple method to reduce disinfection by-product formation, *in Proceedings of 17th Federal Convention, Australia Water and Wastewater Association*, Melbourne, 373-379.

Morris, J.C. and Baum, B. (eds) (1978) Precursors and mechanisms of haloform formation in chlorination of water supplies, Ann Arbor Science Publications, Michigan.

Murphy, E.M., Zachara, J.M. and Smith, S.C. (1990) Influence of mineral-bound humic substances on the sorption of hydrophobic organic compounds. *Environmental Science and Technology*, **24**, 1507-1516.

Myllykangas, T., Nissinen, T.K., Rantakokko, P., Martikainen, P.J. and Vartiainen, T. (2002) Molecular size fractions of treated aquatic humus. *Water Research*, **36**, 3045-3053.

Nakanishi, K. and Solomon, P.H. (1977) Infrared Absorption Spectroscopy, Holden-Day Inc., Oakland.

Nanny, M.A., Minear, R.A. and Leenheer, J.A. (eds) (1997) Nuclear magnetic resonance spectroscopy in environmental chemistry, Oxford University Press Inc., New York.

Newcombe, G., Drikas, M., Assemi, S. and Beckett, R. (1997) Influence of characterised natural organic material on activated carbon adsorption: I. Characterisation of concentrated reservoir water. *Water Research*, **31**, 965-972.

Newman, R.H., Tate, K.R., Barron, P.F. and Wilson, M.A. (1980) Towards a direct, non-destructive method of characterising soil humic substances using ¹³C NMR. *Journal of Soil Science*, **31**, 623-631.

Nguyen, H., Slunjski, M., Bourke, M. and Drikas, M. (1997) DOC removal by MIEX[®] process - Scaling-up and other development issues, in *Proceedings of 17th Federal Convention, Australia Water and Wastewater Association*, Melbourne.

Nissinen, T., Miettinen, I.T., Martikainen, P.J. and Vartiainen, T. (2001) Molecular size distribution of natural organic matter in raw and drinking waters. *Chemosphere*, **45**, 865-873.

Norwood, D.L., Christman, R.F. and Hatcher, P.G. (1987) Structural characterisation of aquatic humic material. 2. Phenolic content and its relationship to chlorination mechanism in an isolated aquatic fulvic acid. *Environmental Science and Technology*, **21**, 791-798.

Norwood, D.L., Johnson, J.D. and Christman, R.F. (1980) Reactions of chlorine with selected aromatic models of aquatic humic material. *Environmental Science and Technology*, **14**, 187-190.

Novak, J., Mills, G.L. and Bertsch, P.M. (1992) Estimating the percent aromatic carbon in soil and aquatic humic substances using ultraviolet absorbance spectroscopy. *Journal of Environmental Quality*, **21**, 144-147.

Obolensky, A. and Singer, P.C. (2005) Halogen substitution patterns among disinfection by-products in the information collection rule database. *Environmental Science and Technology*, **39**, 2719-2730.

Ogston, A.G. (1958) The spaces in a uniform random suspension of fibres. *Transactions of the Faraday Society*, **54**, 1754-1757.

Oliver, B.G. and Thurman, E.M. (1983) Water chlorination: environmental impact and health effects. Jolley, R.L., Gorchev, H. and Hamilton, H.D.J. (eds), Ann Arbor Science, Michigan.

World health Organisation (2004) Guidelines for drinking water quality world health organisation, Geneva. Retrieved 22/03/2007 from <http://www.who.int/en/>

Osram (2007) Osram: Ozone production and surface activation, Retrieved 12/10/2007 from http://www.osram.com/_global/pdf/osram_com/tools_services/downloads/display_optic/123W008GB%2520PI%2520Xeradex.pdf

Owen, D.M., Amy, G. and Chowdhury, Z.K. (1993) Characterisation of natural organic matter and its relationship to treatability, Report #603, American Water Works Association Research Foundation, Denver.

Owen, D.M.A., G.L., Chowdhury, Z.K., Paode, R. and McCoy, G. (1995) NOM characterisation and treatability. *Environmental Science and Technology*, **87**, 46-43

Page, D.W., van Leeuwen, J.A., Spark, K.M. and Mulcahy, D.E. (2002) Pyrolysis characterisation of plant, humus and soil extracts from Australian catchments. *Journal of Analytical and Applied Pyrolysis*, **65**, 269-285.

Parfitt, R.L., Fraser, A.R. and Farmer, V.C. (1977) Adsorption on hydrous oxides. III. Fulvic acid and humic acid on Goethite, Gibbsite and Imogolite. *Journal of Soil Science*, **28**, 289-296.

Parfitt, R.L. and Russell, J.D. (1977) Adsorption on hydrous oxides. IV. Mechanism of adsorption of various ions on Goethite. *Journal of Soil Science*, **28**, 297-305.

Pelekani, C., Drikas, M. and Bursill, D. (2001) Application of direct filtration to MIEX[®] treated river Murray water, in *Proceedings of 19th Federal AWA Convention*, Canberra.

Pereira, V.J., Linden, K.G. and Weinberg, H.S. (2007) Evaluation of UV irradiation for photolytic and oxidative degradation of pharmaceutical compounds in water. *Water Research*, **41**, 4413-4423.

Perminova, I.V., Frimmel, F.H., Kovalevskii, D.V., Abbt-Braun, G., Kudryavtsev, A.V. and Hesse, S. (1998) Development of a predictive model for calculation of molecular weight of humic substances. *Water Research*, **32**, 872-881.

Perminova, I.V., Frimmel, F.H., Kudryavtsev, A.V., Kulikova, N., Abbt-Braun, G., Hesse, S. and Petrosyan, V.S. (2003) Development of a predictive model for calculation of molecular weight of humic substances. *Environmental Science and Technology*, **37**, 2477-2485.

Peschel, G. and Wildt, T. (1988) Humic substances of natural and anthropogeneous origin. *Water Research*, **22**, 105-108.

Peuravuori, J. and Pihlaja, K. (1997) Molecular size distribution and spectroscopic properties of aquatic humic substances. *Analytica Chimica Acta*, **337**, 133-149.

Peuravuori, J. and Pihlaja, K. (2004) Preliminary study of lake dissolved organic matter in light of nanoscale supramolecular assembly. *Environmental Science and Technology*, **38**, 5958-5967.

Piccolo, A., Conte, P., Trivellone, E., van Lagen, B. and Burman, P. (2002) Reduced heterogeneity of a lignite humic acid by preparative HPSEC following interaction with an organic acid. Characterisation of size-separates by Pyr-GC-MS and ¹H-NMR spectroscopy. *Environmental Science and Technology*, **36**, 76-84.

Plechanov, N. (1983) Studies of molecular weight distributions of fulvic and humic acids by gel permeation chromatography. Examination of the solute molecular composition using RI, UV and weight measurement as detection techniques. *Organic Geochemistry*, **5**, 143-149.

Plewa, M.J., Wagner, E.D., Jazwierska, P., Richardson, S.D., Chen, P.H. and McKague, A.B. (2004) Halonitromethane drinking water disinfection by-products: Chemical characterization and mammalian cell cytotoxicity and genotoxicity. *Environmental Science and Technology*, **38**, 62-68.

Popovici, S.T. and Schoenmakers, P.J. (2005) Fast size-exclusion chromatography-theoretical and practical considerations. *Journal of Chromatography A*, **1099**, 92-102.

Porath, J. (1963) Some recently developed fractionation procedures and their applications to peptide and protein hormones. *Journal of Pure and Applied Chemistry*, **6**, 233-244.

Porath, J. and Flodin, P. (1959) Gel filtration: A method for desalting and group separation. *Nature*, **183**, 1657-1659.

Posner, A.M. (1963) Importance of electrolyte in the determination of molecular weights by 'Sephadex' gel filtration with especial reference to humic acid. *Nature*, **198**, 1161-1163.

Pourmoghaddas, H., Stevens, A.A., Kinman, R.N., Dressman, R.C., Moore, L.A. and Ireland, J.C. (1993) Effect of bromide ion on formation of HAAs during chlorination. *Journal of the American Water Works Association*, **85**, 82-87.

Rausa, R., Mazzolari, E. and Calemma, V. (1991) Determination of molecular size distributions of humic acids by high-performance size-exclusion chromatography. *Journal of Chromatography A*, **541**, 419-529.

Reckhow, D.A. and Singer, P.C. (1985) Water chlorination: Environmental impact and health effects. Jolley, R.L., Gorchev, H. and Hamilton, H.D.J. (eds), pp. 1229-1257, Ann Arbor Science, Michigan.

Richardson, S.D. (1998) The encyclopaedia of environmental analysis and remediation. Meyers, R.A. (ed), p. 1398, Wiley, New York.

Richardson, S.D. (2003) Disinfection by-products and other emerging contaminants in drinking water. *Trends in Analytical Chemistry*, **22**, 666-684.

Richardson, S.D., Thruston, A.D., Rav-Acha, C., Groisman, L., Popilevsky, I., Juraev, O., Glezer, V., McKague, A.B., Plewa, M.J. and Wagner, E.D. (2003) Tribromopyrrole, brominated acids, and other disinfection by-products produced by disinfection of drinking water rich in bromide. *Environmental Science and Technology*, **37**, 3782-3793.

Ricker, R.D. and Sandoval, L.A. (1996) Fast, reproducible size-exclusion chromatography of biological macromolecules. *Journal of Chromatography A*, **743**, 43-50.

Robards, K., Haddad, P.R. and Jackson, P.E. (1994) Principles and practice of modern chromatographic methods, Academic Press, Harcourt Brace and Co.

Rook, J. (1974) Formation of haloforms during chlorination of natural waters. *Water Treatment Examination*, **23**, 234-243.

Rook, J. (1976) Haloforms in drinking water. *Journal of the American Water Works Association*, **68**, 168-172.

Rook, J. (1977) Chlorination reactions of fulvic acids in natural waters. *Environmental Science and Technology*, **11**, 478-482.

Saito, Y. and Hayano, S. (1979) Application of high-performance aqueous gel permeation chromatography to humic substances from marine sediment. *Journal of Chromatography A*, **177**, 390-392.

Saiz-Jimenez, C. (1994) Analytical pyrolysis of humic substances: Pitfalls, limitations, and possible solutions. *Environmental Science and Technology*, **28**, 1773-1780.

Saiz-Jimenez, C. (1995) Reactivity of the aliphatic humic moiety in analytical pyrolysis. *Organic Geochemistry*, **23**, 955-961.

Saiz-Jimenez, C. and De Leeuw, J.W. (1986) Chemical characterization of soil organic matter fractions by analytical pyrolysis-gas chromatography-mass spectrometry. *Journal of Analytical and Applied Pyrolysis*, **9**, 99-119.

Schafer, J. and Stejskal, E.O. (1976) Carbon-13 nuclear magnetic resonance of polymers spinning at magic angle. *Journal of the American Chemical Society*, **98**.

Schmitt, D., Saravia, F., Frimmel, F.H. and Schuessler, W. (2003) NOM-facilitated transport of metal ions in aquifers: Importance of complex-dissociation kinetics and colloidal formation. *Water Research*, **37**, 3541-3550.

Schnitzer, M. and Barton, D.H.R. (1963) A new experimental approach to the humic acid problem. *Nature*, **198**, 217-219.

Schnitzer, M. and Khan, S.U. (1972) Humic substances in the environment, Marcel Dekker, New York.

Schnitzer, M. and Skinner, S.I.M. (1968) Isotopes and radiation in soil organic matter studies, International Atomic Energy Agency, Vienna.

Schnoor, J.L., Nitzschke, J.L., Lucas, R.D. and Veenstra, J.N. (1979) Trihalomethane yields as a function of precursor molecular weight. *Environmental Science and Technology*, **13**, 1134-1138.

Schwarzenbach, R.P., Gschwend, P.M. and Imboden, D.M. (1993) Environmental organic chemistry, John Wiley and Sons, New York.

Scott, R.P.W. (ed) (1976) Contemporary liquid chromatography, John Wiley and Sons, New York.

- Semmens, M.J. and Staples, A.B. (1986) The nature of organics removed during treatment of Mississippi river water. *Journal of the American Water Works Association*, **78**, 76-81.
- Serkiz, S.M. and Perdue, E.M. (1990) Isolation of dissolved organic matter from the Suwannee river using reverse osmosis. *Water Research*, **24**, 911-916.
- Sihombing, R., Greenwood, P., Wilson, M.A. and Hanna, J.V. (1996) Composition of size fractions of swamp water and fulvic acid as measured by solid state NMR and pyrolysis GC-MS. *Organic Geochemistry*, **24**, 859-873.
- Silverstein, R.M. and Webster, F.X. (1997) Spectrometric identification of organic compounds, John Wiley and Sons, New York.
- Singer, P. and Bilyk, K. (2000) Enhanced coagulation using a magnetic ion exchange resin, in *Proceedings of AWWA Water Quality Technology Conference, on CD*.
- Singer, P. and Bilyk, K. (2002) Enhanced coagulation using a magnetic ion exchange resin. *Water Research*, **36**, 4009-4022.
- Sinsabaugh, R.L., Hoehn, R.C., Knocke, W.R. and Linkins, A.E. (1986) Removal of dissolved organic carbon by coagulation with iron sulfate. *Journal of the American Water Works Association*, **78**, 74-82.
- Skoog, D.A. (1982) Fundamentals of analytical chemistry, Saunders College Publishing, Philadelphia, PA.
- Slunjski, M., Bourke, M., Nguyen, H., Ballard, M., Morran, J. and Bursill, D. (1999) MIEX[®] DOC Process - A new ion exchange process, in *Proceedings of 18th Federal Convention, Australia Water and Wastewater Association, Adelaide, on CD*.

Slunjski, M., Bourke, M. and O'Leary, B. (2000a) MIEX[®] DOC Process for removal of humics in water treatment, *in Proceedings of International Humic Substances Society, Australia Chapter Seminar, on CD.*

Slunjski, M., Cadee, K., O'Leary, B. and Tattersall, J. (2000b) MIEX[®] Resin water treatment process, *in Proceedings of Aquatech Amsterdam, Amsterdam, on CD.*

Slunjski, M., Nguyen, H., Ballard, M., Eldridge, R., Morran, J., Drikas, M., O'Leary, B. and Smith, P. (2002) MIEX[®] - Good research commercialised. *Water*, **29**, 42-51.

Smith, B.C. (1996) Fundamentals of Fourier transform infrared spectroscopy, CRC Press, Boca Raton, Florida.

Smith, P., Botica, C., Lange, R. and Tattersall, J. (2001) Design and construction of the worlds first large scale MIEX[®] water treatment plant, *in Proceedings of 19th Federal AWA Convention, Canberra, on CD.*

Smith, P., O'Leary, B., Tattersall, J. and Allpike, B.P. (2003) The MIEX[®] process - A year of operation, *in Proceedings of Ozwater Convention, Perth, on CD.*

Smith, W.B. and Kollmansberger, A. (1965) Some aspects of gel permeation chromatography. *Journal of Physical Chemistry*, **69**, 4157-4161.

Specht, C.H. and Frimmel, F.H. (2000) Specific interactions of organic substances in size-exclusion chromatography. *Environmental Science and Technology*, **34**, 2361-2366.

Specht, C.H., Kumke, M.U. and Frimmel, F.H. (2000) Characterisation of NOM adsorption to clay minerals by size exclusion chromatography. *Water Research*, **34**, 4063-4069.

Squire, P.G. (1964) A relationship between the molecular weights of macromolecules and their elution volumes based on a model for Sephadex gel filtration. *Archives of Biochemistry and Biophysics*, **107**, 471-478.

Australian Bureau of Statistics (2007) Australian Bureau of Statistics home page. Retrieved 10/08/2007 from www.abs.gov.au

Stuedel, R. (1996) Mechanism for the formation of elemental sulfur from aqueous sulfide in chemical and microbiological desulfurisation processes. *Industrial Engineering and Chemical Research*, **35**, 1417-1423.

Stevens, A.A. (1979) Oxidative techniques in drinking water treatment. Kuhn, W. and Sontheimer, H. (eds), pp. 145-160, US EPA, Cincinnati, Ohio.

Stevenson, F.J. (1982) Humus chemistry; genesis, composition, reactions, John Wiley and Sons, New York.

Stevenson, F.J. and Goh, K.M. (1971) Infrared spectra of humic acids and related substances. *Geochimica Cosmochimica Acta*, **35**, 471-488.

Sun, L., Perdue, E.M. and McCarthy, J.F. (1995) Using reverse osmosis to obtain organic matter from surface and ground waters. *Water Research*, **29**, 1471-1477.

Symons, J.M., Krasner, S.W., Scilimenti, M.J., Simms, L.A., Sorensen, H.W., Speitel Jr, G.E. and Diehl, A.C. (1996) Disinfection by-products in water treatment. Minear, R.A. and Amy, G.L. (eds), pp. 91-129, CRC Press Inc., New York.

Templier, J., Derenne, S., Croué, J.-P. and Largeau, C. (2005) Comparative study of two fractions of riverine dissolved organic matter using various analytical pyrolytic methods and a ¹³C CP/MAS NMR approach. *Organic Geochemistry*, **36**, 1418-1442.

Thurman, E.M. (1985) Organic geochemistry of natural waters, M. Nijhoff and W. Junk Publishers Dordrecht.

Thurman, E.M. and Malcolm, R.L. (1981) Preparative isolation of aquatic humic substances. *Environmental Science and Technology*, **15**, 463-466.

Thurman, E.M., Wershaw, R.L., Malcolm, R.L. and Pinckney, D.J. (1982) Molecular size of aquatic humic substances. *Organic Geochemistry*, **4**, 27-35.

Tipping, E. and Cooke, D. (1982) The effects of adsorbed humic substances on the surface charge of Goethite (α -FeOOH) in freshwaters. *Geochimica Cosmochimica Acta*, **46**, 75-80.

Traina, S.J., Novak, J. and Smeck, N.E. (1990) An ultraviolet absorbance method of estimating the percent aromatic carbon content in humic acids. *Journal of Environmental Quality*, **19**, 151-153.

Tuschall, J.R. and Brezonik, P.L. (1980) Characterisation of organic Nitrogen in natural waters: Its molecular size, protein content and interactions with heavy metals. *Limnology and Oceanography*, **25**, 495-504.

Unger, K. (1983) The application of size exclusion chromatography to the analysis of biopolymers. *Trends in Analytical Chemistry*, **2**, 271-274.

USEPA (2007) National primary drinking water regulations USEPA, Retrieved 24/08/2007 from <http://www.epa.gov/safewater/index.html>

van der Kaaden, A., Haverkamp, J., Boon, J. and de Leeuw, J.W. (1983) Analytical pyrolysis of carbohydrates : I. Chemical interpretation of matrix influences on pyrolysis-mass spectra of amylose using pyrolysis-gas chromatography-mass spectrometry. *Journal of Analytical and Applied Pyrolysis*, **5**, 199-220

van der Kooij, D. (1990) Drinking water microbiology. Mcfeters, G.A. (ed), John Wiley and Sons, New York

van Heemst, J.D.H., van Bergen, P.F., Stankiewicz, B.A. and de Leeuw, J.W. (1999) Multiple sources of alkylphenol produced upon pyrolysis of DOM, POM and recent sediments. *Journal of Analytical and Applied Pyrolysis*, **52**, 239-256

van Kreveld, M.E. and van Den Hoed, N. (1973) Mechanism of gel permeation chromatography: Distribution coefficient. *Journal of Chromatography*, **83**, 111-124.

Via, S.H. and Dietrich, A.M. (1996) Water disinfection and natural organic matter. Minear, R. and Amy, G. (eds), pp. 282-295.

Vogl, J. and Heumann, V.G. (1998) Development of an ICP-IDMS method for dissolved organic carbon determinations and its application to chromatographic fractions of heavy metal complexes with humic substances. *Analytical Chemistry*, **70**, 2038-2043.

Volk, C., Bell, K., Ibrahim, E., Verges, D., Amy, G. and Lechevallier, M. (2000) Impact of enhanced and optimized coagulation on removal of organic matter and its biodegradable fraction in drinking water. *Water Research*, **34**, 3247-3257.

Vrijennoek, E.M., Childress, A.E., Elimelech, M., Tanka, T.S. and Beuhler, M.D. (1998) Removing particles and THM precursors by enhanced coagulation. *Journal of the American Water Works Association*, **90**, 139-150.

Vuorio, E., Vahala, R., Rintala, J. and Laukkanen, R. (1998) The evaluation of drinking water treatment performed with HPSEC. *Environmental International*, **24**, 617-623.

Wajon, J.E., Kavanagh, B.V., Kagi, R.I., Rosich, R.S., Alexander, R. and Fleay, B.J. (1986) Swampy odour in the drinking water of Perth, Western Australia. *Water*, **September**, 28-32.

Wang, Z.-D., C. Pant, B. and H. Langford, C. (1990) Spectroscopic and structural characterization of a Laurentian fulvic acid: notes on the origin of the colour. *Analytica Chimica Acta*, **232**, 43-49.

Warton, B., Heitz, A., Joll, C.A. and Kagi, R.I. (2006) A new method for determining the chlorine demand of natural and treated waters. *Water Research*, **40**, 2877-2884.

Warton, B., Heitz, A., Zappia, L.R., Franzmann, P.D., Masters, D., Joll, C.A., Alessandrino, M., Allpike, B.P., O'Leary, B. and Kagi, R.I. (2007) Magnetic ion exchange drinking water treatment in a large-scale facility. *Journal of the American Water Works Association*, **99**, 89-101.

Warton, B., Heitz, A., Zappia, L.R., Masters, D., Alessandrino, M., Franzmann, P.D., Joll, C.A., Allpike, B.P., O'Leary, B. and Kagi, R.I. (2005) Natural organic matter budget through Wanneroo groundwater treatment plant: MIEX[®] and enhanced coagulation process streams - Comparison of 'summer' and 'winter' blend waters, Report from ARC SPIRT collaborative project.

Water Corporation (2007) Water Corporation home page. Retrieved 9/8/2007 from www.watercorporation.com.au

Westerhoff, P., Aiken, G., Amy, G. and Debroux, J. (1999) Relationships between the structure of natural organic matter and its reactivity towards molecular ozone and hydroxyl radicals. *Water Research*, **33**, 2265-2276.

Westerhoff, P., Chao, P. and Mash, H. (2004) Reactivity of natural organic matter with aqueous chlorine and bromine. *Water Research*, **38**, 1502-1513.

Westerhoff, P., Song, R.G., Amy, G. and Minear, R. (1998) NOMs role in bromine and bromate formation during ozonation. *Journal of the American Water Works Association*, **90**, 82-94.

Wiesner, M. and Chellam, S. (1992) Mass transport considerations for pressure-driven membrane processes. *Journal of the American Water Works Association*, **90**, 82-94.

Wilson, M.A. (1987) N.M.R. techniques and applications in geochemistry and soil chemistry, Pergamon Press, Oxford, England.

Wilson, M.A. (1989) Humic substances II. In search of structure. Hayes, M.H.B., MacCarthy, P., Malcolm, R.L. and Swift, R.S. (eds), John Wiley and Sons, Chichester.

Wong, S., Hanna, J.V., King, S., Carroll, T.J., Eldridge, R.J., Dixon, D., Bolto, B.A., Hesse, S., Abbt-Braun, G. and Frimmel, F.H. (2002) Fractionation of natural organic matter in drinking water and characterization by ¹³C cross-polarization magic-angle spinning NMR spectroscopy and size exclusion chromatography. *Environmental Science and Technology*, **36**, 3497-3503.

Yau, W.W., Kirkland, J.J. and Bly, D.D. (1979) Modern size exclusion chromatography, John Wiley and Sons, New York.

Yau, W.W. and Malone, C.P. (1967) An approach to diffusion theory of gel permeation chromatographic separation. *Journal of Polymer Science Part B: Polymer Letters*, **5**, 663-669.

Yau, W.W., Malone, C.P. and Fleming, S.W. (1968a) The equilibrium distribution coefficient in gel permeation chromatography. *Journal of Polymer Science Part B: Polymer Letters*, **6**, 803-807.

Yau, W.W., Suchan, H.L. and Malone, C.P. (1968b) Flow-rate dependence of gel permeation chromatography. *Journal of Polymer Science Part A-2: Polymer Physics*, **6**, 1349-1355.

Zappia, L.R., Wylie, J.T., Franzmann, P.D., Warton, B., Alessandrino, M., Heitz, A. Kagi, R.I., Joll, C.A., Scott, D., Hiller, B., Masters, D., Nolan, P. and Thiel, P. (2007) Pilot scale testing of biofilter post-treatment of MIEX[®] treated water. *Journal of Water Supply: research and technology – Aqua*, **56**, 217-232.

Zhou, Q., Cabaniss, S.E. and Maurice, P.A. (2000) Considerations in the use of high-pressure size exclusion chromatography (HPSEC) for determining molecular weights of aquatic humic substances. *Water Research*, **34**, 3505-3514.

Every reasonable effort has been made to acknowledge the owners of copyright material. I would be pleased to hear from any copyright owner who has been omitted or incorrectly acknowledged.